Impacts of climate change and habitat on the health and recovery of Salish Sea shellfish

Eileen H. Bates

A dissertation

submitted in partial fulfillment of the

requirements for the degree of

Doctor of Philosophy

University of Washington

2024

Reading Committee:

Jacqueline Padilla-Gamiño, Chair

Timothy Essington

Jodie Toft

Program Authorized to Offer Degree:

School of Aquatic and Fishery Sciences

University of Washington

Abstract

Impacts of climate change and habitat on the health and recovery of Salish Sea shellfish

Eileen H. Bates

Chair of Supervisory Committee:

Jacqueline Padilla-Gamiño

School of Aquatic and Fishery Sciences

Global climate change is causing ocean acidification (OA), warming, and decreased dissolved oxygen (DO) in coastal areas, which can cause physiological stress and compromise the health of marine organisms. In the Salish Sea, a region that already experiences naturally low pH and seasonal hypoxia and is surrounded by urbanized and industrialized areas, climate change will pose further threats to both economically and ecologically important shellfish species. The first part of this dissertation focuses on trace metal accumulation in mussels (*Mytilus galloprovincialis*), an important harvested species, and Olympia oysters (*Ostrea lurida*), Washington's only native oyster species, and how oceanographic variables that will change with the climate may impact this metal accumulation. Our field study found differences between sites in both the mean metal concentrations and variability around the mean of those concentrations in bivalves. High metal concentrations in bivalves were not associated with high concentrations of

metals in seawater. While we could not eliminate possible confounding factors, we also found higher metal concentrations in shellfish associated with lower pH, lower temperature, and lower dissolved oxygen. These findings increase our understanding of spatial differences in trace metal bioaccumulation in shellfish from the Salish Sea. The rest of this dissertation focused on another native Washington shellfish species, the endangered pinto abalone (*Haliotis kamtschatkana*), which declined by 97% in the state between 1992 to 2017. Their decline is a loss for indigenous tribes, recreational divers, and the health of subtidal rocky reefs and kelp beds. Starting in 2007, conservation aquaculture initiatives to restore pinto abalone have been underway to return the wild population to a self-sustaining level. However, the success of abalone depends not only on restoration efforts but also on the capacity of outplanted abalone to survive and reproduce as threats of ocean acidification and warming continue to increase. We conducted two hatchery-based experiments exposing abalone to different pH and temperature conditions (7.90-7.95 pH/14 °C (ambient), 7.90-7.95 pH/18 °C, 7.55-7.6 pH/14 °C; and 7.55-7.6 pH/18 °C), as well as testing the efficacy of coralline algae (CCA) as a settlement cue and substrate. In our first study, we found that abalone in the ambient treatment had the best survival, those in the 7.60pH/18°C treatment had the worst survival, and those in the two single-stressor treatments had survival in between. For surviving larvae, temperature appeared to have a minor effect on settlement; pH was the dominant stressor determining settlement success, with higher settlement rates for surviving larvae under ambient pH treatments at both temperatures. In our second study, juvenile survival was negatively impacted by low pH but positively impacted by CCA presence. Our results show the potential of CCA to increase pinto abalone juvenile survival and ameliorate the negative effects of low pH. We also conducted a field-based study comparing the survival of outplanted hatchery-reared abalone to oceanographic conditions at abalone restoration sites in

Washington. We found clear differences in salinity and temperature variability between sites. Dissolved oxygen and pH both changed seasonally, and variability increased during spring and summer months with algal growth, but clear spatial patterns could not be determined. Current speeds also varied between sites, and currents seemed to be mostly tidally driven as opposed to having seasonal shifts. Overall, we could not determine clear correlations between any oceanographic variables and abalone survival, but our study provides important data on conditions abalone experience in the wild in Washington and will allow us to track how these conditions change over time.

Table of Contents

Acknowledgements

I would first like to thank my advisor Jackie Padilla-Gamiño for accompanying me on this adventure and for working with me to craft a degree that allowed me to pursue my passions and interests. Her mentorship, help with paper and grant writing, and expertise in ecophysiology have all helped me become a better scientist. And her enthusiasm for coralline algae helped me expand my thinking beyond the shellfish world. I would also like to thank the rest of my committee. Tim Essington for his endless help with statistics and theory and for helping me to understand how my science fits withing in the bigger picture. Jodie Toft for being a critical link to PSRF, for helping ensure my science had tangible and helpful applications, and for her enthusiasm, leadership, expertise, and humor. Jesse Zaneveld for his expertise and his immense help with all things microbiome—although many of the results of these efforts did not end up in my dissertation, we have enough samples in the freezer for another dissertation, and the context his expertise provided has shaped this work and will shape my future research. Jennifer Ruesink, who not only acted as my GSR but also posed questions about my experimental data and environmental data which made me do some of my deepest thinking in grad school. I am grateful to you all.

I thank my lab mates past and present in SAFS. Lindsay Alma, Julietta Martinelli, Tanya Brown, Jeremy Axworthy, Corinne Klohmann, Miranda Roethler, Callum Backstrom, Nuria Viladrich, Craig Norrie, Sarah Tanja, Kat Lasdin, and Xochitl Clare. I especially thank Miranda Roethler and Lindsay Alma for their help with my lab and field work and Jeremy Axworthy for being a constant at the desk next to me for my entire time in SAFS.

Thank you to my classmates and peers within SAFS, especially Writing Group for helping me power through the end of my degree. Katie McElroy, Jenny Stern, Liz Elmstrom,

Megan Feddern, Michaela Lowe, and Miranda Roethler—your assistance made such a difference. I thank the Essington Lab and Friends group for providing a second home lab for me at SAFS, for broadening my scientific world, and for giving me such valuable feedback on my work.

I would like to thank the team at Puget Sound Restoration Fund (PSRF) for their partnership throughout my degree. I thank Jodie Toft, Josh Bouma, and Ryan Crim for their help in designing projects that answered questions relevant to both my interests and their restoration needs. I thank the team, past and present, at the Kenneth K. Chew Center for Shellfish Research and Restoration: Stuart Ryan, Caitlin O'Brien, Malise Yun, Rachel Dalthorp, Mackenzie Weers, Sarah Henneford, and Olivia Cattau. Thanks as well to Mac Gavery, Larken Root, Paul McElhany, Michael Maher, and Danielle Perez for their help with ocean acidification systems and measurements.

The fieldwork for this project was time and energy intensive. The Subtidal Shellfish Team at the Washington Department of Fish and Wildlife made this work possible. Thank you to Katie Sowul, Hank Carson, Emily Loose, Taylor Frierson, Bethany Stevick, and Ocean Working. In addition, Josh Bouma and Jay Dimond from PSRF also helped execute these field projects. Additional thanks to Nate Schwarck and Derek Smith from Western Washington University for captaining boats during off-season sensor work. Thank you to Will Love, UW DSO, for his help in achieving my AAUS scientific diver status and continued SCUBA training. And thanks to Alex Lowe for help in designing the sensor arrays and sharing his experience working on similar studies that helped inspire this one.

Funding for my projects came from Washington Seagrant, the Northwest Climate Adaptation Science Center, the North Pacific Research Board, and the UW School of Aquatic

and Fishery Sciences. Additional support came from The Next Swell, the Pacific Northwest Shell Club, the Women Divers Hall of Fame, and the International Women's Fishing Association. I thank all these organizations and their contributions to my work; this research would not have been possible without their assistance.

Finally, I would like to thank my family, especially my mom Susan, my dad Tim, and my brother Kelvin. I also want to thank my friends from outside of the SAFS community. Without such a wide community—my schoolmates, my friends, my collaborators, my family—this work would not have been possible.

Introduction

Changes to climate and seawater chemistry caused by anthropogenic emission of greenhouse gasses pose a global threat but will particularly impact coastal areas through both land and marine driven changes in precipitation, runoff, sea level rise, and ocean circulation. As global climate change continues, marine species will face increasing seawater temperatures, continued ocean acidification, and lower dissolved oxygen availability. Coastal cities and areas with high river discharge will also encounter increased pollution (Fowler & Oregioni, 1976; Wang et al., 2018), which may have important consequences for the bioaccumulation of metals and chemicals in marine organisms, further impacting their physiology and survival.

Washington State is one such coastal area that is and will be severely impacted by climate change both economically and ecologically. Washington State has an extremely productive shellfish aquaculture industry. It is the largest producer of farmed clams, oysters, and mussels in the United States, and the economic contribution of the industry in 2011 was estimated at $270 million (Washington Sea Grant, 2015). However, this industry is at risk from both climate change and a growing human population. The Salish Sea region is seeing the effects of anthropogenic climate change earlier than many other regions of the global ocean. Waters in the Salish Sea already have naturally low pH from upwelling of deep seawater rich in CO_2 (Feely et al., 2012), which, in conjunction with anthropogenic CO_2 inputs, makes the water in this region especially corrosive for shellfish and other calcifiers. In addition, areas of the Salish Sea, such as Hood Canal, are already seasonally hypoxic, which will only worsen with increased anthropogenic climate change and eutrophication (Keister & Tuttle, 2013).

Changes in seawater pH, temperature, and DO can affect the solubility and speciation of metals, which in turn can affect their bioavailability and their impact on the cellular processes of

marine organisms (Millero, 2001; Millero et al., 2009; Smith et al., 2015). The first chapter of my dissertation analyses the accumulation of trace metals in oysters and mussels in Puget Sound. Extensive modeling has shown that predicting chemical speciation and uptake by animals under different conditions is complex. Laboratory studies have also demonstrated that the impacts vary significantly across species. Therefore, obtaining empirical data specific to Washington State mussels and oysters is crucial for understanding the potential threats local species face.

In addition to the localized environmental conditions that lead to spatial differences in trace metal uptake, these same localized differences, coupled with the overall trend of climate change, pose unique threats and raise scientific questions for the recovery and survival of threatened species. One such endangered species in Washington State is the pinto abalone. The remainder of my dissertation focuses on the effects of climate change on pinto abalone and their associated habitat.

From 1992 to 2017, pinto abalone (*H. kamtschatkana*) experienced a 97% decline in Washington waters (Neuman et al., 2019; Rothaus et al., 2008). Despite the closure of the fishery in 1994, the population remains low and faces challenges associated with disease, illegal harvest, climate change, and low population density (Carson et al., 2019). Reproductively active adults are not prevalent nor densely aggregated enough for successful fertilization to occur (Rothaus et al., 2008). The continued decline of the Washington pinto abalone population is a loss for indigenous tribes, recreational divers, and the health of rocky reefs and kelp beds, and led the Washington Department of Fish and Wildlife (WDFW) to list pinto abalone as an endangered species in Washington in 2019.

Conservation aquaculture is being utilized as a restoration technique by WDFW and Puget Sound Restoration Fund (PSRF). Pinto abalone broodstock are spawned at the Kenneth K.

Chew Center for Shellfish Research and Restoration (Chew Center) that PSRF operates at NOAA's Manchester Research Station. Larvae are raised through settlement and the juveniles are grown for 1 to 2 years before being transitioned to outplant sites in the San Juan Archipelago (Carson et al., 2019). Since 2009, PSRF and WDFW have outplanted over 55,000 juveniles to shallow-water habitats at 36 outplant sites in the San Juan Archipelago.

In addition to their already low numbers, the effects of climate change on seawater may further impact already vulnerable pinto abalone populations. Early life stages of calcifiers have been found particularly vulnerable to the effects of OA—shell deformities, mortality, delayed development, and reduced growth have been demonstrated when larvae of both pinto and European abalone were exposed to pCO_2 conditions resembling those expected in 2100 (Crim et al., 2011; Wessel et al., 2018). My first study on pinto abalone assessed how climate change (temperature and pH shifts) will affect larval survival and settlement.

Pinto abalone specifically depend on macroalgae such as coralline algae for settlement substrate (Morse & Morse, 1984). Chemical cues from coralline algae serve as a critical bridge for invertebrate larvae to recognize settlement substrate, and there is growing recognition that coralline algae biofilms may play an important role in contributing to this cue (Barott et al., 2011; Huggett et al., 2006; Johnson & Sutton, 1994; McCoy & Kamenos, 2015; Negri et al., 2001).

In addition to acting as a settlement inducer, coralline algae can create gradients of pH and oxygen depending on their thickness and composition, further altering their ecosystems, especially at a scale relevant to shellfish larvae (Houlihan et al., 2020; Qian et al., 2007). The third chapter of my dissertation assesses how the presence of coralline algae, in conjunction with acidification and warming, impacts larval and juvenile pinto abalone.

Climate change and habitat, of which coralline algae is one important piece, will impact wild pinto abalone populations and hatchery rearing. Outplant success varies widely across sites. To improve the ultimate success of restoration, there is a need to understand the factors contributing to this variability in outplanted juvenile survival. The last chapter of my dissertation takes what we learned from hatchery studies and then assesses the wild conditions that pinto abalone inhabit.

My four chapters aim to:

(1) Examine how local water chemistry at different sites in Puget Sound affects the accumulation of trace metals in mussels and oysters.

(2) Determine the effect of stressors exacerbated by climate change (elevated temperature, OA) on pinto abalone settlement, shell size, and survival.

(3) Characterize the effectiveness of coralline algae substrate to increase the settlement and survival of pinto abalone under varied OA and temperature conditions.

(4) Characterize environmental conditions at abalone restoration sites and examine how they may relate to the success or failure of juvenile abalone outplant sites.

References

Apprill, A. (2017). Marine animal microbiomes: Toward understanding host–microbiome interactions in a changing ocean. *Frontiers in Marine Science*, *4*, 222.

Babcock, R., & Keesing, J. (1999). Fertilization biology of the abalone Haliotis laevigata: Laboratory and field studies. *Canadian Journal of Fisheries and Aquatic Sciences*, *56*(9), 1668–1678.

Barott, K. L., Rodriguez-Brito, B., Janouškovec, J., Marhaver, K. L., Smith, J. E., Keeling, P., & Rohwer, F. L. (2011). Microbial diversity associated with four functional groups of benthic reef algae and the reef-building coral *Montastraea annularis*. *Environmental Microbiology*, *13*(5), 1192–1204.

Bayraktarov, E., Saunders, M. I., Abdullah, S., Mills, M., Beher, J., Possingham, H. P., Mumby, P. J., & Lovelock, C. E. (2016). The cost and feasibility of marine coastal restoration. *Ecological Applications*, *26*(4), 1055–1074.

Carranza, A., & Zu Ermgassen, P. S. (2020). A Global Overview of Restorative Shellfish Mariculture. *Frontiers in Marine Science*, *7*, 722.

Carson, H. S., Morin, D. J., Bouma, J. V., Ulrich, M., & Sizemore, R. (2019). The survival of hatchery-origin pinto abalone *Haliotis kamtschatkana* released into Washington waters. *Aquatic Conservation: Marine and Freshwater Ecosystems*, *29*(3), 424–441.

Crim, R. N., Sunday, J. M., & Harley, C. D. (2011). Elevated seawater CO2 concentrations impair larval development and reduce larval survival in endangered northern abalone (*Haliotis kamtschatkana*). *Journal of Experimental Marine Biology and Ecology*, *400*(1–2), 272–277.

Doo, S. S., Kealoha, A., Andersson, A., Cohen, A. L., Hicks, T. L., Johnson, Z. I., ... & Busch, D. S. (2020). The challenges of detecting and attributing ocean acidification impacts on marine ecosystems. *ICES Journal of Marine Science*, *77*(7-8), 2411-2422.

Fabricius, K. E., & De'Ath, G. (2004). Identifying ecological change and its causes: A case study on coral reefs. *Ecological Applications*, *14*(5), 1448–1465.

Feely, R. A., Klinger, T., Newton, J. A., & Chadsey, M. (2012). *Scientific summary of ocean acidification in Washington State marine waters* [NOAA OAR Special Report.].

Fowler, S. W., & Oregioni, B. (1976). Trace metals in mussels from the NW Mediterranean. *Marine Pollution Bulletin*, *7*(2), 26–29.

Hilborn, R., & Mangel, M. (1997). *The ecological detective: Confronting models with data* (Vol. 28). Princeton University Press.

Houlihan, E. P., Espinel-Velasco, N., Cornwall, C. E., Pilditch, C. A., & Lamare, M. D. (2020). Diffusive boundary layers and ocean acidification: Implications for sea urchin settlement and growth. *Frontiers in Marine Science*, *7*, 972.

Huggett, M. J., Williamson, J. E., De Nys, R., Kjelleberg, S., & Steinberg, P. D. (2006). Larval settlement of the common Australian sea urchin *Heliocidaris erythrogramma* in response to bacteria from the surface of coralline algae. *Oecologia*, *149*(4), 604–619.

Ianson, D., Allen, S. E., Moore-Maley, B. L., Johannessen, S. C., & Macdonald, and R. W. (2016). Vulnerability of a semi-enclosed estuarine sea to ocean acidification in contrast with hypoxia. *Geophysical Research Letters*, *43*(11), 5793–5801.

Johnson, C. R., & Sutton, D. C. (1994). Bacteria on the surface of crustose coralline algae induce metamorphosis of the crown-of-thorns starfish *Acanthaster planci*. *Marine Biology*, *120*(2), 305–310.

Keister, J. E., & Tuttle, L. B. (2013). Effects of bottom-layer hypoxia on spatial distributions and community structure of mesozooplankton in a sub-estuary of Puget sound, Washington, U.S.A. *Limnology and Oceanography*, *58*(2), 667–680.

Li, Y., & Rogers-Bennett, L. (2017). Evaluating factors affecting restoration of an endangered marine broadcast-spawning invertebrate using an individual-based model of white abalone. *Endangered Species Research*, *32*, 293–308.

Lowe, A. T., Bos, J., & Ruesink, J. (2019). Ecosystem metabolism drives pH variability and modulates long-term ocean acidification in the Northeast Pacific coastal ocean. *Scientific Reports*, *9*(1), 1–11.

Lowe, A. T., Roberts, E. A., & Galloway, A. W. (2016). Improved marine-derived POM availability and increased pH related to freshwater influence in an inland sea. *Limnology and Oceanography*, *61*(6), 2122–2138.

McCoy, S. J., & Kamenos, N. A. (2015). Coralline algae (Rhodophyta) in a changing world: Integrating ecological, physiological, and geochemical responses to global change. *Journal of Phycology*, *51*(1), 6–24.

Millero, F. (2001). Speciation of metals in natural waters. *Geochemical Transactions*, *2*(June), 56–64.

Millero, F. J., Woosley, R., B, D., & Waters, J. (2009). Effect of ocean acidification on the speciation of metals in seawater. *Oceanography*, *22*(4), 72–85.

Morse, A. N., & Morse, D. E. (1984). Recruitment and metamorphosis of *Haliotis* larvae induced by molecules uniquely available at the surfaces of crustose red algae. *Journal of Experimental Marine Biology and Ecology*, *75*(3), 191–215.

Murray, J. W., Roberts, E., Howard, E., O'Donnell, M., Bantam, C., Carrington, E., Foy, M., Paul, B., & Fay, A. (2015). An inland sea high nitrate-low chlorophyll (HNLC) region with naturally high pCO2. *Limnology and Oceanography*, *60*(3), 957–966.

Negri, A. P., Webster, N. S., Hill, R. T., & Heyward, A. J. (2001). Metamorphosis of broadcast spawning corals in response to bacteria isolated from crustose algae. *Marine Ecology Progress Series*, *223*, 121–131.

Neuman, M. J., Wang, S., Busch, S., Friedman, C., Gruenthal, K., Gustafson, R., Kushner, D., Stierhoff, K., Vanblaricom, G. & Wright, S. (2018). A status review of pinto abalone (*Haliotis kamtschatkana*) along the west coast of North America: interpreting trends, addressing uncertainty, and assessing risk for a wide-ranging marine invertebrate. *Journal of Shellfish Research*, *37*(4), 869-910.

Pfister, C. A., Altabet, M. A., & Weigel, B. L. (2019). Kelp beds and their local effects on seawater chemistry, productivity, and microbial communities. *Ecology*, *100*(10), e02798.

Qian, P.-Y., Lau, S. C., Dahms, H.-U., Dobretsov, S., & Harder, T. (2007). Marine biofilms as mediators of colonization by marine macroorganisms: Implications for antifouling and aquaculture. *Marine Biotechnology*, *9*(4), 399–410.

Rothaus, D. P., Vadopalas, B., & Friedman, C. S. (2008). Precipitous declines in pinto abalone (*Haliotis kamtschatkana kamtschatkana*) abundance in the San Juan Archipelago, Washington, USA, despite statewide fishery closure. *Canadian Journal of Fisheries and Aquatic Sciences*, *65*(12), 2703-2711.

Smith, K. S., Balistrieri, L. S., & Todd, A. S. (2015). Using biotic ligand models to predict metal toxicity in mineralized systems. *Applied Geochemistry*, *57*, 55–72.

Suding, K., Higgs, E., Palmer, M., Callicott, J. B., Anderson, C. B., Baker, M., Gutrich, J. J., Hondula, K. L., LaFevor, M. C., & Larson, B. M. (2015). Committing to ecological restoration. *Science*, *348*(6235), 638–640.

Todgham, A. E., & Stillman, J. H. (2013). Physiological responses to shifts in multiple environmental stressors: Relevance in a changing world. *Integrative and Comparative Biology*, *53*(4), 539–544.

Wang, W. X., J, M., & Wenig, N. (2018). Trace metals in oysters: Molecular and cellular mechanisms and ecotoxicological impacts. *Environmental Science: Processes & Impacts*, *20*(6), 892–912.

Washington Sea Grant. (2015). *Shellfish Aquaculture in Washington State: Final Report to Washington State Legislature*. *December*, 1–84.

Weigel, B. L., & Pfister, C. A. (2019). Successional dynamics and seascape-level patterns of microbial communities on the canopy-forming kelps *Nereocystis luetkeana* and *Macrocystis pyrifera*. *Frontiers in Microbiology*, *10*, 346.

Weigel, B. L., & Pfister, C. A. (2020). Oxygen metabolism shapes microbial settlement on photosynthetic kelp blades compared to artificial kelp substrates. *Environmental Microbiology Reports*.

Wessel, N., Martin, S., Badou, A., Dubois, P., Huchette, S., Julia, V., Nunes, F., Harnye, E., Paillard, C. & Auzoux-Bordenave, S. (2018). Effect of CO2–induced ocean acidification on the early development and shell mineralization of the European abalone (*Haliotis tuberculata*). *Journal of Experimental Marine Biology and Ecology*, *508*, 52-63.

Williamson, P., Pörtner, H.-O., Widdicombe, S., & Gattuso, J.-P. (2020). Ideas and Perspectives: When ocean acidification experiments are not the same, reproducibility is not tested. *Biogeosciences Discussions*, 1–7.

Chapter 1: Accumulation of trace metals in shellfish from Puget Sound (Washington, USA) varies with size and location, and may be linked to local water chemistry

Publication history: This study was co-authored with Lindsay Alma, Tamas Ugrai, Alexander Gagnon, Michael Maher, Paul McElhany, and Jacqueline Padilla-Gamiño. At the time this dissertation was published, a version of this chapter was published in Frontiers in Marine Science.

Abstract

Global climate change is causing ocean acidification (OA), warming, and decreased dissolved oxygen (DO) in coastal areas, which can cause physiological stress and compromise the health of marine organisms. While there is increased focus on how these stressors will affect marine species, there is little known regarding how changes in water chemistry will impact the bioaccumulation of trace metals. This study compared trace metal concentrations in tissue of mussels (*Mytilus galloprovincialis*) and Olympia oysters (*Ostrea lurida*) in Puget Sound, Washington, a region that experiences naturally low pH, seasonal hypoxia, and is surrounded by urbanized and industrialized areas. Shellfish were held at three sites where oceanographic data was continuously collected using mooring buoys. Using inductively coupled plasma mass-spectrometry to measure trace metals in the tissue, we found differences in accumulation of trace metals based on species, location, and size. Our study found differences between sites in both the *mean* metal concentrations and *variability* around the mean of those concentrations in bivalves. However, high metal concentrations in bivalves were not associated with high concentrations of metals in seawater. Metal concentrations in shellfish were associated with size: smaller shellfish had higher concentrations of metals. Carr Inlet at 20 m depth had the smallest shellfish and the highest metal concentrations. While we could not eliminate possible confounding factors, we

also found higher metal concentrations in shellfish associated with lower pH, lower temperature, and lower dissolved oxygen (conditions seen at Carr Inlet at 20 m and to a lesser extent at Point Wells at 5 m depth). There were also significant differences in accumulation of metals between oysters and mussels, most notably copper and zinc, which were found in higher concentrations in oysters. These findings increase our understanding of spatial differences in trace metal bioaccumulation in shellfish from Puget Sound. Our results can help inform the Puget Sound aquaculture industry how shellfish may be impacted at different sites as climate change continues and coastal pollution increases.

Introduction

Climate change poses a global threat, but will particularly impact coastal areas such as marginal seas through both land and marine driven changes in precipitation, runoff, sea level rise, ocean circulation, and seawater chemistry (Harley et al., 2006; IPCC, 2014; Scavia et al., 2002). As global climate change continues, marine species will face increasing seawater temperatures, continued ocean acidification, and lower dissolved oxygen availability (IPCC, 2014). Coastal cities and areas with high river discharge will also face the threat of increased pollution (Fowler & Oregioni, 1976; W. X. Wang et al., 2018), which may have important consequences for bioaccumulation of metals and chemicals in marine organisms, further impacting their physiology and survival.

In marginal seas, such as Puget Sound, research has been conducted on the variation of pH, temperature, and DO in coastal zones and how these oceanographic variables may interact to affect physiological performance, reproduction, and survival of species (Gobler & Baumann, 2016; Handisyde et al., 2006; Washington Sea Grant, 2015). To date, though, the indirect effects of water chemistry changes on the accumulation of trace metals in shellfish—a critical intersection of pollution and climate change— has been overlooked.

Changes in seawater pH, temperature, and DO can affect the solubility and speciation of metals, which in turn can affect their bioavailability and their impact on cellular processes of marine organisms (F. Millero, 2001; F. J. Millero et al., 2009; Smith et al., 2015). Aquatic chemistry models have demonstrated that the speciation of metals that are strongly hydrolyzed in seawater (including Al^{3+}, Cr^{3+}, Fe^{3+}) and those dominated by carbonate complexation (including Cu cations) appear to be more heavily influenced by changes in temperature and pH. In contrast, metals that are weakly complexed in seawater (including Mn^{2+}, Fe^{2+}, Co^{2+}, Ni^{2+}, and Zn^{2+}), and

those dominated by chloride complexation (including Cu^{+}, Cd^{2+}) appear less influenced by temperature and pH changes (Byrne et al., 1988). Smith et al. (2015) used a biotic ligand model to predict the toxicity of various metals based on chemical speciation. To date, however, there is limited direct observational data on many of these chemical speciation models, adding a degree of uncertainty to the results they predict and increasing the need for more direct, field-based studies, especially in biological contexts (Byrne et al., 1988). Further, chemical speciation alone cannot always be used to predict metal uptake in organisms, because uptake can vary with species, life stage, metal biochemistry, and CO_2 levels in the water (Ivanina & Sokolova, 2015). These limitations emphasize the importance of collecting empirical data in furthering our understanding of how trace metal accumulation will vary in space and time as temperature and pCO_2 increase due to anthropogenic effects.

Our study uses field experiments to better understand how the trace metal accumulation of shellfish in Puget Sound, Washington, USA will be altered in a changing climate. The Puget Sound region has over 4.8 million inhabitants (*United States Census Bureau*, 2020) and is seeing the effects of anthropogenic climate change earlier than many other regions of the global ocean. Waters in Puget Sound already have naturally low pH from upwelling of deep seawater rich in CO_2 (Feely et al., 2010, 2012), which in conjunction with anthropogenic CO_2 inputs makes the water in this region especially corrosive for shellfish and other calcifiers. In addition, areas of Puget Sound are already seasonally hypoxic, which will only worsen with increased anthropogenic climate change and eutrophication (Keister & Tuttle, 2013). Shellfish aquaculture is a very important industry in this region; Washington state is the largest producer of farmed clams, oysters, and mussels in the United States, and the economic contribution of the industry in 2011 was estimated at $270 million (Washington Sea Grant, 2015). Oyster farmers on the west

coast have already felt the effects of high CO_2 through production failures in oyster aquaculture in the early 2000s (Mabardy et al., 2015).

In addition to their economic value, shellfish such as bivalves are commonly used to monitor and determine toxicity and pollution in coastal areas. In the Mediterranean Sea and the Bohai Sea, studies have found that metal concentrations in mollusks vary with site, and concentrations are correlated with proximity to highly populated areas and industries such as zinc, gold smelting, and paper mills (Fowler & Oregioni, 1976; Y. Wang et al., 2005). In addition to spatial variation in accumulation, studies in Spain, Scotland, and Tasmania have found that bivalves accumulate higher levels of metals than other phyla (Eustace, 1974; Olmedo et al., 2013; Topping, 1972). There are also differences in accumulation between shellfish species: off the coast of China, oysters accumulated metals such as copper, zinc, and cadmium more readily than mussels (W. X. Wang et al., 2018). In Brazil, oysters, as rapid filterers, have been found to be a useful metric for monitoring trace metal pollution levels in estuarine sediments at sites with varying proximity to human impact (Wanick et al., 2012).

Few studies have been conducted on accumulation of specific trace metals in shellfish under ocean acidification scenarios. Short-term hypercapnia (excessive CO_2 in bloodstream) in clams increased copper uptake but suppressed cadmium uptake in mantle tissue (Ivanina et al., 2013). In another study, low pH (pH~ 7.8 and 7.4, compared to control pH~ 8.1) resulted in higher cadmium concentrations after a 30-day experiment on two species of clams and one species of mussel (Shi et al., 2016). Interestingly, Millero et al. (2009) noted that the speciation of cadmium should not change considerably with shifts in pH, perhaps indicating that differences in cadmium accumulation seen in experiments were not necessarily due to speciation changes.

These inconsistent results underscore the need for further studies on trace metal accumulation under ecologically relevant conditions.

To best prepare for the effects of future climate change and coastal population growth, we require a better understanding of how environmental changes will influence the availability of trace metals and how this may affect marine organisms and the humans who rely on them as a food source. Some metals (e.g. iron, copper, zinc, and manganese), are necessary for biological processes, but can be toxic at higher concentrations (Chan & Wang, 2018; F. J. Millero et al., 2009; Olmedo et al., 2013; Sivaperumal et al., 2007). Other metals (e.g. cadmium, mercury, and lead) are toxic even at low levels (Sivaperumal et al., 2007). Detrimental metal accumulation in shellfish can result in oxidative stress, affecting lipids, proteins, and DNA, which in turn impact growth and reproduction and can cause pathological conditions (Chan & Wang, 2018; W. X. Wang et al., 2018).

In Puget Sound, previous research found that heavy metals such as lead, arsenic, and cadmium had the highest concentrations in urban bays such as Commencement Bay near Tacoma and Elliott Bay near Seattle (Long, 1982). In Elliott Bay, particulate copper and zinc were distributed throughout the bay, while dissolved copper and zinc levels were associated with shoreline anthropogenic sources. One study that focused on effluent from Seattle wastewater treatments found that the effluent did not significantly increase the water and biota concentrations of nickel, copper, zinc, and cadmium (Schell & Nevissi, 1977). Sediment cores have revealed that efforts to mitigate point sources of metal pollutants have been relatively effective (for example the closing of a metal smelter in Tacoma, WA decreased arsenic pollution), but as the population around Puget Sound grows, non-point sources of pollutants, which are harder to track, will become more important to consider (Brandenberger et al., 2008).

This collection of research leaves unanswered questions about the current condition of trace metal accumulation in Puget Sound particularly as the effects of climate change intensify. Areas of coastal upwelling and oxygen minimum zones—characteristics of the Puget Sound region—will be informative areas in which to learn how future climate change will impact metal speciation and complexation (F. J. Millero et al., 2009).

This project aimed to determine if concentrations of trace metals in the tissue of oysters (*Ostrea lurida*) and mussels (*Mytilus galloprovincialis*) vary with site and associated environmental variables across Puget Sound. We hypothesized that we would see differences in trace metal accumulation between species and sites, and that relative similarities between sites may be linked to the presence of similar water chemistry properties between sites. We also hypothesized that variability in pH, dissolved oxygen, and temperature at each site would have different impacts on metal accumulation, and these effects would be unique for each metal.

Materials and Methods

Study Sites and oceanographic data collection

Hatchery raised shellfish were used for the experiment. Approximately one-year old Olympia oysters (*Ostrea lurida*) were acquired from Puget Sound Restoration Fund (average length 17.51 mm ± 2.41 mm) and one-year old Mediterranean mussels (*Mytilus galloprovincialis*) were acquired from Taylor Shellfish Farms (average length 28.17 mm ± 4.01 mm). Shellfish were deployed at three sites in mesh bags within cages for one year (Dabob Bay: deployed 7/13/2018, midpoint collection 1/15/2019, final collection 7/11/2019; Carr Inlet: deployed 7/12/2019, midpoint collection 1/8/2019, final collection 7/18/2019; Point Wells: deployed 7/13/2019, midpoint collection 1/23/2019, final collection 7/23/2019). At Dabob Bay (47.803° N, 122.803°

W) and Point Wells (47.761° N, 122.397° W), shellfish cages were hung at 5 m depth (DB5 and PW5), and at Carr Inlet (47.28° N, 122.728° W), shellfish cages were hung at both 5 m and 20 m depths (CI5 and CI20) (Figure 1A). The deployment sites were located at three ORCA (Oceanic Remote Chemical Analyzer) buoys, operated by the University of Washington Applied Physics Laboratory (APL), which allowed environmental data to be continuously collected for each site at the appropriate depths (Figure 1B). Dissolved oxygen, temperature, salinity, pH, and chlorophyll data was collected every 6 hours throughout the water column and made available online through the Northwest Association of Networked Ocean Observing Systems (NANOOS). When sensors malfunctioned during the study, data from the Live Ocean Model were used instead to acquire a continuous profile of conditions (MacCready et al., 2020) at the cage-specific depths.

Trace metal analysis

Shellfish were dissected with ceramic knives to remove tissue from shells. Each individual was bagged, flash frozen, and kept at -80 °C until future analysis. For the field experiment, ten oysters and ten mussels were preserved from each cage at each of the two time points (160 shellfish total). When analysis began, each specimen was transferred to a 50 mL Environmental Express digestion tube which was previously acid leached and rinsed several times in 18 MΩ water to eliminate the possibility of trace metal contamination. Samples were dried in a freeze dryer at approximately -90 °C and 60-80 mtor for ~ 48 hours, at which point dry weight was taken.

Shellfish samples were digested in acid and hydrogen peroxide to break down organic matter into liquid samples that could be processed with the ICP-MS (Inductively Coupled

Plasma Mass Spectrometer). Samples were randomly sorted into 10 groups of 16 tubes (five groups for the January field samples and five groups from the July field samples) for acid digestions. Acid digestion was adapted from two established methods (Ashoka et al., 2009; *Method 3050B Acid Digestion of Sediments, Sludges, and Soils*, 1996). Samples were heated by a graphite hot block at ~ 95 °C in 10 mL of 1:1 HNO_3:H_2O, and three aliquots of 2 mL HNO_3 (Fisher Scientific, trace metal grade) were added 30 minutes apart. A final aliquot of 1 mL H_2O_2 (Fisher Scientific, ACS certified) was added. Samples were then kept on the hot block until liquid had evaporated to 10 - 12 mL, at which point the samples were allowed to cool, and the tubes filled to 50 mL with 18 MΩ water. The samples were then diluted 10x into 10 mL sample tubes and were analyzed using an iCAP RQ ICP-MS at the University of Washington Trace Lab. Calibration curves containing 10 ppt, 100 ppt, 1 ppb, 10 ppb, 50 ppb and 100 ppb of a multielement standard from High Purity Standards were analyzed along with the samples. For Mg, a final standard of 500 ppb was also used in the calibration curves. Four USGS metal standards (T-221, T-231, T-235, and T-239), analyzed in duplicate, were run as a secondary calibration verification. The analysis provided the concentrations of Mg, Al, Ca, Ti, Cr, Mn, Fe, Co, Ni, Cu, Zn, As, and Cd, in each sample. An internal standard solution containing Rh was added continuously to the sample stream during ICP-MS analysis to correct for instrument drift via an apparatus similar to a T-mixer.

Data reduction

Output from the ICP-MS was provided in counts per second. Sample values were corrected based on the signal of the internal standard (Rh) and values from calibration blanks and digest blanks were subtracted from sample values. Then sample metal concentrations were determined

using the slope of the calibration curve and values for metal concentration were normalized to dry weight (mmol metal/g dry tissue). For metals that had ICP-MS data collected for multiple isotopes, the isotope with the better recoveries in the USGS standards were used in analysis. Ti showed poor or inconsistent recoveries for all isotopes and was excluded from the study.

Standards and quality control for trace metal analysis

To ensure consistency and allow for data validation, several quality control measures were used. During each of the 10 batches of acid digestions, the following eight standards were run along with the 16 samples: 2 digestion blanks, where the same additions of HNO_3 and H_2O_2 were performed in the hot block, but no tissue was included; 1 spiked digestion blank, which had 2 ppb of trace metal standard added to the empty tube immediately before digestion; 2 samples of DOLT-5 dogfish liver certified reference material for trace metals and other constituents from NRCC (National Research Council Canada) that also underwent acid digestion; 2 mussel standards, which were freeze dried and blended together to form a uniform powder which was distributed into 2 samples in each of the digestions used as a consistency standard; and 1 spiked mussel standard, which went through the same process but was spiked with 2 ppb of trace metals after freeze-drying but before digestion, consistent with other studies using similar methodology (Schmidt et al., 2013; Waidmann et al., 1994; Weldegebriel et al., 2012).

Seawater sample analysis

Water samples from each study site (5 m at Dabob Bay and Point Wells, and 5 m and 20 m for Carr Inlet) were collected in July 2018 and January 2019. Half of the seawater samples were filtered in an all-plastic filter apparatus using 0.2 μm Millipore filters that had been previously

acid leached. All seawater samples were then acidified to a pH less than 2 using ultra-pure HCl (Optima). Acidification of filtered samples preserves dissolved metals in solution by limiting precipitation and loss of samples to the container sidewalls, while acidification of unfiltered samples preserves the total metals in particulate and dissolved matter. Trace metals in these seawater samples were then separated from matrix ions like Na+ and Cl- using a seaFAST automated preconcentration system (ESI). The concentrated metal samples and processed calibration standards were then analyzed using an Element 2 High-Resolution ICP-MS at the University of Washington Trace Lab. For quality control purposes an analytical duplicate and matrix spike were also processed every ten samples on the seaFAST and then analyzed on the Element. Separate internal standards added prior to preconcentration and just prior to ICP-MS analysis were used to account for any differences in column recovery or ICP-MS stability during analysis. This analysis provided data for six elements in seawater: Fe, Co, Ni, Cu, Zn, and Cd.

Data analysis

All statistical analyses were conducted in R version 4.0.1.

Four samples from the July field collection were removed from the data set due to spills or overflows during the tissue digestion process. Although none of these samples were multivariate outliers, the possibility of lost sample during preparation was sufficient reason to remove them from both multivariate and univariate analyses.

To assess how the levels of individual metals in oyster and mussel tissue related to the metal concentrations in the associated seawater samples (filtered and unfiltered), we used simple linear regression ($metals\ in\ tissue \sim metals\ in\ seawater$) and used the associated adjusted R^2 and p-values to determine the significance of those relationships. Trace metals in the seawater

samples taken in July 2018 and January 2019 were compared to the tissue samples collected in July 2019 and January 2019 respectively. Although the July water and tissue sampling were one year apart due to difficulties in sample collection, they can still be used to approximate a relationship for the summer collection, as water conditions were similar between July 2018 and 2019 (Figure 2). A Bonferroni correction was applied to the original alpha value of 0.05 because the regression was being repeated six times for the six metals analyzed in seawater, so the corrected alpha level used was 0.0083 to reduce the likelihood of Type I error.

To test the hypothesis that the overall metal accumulation would differ between species and sampling time, the Adonis function was used to perform perMANOVA using a Euclidean distance matrix on the cube root transformed data (Oksanen et al., 2016). Accumulation of the 12 metals was compared between the two species and the two sampling times. An alpha level of 0.05 was chosen. Concentrations of the twelve metals individually were also compared between mussels and oysters using t-tests. A Bonferroni correction was again applied to account for 12 repeated t-tests, resulting in an alpha level of 0.004.

Principal component analysis (PCA) was performed on correlation matrices (to mitigate differences in scale between concentrations of different trace metals) of the oyster and mussel data to evaluate whether accumulation of certain metals was correlated and whether there were patterns of metal accumulation based on treatment or location (Husson et al., 2013; Kassambara & Mundt, 2017). The broken-stick model (Jackson, 1993) was used to determine if eigenvalues for each principal component were greater than would be expected by chance (the broken-stick expectation), and therefore considered to represent a statistically significant fraction of the original variation in the data. Eigenvector coefficients (variable loadings) were converted into Pearson product-moment correlations and these structure coefficients represented the correlation

between the original variables and each of the principal component scores. Biplots were created to visualize the location of samples and magnitude of variable importance in ordination space. We screened for multivariate outliers in the data sets for the PCA. Although several data points were more than three standard deviations from the mean of average distances (using Euclidean distance), we did not exclude these data points.

In addition to multivariate analyses on the metals in aggregate, we also wanted to assess the effects of location on individual metal levels. To determine which dependent variables (metals) were impacted by season at each site, one-way ANOVAs and Tukey Post-Hoc tests were run for each metal to compare differences in metal concentrations between the four locations at the two time points (treated as 8 distinct groups) for each of the two species (Huberty & Morris, 1992). While this produced results for every pair of season-specific locations, only those comparing the same location across seasons were included. Again, Bonferroni correction was applied because the ANOVA was being repeated twelve times for the twelve metals, so the corrected alpha level used was 0.004. To assess the difference in metal accumulation between sites *within* each sampling period, ANOVA and Tukey Post-Hoc Tests were again run, this time for the mussel and oyster data separately for January and July, again with an alpha value of 0.004 after a Bonferroni correction.

To assess how the size of the shellfish affected the accumulation of trace metals, we again performed regression, this time exponential ($metals\ in\ tissue \sim \ln(sample\ dry\ weight)$), and used adjusted R^2 and p-values from that regression to determine significance of these relationships. After a Bonferroni correction was used to account for repeated regressions for the twelve metals, the alpha level was 0.004.

Toxicity and consumption estimates

Various available metrics (adequate daily intake, average daily intake, upper level of intake per day, and maximum level permitted) were found for each of the analyzed metals (Table 1). There was no single regulating agency with metrics available for all metals, and no upper suggested limits on consumption exist for certain metals, which is why a variety of metrics were used. To estimate how intake of metals from consuming Puget Sound shellfish compared to these regulated levels, concentration of metals in wet shellfish tissue samples was estimated by multiplying the concentration of metal in dried samples by 0.22 (the average dry to wet weight ratio for the January samples). Using molecular weight and assuming 227 grams (0.5 lbs) daily consumption, the daily level of metals consumed was calculated for mussels and oysters from each site to be compared to regulated levels.

Results

Quality Control

As samples were processed in two batches using ICP-MS, controls were compared between those two runs. Supplementary Table 1 summarizes the recoveries for the four USGS standards from each run. Supplementary Table 2 summarizes the recoveries of the DOLT-5 standard reference material, replicates of which were included in each tissue digestion and were processed with the ICP-MS in the same batch as the corresponding digestion group. For the USGS standards, recoveries were lower for the July field data than for the January field data. The lower percent recovery may mean that some metals are underestimated in the July samples by 10s of percent, but this does not affect our conclusions when comparing metal accumulation at different sites or between different species (Supplementary Table 1). For the DOLT-5 standard reference material, the average recoveries for the ICP-MS runs for the January data and the July

data were within 10% of each other, with the exception of Mg, where the July data had a lower average recovery. All DOLT-5 samples showed a relatively lower percent recovery than the USGS standards, which means there is either some consistent loss in all samples (which would not change patterns we find for metals) or that the dry weight normalization in the dogfish is different in some way from our shellfish samples (Supplementary Table 2). This is not unheard of, as Ashoka et al. (2009) found upon comparing digestion methods that multiple digestion techniques show low recoveries for certain elements, and that no one method produced the best recoveries across all targeted elements for the different sample types they tested.

Environmental data

All three sites (at 5 m) showed lower pH values in the late fall and early winter months (Figure 2A). Carr Inlet 20 m consistently had the lowest pH throughout the year, with minimum pH values in late summer. Throughout the year Dabob Bay 5 m showed the highest pH values, Carr Inlet 5 m the second highest, and Point Wells 5 m the third highest. Dabob Bay showed the greatest fluctuations in pH, with a few peaks well below the minimum level at any other site. From July 2018 through July 2019, at Carr Inlet 20 m, the minimum and maximum pH were 7.62 and 8.12, for Carr Inlet 5 m: 7.67 and 8.29, for Point Wells 5 m: 7.73 and 8.30, and for Dabob Bay 5 m: 7.46 and 8.29 (Figure 2A).

Minimum temperatures at all sites were found in February and March, while maximum temperatures were found in July and August (Figure 2B). Dabob Bay 5 m showed the greatest variability in temperature especially during the summer months. For Dabob Bay 5 m, the minimum and maximum temperature were: 6.98 °C and 18.03 °C; for Point Wells 5 m: 7.99 °C and 14.98 °C; for Carr Inlet 5 m: 7.79 °C and 16.99 °C; and for Carr Inlet 20 m: 7.87 °C and

13.87 °C (Figure 2B). For dissolved oxygen, the minimum and maximum values for Dabob Bay 5 m were 2.29 mg/L and 15.27 mg/L; for Point Wells 5 m were 4.35 mg/L and 13.52 mg/L; for Carr Inlet 5 m were 3.36 mg/L and 13.79 mg/L; and for Carr Inlet 20 m were 2.82 mg/L and 9.46 mg/L. Carr Inlet 20 m showed less variability compared to the 5 m sites. High variability in dissolved oxygen occurred from spring through fall at Carr Inlet 5 m, winter through mid-summer for Dabob Bay 5 m, and just in late spring and summer for Point Wells 5 m (Figure 2C).

Trace metal seawater analysis

Comparing filtered to unfiltered samples should allow determination of what fraction of metals were dissolved in the seawater as opposed to in particulate matter. There is a trend across all six metals analyzed in seawater that the unfiltered water samples had higher concentrations of metals than the filtered samples. Fe, Co, Zn and Cu showed particularly large differences between filtered and unfiltered seawater, though lack of replicate water samples prevent statistical analyses. Largest seasonal changes for unfiltered metals were seen for Fe and Zn, with higher concentrations in January than July. Larger differences in trace metals abundance were found between seasons than between sites. Notable exceptions include lower levels of Zn at Carr Inlet 20 m in January and higher levels of Fe and Co at Carr Inlet 5 m in January (Figure 3).

Trace metal tissue analysis

For oysters, no relationships were found significant in the regressions comparing tissue metal concentrations to metals in filtered water (Figure 4). For unfiltered seawater samples, only Fe had a significant relationship between oyster tissue and seawater concentrations in July ($R^2 = 0.156$, $p = 0.0082$). In January, the only significant relationship showed the

concentration of Zn in oyster tissue actually decreased as concentrations of Zn in unfiltered seawater increased ($R^2 = 0.319$, $p = 8.79 \times 10^{-5}$) (Figure 5).

For mussels, no metals had a significant relationship between tissue and filtered water for the January data. For the July filtered water data, two metals had significant relationships between the tissue and unfiltered water, Fe ($R^2 = 0.201$, $p = 0.003$) and Co ($R^2 = 0.441$, $p = 3.28 \times 10^{-6}$) (Figure 6). For the unfiltered data in January, Fe ($R^2 = 0.251$, $p < 0.001$), Co ($R^2 = 0.566$, $p = 1.33 * 10^{-8}$), and Zn ($R^2 = 0.271$, $p = 0.0003$) all showed significant relationships between tissue and seawater concentrations in January, but the relationships were negative, not positive. For July, Cd ($R^2 = 0.226$, $p = 0.002$) had a significant relationship between tissue concentration and seawater concentration (Figure 7).

There was a significant difference in metal concentrations found when comparing the two species when looking across both sampling periods (perMANOVA, $p = 0.0001$ with 10,000 permutations). Comparing each individual metal between the two species, oysters had higher concentrations than mussels of Zn and Cu in both sampling periods ($p < 0.0001$ for all), and in July, oysters had a higher concentration of Fe than mussels ($p < 0.0001$), while mussels in July had a higher concentration of Mg than oysters ($p = 0.003$). Notably, the average concentration of Zn and Cu in oysters were 19.4 and 25.2 times higher in oysters than in mussels respectively (Supplementary Table 3).

Oysters had higher variation in metal accumulation between sites in January than in July. In January, Carr Inlet 20 m most frequently had the highest average levels of metals, with Point Wells 5 m frequently having the second highest levels of metals. In July, almost no significant differences in metal accumulation were found between sites. Oysters from Carr Inlet 20 m

showed significant seasonal changes for the most metals, with higher levels found in January than July (Figure 8).

In mussels, trace metal concentrations were generally higher in January than in July. Carr Inlet 20 m generally had the highest concentrations of metals, with Point Wells 5 m having the second highest concentrations. One notable exception was the highest average concentrations of Cd in both January and July at Dabob Bay 5 m. Mussel bioaccumulation of Al, Fe and Cr had lower variability in July than in January (Figure 9).

Smaller shellfish generally had higher concentrations of metals (Figures 10 and 11). Metal concentration decreased significantly with increasing oyster size for eight of the metals analyzed using an exponential regression: Mg ($R^2 = 0.14$, $p = 0.0004$), Al ($R^2 = 0.14$, $p = 0.0004$), Cr ($R^2 = 0.13$, $p = 0.0007$), Mn ($R^2 = 0.37$, $p < 0.0001$), Fe ($R^2 = 0.25$, $p < 0.0001$), Cu ($R^2 = 0.44$, $p < 0.0001$), Zn ($R^2 = 0.41$, $p < 0.0001$), and Cd ($R^2 = 0.38$, $p < 0.0001$) (Figure 10).

For mussels, the negative relationship between size and metal concentration was significant for every metal analyzed except Cd: Mg ($R^2 = 0.26$, $p < 0.0001$), Al ($R^2 = 0.43$, $p < 0.0001$), Ca ($R^2 = 0.13$, $p = 0.0006$), Cr ($R^2 = 0.57$, $p < 0.0001$), Mn ($R^2 = 0.63$, $p < 0.0001$), Fe ($R^2 = 0.44$, $p < 0.0001$), Co ($R^2 = 0.36$, $p < 0.0001$), Ni ($R^2 = 0.56$, $p < 0.0001$), Cu ($R^2 = 0.48$, $p < 0.0001$), Zn ($R^2 = 0.36$, $p < 0.0001$), As ($R^2 = 0.31$, $p < 0.0001$) (Figure 11).

Principal component analysis for oysters revealed that principal components 1 and 2 explained 58.3% and 12.9% of the variance for January sampling and explained 39.9% and 19% of the total variance for July sampling (Figure 12). The first principal component from the January sampling data, and the first two principal components from the July sampling data, explained a higher percent of the variance than would be expected using the Broken Stick model. The PCA showed that Carr Inlet 20 m site had the largest variability in metal concentration

during both sampling times (January and July). Carr Inlet 5 m, in contrast, had considerably smaller variability in sample concentration at the two time points. The variability in metal concentrations relative to other sites increased between January and July for Dabob Bay 5 m but decreased for Point Wells 5 m. All metals were more closely correlated in January, while in July they diverged more into two groups, with Ni, Cr, and Co correlated with each other but not with the rest of the 12 metals (Figure 12).

Principal component analysis for mussels revealed that principal components 1 and 2 explained 67.5% and 12% of the variance for January sampling and explained 53.6% and 15.4% of the total variance for July sampling. Only the first principal component from both sampling periods explained a higher percent of the variance than would be expected using the Broken Stick model. The PCA showed that Carr Inlet 20 m was associated with overall higher metal concentrations during both the January and July sampling and had larger variability in metal concentrations. The most evident change on these plots between seasons is with Cd, which is more correlated with the other metals in July than in January. Based on location in multivariate space, Dabob Bay 5 m and Point Wells 5 m were more influenced by higher Cd during the January sampling. Ca was not correlated with other metals in either time period (Figure 13).

Average values of metals that would be consumed if a person ate 0.5 lbs of Puget Sound mussels or oysters per day were sometimes above “average daily intake” or “adequate intake” levels (as defined for adults in the USA and Australia/New Zealand respectively), but these metals (Cr, Mn, Al, Co, Ni) do not have regulated maximum values for consumption. This occurred most often in Carr Inlet 20 m samples (Table 2) (Agency for Toxic Substances and Disease Registry (ATSDR), 2005, 2008; Capra, 2006; Faroon et al., 2004).

For those metals where there are upper recommended daily intake levels (Mg, Ca, Fe, Cu, and Zn), only copper (at Carr Inlet 20 m) and zinc (at all sites) were over the recommended level for oysters, and no metals were over the recommended level for mussels (upper recommended daily intake in Australia/New Zealand defined as the "highest average daily nutrient intake level likely to pose no adverse health effects") (Capra, 2006). Codes Alimentarius, the international commission that sets food guidelines, only provides maximum allowable limits for *inorganic* arsenic, but the levels we measured were organic *and* inorganic arsenic together, so a direct comparison cannot be made (Codex Alimentarius Commission, 2015). Cadmium also has a maximum level permitted in mollusks by Codex Alimentarius, and in some cases the estimates from Puget Sound shellfish were over these levels (Table 2) (Codex Alimentarius Commission, 2015).

Discussion

This study used experimental data from the field to investigate how effects of temperature, pH, and DO are associated with the accumulation of trace metals in mussels and oysters from Puget Sound.

Spatial and seasonal variability in shellfish trace metal bioaccumulation

Our results provide evidence that (1) lower pH is associated with higher metal concentrations in shellfish, and (2) depth may have more impact than site on metal bioaccumulation in Puget Sound. The deepest location, Carr Inlet 20 m, showed the lowest pH and the highest bioaccumulation in both oysters and mussels. Low pH has been shown to increase the solubility of certain trace metals. For example, models indicate a pH shift from 8.1

to 7.4 could increase the water solubility of Fe(III) by 40%, which would make it more bioavailable to plankton (Brand, 1991; F. J. Millero et al., 2009), and in turn likely available to higher trophic levels. It is important to note that other variables may play a role in the shellfish physiological performance and bioaccumulation of trace metals. Carr Inlet 20 m also had lower light levels and lower and less variable dissolved oxygen levels, which may impact shellfish directly as well as indirectly through plankton abundance (Alma, n.d.in prep.).

Interestingly, Carr Inlet 20 m showed the largest seasonal differences in bioaccumulation. At this site we found seasonal changes in metal abundance in mussels and oysters (Mg, Al, Cr, Mn, and Fe for mussels, Mg, Ca, Mn, and Fe for oysters). Higher levels of metals in shellfish at Carr Inlet 20 m were found in January. This site had experienced its lowest pH levels in the months leading up to this sampling, potentially causing the higher metal bioaccumulation. However, we did not see this trend at shallow sites which also had lower pH leading up to the January sampling, suggesting that there are other physical and biological factors that also fluctuate seasonally that may impact the abundance of trace metals in our study.

In our study, the highest concentrations of cadmium in mussels were found at Dabob Bay (which on average had the highest pH but showed extreme drops in pH levels during winter), and at Carr Inlet 20 m in the July sampling (the site which overall had the lowest pH). The variability in results of previous laboratory studies (Ivanina et al., 2013; F. J. Millero et al., 2009; Shi et al., 2016) and our field study may be an indication that some unknown environmental factor—separate from aqueous speciation—is influencing the accumulation of cadmium in all these studies. In the field, Carr Inlet 20 m and Point Wells 5 m also had higher copper concentrations for mussels, and Carr Inlet 20 m had higher copper concentrations for oysters. These two sites are colder, have less variability in dissolved oxygen, and have slightly lower pH, and this lower

pH is consistent with increased copper uptake seen in other studies (Götze et al., 2014; Ivanina et al., 2013).

Multivariate analyses also revealed that most of the metals were positively correlated to each other—i.e. some samples have higher amounts of all the metals or few of all the metals, as opposed to some sites having more of one and less of another metal. Our evidence did not link warmer sites (which would have caused increased metabolism) to higher levels of metals in shellfish.

Trace metals in seawater

For both mussels and oysters, there were few significant positive correlations between the concentrations of trace metals in seawater and tissue samples (and some were even negative). This does not establish a clear relationship between water and tissue concentrations for either species or for any specific metal and does not explain the differences in metal accumulation in shellfish between sites. Previous studies did not find correlation between metal concentrations in *filtered* water and mussel tissue (Fowler & Oregioni, 1976). This may have been due to the ability of filter feeders to ingest metals that are suspended in particulate matter in the water, as particulate matter is not accounted for in filtered water samples (Fowler & Oregioni, 1976). We had expected to explain this discrepancy further by analyzing both *filtered* and *unfiltered* water samples, but also found little correlation between metal concentration in shellfish and seawater, indicating that including particulate matter in the analysis still did not account for how the shellfish are ingesting and processing trace metals. The field seawater samples did reveal generally higher concentrations in unfiltered samples, supporting the idea that more metals are available if shellfish ingest both the dissolved and particulate matter in the water. The ability of

shellfish to selectively feed—whether this results in a higher or lower intake of metals than through random feeding, could be responsible for the discrepancy (Purroy et al., 2018). This lack of correlation could also be confounded by the difference in sizes between shellfish at different sites.

Shellfish size and trace metal accumulation

We found that trace metal bioaccumulation was higher in shellfish of smaller size. Higher metal concentration in smaller shellfish could be due to a residual effect of a prior metal signal from the common pool the shellfish were sourced from. The shellfish that grew less after being deployed in the cages would have less tissue to "dilute" that original signal. Because we sampled tissue as opposed to shell, we would expect some turnover in metal concentration with time, so this seems unlikely, but is a possibility. This trend could also be due to localization of metals to specific regions of the shellfish body, if the relative contribution of these regions to total dry weight changes with age and size. For example, if metals accumulated more in internal organs as opposed to the lipids of the shellfish, then they could appear more concentrated in smaller shellfish when these organs make up more of the dry weight. Various other studies have focused on specific tissues within the shellfish such as the digestive gland of oysters or mantle cells of clams (Ivanina et al., 2013), and it has been noted that some metals tend to accumulate more in certain oyster tissues (W. X. Wang et al., 2018). Our study used the entire shellfish tissue to obtain a measurement of bioaccumulation per individual because the entire soft tissue of mussels and oysters is typically consumed. The inverse relationship between metal concentration and size could influence the values we obtained at Carr Inlet 20 m. The shellfish at that location showed higher metal concentrations and weighed less than shellfish from other sites.

Other studies have also noted, both incidentally and intentionally, relationships between shellfish size and metal accumulation. In *Mytilus* species, it was noted that cadmium concentrations were independent of size, while zinc, manganese, nickel, and iron all had higher concentrations in smaller mussels (Boyden, 1977). For oysters (*Ostrea spp.*), previous studies found that cadmium and zinc concentrations were independent of body size, but zinc concentrations were more variable in polluted environments. For copper, it was noted that particularly large individuals took longer to equilibrate to the local copper conditions (Boyden, 1977)—corresponding to the slower (relative to mussels) depuration rates of copper in oysters noted in other studies (Han et al., 1993).

Trace metal accumulation in oysters vs. mussels

In addition to differences based on shellfish size and site, our study found clear differences in the metal accumulation between the two species. The oysters in our study had significantly higher levels of copper and zinc (about 25.2 and 19.4 times higher respectively), which may in part be due to a faster turnover of copper in the mussel species (Han et al., 1993). A previous study focusing on the depuration of copper and zinc by bivalves in Taiwan moved from polluted to clean waters showed faster depuration rates of copper in blue mussels than green oysters (Han et al., 1993). In the Patuxent River Estuary in Maryland, another study found that eastern oysters accumulated varying amounts of copper depending on site, while mussels had more constant levels of copper throughout the estuary (Riedel et al., 1995). In our study, mussels and oysters experienced the same environments with common food sources, indicating that their species-specific responses to the environment contributed to their different bioaccumulation rates (Riedel et al., 1995). Previous studies have also shown evidence that

mussels have some capacity to metabolically regulate trace metal concentrations of zinc and copper (Davenport & Manley, 1978; Phillips & Yim, 1981; Scott & Major, 1972), a trait that oysters do not possess, resulting in the higher accumulation in oysters (Phillips & Yim, 1981). They also note that oysters and mussels have different pathways of trace-element incorporation. With iron, for example, oysters incorporate the metal into their shells while mussels incorporate more iron into the byssus (Phillips & Yim, 1981).

Multivariate trends we found between sites (most prominently the higher concentration of metals at Carr Inlet 20m) stayed relatively consistent for mussels between the January and July samplings, but for oysters, PCA reveals a different pattern in prevalence of metals at certain sites between the two sampling times. This may be related to different abilities to regulate trace metal concentrations or different depuration times (Davenport & Manley, 1978; Han et al., 1993; Phillips & Yim, 1981; Riedel et al., 1995; Scott & Major, 1972). Alternatively, these patterns could reflect biological differences between the species—as faster filterers, oysters may change their internal concentrations of certain elements more rapidly than mussels (W. X. Wang et al., 2018). These physiological differences between species are important and emphasize the need for species-specific studies to better understand the mechanisms involved in accumulation and regulation of trace metals and how these species can or should be used as pollution indicators (Phillips & Yim, 1981). In addition, this could provide a physiological explanation for some of the discrepancies between seawater and tissue concentrations of trace metals we found in this study.

Applications to aquaculture

The apparent trend in lower metals concentrations for larger shellfish is encouraging for the aquaculture industry, in that those mussels and oysters that are harvested and sold are generally of a larger size, and therefore would have lower concentration of metals by weight. Among the cages deployed at 5 m depths, the shellfish at Point Wells (Central Sound) had the highest concentrations of metals. This area of the central sound has less shellfish farming than the Dabob Bay site (Hood Canal), and the Carr Inlet site at 5 m (South Sound), which have more dense shellfish aquaculture. The higher metal concentrations found in shellfish located at the Carr Inlet 20 m site reveal a notable effect of depth, which is important information for shellfish farmers—although most shellfish are grown in the intertidal, some mussels in Puget Sound are grown hanging from lines on rafts and reach deeper levels. Metal accumulation may be more of a concern for those shellfish, but again, our findings may have been constrained by the smaller size (slower growth) of shellfish at that depth.

While this was not a toxicology study, and the intention was to compare shellfish metal concentrations between sites and species as opposed to comparing them to regulatory levels, we did estimate concentrations of metals in the wet shellfish tissue to see whether they were comparable to regulations for daily intake, and in certain cases, maximum allowable levels. The most notable of our findings are the much higher concentrations of copper and zinc in oysters, which were in some cases over recommended daily values if an adult were to eat 0.5 pounds of shellfish daily. Shellfish are known to have particularly high concentrations of copper: The National Institute of Health found that three ounces of cooked eastern oyster could result in over 500% of the listed adult Daily Value for copper (National Institute of Health, 2020). Codex Alimentarius, the international commission that sets food guidelines, does not consider all metals

to be contaminants. Copper, for example, is considered to have significance in terms of food quality, but not public health significance, so strict upper limits are not set (Codex Alimentarius Commission, 2015). Cadmium, however, is considered a contaminant by Codex, and cadmium pollution in Puget Sound shellfish has been studied, as levels over the Codex standard could be detrimental to the shellfish industry (Pacific Shellfish Institute, 2008). The commission set the limit as 1 ppm in molluscan shellfish in 2003, but later changed the limited to 2 ppm (Pacific Shellfish Institute, 2008). A study focused on Hood Canal oysters found that most shellfish were below this 2 ppm limit, but 15% exceeded it (Pacific Shellfish Institute, 2008). Our study had average levels over this 2 ppm limit at the Carr Inlet 5 m site for mussels and the Carr Inlet 20 m site for oysters—indicating higher levels in central sound than in Hood Canal.

The variation in metal concentrations between our sites indicates that water properties may have some impact on metal concentrations. The variability in trace metal accumulation we found in the field based on size, site, water properties, and depth all point to the necessity to continue testing trace metal accumulation at local levels, especially in regions with important aquaculture industries.

Acknowledgements

The authors would like to thank Miranda Roethler for her help with mapping, along with the other members of the Padilla-Gamiño lab at UW SAFS (Jeremy Axworthy, Corinne Klohmann, and Tanya Brown) for their support throughout analysis and writing. The authors would also like to thank Chris Archer and Robert Daniels for their assistance with SCUBA fieldwork; Jan Newton, John Mickett, and Ryan Newell for contributing to project planning, field deployments, and providing data from APL; Parker MacCready for providing data from the LiveOcean Model;

Gordon King for providing mussels from Taylor Shellfish; and Ryan Crim, Stuart Ryan, and Betsy Peabody for providing oysters from Puget Sound Restoration Fund.

Figures and Tables

Table 1. Regulations/recommendations for metal intake for adult humans for Cr, Mn, Al, Co, Ni, Mg, Ca, Fe, Cu, and Zn, and the maximum concentrations allowed in shellfish for As (inorganic) and Cd.

Metal	Metric available	Concentration	Regulation Source
Chromium	Adequate intake	**30 µg/day** (35 µg adult men, 25 µg adult women)	Australia/New Zealand (Capra, 2006)
Manganese	Adequate intake	**5.25 mg/day** (5.5mg/day adult men, 5mg/day adult women)	Australia/New Zealand (Capra, 2006)
Aluminum	Average daily intake	**7.7 mg/day** (0.10-0.12 mg Al/kg body weight/day for adults) assuming 70 kg adult	USA (Agency for Toxic Substances and Disease Registry (ATSDR), 2008)
Cobalt	Average daily intake	**11 µg/day** average	USA (Faroon et al., 2004)
Nickel	Average daily intake	**115.5 µg/day** (69-162 µg /day adult average)	USA (Agency for Toxic Substances and Disease Registry (ATSDR), 2005)
Magnesium	Upper level of daily intake	**350 mg/day** adults	Australia/New Zealand (Capra, 2006)
Calcium	Upper level of daily intake	**2,500 mg/day** adults	Australia/New Zealand (Capra, 2006)
Iron	Upper level of daily intake	**45 mg/day** adults	Australia/New Zealand (Capra, 2006)
Copper	Upper level of daily intake	**10 mg/day** adults	Australia/New Zealand (Capra, 2006)
Zinc	Upper level of daily intake	**40 mg/day** adults	Australia/New Zealand (Capra, 2006)
Arsenic	Maximum level in in edible fats and oils	**0.1 ppm (inorganic)** in edible fats and oils	Codex Alimentarius (Codex Alimentarius Commission, 2015)
Cadmium	Maximum level in molluscan shellfish	**2.0 ppm** in molluscan shellfish	Codex Alimentarius (Codex Alimentarius Commission, 2015)

Table 2. Average concentrations of metals found in mussels and oysters from each of the four sites. Levels in red are above the levels recommended by different regulatory agencies. There was no single regulating agency with metrics available for all metals, and no upper suggested limits on consumption exist for certain metals, which is why a variety of metrics were used. *For arsenic, the limits are on inorganic arsenic, known to be toxic, and are for edible fats and oils. The values in the shellfish in our experiment are total (organic and inorganic) arsenic.

Mussels					Oysters			
Carr Inlet 20 m	**Carr Inlet 5 m**	**Dabob Bay 5 m**	**Point Wells 5 m**	**Metal (Regulated value)**	**Carr Inlet 20 m**	**Carr Inlet 5 m**	**Dabob Bay 5 m**	**Point Wells 5 m**
Mean intake from mussels (if consume 227 g/day)					**Mean intake from oysters (if consume 227 g/day)**			
				Adequate intake (AUS/NZ)				
57.5 µg	17.8 µg	22.2 µg	35.4 µg	**Chromium** 30 µg/day	66.9 µg	18.9 µg	29.8 µg	44.6 µg
5.6 mg	1.3 mg	0.7 mg	2.1 mg	**Manganese 5.25 mg/day**	6.3 mg	2.6 mg	1.6 mg	3.3 mg
				Average daily intake (USA)				
20.9 mg	4.9 mg	4.5 mg	9.7 mg	**Aluminum 7.7 mg/day**	21.2 mg	15.0 mg	6.4 mg	13.3 mg
31.4 µg	11.8 µg	20.6 µg	30.1 µg	**Cobalt 11 µg/day**	22.1 µg	1.7 µg	13.0 µg	27.1 µg
128.5 µg	38.9 µg	54.7 µg	79.4 µg	**Nickel 115.5 µg/day**	148.3 µg	13.8 µg	53.0 µg	127.5µg
				Upper level of daily intake (AUS/NZ)				
214.9 mg	133.4 mg	153.4 mg	191.1 mg	**Magnesium 350 mg/day**	168.56 mg	139.8 mg	128.1 mg	129.9 mg
136.3 mg	11.4 mg	20.8 mg	39.1 mg	**Calcium 2,500 mg/day**	172.5 mg	86. 6mg	56.9 mg	93.7 mg
24.5 mg	7.3 mg	9.3 mg	16.0 mg	**Iron 45 mg/day**	26.2 mg	13.7 mg	16.3 mg	21.8 mg
0.4 mg	0.3 mg	0.3 mg	0.4 mg	**Copper 10 mg/day**	14.1 mg	5.7 mg	5.1 mg	7.9 mg
10.7 mg	6.7 mg	6.4 mg	6.5 mg	**Zinc 40 mg/day**	223.1 mg	126.9 mg	113.5 mg	124.8 mg
Mean concentration in mussels					**Mean concentration in oysters**			
				Maximum level (Codex Alimentarius)				
1.93ppm	1.37 ppm	1.52 ppm	1.86 ppm	**Arsenic 0.1 ppm***	1.84 ppm	1.81 ppm	1.56 ppm	1.61 ppm
1.27ppm	2.35 ppm	1.67 ppm	1.76 ppm	**Cadmium 1.0 ppm**	2.22 ppm	1.46 ppm	1.53 ppm	1.99 ppm

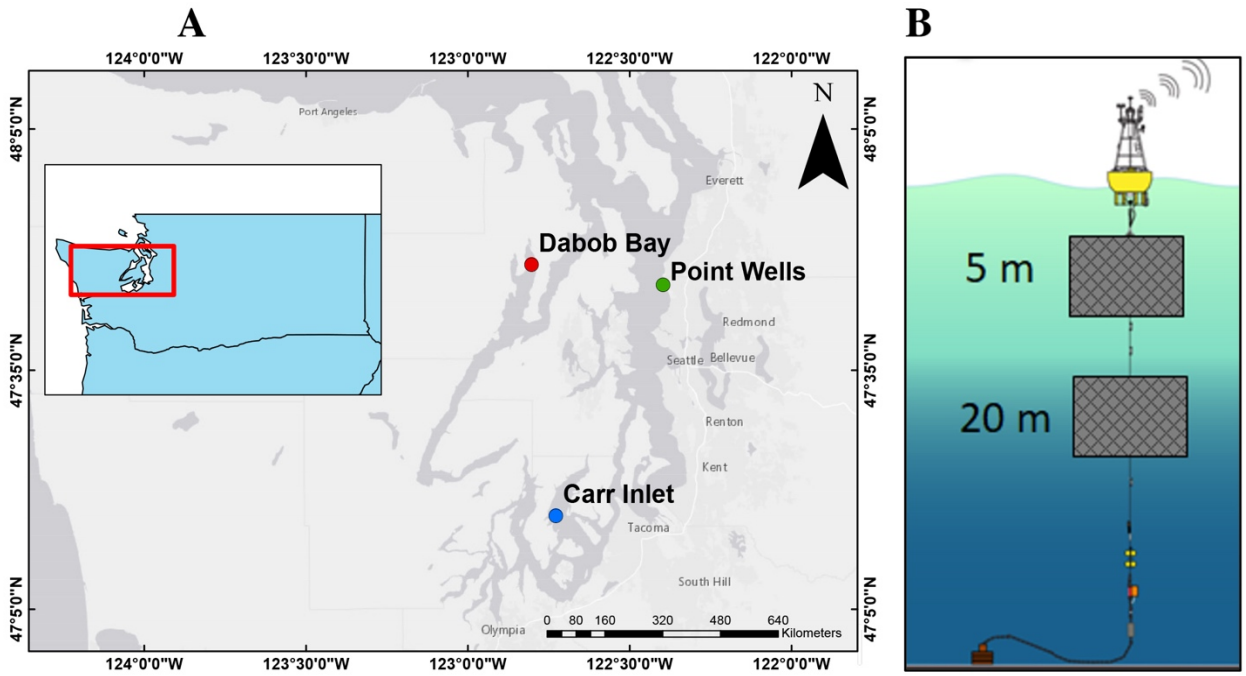

Figure 1. (A) Map of Puget Sound showing the locations of ORCA buoys where shellfish were deployed. Oysters and mussels were deployed at Dabob Bay (Hood Canal) at 5 m depth, Point Wells (central Puget Sound) at 5 m depth, and Carr Inlet (south Puget Sound) at both 5 m and 20 m depths. **(B)** A diagram of how shellfish were deployed below ORCA buoys in the field. Two locations had 5m cages, and the third location had a cage at both 5 m and 20 m depths.

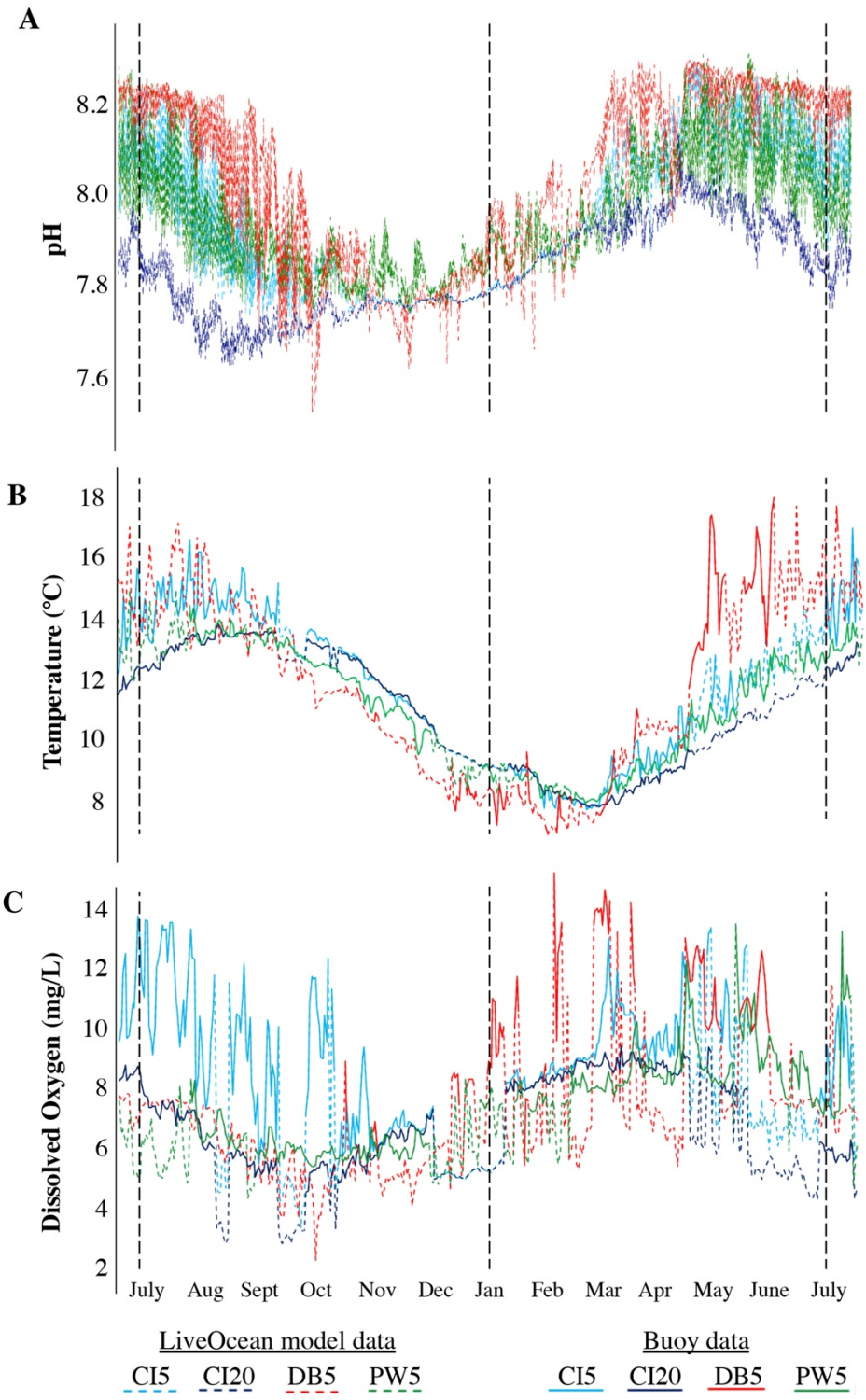

Figure 2. Environmental data at the four shellfish cage locations from July 2018– July 2019 for **(A)** pH calculated using TIC and Alkalinity from Live Ocean Model data**, (B)** temperature, and **(C)** dissolved oxygen. Dotted lines indicate data from the Live Ocean Model. Solid lines indicate

data from the ORCA buoys. Dotted vertical lines indicate approximately when the shellfish were deployed (July 2018), when the first shellfish samples were taken (January 2019), and when the final shellfish samples were taken (July 2019).

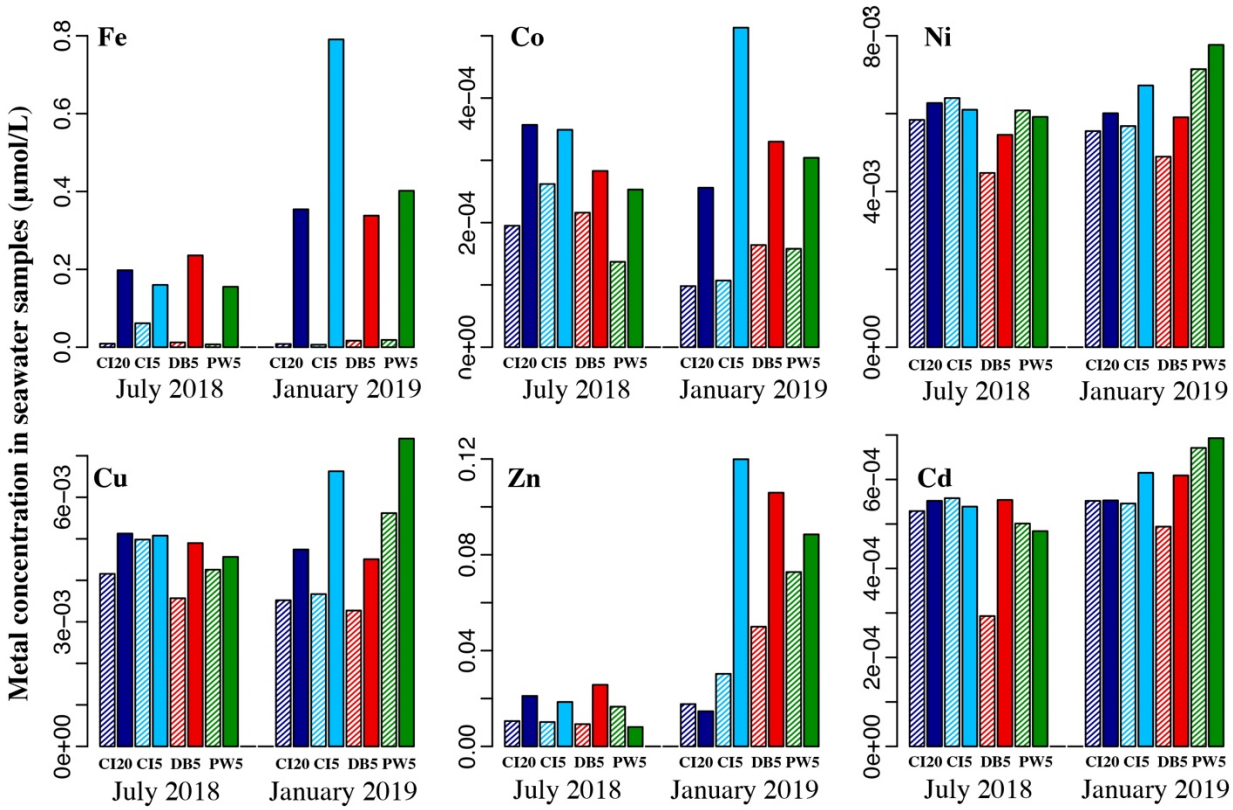

Figure 3. Trace metal analysis of seawater samples collected at the sites when the shellfish cages were deployed (July 2018), and six months after deployment began (January 2019). For each pair, the first bar (striped) is the filtered seawater sample, and the second bar (solid) is the unfiltered seawater sample—comparing the two should allow determination of what metals were dissolved in the seawater as opposed to in particulate matter. Dark blue = Carr Inlet 20 m, light blue = Carr Inlet 5 m, green = Point Wells 5 m, and red = Dabob Bay 5 m.

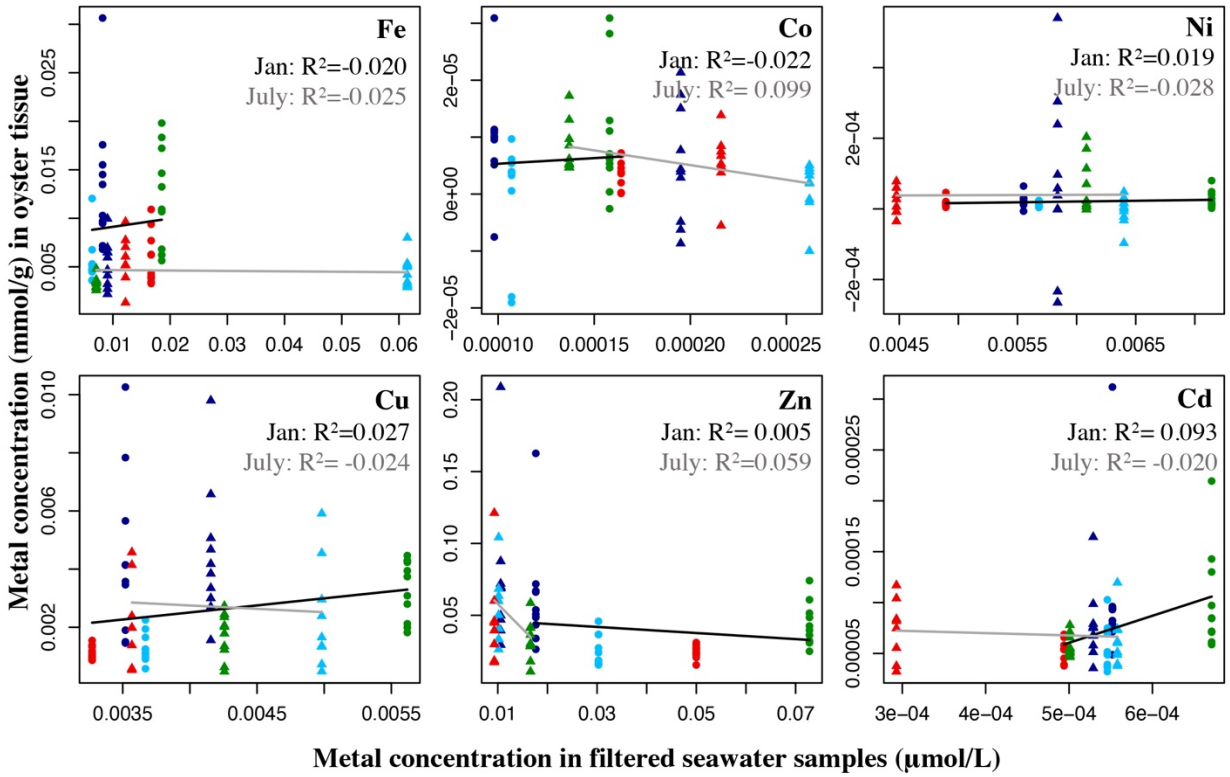

Figure 4. Metal concentration (µmol/L) in *filtered* seawater samples from July 2018 and Jan 2019 plotted against the metal concentration the oyster tissue samples (mmol/g) from the four locations collected in July 2019 and Jan 2019. Circles represent the January samples; triangles represent the July samples. Dark blue = Carr Inlet 20 m, light blue = Carr Inlet 5 m, green = Point Wells 5 m, and red = Dabob Bay 5 m. Linear regression was used to assess the relationship between the two variables for Jan (black line) and July (grey line) separately (* indicates the adjusted R^2 value is significant, $p < 0.0083$).

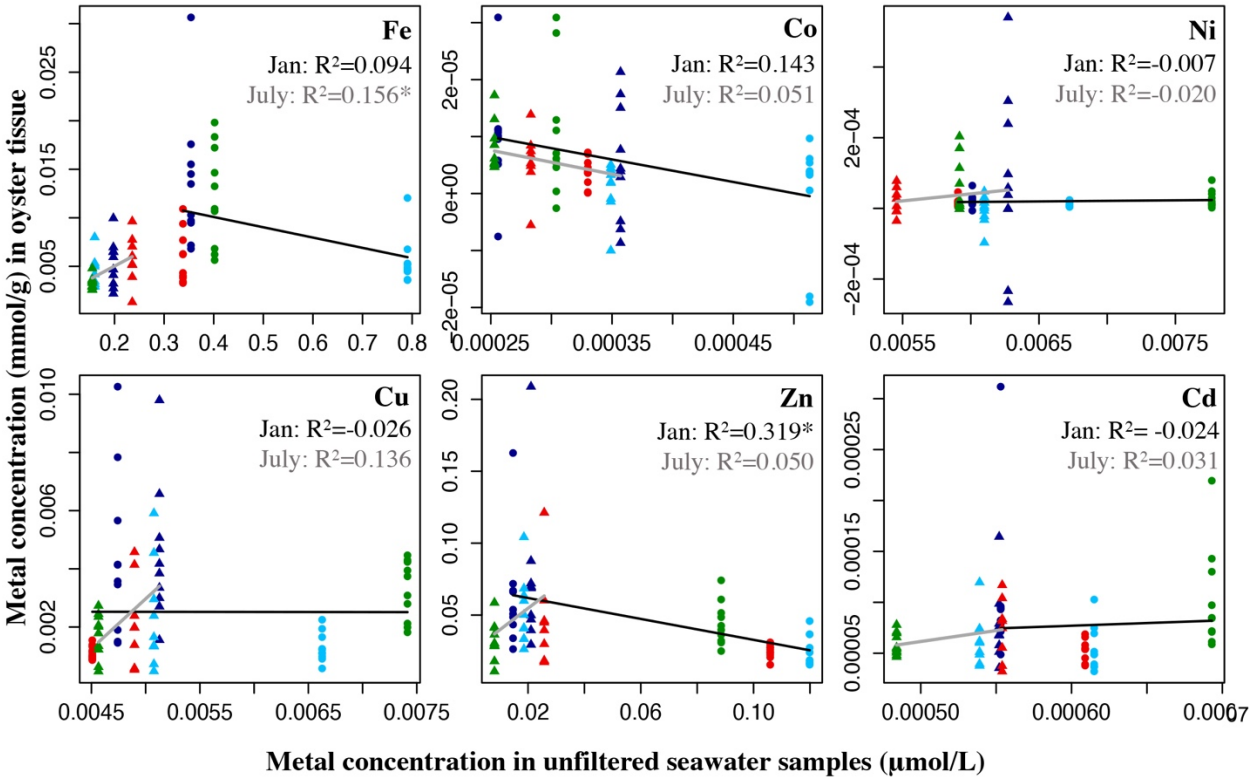

Figure 5. Metal concentration (µmol/L) in *unfiltered* seawater samples from July 2018 and Jan 2019 plotted against the metal concentration the oyster tissue samples (mmol/g) from the four locations collected in July 2019 and Jan 2019. Circles represent the January samples; triangles represent the July samples. Dark blue = Carr Inlet 20 m, light blue = Carr Inlet 5 m, green = Point Wells 5 m, and red = Dabob Bay 5 m. Linear regression was used to assess the relationship between the two variables for Jan (black line) and July (grey line) separately (* indicates the adjusted R^2 value is significant, $p < 0.0083$).

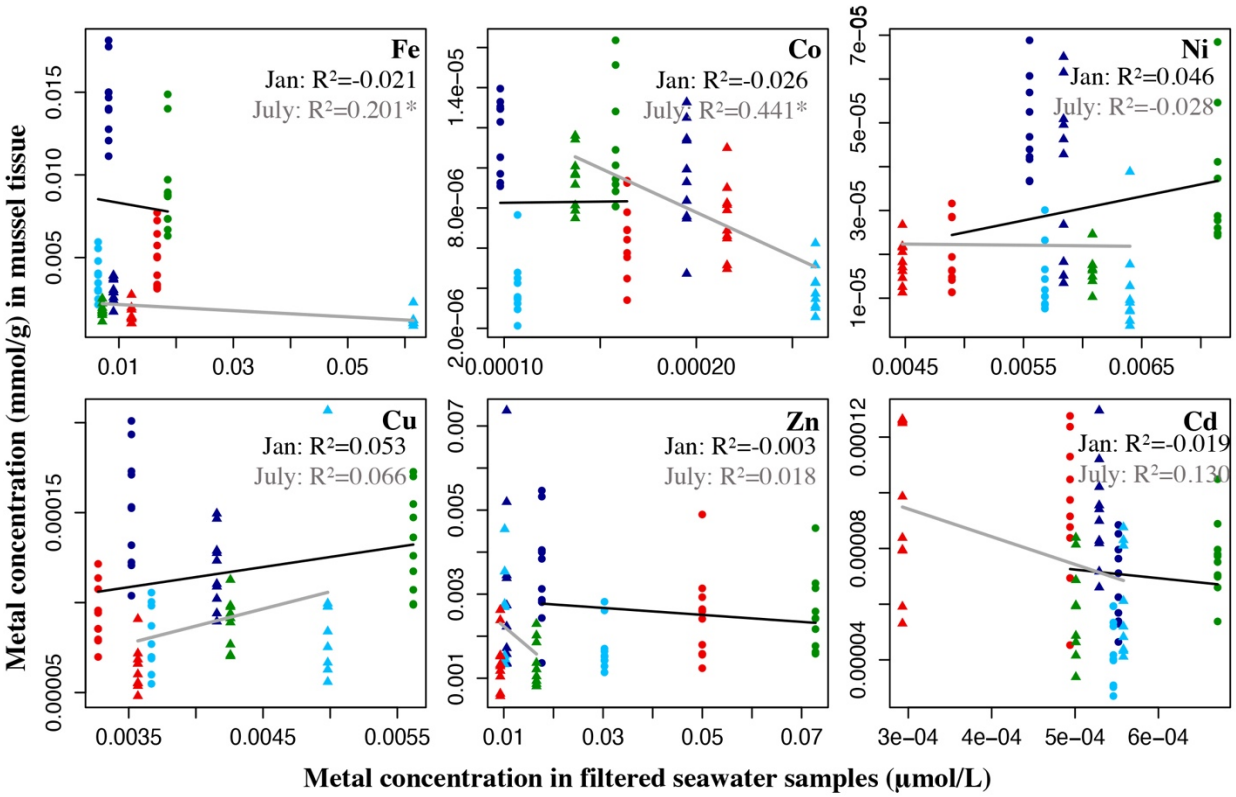

Figure 6. Metal concentration (µmol/L) in *filtered* seawater samples from July 2018 and Jan 2019 plotted against the metal concentration of mussel tissue samples (mmol/g) from the four locations collected in July 2019 and Jan 2019. Circles represent the January samples; triangles represent the July samples. Dark blue = Carr Inlet 20 m, light blue = Carr Inlet 5 m, green = Point Wells 5 m, and red = Dabob Bay 5 m. Linear regression was used to assess the relationship between the two variables for January (black line) and July (grey line) separately (* indicates adjusted the R^2 value is significant, $p < 0.0083$).

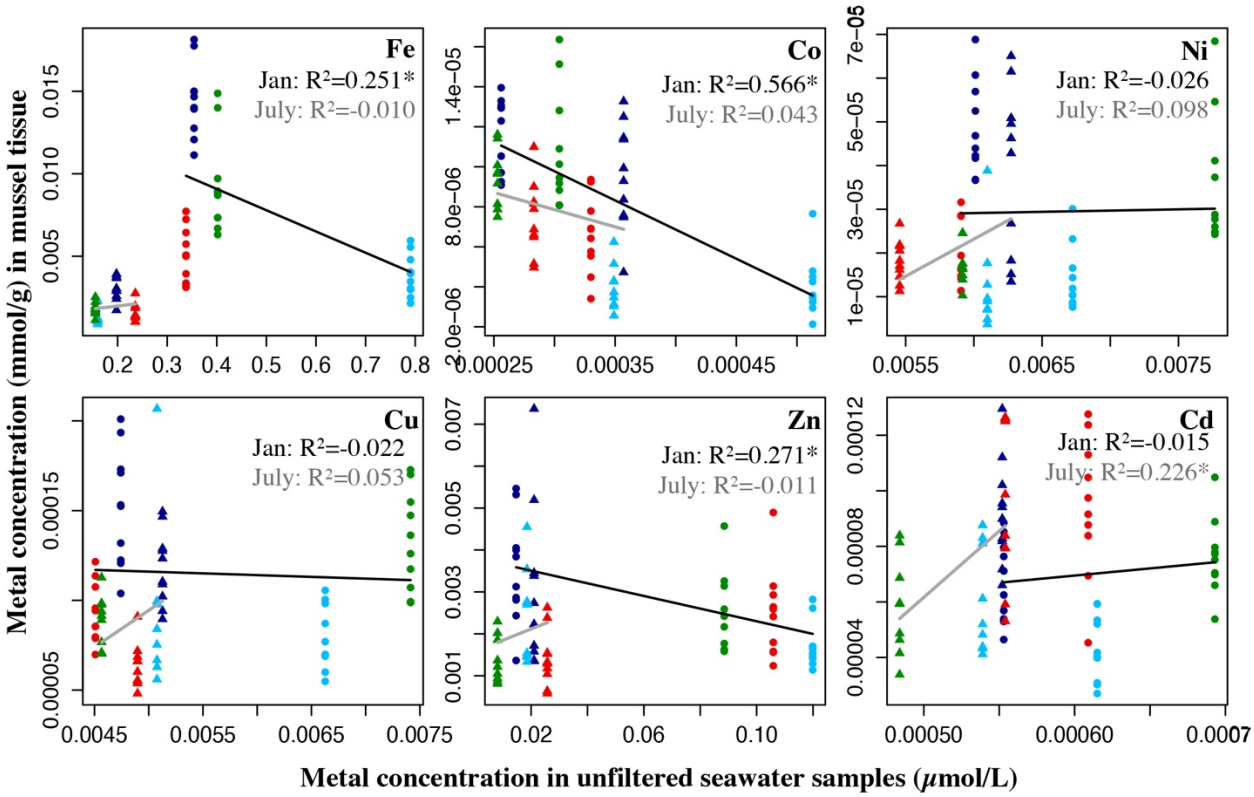

Figure 7. Metal concentration (µmol/L) in *unfiltered* seawater samples from July 2018 and Jan 2019 plotted against the metal concentration of mussel tissue samples (mmol/g) from the four locations collected in July 2019 and Jan 2019. Circles represent the January samples; triangles represent the July samples. Dark blue = Carr Inlet 20 m, light blue = Carr Inlet 5 m, green = Point Wells 5 m, and red = Dabob Bay 5 m. Linear regression was used to assess the relationship between the two variables for January (black line) and July (grey line) separately (* indicates the adjusted R^2 value is significant, $p < 0.0083$).

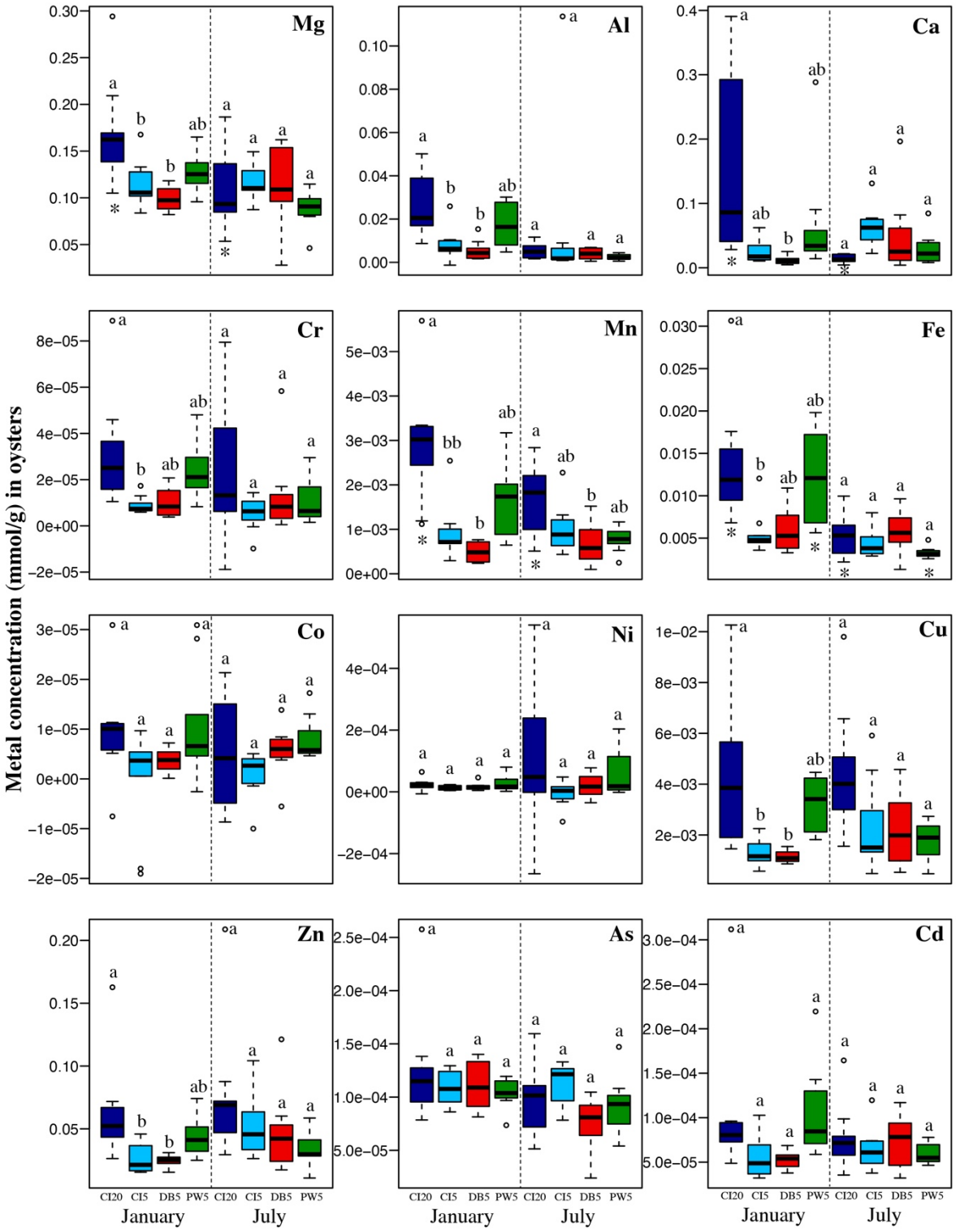

Figure 8. Concentrations in mmol/g for each of the twelve analyzed trace metals in oysters held for six months (January) and one year (July) in four locations: Carr Inlet 20 m (dark blue), Carr

Inlet 5 m (light blue), Dabob Bay 5 m (red), and Point Wells 5 m (green). ANOVAs and Tukey Post Hoc Tests with a Bonferroni correction were used to see if there were significant differences ($p < 0.004$) *between location for January and July separately*, and differences are indicated by letter above each boxplot. Separate ANOVA and Tukey Post Hoc Tests were also completed to compare across time periods. Asterisks below the box plot indicate a significant difference ($p < 0.004$) in the concentration of a metal at one site *between January and July*.

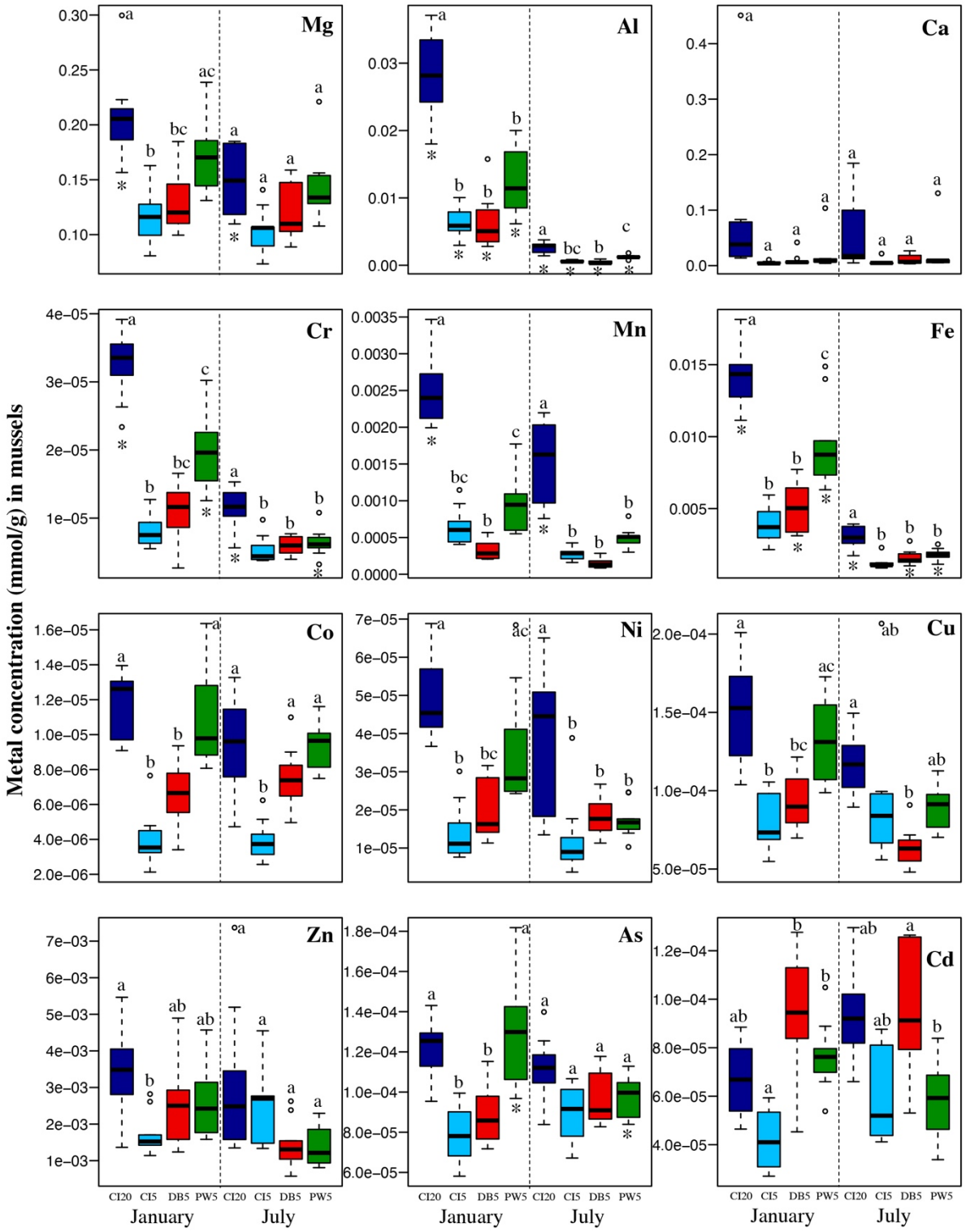

Figure 9. Concentrations in mmol/g for each of the twelve analyzed trace metals in mussels held for six months (January) and one year (July) in four locations: Carr Inlet 20 m (dark blue), Carr

Inlet 5 m (light blue), Dabob Bay 5 m (red), and Point Wells 5 m (green). ANOVAs and Tukey Post Hoc Tests with a Bonferroni correction were used to see if there were significant differences ($p < 0.004$) *between location for January and July separately*, and differences are indicated by letter above each boxplot. Separate ANOVA and Tukey Post Hoc Tests were also completed to compare across time periods. Asterisks below the box plot indicate a significant difference ($p < 0.004$) in the concentration of a metal at one site *between January and July*.

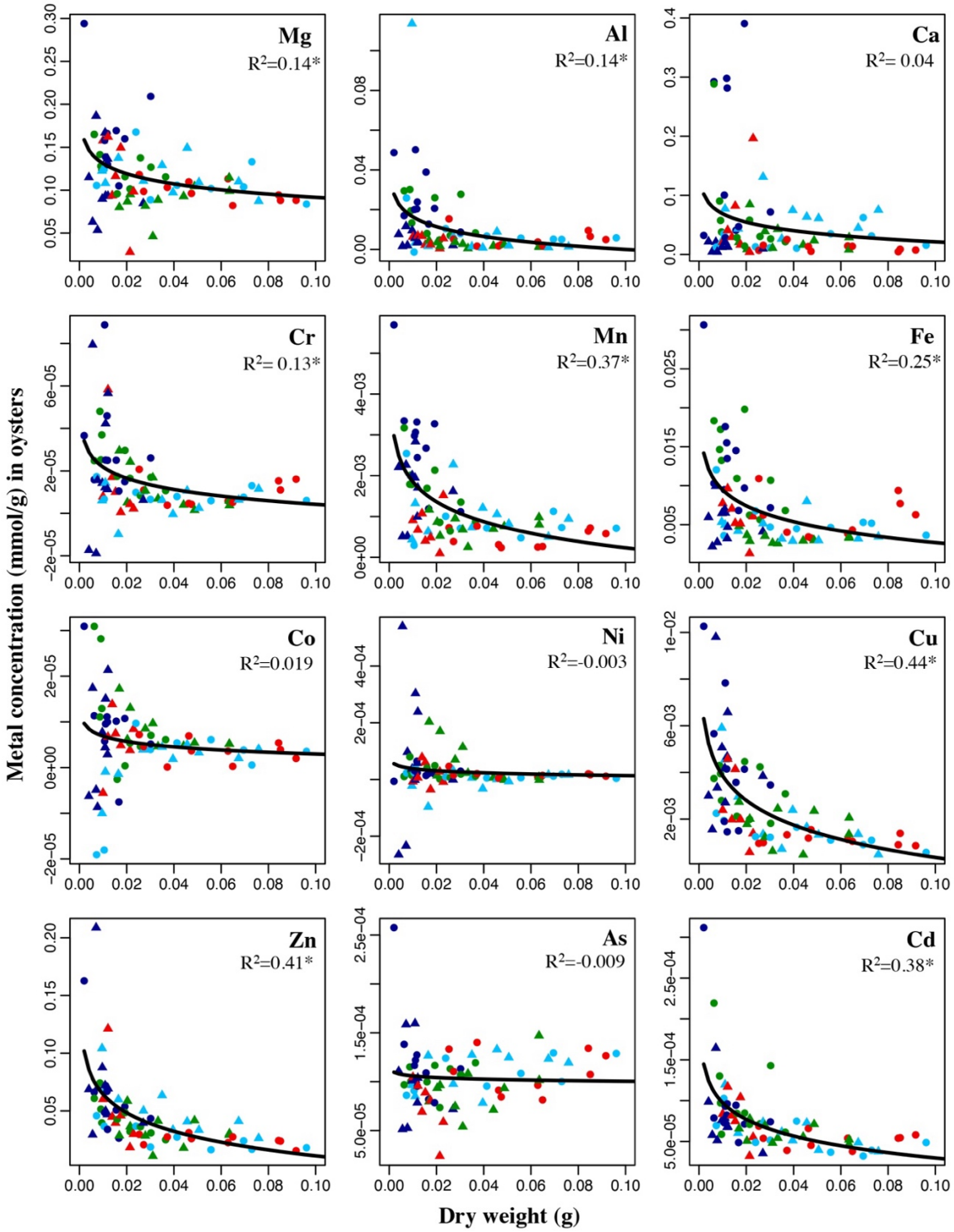

Figure 10. Concentrations in mmol/g for each of the twelve analyzed trace metals in oysters held for six months (January: circles) and one year (July: triangles) in four locations: Point Wells 5 m (green), Dabob Bay 5 m (red), Carr Inlet 5 m (light blue), and Carr Inlet 20 m (dark blue), all

plotted against the dry weight (grams) of the oysters. Adjusted R^2 values from exponential regression are shown in each panel (* indicates the R^2 value is significant, $p < 0.004$).

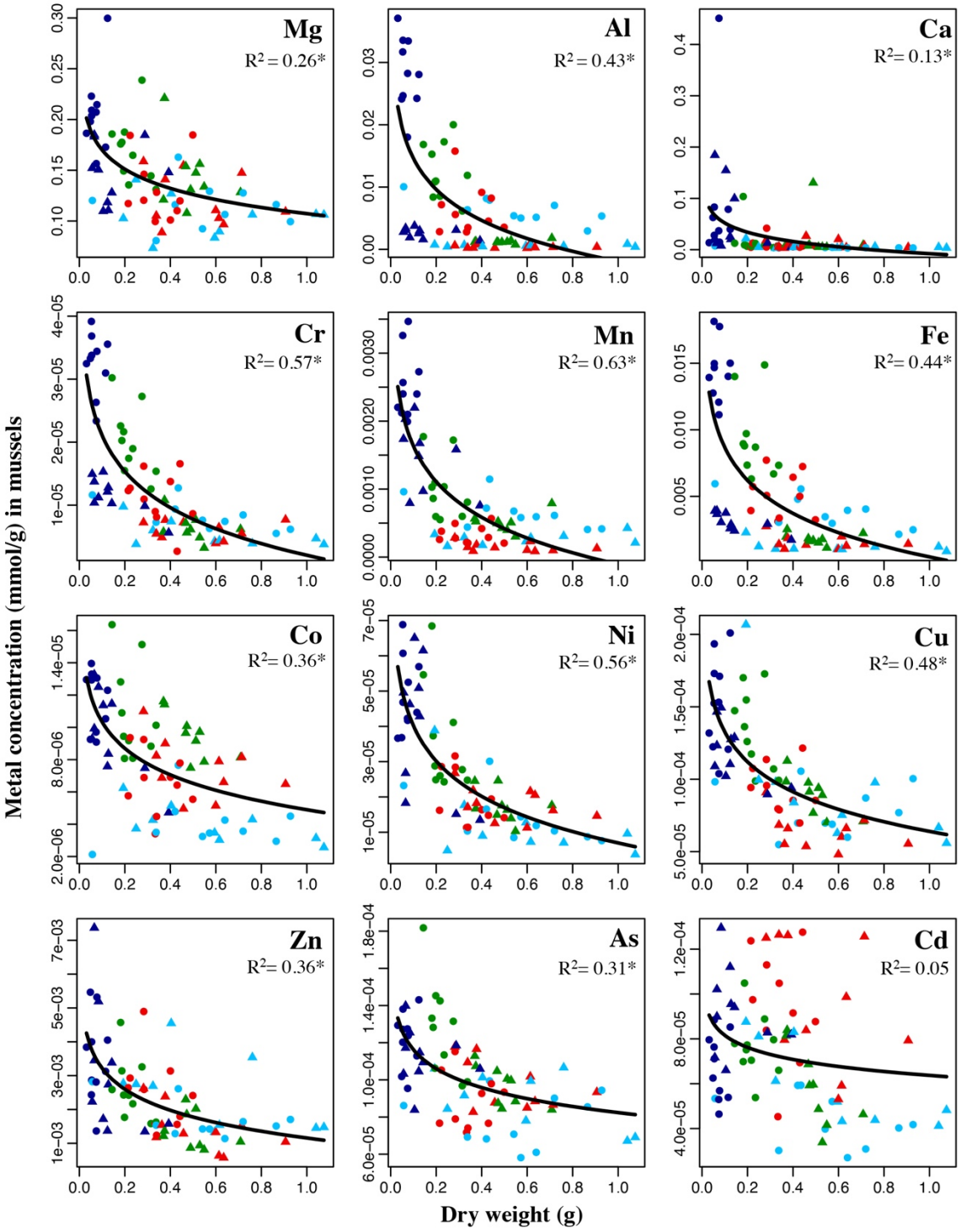

Figure 11. Concentrations in mmol/g for each of the twelve analyzed trace metals in mussels held for six months (January: circles) and one year (July: triangles) in four locations: Point Wells 5 m (green), Dabob Bay 5 m (red), Carr Inlet 5 m (light blue), and Carr Inlet 20 m (dark blue), all plotted against the dry weight (grams) of the oysters. Adjusted R^2 values from exponential regression are shown in each panel (* indicates the R^2 value is significant, $p < 0.004$). One mussel sample that weighed ~ 0.15 g was not graphed to better view the majority of samples but was included in analyses.

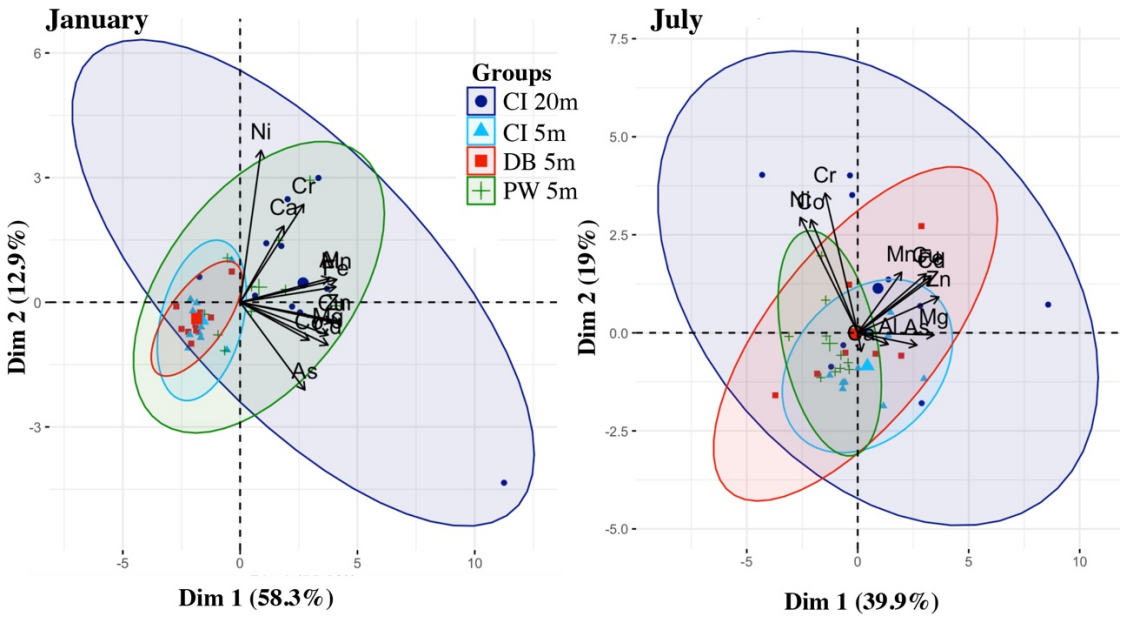

Figure 12: PCA of the trace metals data from oysters from January and July, colored by location (Carr Inlet 20 m = dark blue, Carr Inlet 5 m = light blue, Dabob Bay 5 m = red, Point Wells 5 m = green).

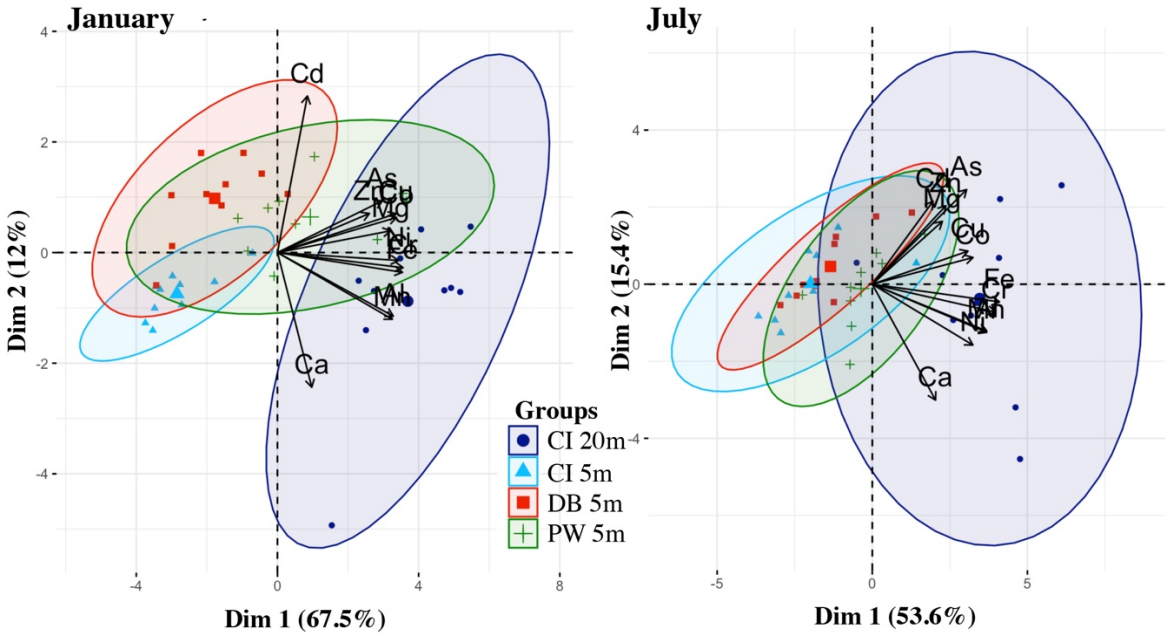

Figure 13. PCA of the trace metals data from mussels from January and July, colored by location (Carr Inlet 20 m = dark blue, Carr Inlet 5 m = light blue, Dabob Bay 5 m = red, Point Wells 5 m = green).

References

Agency for Toxic Substances and Disease Registry (ATSDR). (2005). *Toxicological profile for Nickel*. US Department of Health and Human Services, Public Health Service.

Agency for Toxic Substances and Disease Registry (ATSDR). (2008). *Toxicological profile for Aluminum*. U.S. Department of Health and Human Services, Public Health Service.

Alma, L. (n.d.). *Unpublished data*.

Ashoka, S., Peake, B. M., Bremner, G., Hageman, K. J., & Reid, M. R. (2009). Comparison of digestion methods for ICP-MS determination of trace elements in fish tissues. *Analytica Chimica Acta*, *653*(2), 191–199.

Boyden, C. R. (1977). Effect of size upon metal content of shellfish. *Journal of the Marine Biological Association of the United Kingdom*, *57*(3), 675–714.

Brand, L. E. (1991). Minimum iron requirements of marine phytoplankton and the implications for the biogeochemical control of new production. *Limnology and Oceanography*, *36*(8), 1756–1771.

Brandenberger, J. M., Crecelius, E. A., & Louchouarn, P. (2008). Historical inputs and natural recovery rates for heavy metals and organic biomarkers in Puget Sound during the 20th century. *Environmental Science and Technology*, *42*, 6786-6790.

Byrne, R., Kump, L. R., & Cantrell, K. J. (1988). The influence of temperature and pH on trace metal speciation in seawater. *Marine Chemistry*, *25*(2), 163–181.

Capra, S. (2006). *Nutrient reference values for Australia and New Zealand: Including recommended dietary intakes*.

Chan, C. Y., & Wang, W.X. (2018). A lipidomic approach to understand copper resilience in oyster *Crassostrea hongkongensis*. *Aquatic Toxicology*, *204*, 160–170.

Commission, C. A. (2015). *General standard for contaminants and toxins in food and feed (Codex Stan 193-1995)*. Amended.

Davenport, J., & Manley, A. (1978). The detection of heightened sea-water copper concentrations by the mussel *Mytilus edulis. Journal of the Marine Biological Association of the United Kingdom*, *58*(4), 843–850.

Eustace, I. J. (1974). Zinc, cadmium, copper, and manganese in species of finfish and shellfish caught in the Derwent Estuary, Tasmania. *Marine and Freshwater Research*, *25*(2), 209–220.

Faroon, O. M., Abadin, H., Keith, S., Osier, M., Chappell, L. L., Diamond, G., & Sage, G. (2004). Toxicological profile for cobalt. US Department of Health and Human Services. *Public Health Service Agency for Toxic Substances and Disease-Registry*.

Feely, R. A., Alin, S. R., Newton, J., Sabine, C. L., Warner, M., Devol, A., & Maloy, C. (2010). The combined effects of ocean acidification, mixing, and respiration on pH and carbonate saturation in an urbanized estuary. *Estuarine, Coastal and Shelf Science*, *88*(4), 442–449.

Feely, R. A., Klinger, T., Newton, J. A., & Chadsey, M. (2012). *Scientific summary of ocean acidification in Washington State marine waters* [NOAA OAR Special Report.].

Fowler, S. W., & Oregioni, B. (1976). Trace metals in mussels from the NW Mediterranean. *Marine Pollution Bulletin*, *7*(2), 26–29.

Gobler, C. J., & Baumann, H. (2016). Hypoxia and acidification in ocean ecosystems: Coupled dynamics and effects on marine life. *Biology Letters*, *12*: 20150976.

Götze, S., Matoo, O. B., Beniash, E., Saborowski, R., & Sokolova, I. M. (2014). Interactive effects of CO2 and trace metals on the proteasome activity and cellular stress response of marine bivalves *Crassostrea virginica* and *Mercenaria mercenaria*. *Aquatic Toxicology*, *149*, 65–82.

Han, B.C., Jeng, W.L., Tsai, Y.-N., & Jeng, M.-S. (1993). Depuration of copper and zinc by green oysters and blue mussels of Taiwan. *Environmental Pollution*, *82*(1), 93–97.

Handisyde, N. T., Ross, L. G., Badjeck, M. C., & Allison, E. H. (2006). *The effects of climate change on world aquaculture: A global perspective. Aquaculture and Fish Genetics Research Programme, Stirling Institute of Aquaculture* (p. 151) [Final Technical Report,]. DFID.

Harley, C. D., Randall Hughes, A., Hultgren, K. M., Miner, B. G., Sorte, C. J., Thornber, C. S., Rodriguez, L. F., Tomanek, L., & Williams, S. L. (2006). The impacts of climate change in coastal marine systems. *Ecology Letters*, *9*(2), 228–241.

Huberty, C. J., & Morris, J. D. (1992). *Multivariate analysis versus multiple univariate analyses.*

Husson, F., Josse, J., Le, S., & Mazet, J. (2013). FactoMineR: multivariate exploratory data analysis and data mining with R. *R Package Version* 1.1.29.

IPCC (2014). *Climate Change 2014: Synthesis Report. Contribution of Working Groups I, II and III to the Fifth Assessment Report of the Intergovernmental Panel on Climate Change [Core Writing Team* (R. K. Pachauri & L. A. Meyer, Eds.). IPCC

Ivanina, A. V., Beniash, E., Etzkorn, M., Meyers, T. B., AH, R., & Sokolova, I. M. (2013). Short-term acute hypercapnia affects cellular responses to trace metals in the hard clams *Mercenaria mercenaria. Aquatic Toxicology*, *140*, 123–133.

Ivanina, A. V., & Sokolova, L. M. (2015). Interactive effects of metal pollution and ocean acidification on physiology of marine organisms. *Current Zoology*, *61*(4), 653–668.

Jackson, D. A. (1993). Stopping rules in principal components analysis: A comparison of heuristical and statistical approaches. *Ecology*, *74*(8), 2204–2214.

Kassambara, A., & Mundt, F. (2017). Factoextra: Extract and visualize the results of multivariate data analyses. *R Package Version 1.5.*

Keister, J. E., & Tuttle, L. B. (2013). Effects of bottom-layer hypoxia on spatial distributions and community structure of mesozooplankton in a sub-estuary of Puget sound, Washington, U.S.A. *Limnology and Oceanography*, *58*(2), 667–680. https://doi.org/10.4319/lo.2013.58.2.0667

Long, E. R. (1982). An assessment of marine pollution in Puget Sound. *Marine Pollution Bulletin*, *13*(11), 380–383.

Mabardy, R. A., Waldbusser, G. G., Conway, F., & Olsen, C. S. (2015). Perception and response of the US west coast shellfish industry to ocean acidification: The voice of the canaries in the coal mine. *Journal of Shellfish Research*, *34*(2), 565–572.

MacCready, P., McCabe, R. M., Siedlecki, S. A., Lorenz, M., Giddings, S. N., Bos, J., Albertson, S., Banas, N., & Garnier, S. (2020). *Estuarine Circulation, Mixing, and Residence Times in the Salish Sea*.

Method 3050B Acid Digestion of Sediments, Sludges, and Soils. (1996). Environmental Protection Agency.

Millero, F. (2001). Speciation of metals in natural waters. *Geochemical Transactions*, *2*, 56–64.

Millero, F. J., Woosley, R., B, D., & Waters, J. (2009). Effect of ocean acidification on the speciation of metals in seawater. *Oceanography*, *22*(4), 72–85.

National Institute of Health: Office of Dietary Supplements (2020). *Copper (Fact Sheet for Health Professionals. Retrieved from https://ods.od.nih.gov/factsheets/Copper-HealthProfessional/#en9*

Oksanen, J., Blanchet, F. G., Friendly, M., Kindt, R., Legendre, P., McGlinn, D., Minchin, P. R., O'hara, R. B., Simpson, G. L., & Solymos, P. (2016). Vegan: Community Ecology Package. R package version 2.4-3. *Vienna: R Foundation for Statistical Computing*.

Olmedo, P., Hernández, A. F., Pla, A., Femia, P., Navas-Acien, A., & Gil, F. (2013). Determination of essential elements (copper, manganese, selenium and zinc) in fish and shellfish samples. Risk and nutritional assessment and mercury–selenium balance. *Food and Chemical Toxicology*, *62*, 299–307.

Pacific Shellfish Institute, Olympia, WA. (2008). *Characterization of the Cadmium Health Risk, Concentrations and Ways to Minimize Cadmium Residues in Shellfish: Sampling and Analysis of Cadmium in U.S. West Coast Bivalve Shellfish*.

Phillips, D. J. H., & Yim, W. W. S. (1981). A comparative evaluation of oysters, mussels and sediments as indicators of trace metals in Hong Kong waters. *Marine Ecology*, *6,*285-292.

Purroy, A., Najdek, M., Isla, E., Župan, I., Thebault, J., & Peharda, M. (2018). Bivalve trophic ecology in the Mediterranean: Spatio-temporal variations and feeding behavior. *Marine Environmental Research*, *142*, 234–249.

Riedel, G. F., Abbe, G. R., & Sanders, J. G. (1995). Silver and copper accumulation in two estuarine bivalves, the eastern oyster (*Crassostrea virginica*) and the hooked mussel (*Ischadium recurvum*) in the Patuxent River estuary, Maryland. *Estuaries*, *18*(3), 445-455.

Scavia, D., Field, J. C., Boesch, D. F., Buddemeier, R. W., Burkett, V., Cayan, D. R., Fogarty, M., Harwell, M. A., Howarth, R. W., & Mason, C. (2002). Climate change impacts on US coastal and marine ecosystems. *Estuaries*, *25*(2), 149–164.

Schell, W. R., & Nevissi, A. (1977). Heavy metals from waste disposal in central Puget Sound. *Environmental Science & Technology*, *11*(9), 887–893.

Schmidt, L., Bizzi, C. A., Duarte, F. A., VL, D., & Flores, E. M. (2013). Evaluation of drying conditions of fish tissues for inorganic mercury and methylmercury speciation analysis. *Microchemical Journal*, *108*, 53–59.

Scott, D. M., & Major, C. W. (1972). The effect of copper (II) on survival, respiration, and heart rate in the common blue mussel, *Mytilus edulis*. *The Biological Bulletin*, *143*(3), 679–688.

Shi, W., Zhao, X., Han, Y., Che, Z., X, C., & Liu, G. (2016). Ocean acidification increases cadmium accumulation in marine bivalves: A potential threat to seafood safety. *Scientific Reports*, *6*, 20197.

Sivaperumal, P., Sankar, T. V., & Viswanathan Nair, P. G. (2007). Heavy metal concentrations in fish, shellfish and fish products from internal markets of India vis-a-vis international standards. *Food Chemistry*, *102*(3), 612–620.

Smith, K. S., Balistrieri, L. S., & Todd, A. S. (2015). Using biotic ligand models to predict metal toxicity in mineralized systems. *Applied Geochemistry*, *57*, 55–72.

Topping, G. (1972). Heavy metals in shellfish from Scottish waters. *Aquaculture*, *1*, 379–384.
United States Census Bureau. (2020, August 17). Quickfacts WA. https://www.census.gov/quickfacts/fact/map/WA/PST045219

Waidmann, E., H, E., & Duerbeck, H. W. (1994). Trace determination of Tl, Cu, Pb, Cd, and Zn in specimens of the limnic environment using isotope dilution mass spectrometry with thermal ionization. *Fresenius' Journal of Analytical Chemistry*, *350*, 293–297.

Wang, W. X., J, M., & Wenig, N. (2018). Trace metals in oysters: Molecular and cellular mechanisms and ecotoxicological impacts. *Environmental Science: Processes & Impacts*, *20*(6), 892–912.

Wang, Y., Liang, L., Shi, J., & Jiang, G. (2005). Study on the contamination of heavy metals and their correlations in mollusks collected from coastal sites along the Chinese Bohai Sea. *Environment International*, *31*(8), 1103–1113.

Wanick, R. C., Kütter, V. T., Teixeira, C. L., Cordeiro, R. C., & Santelli, R. E. (2012). Use of the digestive gland of the oyster *Crassostrea rhizophorae* (Guilding, 1828) as a bioindicator of Zn, Cd and Cu contamination in estuarine sediments (south-east Brazil). *Chemistry and Ecology*, *28*(2), 103–111.

Washington Sea Grant. (2015). *Shellfish Aquaculture in Washington State: Final Report to Washington State Legislature*. *December*, 1–84.

Weldegebriel, Y., BS, C., & Wondimu, T. (2012). Concentration levels of metals in vegetables grown in soils irrigated with river water in Addis Ababa, Ethiopia. *Ecotoxicology and Environmental Safety*, *77*, 57–63.

Supplementary Tables

Supplementary Table 1. The percent recovery from four different USGS standards run in duplicate for the two runs of the ICP-MS, and the average recovery for each isotope, are shown. For isotopes where there was a greater than 10% difference between the sample recoveries from January and July sampling, numbers are shown in red.

		Percent Recoveries for Isotopes Used in Analysis											
	USGS Standard	**^{25}Mg**	**^{27}Al**	**^{43}Ca**	**^{52}Cr**	**^{55}Mn**	**^{56}Fe**	**^{59}Co**	**^{62}Ni**	**^{63}Cu**	**^{66}Zn**	**^{75}As**	**^{111}Cd**
Field Samples January	T-221	97.3	97.7	107.2	110.4	106.1	110.4	103.6	78.0	101.7	99.0	96.9	72.1
	T-239	102.9	104.8	111.3	114.6	113.1	112.7	107.0	115.6	100.9	108.2	101.5	103.2
	T-231	102.1	101.7	116.2	120.4	108.1	112.0	101.4	111.1	101.8	99.5	94.1	96.5
	T-235	101.1	100.4	111.3	125.2	108.3	112.8	103.3	110.9	106.4	100.2	100.0	79.1
	Average	100.8	101.1	111.5	117.6	108.9	112.0	103.8	103.9	102.7	101.7	98.2	87.7
Field Samples July	T-221	66.2	70.5	79.1	85.3	79.8	81.4	86.1	58.2	91.0	92.2	78.7	96.0
	T-239	70.7	74.4	81.9	87.0	84.7	85.9	88.4	82.5	96.1	103.5	81.8	107.3
	T-231	69.1	72.9	84.3	107.5	82.2	84.9	85.7	59.1	89.8	94.3	76.5	100.6
	T-235	68.1	69.8	80.4	93.2	81.2	82.0	86.1	73.1	92.5	111.4	81.4	92.6
	Average	68.5	71.9	81.4	93.2	82.0	83.5	86.6	68.2	92.3	100.4	79.6	99.1

Supplementary Table 2. The percent recovery from DOLT-5 dogfish liver standard reference material. The average percent recovery for the ICP-MS run, the SD between the DOLT-5 sample recoveries, and the SD between the mean recovery from each tissue digestion batch, are included for the two runs of the ICP-MS. For isotopes where there was a greater than 10% difference between the recoveries from January and July, numbers are shown in red.

Percent Recovery for DOLT-5 Standard Reference Material

	Recovery	^{25}Mg	^{27}Al	^{43}Ca	^{52}Cr	^{55}Mn	^{56}Fe	^{59}Co	^{62}Ni	^{63}Cu	^{66}Zn	^{75}As	^{111}Cd
Field Samples January	**Average**	98.7	31.2	10.8	39.8	90.7	95.2	84.0	45.4	95.2	90.9	75.9	89.8
	SD	9.9	9.8	1.0	2.9	3.8	3.7	4.9	3.5	3.9	8.1	2.3	1.8
	SD between digests	3.7	9.5	0.3	2.9	1.5	1.4	4.2	3.3	1.9	3.0	0.9	1.3
Field Samples July	**Average**	78.2	25.1	9.4	41.6	83.0	85.4	82.1	47.6	89.8	89.6	77.5	91.1
	SD	13.8	4.5	1.5	5.4	8.6	8.0	5.5	4.5	7.5	5.9	4.9	1.7
	SD between digests	8.6	2.5	1.0	3.9	5.2	4.8	3.5	1.2	4.4	3.7	3.1	0.9

Supplementary Table 3. Summary of mean trace metal concentrations in oyster and mussel tissues for each of the four locations at the two time points (mmol/g). P-values are from Welch's Two Samples T-test for each metal comparing the two species across all four cage locations. Arrow indicates which species had the larger mean concentration of metals, and red color indicates the difference between species was significant (alpha level of 0.004 was chosen after Bonferroni correction).

Oysters					Mussels			
Carr Inlet 20m	Carr Inlet 5m	Dabob Bay 5m	Point Wells 5m	Metal (p value)	Carr Inlet 20m	Carr Inlet 5m	Dabob Bay 5m	Point Wells 5m
January					January			
1.69E-01	1.14E-01	9.92E-02	1.25E-01	Mg (0.004)→	2.07E-01	1.15E-01	1.31E-01	1.69E-01
2.61E-02	8.15E-03	5.31E-03	1.74E-02	←Al (0.737)	2.83E-02	6.34E-03	6.31E-03	1.26E-02
1.58E-01	2.45E-02	1.15E-02	6.53E-02	←Ca (0.065)	8.25E-02	5.07E-03	1.01E-02	1.78E-02
3.14E-05	8.80E-06	9.78E-06	2.35E-05	←Cr (0.916)	3.26E-05	8.25E-06	1.11E-05	2.02E-05
2.91E-03	9.00E-04	4.88E-04	1.63E-03	←Mn (0.147)	2.52E-03	6.55E-04	3.32E-04	1.01E-03
1.35E-02	5.52E-03	5.94E-03	1.24E-02	←Fe (0.325)	1.44E-02	3.84E-03	5.09E-03	9.27E-03
9.72E-06	-7.72E-08	3.77E-06	1.04E-05	Co (0.157) →	1.17E-05	4.00E-06	6.58E-06	1.09E-05
2.37E-05	1.33E-05	1.66E-05	2.64E-05	Ni (0.015) →	4.87E-05	1.42E-05	1.92E-05	3.58E-05
4.39E-03	1.30E-03	1.14E-03	3.25E-03	←Cu (4.17E-09)	1.52E-04	7.91E-05	9.31E-05	1.33E-04
6.24E-02	2.56E-02	2.48E-02	4.41E-02	←Zn (4.51E-11)	3.53E-03	1.71E-03	2.48E-03	2.56E-03
1.24E-04	1.09E-04	1.11E-04	1.04E-04	←As (0.220)	1.22E-04	7.83E-05	8.83E-05	1.28E-04
1.02E-04	5.41E-05	5.31E-05	1.02E-04	←Cd (0.405)	6.73E-05	4.34E-05	9.44E-05	7.64E-05
July					July			
1.08E-01	1.16E-01	1.13E-01	8.90E-02	Mg (0.003) →	1.47E-01	1.04E-01	1.22E-01	1.44E-01
5.36E-03	1.41E-02	3.98E-03	2.35E-03	←Al (0.077)	2.67E-03	5.92E-04	4.28E-04	1.24E-03
1.41E-02	6.20E-02	4.96E-02	2.83E-02	←Ca (0.131)	5.37E-02	6.40E-03	1.07E-02	2.14E-02
2.02E-05	5.79E-06	1.36E-05	1.09E-05	←Cr (0.110)	1.16E-05	5.34E-06	6.04E-06	6.38E-06
1.66E-03	9.93E-04	6.78E-04	7.67E-04	←Mn (0.005)	1.53E-03	2.69E-04	1.49E-04	5.04E-04
5.28E-03	4.34E-03	5.76E-03	3.27E-03	←Fe (1.58E-09)	3.09E-03	1.22E-03	1.55E-03	1.82E-03
5.29E-06	1.24E-06	5.61E-06	7.98E-06	Co (0.032) →	9.59E-06	3.99E-06	7.44E-06	9.46E-06
7.74E-05	-3.90E-06	1.99E-05	6.06E-05	←Ni (0.421)	3.90E-05	1.23E-05	1.81E-05	1.74E-05
4.47E-03	2.27E-03	2.20E-03	1.71E-03	←Cu (8.67E-10)	1.18E-04	9.41E-05	6.36E-05	8.90E-05
7.42E-02	5.21E-02	4.72E-02	3.23E-02	←Zn (1.92E-10)	3.04E-03	2.46E-03	1.41E-03	1.38E-03
9.90E-05	1.11E-04	7.54E-05	9.20E-05	As (0.504) →	1.12E-04	8.93E-05	9.69E-05	9.66E-05
7.73E-05	6.39E-05	7.33E-05	5.92E-05	Cd (0.132) →	9.26E-05	6.01E-05	9.57E-05	5.81E-05

Supplementary Table 4. P values for ANOVAs and Tukey Post-Hoc Tests comparing tissue metal concentration across sites within sampling time and between sites across sampling time for oysters and mussels. Green outlined boxes are comparing different sites during January sampling, blue outlined boxes are comparing different sites during July sampling, and the diagonal in the middle is comparing each site between January and July. Asterisks indicate p-values are significant ($p < 0.004$, because Bonferroni correction was used).

Oysters					**Mussels**				
Magnesium									
	CI20	CI5	PW5	DB5		CI20	CI5	PW5	DB5
CI20	0.0014*	0.0016*	0.0141	<0.0001*	CI20	0.0006*	<0.0001*	0.0491	<0.0001*
CI5	0.9500	1.0000	0.8598	0.7002	CI5	0.0098	0.9920	0.0027*	0.6680
PW5	0.5593	0.2681	0.1977	0.2573	PW5	0.9972	0.0198	0.6244	0.0504
DB5	0.9872	0.9981	0.4074	0.9806	DB5	0.1895	0.5265	0.2910	0.9960
Aluminum									
	CI20	CI5	PW5	DB5		CI20	CI5	PW5	DB5
CI20	0.0409	0.0013*	0.2153	0.0002*	CI20	<0.0001*	<0.0001*	<0.0001*	<0.0001*
CI5	0.7081	0.9835	0.1694	0.9163	CI5	<0.0001*	0.0032*	0.0121	1.0000
PW5	0.9823	0.4816	0.2953	0.0433	PW5	<0.0001*	0.0233	<0.0001*	0.0117
DB5	0.9985	0.6481	0.9976	1.0000	DB5	<0.0001*	0.8593	0.0024*	0.0016*
Calcium									
	CI20	CI5	PW5	DB5		CI20	CI5	PW5	DB5
CI20	<0.0001*	0.0042	0.0688	0.0015*	CI20	0.9445	0.0693	0.1633	0.0986
CI5	0.0240	0.8879	0.6807	0.9842	CI5	0.0682	1.0000	0.9749	0.9984
PW5	0.8097	0.1671	0.8949	0.4628	PW5	0.3160	0.8568	1.0000	0.9942
DB5	0.1728	0.8818	0.5922	0.9087	DB5	0.0975	0.9956	0.9365	1.0000

Chromium									
	CI20	CI5	PW5	DB5		CI20	CI5	PW5	DB5
CI20	0.7903	0.0031*	0.5537	0.0048	CI20	<0.0001*	<0.0001*	<.0001*	<0.0001*
CI5	0.3462	0.9999	0.0850	0.9984	CI5	<0.0001*	0.6039	<0.0001*	0.4718
PW5	0.6967	0.9330	0.6750	0.1192	PW5	<0.0001*	0.7400	<0.0001*	0.0002
DB5	0.8869	0.8221	0.9899	0.9997	DB5	<0.0001*	0.8961	0.9858	0.0348
Manganese									
	CI20	CI5	PW5	DB5		CI20	CI5	PW5	DB5
CI20	0.0035*	<0.0001*	0.0063	<0.0001*	CI20	<0.0001*	<0.0001*	<0.0001*	<0.0001*
CI5	0.0448	1.0000	0.1994	0.6702	CI5	<0.0001*	0.1737	0.1434	0.1983
PW5	0.0043	0.7894	0.1150	0.0163	PW5	<0.0001*	0.3098	0.0243	0.0009*
DB5	0.0030*	0.6181	0.9857	0.9990	DB5	<0.0001*	0.7902	0.0464	0.9084
Iron									
	CI20	CI5	PW5	DB5		CI20	CI5	PW5	DB5
CI20	<0.0001*	0.0029*	0.9453	0.0051	CI20	<0.0001*	<0.0001*	<0.0001*	<0.0001*
CI5	0.6817	0.9959	0.0130	0.9971	CI5	<0.0001*	0.0118	<0.0001*	0.5642
PW5	0.1013	0.5950	<0.0001*	0.0215	PW5	<0.0001*	0.1110	<0.0001*	0.0005*
DB5	0.9515	0.4020	0.0428	1.0000	DB5	<0.0001*	0.5496	0.7163	<0.0001*
Cobalt									
	CI20	CI5	PW5	DB5		CI20	CI5	PW5	DB5
CI20	0.9116	0.0832	0.9981	0.4501	CI20	0.2795	<0.0001*	0.8259	<0.0001*
CI5	0.5927	0.9999	0.0570	0.7688	CI5	<0.0001*	1.0000	<0.0001*	0.0466
PW5	0.8026	0.1256	0.9971	0.3547	PW5	0.9986	<0.0001*	0.7725	0.0003*
DB5	0.9996	0.5165	0.8747	0.9997	DB5	0.0671	0.0018*	0.1084	0.9792
Nickel									
	CI20	CI5	PW5	DB5		CI20	CI5	PW5	DB5
CI20	0.8998	0.5056	0.9844	0.7738	CI20	0.5181	<0.0001*	0.0471	<0.0001*

CI5	0.5252	0.9999	0.3098	0.9701	CI5	0.0001*	1.0000	0.0003*	0.7131
PW5	0.9919	0.6990	0.9912	0.5610	PW5	0.0016*	0.7905	0.0131	0.0068
DB5	0.7974	0.9811	0.9159	1.0000	DB5	0.0017*	0.7046	0.9992	1.0000
Copper									
	CI20	CI5	PW5	DB5		CI20	CI5	PW5	DB5
CI20	1.0000	0.0004*	0.3568	0.0002*	CI20	0.0654	<0.0001*	0.3094	<0.0001*
CI5	0.0302	0.8770	0.0355	0.9952	CI5	0.2065	0.9017	0.0001*	0.5844
PW5	0.0045	0.8774	0.4003	0.0198	PW5	0.0906	0.9757	0.0075	0.0048
DB5	0.0360	0.9997	0.9278	0.8602	DB5	0.0003*	0.0707	0.1672	0.1691
Zinc									
	CI20	CI5	PW5	DB5		CI20	CI5	PW5	DB5
CI20	0.9792	0.0023*	0.2367	0.0019*	CI20	0.9741	0.0012*	0.1416	0.0998
CI5	0.4506	0.3930	0.2249	0.9998	CI5	0.7262	0.8193	0.2396	0.3176
PW5	0.0364	0.5434	0.9788	0.1955	PW5	0.0264	0.2549	0.2978	0.9981
DB5	0.3253	0.9888	0.7792	0.6823	DB5	0.0251	0.2590	0.9999	0.3869
Arsenic									
	CI20	CI5	PW5	DB5		CI20	CI5	PW5	DB5
CI20	0.5293	0.6751	0.4454	0.7395	CI20	0.8824	<0.0001*	0.8867	0.0011*
CI5	0.7630	1.0000	0.9815	0.9995	CI5	0.0048	0.8142	<0.0001*	0.6135
PW5	0.9430	0.4266	0.9805	0.9618	PW5	0.0810	0.6760	0.0019*	0.0001*
DB5	0.3017	0.0502	0.6012	0.1835	DB5	0.0790	0.6246	0.9999	0.9287
Cadmium									
	CI20	CI5	PW5	DB5		CI20	CI5	PW5	DB5
CI20	0.8224	0.1136	1.0000	0.1029	CI20	0.0885	0.0177	0.6443	0.0061
CI5	0.6669	0.9991	0.1159	1.0000	CI5	0.0129	0.5733	0.0007*	<0.0001*
PW5	0.4233	0.9776	0.2044	0.1050	PW5	0.0076	0.9972	0.4626	0.1047
DB5	0.9879	0.8757	0.6736	0.9511	DB5	0.9882	0.0057	0.0033*	1.0000

Chapter 2: Exposure of larval pinto abalone to ocean acidification and warming negatively impacts survival, settlement, and size

Publication history: This study was co-authored with Ryan Crim, Josh Bouma, Jodie Toft, and Jacqueline Padilla-Gamiño. At the time this dissertation was published, this chapter was not published separately.

Abstract

Pinto abalone (*Haliotis kamtschatkana*) the only abalone species native to Washington waters, declined by 97% in the state between 1992 to 2017. Their decline is a loss for indigenous tribes, recreational divers, and the health of subtidal rocky reefs and kelp beds. Current restoration actions are facing ocean acidification and warming in the northeast Pacific, further threatening pinto abalone recovery. This research aims to deepen our understanding of the tolerance and physiological flexibility of early life history stages of pinto abalone and inform hatchery practices under future climate change scenarios. We conducted an experiment to test how pH and temperature stress will impact abalone larvae. We exposed abalone post-fertilization to four treatments for ten days spanning their lecithotrophic larval development period: (1) 7.95pH/14°C (ambient) (2) 7.60pH/14°C, (3) 7.95pH/18°C and (4) 7.60pH/18°C. Abalone in the ambient treatment had the best survival, those in the 7.60pH/18°C treatment had the worst survival, and those in the two single-stressor treatments had survival in between. For surviving larvae, temperature appeared to have a minor effect on settlement; pH was the dominant stressor determining settlement success, with higher settlement rates for surviving larvae under ambient pH treatments at both temperatures. pH also had a stronger effect than temperature on shell length. Our study shows how warming and ocean acidification impact the early life stages of

pinto abalone. This information is essential for optimizing future restoration aquaculture and determining their ideal habitat and potential geographic range.

Introduction

Pinto abalone (*Haliotis kamtschatkana)* are ecologically important grazers for the intertidal and subtidal ecosystems they inhabit and are prized for their economic and subsistence value (Tomascik & Holmes, 2003). While pinto abalone can be found from southeast Alaska, USA, to Baja California, Mexico, their populations have declined drastically along much of this range (Neuman et al., 2019). In Washington State (USA), pinto abalone experienced a 97% decline at 10 permanent index stations monitored for population trends from 1992 to 2017 (Rothaus et al., 2008) (WDFW unpublished data), and in 2019, they were listed as a state endangered species (Neuman et al., 2019; Rogers-Bennett et al., 2011; Sowul et al., 2022).

Pinto abalone have historically been harvested to varying degrees by indigenous and non-indigenous people throughout their range (Neuman et al., 2019). While their decline was noted, and the Washington pinto abalone sport fishery closed in 1994, the population has yet to recover (Carson et al., 2019; Rothaus et al., 2008). The continued decline of pinto abalone could be caused by a combination of disease, illegal harvest, or changing water conditions, but the principal reason is their low population density (Rothaus et al., 2008; Tegner et al., 2001; Tomascik & Holmes, 2003). The sparse distribution of reproductive adults hinders successful fertilization due to insufficient aggregation (Rothaus et al., 2008). Gascoigne & Lipcius (2004), in their exploration of the Allee effect in marine ecosystems, emphasized that broadcast spawners and exploited populations, characteristics of pinto abalone, are particularly susceptible to exhibiting the Allee effect (Allee, 1931).

Pinto abalone populations in Washington are unlikely to recover without human intervention. To rebuild the pinto abalone population to historical levels, hatchery-based restoration efforts were initiated over a decade ago. These efforts have been led by the

Washington Department of Fish and Wildlife (WDFW) and Puget Sound Restoration Fund (PSRF), with support from various other partners. Pinto abalone broodstock are spawned, and gametes are mixed to create diverse families. Larvae are raised through settlement competency, and juveniles are grown in nursery tanks for one to two years before they are outplanted to locations within the San Juan Archipelago (Carson et al., 2019).

As restoration occurs, however, climate change is already impacting the waters where vulnerable pinto abalone populations reside. Climate change, caused by increasing atmospheric CO_2 concentrations, contributes to ocean warming, as well as ocean acidification through CO_2 absorption in the oceans (Caldeira & Wickett, 2003; Feely et al., 2004; IPCC, 2014). While previous research has informed understanding of optimal environmental conditions for pinto abalone, there is increasing recognition that looking at single stressors in isolation will not give an accurate picture of what will occur in the natural environment. Depending on the direction, extent, and mechanism in which each stressor affects a given species, multiple stressors can act in additive, antagonistic, or synergistic ways (Piggott et al., 2015). By understanding the impact of multiple stressors at an individual level, we can scale up findings to make more accurate projections about how climate change will impact entire populations. However, it is essential to recognize that these impacts depend on the contexts of specific communities and ecosystems (Griffen et al., 2016).

In the San Juan Islands of Washington, abalone already experience persistently low pH and are expected to experience higher temperatures more frequently in coming years (Ianson et al., 2016; Lowe et al., 2016; Murray et al., 2015). Ocean acidification can reduce carbonate ion availability, or the mineral saturation state of seawater, and have detrimental consequences for species that use calcium carbonate to build their skeletons (Waldbusser et al., 2015). Early life

stages of marine calcifiers such as shellfish have been found particularly vulnerable to the effects of ocean acidification (Byrne, 2011). Impacts such as shell deformities, mortality, delayed development, and reduced growth have been demonstrated when pinto and European abalone larvae were exposed to pCO_2 conditions resembling those expected in 2100 (Crim et al., 2011; Wessel et al., 2018). Larvae of Ezo abalone had smaller shells and more shell deformities when exposed to increased pCO_2 conditions (Kimura et al., 2011; Onitsuka et al., 2018). One study found a threshold for these impacts at an aragonite saturation of around 1.1 (Onitsuka et al., 2018).

Simultaneously, increased ocean temperatures due to global warming can impact physiology and critical performance traits such as growth rate, reproductive output, and disease susceptibility of marine species (Brander, 2007; Cochrane et al., 2009, p. 2012; De Silva et al., 2012; Handisyde et al., 2006). Temperature tolerances of abalone have been studied across a wide range of species, varying between species and life stages (Morash & Alter, 2016; Rogers-Bennett et al., 2010). Pinto abalone larvae showed sharp declines at 24°C compared to larvae at 21°C, suggesting a thermal tolerance limit in that 3°C range (Bouma, 2007).

When experienced together, ocean acidification and warming also negatively impact larval abalone. For example, larval reddish-rayed abalone had developmental failures, reduced calcification, and higher mortality when exposed to warmer (+2°C and +4°C) and more acidified (-0.4 and -0.6 pH units) conditions, but these stressors did not have interactive effects (Byrne et al., 2011). In European abalone, a 0.3-unit pH drop and 2°C temperature increase caused significant negative impacts on larvae, especially in terms of shell length and calcification, but as with reddish-rayed abalone, no interactive effects of the stressors were found (Kavousi et al., 2022).

Beyond survival, other important components of pinto abalone's early life cycle may be impacted by climate change. Pinto abalone have a free-swimming larval phase after they hatch. After this period, they settle onto the substrate and metamorphose into juveniles (Figure 1). Abalone larvae are lecithotrophic (non-feeding). Thus, development progresses with finite energy reserves and settlement occurs within a relatively short window of seven to 10 days (Sloan, 1988), depending largely on temperature. In the wild, this settlement is triggered by specific environmental cues, while in hatcheries, a chemical inducer (gamma-aminobutyric acid [GABA]) is commonly used (Leighton, 2008; Morse & Morse, 1984). Therefore, in addition to studying the survival and size of abalone larvae exposed to different ocean warming and acidification scenarios, it is essential to assess how climate change will impact larval settlement. Ocean acidification may result in abalone depleting energy reserves faster as they attempt to regulate pH, and ocean acidification can slow metabolism, which could delay settlement (Avignon et al., 2020; Gazeau et al., 2013; Palmer, 1981, 1992; Waldbusser et al., 2015). Negative impacts during early life stages such as these, can lead to bottleneck effects on the population of the species as a whole (Byrne, 2011). Despite the importance of early life stages, in ecological studies of marine invertebrates the larval phase is often considered a "black box" due to the difficulty in measuring larval behavior and survival in the natural environment (Chan et al., 2018). Opening this "black box" allows us to understand how variability in larval distribution and recruitment will impact abalone conservation under future climate change.

This study aimed to understand how climate change will affect the early life stages of pinto abalone to inform hatchery-based restoration practices. We studied how individual temperature and pH stressors and the combination of those stressors would affect larval abalone

hatching, survival, settlement, and size. This study provides the first look at multiple stressor impacts of climate change on pinto abalone.

Methods

Spawning of broodstock

Fertilized gametes were acquired from the Kenneth K. Chew Center for Shellfish Research and Restoration (Chew Center) as part of their conservation breeding program. Broodstock were induced to spawn by submerging them in a 0.024% hydrogen peroxide bath for three hours and then returned to filtered seawater, a procedure commonly used in commercial abalone aquaculture (D. E. Morse et al., 1977). Gametes from two males and two females were collected, and fertilizations were made with each possible cross of the adults (four total). Each experimental replicate received the same number of embryos (n=3,750) from each cross, estimated by volume, so ratios of embryos from different families were consistent between replicates. Fertilization rates were assessed for each cross in the hatchery, showing significant variation (6%, 80%, 2%, and 83%). Notably, both families from one male exhibited considerably lower fertilization rates. Given the transfer of 15,000 eggs (3,750 from each cross) into each replicate tank and the known fertilization rates for each cross, it is estimated that the total number of fertilized embryos in each replicate was approximately 6,400 at the start of the experiment.

Experimental Treatments

Gamete groups were divided into four distinct experimental groups with three replicates each. We used a 14°C treatment (ambient temperature), which is the temperature normally used

for larval rearing at the hatchery, and an 18°C treatment (high temperature), representing a temperature not currently experienced in the San Juan Archipelago but that will be more commonly seen under future climate change (IPCC, 2014; Weigel et al., 2023). Half of the treatment tanks used the pH of the hatchery flow-through seawater system, which was 7.9-8.0 (ambient pH), and the other half used future forecasted pH levels, targeting a pH of 7.6 (low pH). Expected atmospheric CO_2 levels by 2050 could lead to an average drop of 0.3 pH units in oceans (Cooley et al., 2009). Coastal regions where abalone reside may experience even faster pH declines and greater pH variability. Therefore, we selected a pH difference just over this 0.3-unit average (Cooley et al., 2009; Strong et al., 2014).

Larval Hatching and Rearing

A total of fifteen thousand eggs, (see above for fertilization rates) were placed in three replicate tanks for each of the four treatments. Water outflow occurred at the top of the tanks, enabling hatched embryos to ascend into the water column and move into a second tier of tanks. Here, they were contained in silos—tubes equipped with mesh bottoms that facilitated water flow while preventing larvae from being flushed out of the system (Figure 2a). On the third day (experiment days are counted as days post-spawn [dpf]) of the experiment, we removed the embryo tanks from the system. This decision assumed that any larvae destined to hatch had already completed this process by that time. Additionally, this step aimed to minimize the introduction of bacteria from deceased embryos into the system. For days three through 10 of the experiment, the header tanks fed directly into the larval tanks with silos (Figure 2b). Counts were performed on days one through three and days six through 10. Counts, in triplicate, were taken from each silo by removing a known volume of water, counting the larvae present, and

extrapolating to the number in the whole silo using its known volume. Next, we added the numbers of larvae initially removed from the current and previous days' survival counts and settlement trials. This approach ensured that the larvae removed for experimental purposes were not counted as mortalities. On day 10, after the final counts of larvae had been taken, the silos were cleaned, and the remaining abalone stuck either on the sides or mesh screens were removed forcefully with water. Flow rates in each replicate were modulated with irrigation drippers throughout the experiment (approximately 10L per hour); see supplementary Table 1 for more details.

Larval Settlement Trials

A subset of larvae (50-200 depending on living larvae available in each replicate) from each treatment were removed and induced to set each day from 6-10dpf. Larvae were placed in a glass mason jar of seawater with 1 mmol gamma-aminobutyric acid (GABA, Acros Organics), commonly used to induce settlement in abalone hatcheries. The jars were filled with water of the corresponding treatment pH and temperature, sealed with plastic lids, and placed in a water bath for ~24 hours to maintain those conditions. After this period, the jars were gently rinsed with seawater to collect larvae still in the water column and then rinsed aggressively with freshwater and propanol to remove larvae that had settled onto the sides and bottom of the jar. Counts of the swimming and settled larvae were used to calculate the percent settlement in each replicate jar for each of the five days. These larvae were not included as mortalities in the larval survival data.

Water chemistry

Temperature and pH in each of the four header tanks were measured continuously with Durafet probes. Seawater pH was controlled by the automated addition of CO_2 with a solenoid valve. Submersion heaters (Finnex, 800Watt) increased the temperature of ambient inflowing seawater in an initial header tank equipped with a degassing column. Seawater then passed through a UV sterilizer and into the four experimental header tanks equipped with chillers (Teco TK2000H) for temperature control.

In addition to the Durafet probe measurements, temperature, salinity, and pH were assessed daily. For each header and treatment tank, temperature and salinity probes were used, and water samples were taken and analyzed using m-cresol purple dye spectrometry to assess pH (Dickson et al., 2007). Additionally, water samples were taken for alkalinity analyses on three days (0, 6, and 9dpf) during the experiment. These samples were preserved with mercuric chloride. Samples from days zero and nine were analyzed via titration with HCl using a Mettler Toledo T5 Excellence Titrator. Alkalinity values were used to calculate temperature-corrected pH values for each spectrometer measurement using the R package Seacarb (Gattuso et al., 2015). Alkalinity, pH, salinity, and temperature were then used to calculate pCO_2 and aragonite saturation state ($\Omega_{aragonite}$). Water chemistry variables for both larval and embryo tanks were compared using ANOVA to assess whether there were treatment differences.

Temperature loggers (Onset HOBO Pendant) were placed in one of the replicate tanks from each treatment throughout the experiment. Temperature loggers were also placed in the water baths used for the settlement jars on days six through 11 (as larvae 10dpf were left overnight for the final settlement trial, the experiment lasted 11 days) of the experiment to ensure they had remained at the targeted high and low temperature levels.

Shell length

Abalone larvae from each replicate tank were sampled daily and preserved in 30% isopropyl alcohol. Larvae were photographed using a compound scope (Nikon Eclipse Ni) and camera (Nikon DS-Fi3). Shell length along the longest axis was measured for 30 shells from each tank on their sides. If fewer than 30 surviving or settled larvae were available in a replicate on a given day, measurements were taken for as many shells as possible. Measurements were done for larvae on days three, seven, and ten of the experiment. On day three, larvae from the flow-through silos that were used for counts were also measured. On days seven and ten, the larvae counted as "settled" in the jars were measured (the settlement trials for these larvae started 6 and 9dpf respectively).

One individual conducted the shell measurements to ensure a consistent protocol was applied, especially for shells with unclear edges or no clear distinction between shell and tissue. Shell length could be affected when shells were crushed, positioned on one side, fragmented, or missing. However, the first 30 abalone shells encountered in each replicate were photographed regardless of their condition. This was done to ensure consistency between treatments. When the shell could be distinguished from the abalone foot or other tissue protruding from the shell, only the shell length was measured. However, when the shell and tissue could not be distinguished, the entire length of the abalone was measured.

Data analysis

Data analyses were completed in R. To assess the impact of pH and temperature while considering the day of measurement, we used multi-model inference to determine the relative importance of different factors. Using the lme4 package in R, we used linear models for

hatching, settlement (arcsine transformed the proportional data), and survival data, and a mixed-effects linear model for larval size using a random effect to account for repeated measurements from the same tanks (Bates et al., 2015). All models included day as a continuous predictor. When included, temperature and pH were treated as categorical (factor) variables. Residuals were assumed to be normally distributed.

For these analyses, alternative models (14 models each for hatching and survival, six for settlement, and five for size; see Supplementary Tables 2-5) were compared using AICc (Akaike Information Criterion, corrected for small sample size). In addition to AICc, model complexity was also considered when selecting the best models, with simpler models favored when a substantial drop in AICc was not noted with the addition of more terms. QQ plots and residual vs. fitted value plots were assessed for any of the best performing models that we considered in interpretation.

Results

Water Chemistry

Flow rates were approximately 10 liters per hour on average for each treatment. Details of flow rates for each tank and treatment are summarized in Supplementary Table 1.

Data for pH, temperature, salinity, alkalinity, aragonite saturation, and pCO_2 based on our daily measurements are summarized for each treatment in Table 1. We successfully maintained temperature treatments just under 4°C apart in both of the larval tanks (17.88 ± 0.18°C and 14.11 ± 0.25°C for the ambient pH treatments and 17.97 ± 0.17°C and 14.04 ± 0.21°C for the low pH treatments) and embryo tanks (17.75 ± 0.20°C and 14.26 ± 0.21°C for the ambient pH treatments and 17.80 ± 0.23°C and 14.10 ± 0.20 °C for the low pH treatments). We also successfully

maintained a pH difference of just over 0.3 units between treatments in larval tanks (7.92 ± 0.02 and 7.58 ± 0.05 for high temperature treatments and 7.95 ± 0.04 and 7.60 ± 0.04 for low temperature treatments) and in embryo tanks (7.92 ± 0.02 and 7.58 ± 0.04 for high temperature treatments and 7.97 ± 0.06 and 7.60 ± 0.04 for low temperature treatments). Daily temperature and pH by treatment during the experiment are included in Supplementary Figures 1-4. The aragonite saturation in our ambient pH treatments was just over 2, while the aragonite saturation for the low pH treatments was around 1.

The continuous temperature loggers in the larval tanks showed minimal daily fluctuations in temperature (Supplementary Figure 5). The temperature loggers in the settlement water baths showed rapid but minimal temperature fluctuations as the water chillers turned on and off to maintain temperature around the targeted levels (Supplementary Figure 6). While we were not able to take measurements in the settlement jars, we are confident that with the lack of air space in each jar and submersion in water baths, temperature and pH remained close to the starting targeted values as jars were filled with water from each respective header tank.

Larval Hatching

The number of hatched larvae was highest in the ambient treatment, followed by both single stressor treatments, with the multiple stressor treatment showing the lowest hatching success. On day three, percent surviving hatched larvae compared to estimated number of fertilized embryos was 74% in the control treatment, 63% in the high temperature treatment, 56% in the low pH treatment, and 35% in the multiple stressor treatment. Notably, hatching occurred earlier in the high temperature treatments compared to the low temperature treatments. On day one post fertilization, the control only had 2% hatched and swimming larvae and the low

pH treatment had 3%, while the high temperature treatment had 66% and the high temperature low pH treatment had 59% (Figure 3).

Model comparison revealed that pH, temperature, and day influenced hatching success, and further that temperature influenced hatch timing, as was reflected visually in the data (Supplementary Table 2). Model parameter coefficients are summarized in Table 2 for the best fitting model. Model diagnostics showed a normal QQ plot and a slight trend of positive residuals all falling in the middle of the predictions range. Given the complicated biological processes at play with larvae hatching and dying in the system, we felt this model satisfactorily represented the data. The model with temperature, day, and the interaction of temperature and day also had reasonable support, indicating that support for the effect of pH is minimal. The estimated effect sizes in our best fitting model also indicate a stronger effect of temperature than pH treatment.

Larval Settlement

Larval settlement (measured as the proportion of larvae that settled out of the total abalone added to each jar) was much higher in the two ambient pH treatments than in the two low pH treatments. Averaged across the five days of settlement trials, we had 81% settlement in the ambient treatment, 89% settlement in the high temperature treatment, 58% settlement in the low pH treatment, and 50% settlement in the high temperature low pH treatment. High temperature may have slightly enhanced settlement and decreased the time to settlement in the ambient pH treatment. However, higher temperature did not appear to have any positive effect on settlement when combined with low pH (Figure 4).

For larval settlement, we compared 13 models using AICc (Supplementary Table 3). Two models had notable support: one included day, pH, temperature, pH*temperature, and temperature*day as factors impacting settlement., the other included day, pH, temperature, and temperature*day. The data do not provide strong evidence to judge one as being more supported than the other (though the first model had slightly more support). The data provide support to models that include interaction terms, although the support is not so overwhelming to dismiss a simpler model only including day and pH which had an AICc just 4.14 higher. For the best fitting model, residuals appeared randomly distributed for the best fitting model apart from a few low outliers, and QQ plot showed a very slight left skew. Parameter coefficients for the two best performing models and the simpler 3 parameter model are shown in Table 3.

As our experimental design required us to maintain tanks of swimming larvae throughout the entire window for settlement, we anticipated that some larvae could settle onto the silos used for larval rearing during this time. The larvae stuck to the silos that were removed on day ten were not included in any statistical analysis for survival. There was no way to determine if these abalone had settled on the sides or bottom of the silos or if they had somehow become stuck in the silo mesh, nor was there a way to determine if they were alive or dead at the time the experiment ended. At the conclusion of the experiment, the mean number of larvae stuck in the silo was 157 in the control treatment, 246 in the high temperature treatment, eight in the low pH treatment, and four in the high temperature low pH treatment. There were significantly more larvae from both ambient pH treatments left in the silos than there were from either of the low pH treatments (Two-way ANOVA, $F_{1,9}$=11.8, p=0.007), but there was no significant effect of temperature on number of larvae stuck in the silos (Two-way ANOVA, $F_{1,9}$=0.56, p=0.475) (Supplementary Figure 7).

Due to a spill of experimental replicates, we only had N=4 instead of the usual N=12 on day 11 of the experiment. Two of these replicates were from the low pH treatment, one from the high temperature low pH treatment, one from the high temperature treatment, and none from the ambient treatment. This data loss may limit our statistical power but does not impact the accuracy of the study's results.

Larval Survival

Because of the significant differences in surviving hatched abalone after day three, when we removed the embryo tanks and halted new hatching in the experiment, we opted to analyze survival in the larval stage separately from the hatching stage. While the number of living larvae was dependent on treatment during this larval phase, the declines in abalone numbers we saw across the larval phase were very similar between treatments. On day six of the experiment, mean larval survival compared to fertilized embryos in each tank was 84% in the ambient treatment, 64% in the high temperature treatment, 58% in the low pH treatment, and 31% in the high temperature low pH treatment (increases in larval survival between days three and six are due only to variability in sampling—no additional larvae could enter the system after day three when we removed the embryo tanks). On day 10, these numbers were 71%, 56%, 48%, and 27%, respectively; they had declined by 13%, 13%, 17%, and 15%, respectively, during the four-day period. Both pH and temperature impacted the maximum survival rate, but neither factor nor their interaction appeared to dramatically impact the rate of larval mortality in the latter half of the larval stage.

Our models supported these findings. Model selection indicated strong support for the model with pH, temperature, and day effects. While some other models had marginally larger

delta AIC, these models were always more complex version of this simpler model (Table 4, Supplementary Table 4). QQ plot and plotted residuals vs. fitted values showed normal results with a random distribution of residuals.

Shell Length

Low pH appeared to have the greatest negative impact on the shell length of larval abalone across all three days where shell length was measured. Shells in the low pH treatments were 9%, 18%, and 16% smaller than shells in the two ambient pH treatments on days three, seven, and ten, respectively. Temperature had minimal impact on shell size, with shells being only 4%, 0.1%, and 0.6% smaller in the ambient relative to high temperature treatments on days three, seven, and ten, respectively (Figure 5).

Comparison of 18 mixed models showed that the full model with pH, temperature, day, and all three 2-way interactions, as well as the random effect of larval tank had the lowest AICc (Supplementary Table 5). The parameter coefficients in this model (Table 5) demonstrated the larger influence of pH, which we noted visually in the data, followed by the influence of temperature. QQ plots for the best fitting model indicated slightly heavy-tailed data, and comparisons of residuals and predicted values showed random distribution.

While our approach of measuring the entire abalone length when distinguishing between the shell and tissue was difficult might have introduced some measurement bias by potentially overestimating length, it is noteworthy that abalone from low pH treatments were smaller. Consequently, any potential bias would likely make the shell lengths of the low and ambient pH treatments more similar rather than artificially increasing the difference in shell length between treatments.

Discussion

This study investigated the interacting effect of two environmental stressors, temperature and pH, on pinto abalone, a species designated as endangered in Washington state. Our experimental results suggest that both high temperature and low pH have the capacity to negatively impact early developmental processes in pinto abalone in the near future. Warmer temperatures led to faster hatching of abalone embryos in our experiment, but overall, higher temperatures and lower pH led to fewer surviving hatched abalone 3dpf. Mortality rates were relatively low in the latter half of the larval phase and were similar between treatments. pH stood out as the main stressor impacting abalone larval settlement and size.

Hatching

In our study, pinto abalone hatching was negatively impacted by increased temperature and decreased pH. The high hatching rates in both high temperature treatments (ambient and low pH) 1dpf were likely due to increased metabolism and faster development of embryos in the warmer temperature (Gillooly et al., 2001). The positive relationship between temperature and rate of development has been noted for other abalone species such as donkey's ear, white, South African, greenlip, and blacklip, among others (Grubertt & Ritar, 2004; Mccormick et al., 2016; Mzozo et al., 2021; Pedroso, 2017). In our study, this faster development, however, was less apparent after the embryonic phase. By 3dpf (measured just before we removed the embryo tanks from the larval rearing system), both low pH treatments (high and ambient temperatures) had the lowest number of larvae remaining. The data show a lower hatching rate in the low pH treatment, which is distinct from the lower post-hatching immediate survival in the high

temperature low pH treatment, but our sampling interval is insufficient to confirm this difference. Results from other studies do not show clear trends that would support one of these scenarios over the other. A metanalysis of multiple stressors on marine embryos and larvae found that embryos are more resilient to environmental stressors than larvae (Przeslawski et al., 2015). However, negative impacts of ocean acidification have been seen in both stages. Delayed development of embryos, delayed hatching, and longer hatching duration have been seen in various invertebrates under low pH conditions (Findlay et al., 2009; Long et al., 2013). Traits such as embryonic and larval development, larval size, and survival can be negatively impacted by low pH in marine molluscs (Gazeau et al., 2013). For instance, a study on donkey's ear abalone demonstrated that hatching and trochophore larval survival decreased with declining pH levels (Tahil & Dy, 2016). Based on our results and information gleaned from previous studies on marine invertebrate development, it is likely that the pinto abalone embryos in our study had faster development due to high temperatures and hindered development due to low pH. After the embryonic phase, hatched larvae seemed more susceptible to higher temperatures and continued to be negatively impacted by low pH in the first 3dpf.

Survival in the late larval stage

During the latter half of our experiment, minimal larval mortality occurred and was relatively consistent across all four treatments. It appears that the impacts of increased temperature and decreased pH on survival may have been more pronounced primarily during the early larval stage. The trend we saw could also have been due to variability in vulnerability between individual larvae—the less resilient individuals may have died quickly, leaving more resilient larvae that survived better throughout the rest of the experiment. Additional

investigation is necessary to determine what specific periods of the embryonic and larval phases are most susceptible to ocean acidification.

In the wild, this vulnerability of larvae implies that changing ocean conditions could lead to reduced recruitment if, for example, a heat wave or period of upwelling coincided with abalone larval periods. As ocean conditions change, pH drops and temperature spikes may become more frequent or sustained (IPCC, 2014; Oliver et al., 2018). In the hatchery, this also suggests that greater emphasis should be placed on buffering water during the early days of the larval phase to reduce mortalities.

Settlement

pH but not temperature significantly impacted pinto abalone settlement timing and success in our study. Other investigations have also found that low pH can decrease larval settlement and increase developmental time in shelled molluscs and other invertebrate taxa (Doropoulos et al., 2012; Gazeau et al., 2013; Webster et al., 2013). A review of larval settlement under ocean acidification highlighted that changes in larval perception of settlement substrate and cues in lower pH conditions could lead to delayed or decreased settlement and metamorphosis across various taxa (Espinel-Velasco et al., 2018). This delayed or decreased settlement, combined with the inability of abalone larvae to acquire more energy through feeding in the larval phase, could pose a substantial bottleneck for pinto abalone. As larval survival of marine species generally decreases as larval duration increases (O'Connor et al., 2007; Rumrill, 1990), any slowing of the settlement process overall could negatively impact the abalone population. In the Salish Sea, pH levels undergo seasonal fluctuations due to a combination of physical and biological processes (Lowe et al., 2019). Higher pH values are typically observed

during the spring and summer months. This seasonal variation is noteworthy as it aligns with the spawning season of pinto abalone, potentially providing favorable conditions for their reproduction and development.

We did not expect the lack of any temperature effect during the settlement trials. Although we observed a very slight decrease in larval duration in the high temperature (ambient pH) treatment, temperature did not influence settlement statistically. Generally, temperature is one of the most dominant factors in predicting larval duration (O'Connor et al., 2007). Previous studies in white and South African abalone found faster settlement or increased competency to settle with increased temperature (D. L. Leighton, 1972; Mzozo et al., 2021). However, these results likely only hold within the ideal temperature range of a given species. The abalone in our experiment were stressed by the increased temperature, as demonstrated by the higher mortalities in the early larval stage. While our selected temperature did not result in complete mortality, the stress experienced by the surviving larvae might have slowed down settlement, contrary to our expectations. Our experiment with two temperatures does not allow the construction of a complete thermal performance curve for pinto abalone. However, existing studies suggest that survival and other metrics of larval success or development may not align precisely on the same thermal performance curves (Buckley et al., 2023). This means there could be differences in the temperatures at which performance failure vs. mortality occur (Buckley et al., 2023).

Larval duration also affects dispersal, with long larval duration increasing dispersal distances (Kinlan et al., 2005; O'Connor et al., 2007). If low pH increases larval duration by reducing or delaying abalone competency, it could have important implications for abalone population connectivity, especially in a broadcast spawning species where the proximity of adults is critical for successful reproduction (Allee, 1931; Gascoigne & Lipcius, 2004). A more

widespread but sparser population could impact the efforts of restoration practitioners in Washington State. Abalone could end up further from optimal habitat and from each other, potentially complicating restoration efforts.

Shell length

Our results were consistent with other studies that found reduced growth or increased abnormalities in low pH conditions for pinto abalone, European abalone, Ezo abalone, and reddish-rayed abalone (Avignon et al., 2020; Byrne et al., 2011, 2011; Crim et al., 2011; Kimura et al., 2011; Onitsuka et al., 2018). A decrease in shell strength and growth in European abalone represented trade-offs necessary to sustain metabolism under low pH conditions (Avignon et al., 2020). The lack of temperature impact on shell length in our study was counterintuitive given what is known about the relationship between metabolism, development, and temperature (Gillooly et al., 2001; Mccormick et al., 2016; Mzozo et al., 2021). However, a study on tropical donkey's ear abalone noted a decrease in larval size above a certain temperature threshold (Pedroso, 2017). In our study, faster hatching rates suggest that abalone in the high-temperature treatment were developing faster, but perhaps physiological stress from those high temperatures prevented the faster shell growth we might expect at higher temperatures. Larval size has been linked to predation rates in other species (Allen, 2008; Bailey, 1984), so it is possible that declines in larval and spat size would lead to higher predation of abalone. Further, in a study on a bryozoan with nonfeeding larvae, links were found between larval size and survival post-metamorphosis (Marshall et al., 2003), indicating that smaller size at settlement could lead to lower survival through the juvenile stage.

Implications for conservation aquaculture

Although water conditions can be controlled to some extent in a hatchery setting, the changing oceanographic conditions in pinto abalone habitat raise the question of how restoration practitioners should prepare abalone for maximum success in the wild. As climate change has increasingly affected shellfish and, specifically, the aquaculture industry, more research has been conducted into the efficacy of selective breeding on building climate resilience in various species (Tan et al., 2020). Research has been conducted on the potential use of genetics or genomics for conveying heat tolerance in abalone and the potential of acclimation within generations (Liu et al., 2022; Yu et al., 2023). Fewer consistent results regarding the potential of acclimation or transgenerational effects of ocean acidification on abalone have been found. In European abalone, no carryover effects were seen after parental exposure to ocean acidification, with larval and juvenile fitness negatively affected by a drop in pH (Auzoux-Bordenave et al., 2022). Evidence from a recent experiment on red abalone indicated that exposure to ocean acidification during early life stages negatively affected adult growth and offspring survival (Neylan et al., 2023). More research is needed to understand whether exposure to ocean acidification during early stages could harden abalone against unfavorable conditions that they or their offspring might experience outside the hatchery. An alternative approach would be to prevent the exposure of offspring to ocean acidification at critical early life stages.

When it comes to outplanting, there are also decisions that need to be made. If the goal is to restore abalone populations to their former abundance and distribution, it is essential to release abalone into the wild that possess the highest level of climate resilience possible. An alternative option, however, is to find sites that are natural refugia to ocean acidification and other damaging factors. In Mexico, a study on green abalone found substantial differences in juvenile survival

and growth between two sites with different exposure to oceanographic stressors (Boch et al., 2018). Targeting the best sites for outplanting abalone could enhance their survival rates. However, considering the rapid pace of climate change, this strategy might only postpone the inevitable impacts on the species. It is possible that abalone could be better equipped to handle these challenges with genetic priming or individual exposure to environmental conditions.

Conclusions

Our study can help determine the best hatchery conditions for rearing pinto abalone larvae and help inform what conditions are essential to monitoring at restoration sites in Washington. This study is an important step in understanding the possible effects of climate change on abalone larval survival and settlement and, therefore, understanding population level changes to pinto abalone that would result from climate change. Our results showed that ocean acidification will have a negative impact on larval survival, growth, and settlement. While the effects of temperature were not as pronounced, the increased temperature still negatively impacted larval survival. Combined stressors had additive effects on larval survival when both low pH and high temperature were imposed concurrently. Understanding the impact of these stressors will help optimize the hatchery rearing of abalone, understand how they will survive and reproduce in the wild, and improve chances of successfully restoring this endangered species.

Our study also offers a first look at how temperature and pH could differentially contribute to changes in pinto abalone development rate and survival. As we look forward, it will be necessary to study these impacts when pH and temperature levels are variable instead of constant—growing evidence suggests that variability, in addition to mean temperature, may have

important physiological implications as the climate changes (Buckley et al., 2023; Dillon & Woods, 2016). Performance curves can look different for development than they do for survival—both in shape and in the magnitude of the optima (Abarca et al., 2024). We may have seen some evidence of this in our distinct results for hatching, settlement, survival, and size, and further investigation into these distinctions and how they may impact species like abalone at population levels would help bolster our understanding of the species and how climate change may impact their recovery.

Acknowledgements

The authors would like to thank Stuart Ryan, Sarah Henneford, and Lindsay Alma for their assistance in experimental setup and execution. Thanks to Mike Maher, Danielle Perez, Paul McElhany, and Larken Root for training and troubleshooting the spec pH system and calculations. We thank Tim Essington for his help in designing and discussing the best options for statistical analysis and reviewing the manuscript. Thanks to Jennifer Ruesink and Jesse Zaneveld for their reviews of the manuscript. Thank you to Sarah Ghandour and Ella Persson for help photographing larval shells for size analysis.

Figures and Tables

Table 1. Mean and standard deviation of water chemistry values for each treatment in larvae and embryo tanks.

Treatment	pH	Temperature (°C)	Aragonite Saturation	pCO_2 (µatm)	Salinity (PSU)	Alkalinity (µmol/kg)
Larval Tanks						
High Temp	7.92 ± 0.02	17.88 ± 0.18	2.19 ± 0.11	651.7 ± 41.43	30.01 ± 0.07	2612.98 ± 51.85
High Temp/ Low pH	7.58 ± 0.05	17.97 ± 0.17	1.11 ± 0.11	1604.6 ± 173.5	30.01 ± 0.07	2650.91 ± 45.08
Ambient	7.95 ± 0.04	14.11 ± 0.25	2.02 ± 0.20	609.3 ± 59.7	30.00 ± 0.07	2585.13 ± 13.84
Low pH	7.60 ± 0.04	14.04 ± 0.21	1.00 ± 0.09	1480.3 ± 137.9	30.00 ± 0.07	2664.12 ± 14.67
Embryo Tanks						
High Temp	7.92 ± 0.02	17.75 ± 0.20	2.19 ± 0.13	665.6 ± 46.3	29.97 ± 0.06	2607.66 ± 11.22
High Temp/ Low pH	7.58 ± 0.04	17.80 ± 0.23	1.10 ± 0.09	1598.1 ± 155.2	29.98 ± 0.06	2661.41 ± 29.83
Ambient	7.97 ± 0.06	14.26 ± 0.21	2.13 ± 0.30	577.5 ± 83.6	29.90 ± 0.13	2588.03 ± 10.57
Low pH	7.60 ± 0.04	14.10 ± 0.20	1.00 ± 0.10	1484.4 ± 139.8	29.94 ± 0.07	2661.93 ± 26.26

In larval tanks, N=33 for pH, temperature, aragonite saturation, pCO_2, and salinity. N= 6 for alkalinity. In embryo tanks, N=12 for pH, temperature, aragonite saturation, pCO_2, and salinity, N=3 for alkalinity.

Table 2. Summary of the best fitting hatching model

Term	Estimate	Std. Error
(Intercept)	4411.5	692.8
pH (low)	-812.5	357.7
Temp (low)	-5100.4	946.5
Day	-415.6	309.8
Temp (low)*day	2416.5	438.1

Table 3a. Parameter coefficients for the best fitting settlement model.

Term	Estimate	Std. Error
(Intercept)	1.00	0.20
pH (low)	-0.46	0.06
Temp (low)	-0.82	0.27
Day	0.03	0.02
pH(low)*temp(low)	0.14	0.08
Temp (low)*day	0.09	0.03

Table 3b. Parameter coefficients for the second-best fitting settlement model.

Term	Estimate	Std. Error
(Intercept)	1.00	0.20
pH (low)	-0.40	0.04
Temp (low)	-0.79	0.28
Day	0.03	0.02
Temp (low)*day	0.09	0.03

Table 3c. Parameter coefficients for alternate settlement model

Term	Estimate	Std. Error
(Intercept)	0.57	0.15
pH (low)	-0.39	0.04
Day	0.07	0.02

Table 4. Parameter coefficients for the best-fitting survival model

Term	Estimate	Std. Error
(Intercept)	4995.61	314.31
pH (low)	-1823.51	106.26
Temp (low)	1378.05	106.26
Day	-148.76	37.57

Table 5. Parameter coefficients for the best-fitting size model

Term	Estimate	Std. Error
(Intercept)	273.400	3.173
pH (low)	-18.826	4.011
Temp (low)	12.717	4.040
Day	2.422	0.375
pH (low)* temp (low)	1.625	4.003
pH (low) * day	-3.389	0.442
Temp (low)* day	-0.984	0.442

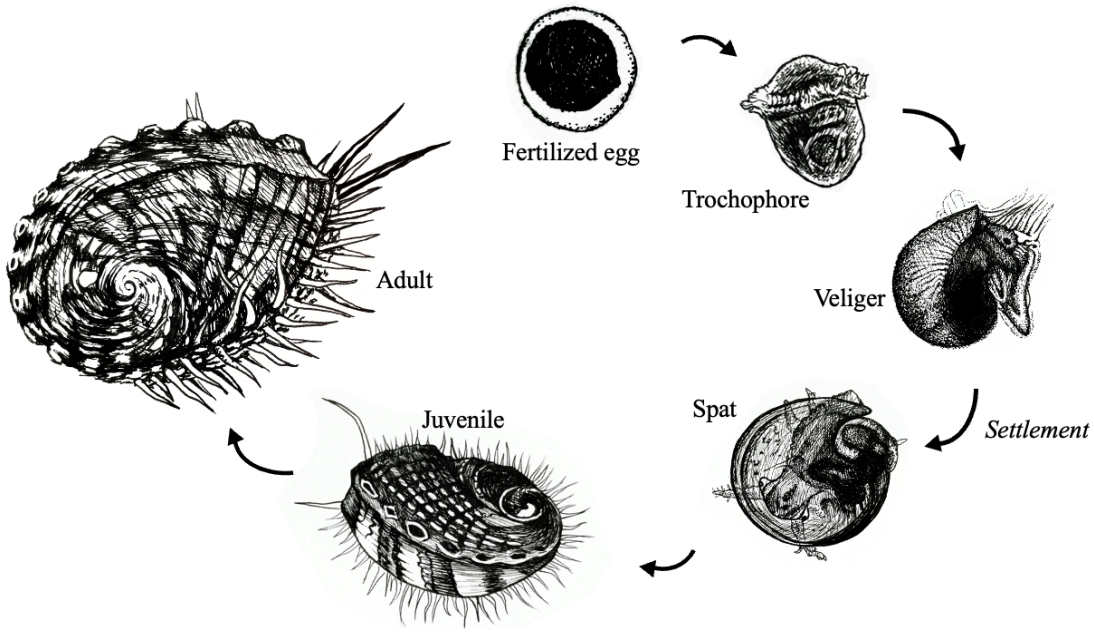

Figure 1. Abalone life cycle. Fertilized eggs hatch 1-3 days post spawn, then the larval phase (trochophore and veliger) lasts 7-10 days before settlement onto the benthos occurs and metamorphosis into spat occurs. Spat grow into juvenile and eventually adult abalone. Illustrations by Katie Craighill.

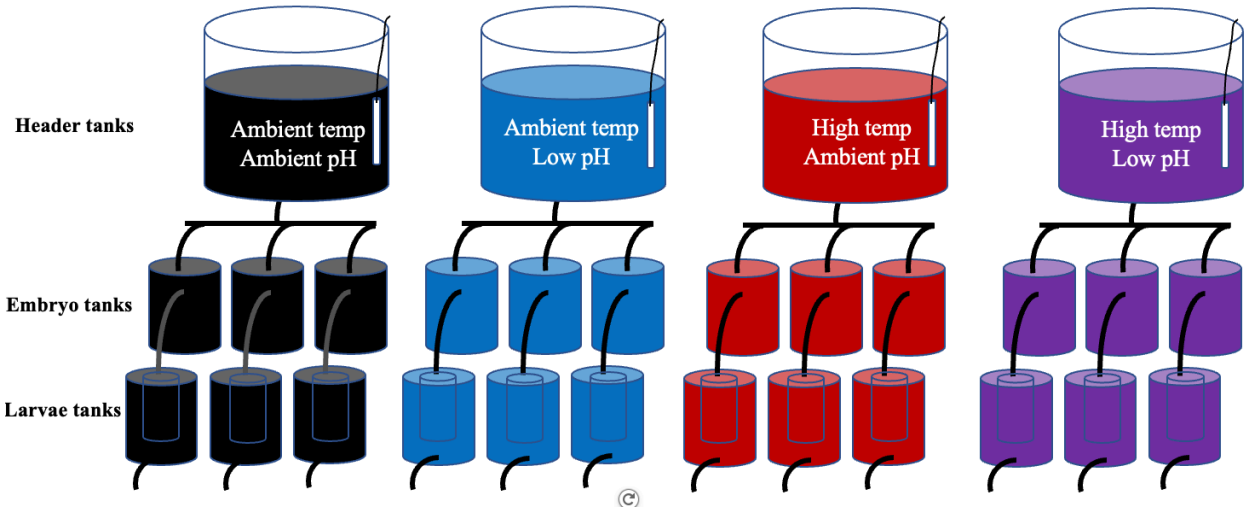

Figure 2a. Schematic of experiment setup for days 0-3. One header tank was adjusted to each of the four temperature and pH level combinations. Each header fed three experimental tanks. Embryos were placed on the floor of each tank. As embryos hatched, larvae would be pulled through into the second tier of tanks which included silos to prevent loss of abalone. Larval abalone lived in these silos until day 10 of the experiment or until they were removed for settlement trials.

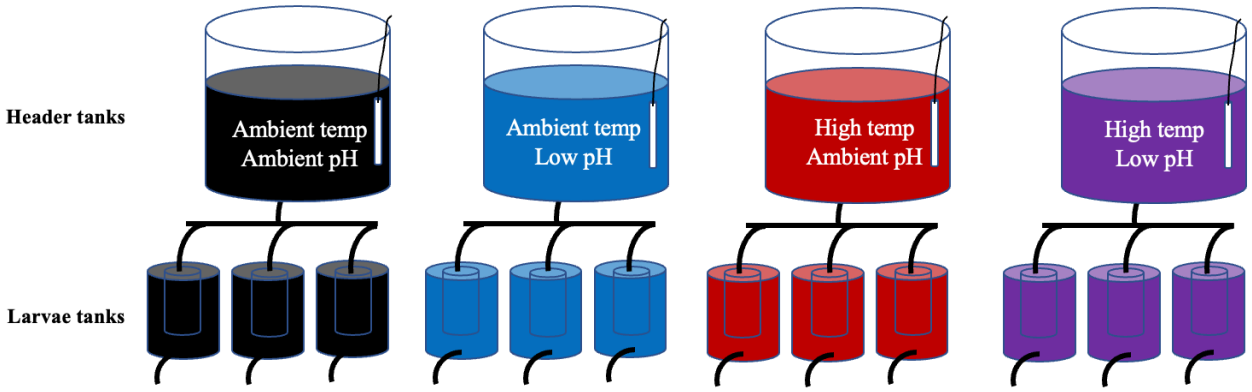

Figure 2b. Schematic of experimental setup for days 3-10. On the third day after fertilization, the embryo tanks were removed from the system, so the header tanks fed directly into the larval silos.

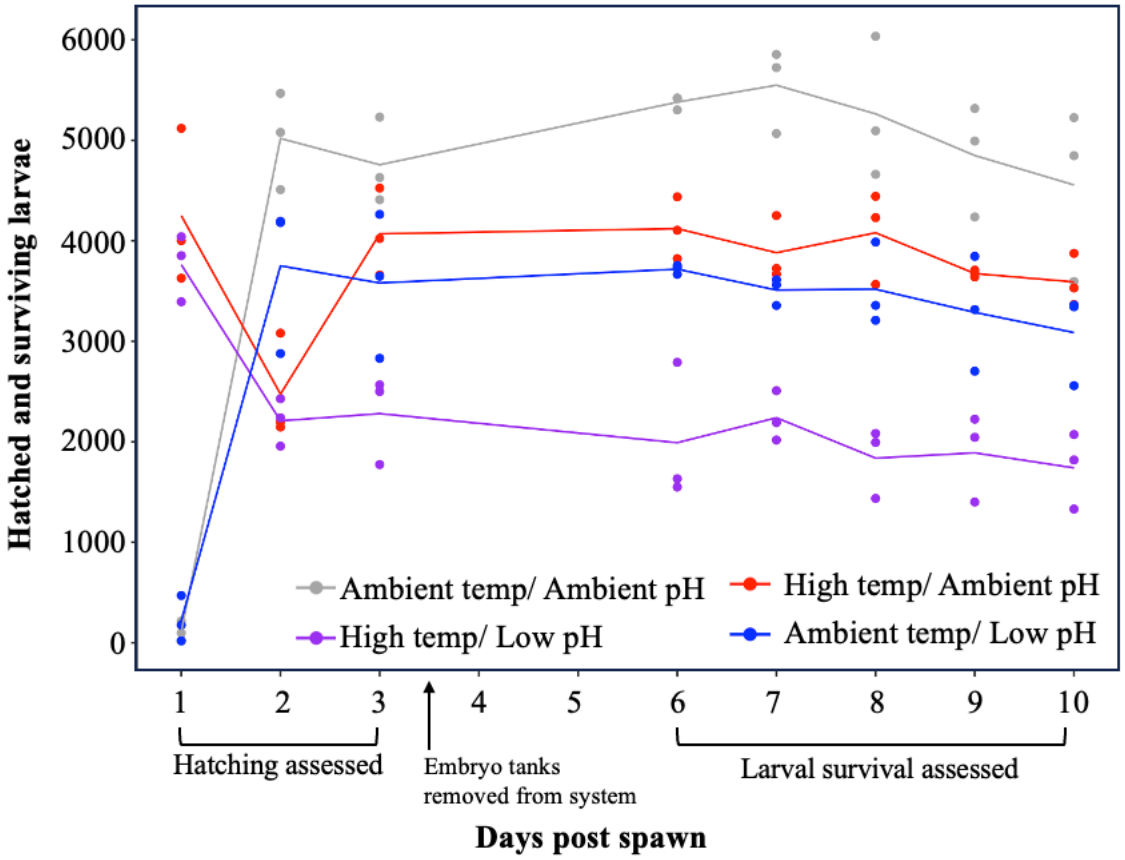

Figure 3. Approximated number of larvae in each replicate tank from days 1-10 of the experiment. Lines represent the mean number of larvae for each treatment, while each of the replicates is shown by colored dots. The increasing numbers at the beginning are due to embryos hatching and more larvae entering the larval tanks from the embryo tanks. Embryo tanks were removed from the system on day 3, so days 6-10 track surviving larvae of those that hatched on days 1-3. Grey=ambient, red= high temperature, blue= low pH, purple=high temperature/ low pH.

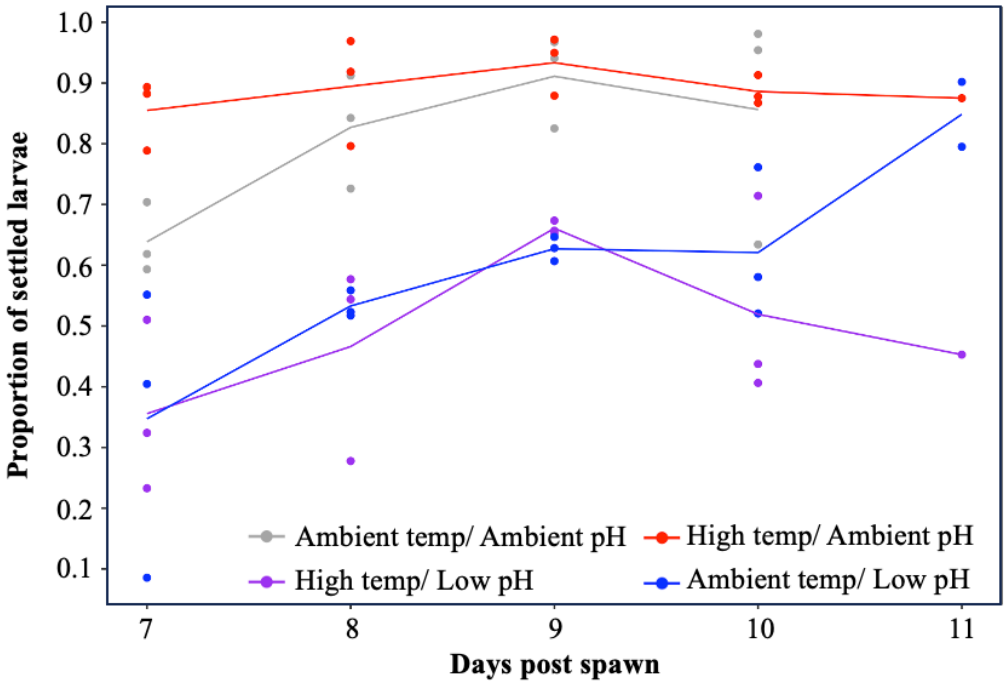

Figure 4. Fraction of larvae that settled during trials from days 7-11 of the experiment. Different larvae were used for each trial. Lines represent the mean settlement rate for each treatment, while each of the replicates are shown by colored dots. Grey=ambient, red= high temperature, blue= low pH, purple= high temperature/ low pH.

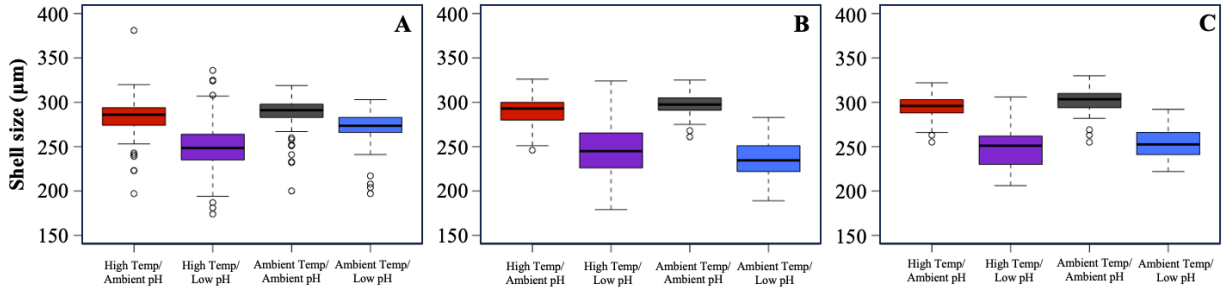

Figure 5. Abalone shell size along longest axis measured for 30 (or as many as available) larvae from each replicate tank on day 3 (A), day 7 (B) and day 10 (C) grouped by treatment. Comparison of linear mixed effects models with replicate tank as a random effect showed that temperature, pH, and temperature*pH were all relevant fixed effects.

References

Abarca, M., Parker, A. L., Larsen, E. A., Umbanhowar, J., Earl, C., Guralnick, R., Kingsolver, J., & Ries, L. (2024). How development and survival combine to determine the thermal sensitivity of insects. *Plos One*, *19*(1), e0291393.

Allee, W. C. (1931). *Animal aggregations, a study in general sociology., (The University of Chicago Press: Chicago, IL, USA)*.

Allen, J. D. (2008). Size-specific predation on marine invertebrate larvae. *The Biological Bulletin*, *214*(1), 42–49.

Auzoux-Bordenave, S., Ledoux, A., Martin, S., Di Poi, C., Suquet, M., Badou, A., Gaillard, F., Servili, A., Le Goïc, N., & Huchette, S. (2022). Responses of early life stages of European abalone (*Haliotis tuberculata*) to ocean acidification after parental conditioning: Insights from a transgenerational experiment. *Marine Environmental Research*, *181*, 105753.

Avignon, S., Auzoux-Bordenave, S., Martin, S., Dubois, P., Badou, A., Coheleach, M., Richard, N., Di Giglio, S., Malet, L., & Servili, A. (2020). An integrated investigation of the effects of ocean acidification on adult abalone (*Haliotis tuberculata*). *ICES Journal of Marine Science*, *77*(2), 757–772.

Bailey, K. M. (1984). Comparison of laboratory rates of predation of five species of marine fish larvae by three planktonic invertebrates: Effects of larval size on vulnerability. *Marine Biology*, *79*(3), 303–309.

Bates, D., Maechler, M., Bolker, B., Walker, S., Christensen, R. H. B., Singmann, H., Dai, B., Grothendieck, G., Green, P., & Bolker, M. B. (2015). Package 'lme4.' *Convergence*, *12*(1), 2.

Boch, C. A., Micheli, F., AlNajjar, M., Monismith, S. G., Beers, J. M., Bonilla, J. C., Espinoza, A. M., Vazquez-Vera, L., & Woodson, C. B. (2018). Local oceanographic variability influences the performance of juvenile abalone under climate change. *Scientific Reports*, *8*(1), 5501.

Bouma, J. V. (2007). *Early life history dynamics of pinto abalone (Haliotis kamtschatkana) and implications for recovery in the San Juan Archipelago, Washington State*. University of Washington.

Buckley, L. B., Carrington, E., Dillon, M. E., García-Robledo, C., Roberts, S. B., Wegrzyn, J. L., & Urban, M. C. (2023). Characterizing biological responses to climate variability and extremes to improve biodiversity projections. *PLOS Climate*, *2*(6), e0000226.

Byrne, M. (2011). Impact of ocean warming and ocean acidification on marine invertebrate life history stages: Vulnerabilities and potential for persistence in a changing ocean. *Oceanography and Marine Biology Annual Review*, *49*, 1–42.

Byrne, M., Ho, M., Wong, E., Soars, N. A., Selvakumaraswamy, P., Shepard-Brennand, H., Dworjanyn, S. A., & Davis, A. R. (2011). Unshelled abalone and corrupted urchins: Development of marine calcifiers in a changing ocean. *Proceedings of the Royal Society B: Biological Sciences*, *278*(1716), 2376–2383.

Caldeira, K., & Wickett, M. E. (2003). Anthropogenic carbon and ocean pH. *Nature*, *425*(6956), 365–365.

Carson, H. S., Morin, D. J., Bouma, J. V., Ulrich, M., & Sizemore, R. (2019). The survival of hatchery-origin pinto abalone *Haliotis kamtschatkana* released into Washington waters. *Aquatic Conservation: Marine and Freshwater Ecosystems*, *29*(3), 424–441.

Chan, K. Y. K., Sewell, M. A., & Byrne, M. (2018). Revisiting the larval dispersal black box in the Anthropocene. *ICES Journal of Marine Science*, *75*(6), 1841–1848.

Cooley, S. R., Kite-Powell, H. L., & Doney, S. C. (2009). Ocean acidification's potential to alter global marine ecosystem services. *Oceanography*, *22*(4), 172–181.

Crim, R. N., Sunday, J. M., & Harley, C. D. (2011). Elevated seawater CO_2 concentrations impair larval development and reduce larval survival in endangered northern abalone (*Haliotis kamtschatkana*). *Journal of Experimental Marine Biology and Ecology*, *400*(1–2), 272–277.

Dickson, A. G., Sabine, C. L., & Christian, J. R. (2007). *Guide to best practices for ocean CO2 measurements.* North Pacific Marine Science Organization.

Dillon, M. E., & Woods, H. A. (2016). Introduction to the symposium: Beyond the mean: Biological impacts of changing patterns of temperature variation. *Integrative and Comparative Biology*, *56*(1), 11–13.

Doropoulos, C., Ward, S., Diaz-Pulido, G., Hoegh-Guldberg, O., & Mumby, P. J. (2012). Ocean acidification reduces coral recruitment by disrupting intimate larval-algal settlement interactions. *Ecology Letters*, *15*(4), 338–346.

Espinel-Velasco, N., Hoffmann, L., Agüera, A., Byrne, M., Dupont, S., Uthicke, S., Webster, N. S., & Lamare, M. (2018). Effects of ocean acidification on the settlement and metamorphosis of marine invertebrate and fish larvae: A review. *Marine Ecology Progress Series*, *606*, 237–257.

Feely, R. A., Sabine, C. L., Lee, K., Berelson, W., Kleypas, J., Fabry, V. J., & Millero, F. J. (2004). Impact of anthropogenic CO_2 on the $CaCO_3$ system in the oceans. *Science*, *305*(5682), 362–366.

Findlay, H. S., Kendall, M. A., Spicer, J. I., & Widdicombe, S. (2009). Future high CO_2 in the intertidal may compromise adult barnacle *Semibalanus balanoides* survival and embryonic development rate. *Marine Ecology Progress Series*, *389*, 193–202.

Gascoigne, J., & Lipcius, R. N. (2004). *Allee effects in marine systems*. *269*, 49–59.

Gattuso, J.-P., Epitalon, J.-M., Lavigne, H., Orr, J., Gentili, B., Hagens, M., Hofmann, A., Mueller, J.-D., Proye, A., & Rae, J. (2015). Package 'seacarb.'

Gazeau, F., Parker, L. M., Comeau, S., Gattuso, J.-P., O'Connor, W. A., Martin, S., Pörtner, H.-O., & Ross, P. M. (2013). Impacts of ocean acidification on marine shelled molluscs. *Marine Biology*, *160*, 2207–2245.

Gillooly, J. F., Brown, J. H., West, G. B., Savage, V. M., & Charnov, E. L. (2001). Effects of size and temperature on metabolic rate. *Science*, *293*(5538), 2248–2251.

Griffen, B. D., Belgrad, B. A., Cannizzo, Z. J., Knotts, E. R., & Hancock, E. R. (2016). Rethinking our approach to multiple stressor studies in marine environments. *Marine Ecology Progress Series*, *543*, 273-281.

Grubert, M. A., & Ritar, A. J. (2004). The effect of temperature on the embryonic and larval development of blacklip (*Haliotis rubra*) and greenlip (*H. laevigata*) abalone. *Invertebrate Reproduction & Development*, *45*(3), 197–203.

Ianson, D., Allen, S. E., Moore-Maley, B. L., Johannessen, S. C., & Macdonald, and R. W. (2016). Vulnerability of a semi-enclosed estuarine sea to ocean acidification in contrast with hypoxia. *Geophysical Research Letters*, *43*(11), 5793–5801.

IPCC, 2014: Climate Change 2014: Synthesis Report. Contribution of Working Groups I, II and III to the Fifth Assessment Report of the Intergovernmental Panel on Climate Change [Core Writing Team, R.K. Pachauri and L.A. Meyer (eds.)]. IPCC, Geneva, Switzerland, 151 pp.

Kavousi, J., Roussel, S., Martin, S., Gaillard, F., Badou, A., Di Poi, C., Huchette, S., Dubois, P., & Auzoux-Bordenave, S. (2022). Combined effects of ocean warming and acidification on the larval stages of the European abalone *Haliotis tuberculata*. *Marine Pollution Bulletin*, *175*, 113131.

Kimura, R. Y. O., Takami, H., Ono, T., Onitsuka, T., & Nojiri, Y. (2011). Effects of elevated pCO_2 on the early development of the commercially important gastropod, Ezo abalone *Haliotis discus hannai*. *Fisheries Oceanography*, *20*(5), 357–366.

Kinlan, B. P., Gaines, S. D., & Lester, S. E. (2005). Propagule dispersal and the scales of marine community process. *Diversity and Distributions*, *11*(2), 139–148.

Leighton, D. L. (1972). Laboratory observations on the early growth of the abalone, *Haliotis sorenseni*, and the effect of temperature on larval development and settling success. *Fishery Bulletin*, *70*(2), 373–381.

Leighton, P. (2008). *Abalone hatchery manual* (pp. 1-88). Bord Iascaigh Mhara, Aquaculture Technical Section, Aquaculture Development Division.

Liu, J., Peng, W., Yu, F., Shen, Y., Yu, W., Lu, Y., Lin, W., Zhou, M., Huang, Z., & Luo, X. (2022). Genomic selection applications can improve the environmental performance of aquatics: A case study on the heat tolerance of abalone. *Evolutionary Applications*, *15*(6), 992–1001.

Long, W. C., Swiney, K. M., & Foy, R. J. (2013). Effects of ocean acidification on the embryos and larvae of red king crab, *Paralithodes camtschaticus*. *Marine Pollution Bulletin*, *69*(1–2), 38–47.

Lowe, A. T., Bos, J., & Ruesink, J. (2019). Ecosystem metabolism drives pH variability and modulates long-term ocean acidification in the Northeast Pacific coastal ocean. *Scientific Reports*, *9*(1), 963.

Marshall, D. J., Bolton, T. F., & Keough, M. J. (2003). Offspring size affects the post-metamorphic performance of a colonial marine invertebrate. *Ecology*, *84*(12), 3131–3137.

Mccormick, T. B., Navas, G., Buckley, L. M., & Biggs, C. (2016). Effect of temperature, diet, light, and cultivation density on growth and survival of larval and juvenile white abalone *Haliotis sorenseni* (Bartsch, 1940). *Journal of Shellfish Research*, *35*(4), 981–992.

Morash, A. J., & Alter, K. (2016). Effects of environmental and farm stress on abalone physiology: perspectives for abalone aquaculture in the face of global climate change. *Reviews in Aquaculture*, *8*(4), 342-368.

Morse, A. N., & Morse, D. E. (1984). Recruitment and metamorphosis of *Haliotis* larvae induced by molecules uniquely available at the surfaces of crustose red algae. *Journal of Experimental Marine Biology and Ecology*, *75*(3), 191–215.

Morse, D. E., Duncan, H., Hooker, N., & Morse, A. (1977). Hydrogen peroxide induces spawning in mollusks, with activation of prostaglandin endoperoxide synthetase. *Science*, *196*(4287), 298-300.

Murray, J. W., Roberts, E., Howard, E., O'Donnell, M., Bantam, C., Carrington, E., Foy, M., Paul, B., & Fay, A. (2015). An inland sea high nitrate-low chlorophyll (HNLC) region with naturally high pCO_2. *Limnology and Oceanography*, *60*(3), 957–966.

Mzozo, Z. B., Hugo, S., & Vine, N. G. (2021). Effect of Temperature on the Development and Settlement of the Abalone Larvae *Haliotis midae*: Considerations for Abalone Hatchery Management and Stock Enhancement. *Journal of Shellfish Research*, *40*(1), 119–125.

Neuman, M. J., Wang, S., Busch, S., Friedman, C., Gruenthal, K., Gustafson, R., Kushner, D., Stierhoff, K., Vanblaricom, G. & Wright, S. (2018). A status review of pinto abalone (*Haliotis kamtschatkana*) along the west coast of North America: interpreting trends, addressing uncertainty, and assessing risk for a wide-ranging marine invertebrate. *Journal of Shellfish Research*, *37*(4), 869-910.

Neylan, I. P., Swezey, D. S., Boles, S. E., Gross, J. A., Sih, A., & Stachowicz, J. J. (2023). Within-and transgenerational stress legacy effects of ocean acidification on red abalone (*Haliotis rufescens*) growth and survival. *Global Change Biology*, e17048.

O'Connor, M. I., Bruno, J. F., Gaines, S. D., Halpern, B. S., Lester, S. E., Kinlan, B. P., & Weiss, J. M. (2007). Temperature control of larval dispersal and the implications for marine ecology, evolution, and conservation. *Proceedings of the National Academy of Sciences*, *104*(4), 1266–1271.

Oliver, E. C., Donat, M. G., Burrows, M. T., Moore, P. J., Smale, D. A., Alexander, L. V., Benthuysen, J. A., Feng, M., Sen Gupta, A., & Hobday, A. J. (2018). Longer and more frequent marine heatwaves over the past century. *Nature Communications*, *9*(1), 1–12.

Onitsuka, T., Takami, H., Muraoka, D., Matsumoto, Y., Nakatsubo, A., Kimura, R., Ono, T., & Nojiri, Y. (2018). Effects of ocean acidification with pCO2 diurnal fluctuations on survival and larval shell formation of Ezo abalone, *Haliotis discus hannai*. *Marine Environmental Research*, *134*, 28–36.

Palmer, A. R. (1981). Do carbonate skeletons limit the rate of body growth? *Nature*, *292*(5819), 150–152.

Palmer, A. R. (1992). Calcification in marine molluscs: How costly is it? *Proceedings of the National Academy of Sciences*, *89*(4), 1379–1382.

Pedroso, F. L. (2017). Effects of elevated temperature on the different life stages of tropical mollusk, donkey's ear abalone (*Haliotis asinina*). *Aquaculture, Aquarium, Conservation & Legislation*, *10*(6), 1421–1427.

Piggott, J. J., Townsend, C. R., & Matthaei, C. D. (2015). Reconceptualizing synergism and antagonism among multiple stressors. *Ecology and Evolution*, *5*(7), 1538–1547.

Przeslawski, R., Byrne, M., & Mellin, C. (2015). A review and meta-analysis of the effects of multiple abiotic stressors on marine embryos and larvae. *Global Change Biology*, *21*(6), 2122–2140.

Rogers-Bennett, L., Allen, B. L., & Rothaus, D. P. (2011). Status and habitat associations of the threatened northern abalone: importance of kelp and coralline algae. *Aquatic Conservation: Marine and Freshwater Ecosystems*, *21*(6), 573-581.

Rogers-Bennett, L., Dondanville, R. F., Moore, J. D., & Vilchis, L. I. (2010). Response of red abalone reproduction to warm water, starvation, and disease stressors: Implications of ocean warming. *Journal of Shellfish Research*, *29*(3), 599–611.

Rothaus, D. P., Vadopalas, B., & Friedman, C. S. (2008). Precipitous declines in pinto abalone (*Haliotis kamtschatkana kamtschatkana*) abundance in the San Juan Archipelago, Washington, USA, despite statewide fishery closure. *Canadian Journal of Fisheries and Aquatic Sciences*, *65*(12), 2703-2711.

Rumrill, S. S. (1990). Natural mortality of marine invertebrate larvae. *Ophelia*, *32*(1–2), 163–198.

Sloan, N. A. (1988). Northern abalone, *Haliotis kamtschatkana*, in British Columbia: Fisheries and synopsis of life history information. *Canadian Special Publication of Fisheries and Aquatic Sciences*, *103*, 46.

Sowul, K., Carson, H., Bouma, J., & Fyfe, D. (2022). *Washington State Recovery Plan for the Pinto Abalone* (p. 65 +iv pp). Washington Department of Fish and Wildlife.

Strong, A. L., Kroeker, K. J., Teneva, L. T., Mease, L. A., & Kelly, R. P. (2014). Ocean acidification 2.0: Managing our changing coastal ocean chemistry. *BioScience*, *64*(7), 581–592.

Tahil, A. S., & Dy, D. T. (2016). Effects of reduced pH on the early larval development of hatchery-reared Donkey's ear abalone, *Haliotis asinina* (Linnaeus 1758). *Aquaculture*, *459*, 137–142.

Tan, K., Zhang, H., & Zheng, H. (2020). Selective breeding of edible bivalves and its implication of global climate change. *Reviews in Aquaculture*, *12*(4), 2559–2572.

Tegner, M. J., Haaker, P. L., Riser, K. L., & Vilchis, L. I. (2001). Climate variability, kelp forests, and the southern California red abalone fishery. *Journal of Shellfish Research*, *20*(2), 755–764.

Tomascik, T., & Holmes, H. (2003). Distribution and abundance of *Haliotis kamtschatkana* in relation to habitat, competitors and predators in the Broken Group Islands, Pacific Rim National Park Reserve of Canada. *Journal of Shellfish Research*, *22*(3), 831–838.

Waldbusser, G. G., Hales, B., Langdon, C. J., Haley, B. A., Schrader, P., Brunner, E. L., Gray, M. W., Miller, C. A., & Gimenez, I. (2015). Saturation-state sensitivity of marine bivalve larvae to ocean acidification. *Nature Climate Change*, *5*(3), 273–280.

Webster, N. S., Uthicke, S., Botté, E. S., Flores, F., & Negri, A. P. (2013). Ocean acidification reduces induction of coral settlement by crustose coralline algae. *Global Change Biology*, *19*(1), 303–315.

Weigel, B. L., Small, S. L., Berry, H. D., & Dethier, M. N. (2023). Effects of temperature and nutrients on microscopic stages of the bull kelp (*Nereocystis luetkeana*, Phaeophyceae). *Journal of Phycology*, *59*(5), 893–907.

Wessel, N., Martin, S., Badou, A., Dubois, P., Huchette, S., Julia, V., Nunes, F., Harnye, E., Paillard, C. & Auzoux-Bordenave, S. (2018). Effect of CO2–induced ocean acidification on the early development and shell mineralization of the European abalone (*Haliotis tuberculata*). *Journal of Experimental Marine Biology and Ecology*, *508*, 52-63.

Yu, F., Shen, Y., Peng, W., Chen, N., Gan, Y., Xiao, Q., Liu, J., Lu, Y., Lin, W., & Han, Z. (2023). Metabolic and transcriptional responses demonstrating enhanced thermal tolerance in domesticated abalone. *Science of The Total Environment*, *872*, 162060.

Supplementary Figures and Tables

Supplementary Table 1. Flow rates (L/hr) for each replicate tank and average flow rate (L/hr) for each treatment

	Ambient			High Temperature			High Temperature/Low pH			Low pH		
	Rep 1	Rep 2	Rep 3	Rep 4	Rep 5	Rep 6	Rep 7	Rep 8	Rep 9	Rep 10	Rep 11	Rep 12
Day 1	11.73	9.47	9.51	9.22	10.00	11.69	10.59	11.34	9.18	11.02	10.07	9.34
Mean	10.24			10.30			10.37			10.15		
Day 4	11.92	9.38	9.38	12.00	9.38	10.29	10.65	10.29	11.04	11.39	9.89	8.91
Mean	10.22			10.55			10.66			10.06		

Supplementary Table 2. Model comparison for larval hatching across treatments.

Model Terms	Model Rank	Parameters	ΔAICc
pH + temp + day + temp*day	1	5	0
pH + temp + day + pH*day + temp*day	2	6	0.270
temp + day +temp*day	3	4	2.831
pH + temp + day + pH*temp + temp*day	4	6	2.885
pH + temp + day + pH*temp + pH*day + temp*day	5	7	3.362
pH + day	6	3	19.690
day	7	2	20.182
pH + day + pH*day	8	4	20.941
pH + temp + day	9	4	21.904
temp + day	10	3	22.267
pH + temp + day + pH*day	11	5	23.313
pH + temp + day + pH*temp	12	5	24.609
pH + temp + day + pH*temp + pH*day	13	6	26.203

Supplementary Table 3. Model comparison for larval settlement across treatments.

Model Elements	Model Rank	# of parameters	ΔAICc
pH + temp + day + pH*temp + temp*day	1	6	0
pH + temp + day + temp*day	2	5	0.755
pH + temp + day + pH*temp + pH*day + temp*day	3	7	1.947
pH + temp + day + pH*day + temp*day	4	6	2.701
pH + day	5	3	4.137
pH + day + pH*day	6	4	5.327
pH + temp + day + pH*temp	7	5	5.403
pH + temp + day	8	4	6.486
pH + temp + day + pH*temp + pH*day	9	6	6.641
pH + temp + day + pH*day	10	5	7.763
day	11	2	53.092
temp + day	12	3	55.285
temp + day + temp*day	13	4	55.981

Supplementary Table 4. Model comparison for larval survival (days 6-10) across treatments.

Model Elements	Model Rank	# of parameters	ΔAICc
pH + temp + day	1	4	0
pH + temp + day + pH*temp	2	5	0.802
pH + temp + day + temp*day	3	5	0.976
pH + temp + day + pH*day	4	5	1.599
pH + temp + day + pH*temp + temp*day	5	6	1.829
pH + temp + day + pH*temp + pH*day	6	6	2.470
pH + temp + day + pH*day + temp*day	7	6	2.646
pH + temp + day + pH*temp + pH*day + temp*day	8	7	3.573
pH + day	9	3	80.931
pH + day + pH*day	10	4	83.035
temp + day	11	3	107.743
temp + day + temp*day	12	4	109.819
day	13	2	129.042

Supplementary Table 5. Model comparison for abalone length.

Model Elements	Model Rank	# of parameters	ΔAICc
pH + temp + day + pH*temp + pH*day + temp*day + (1|tank)	1	7	0
pH + temp + day + pH*day + temp*day + (1|tank)	2	6	2.696
pH + temp + day + pH*temp + pH*day + (1|tank)	3	6	3.129
pH + temp + day + pH*day + (1|tank)	4	5	5.911
pH + day + pH*day + (1|tank)	5	4	16.35
pH + temp + day + pH*temp + temp*day + (1|tank)	6	6	55.46
pH + temp + day + temp*day + (1|tank)	7	5	58.09
pH + temp + day + pH*temp + (1|tank)	8	5	60.473
pH + temp + day + (1|tank)	9	4	63.125
pH + day + (1|tank)	10	3	72.584
temp + day +temp*day + (1|tank)	11	4	97.273
temp + day + (1|tank)	12	3	102.595
day + (1|tank)	13	2	107.772

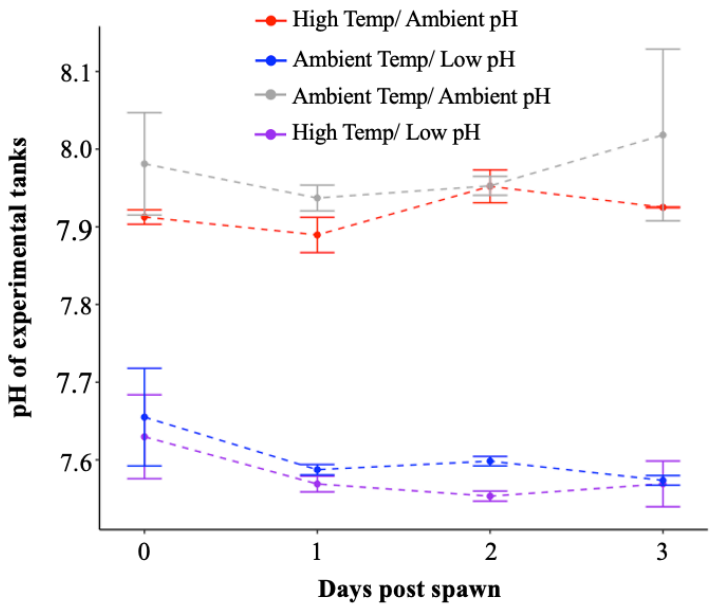

Supplementary Figure 1. Daily spec measurements of pH in each of the embryo tanks grouped by treatment. Grey=ambient, red= high temperature, blue= low pH, purple=high temperature/ low pH. Error bars show standard deviation.

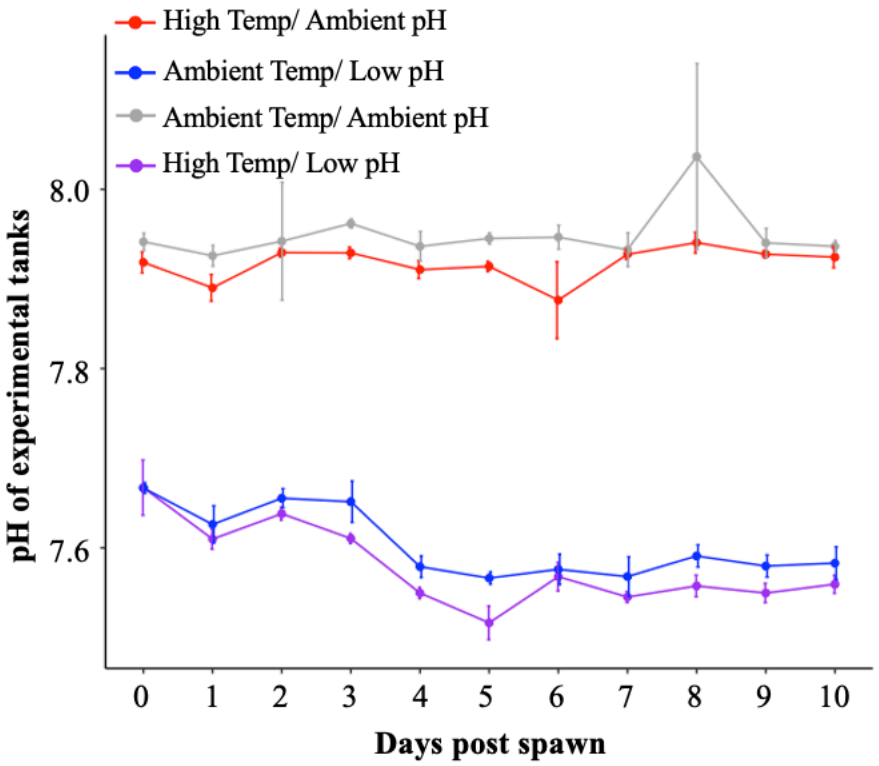

Supplementary Figure 2. Daily spec measurements of pH in each of the larval tanks grouped by treatment. Grey=ambient, red= high temperature, blue= low pH, purple=high temperature/ low pH. Error bars show standard deviation.

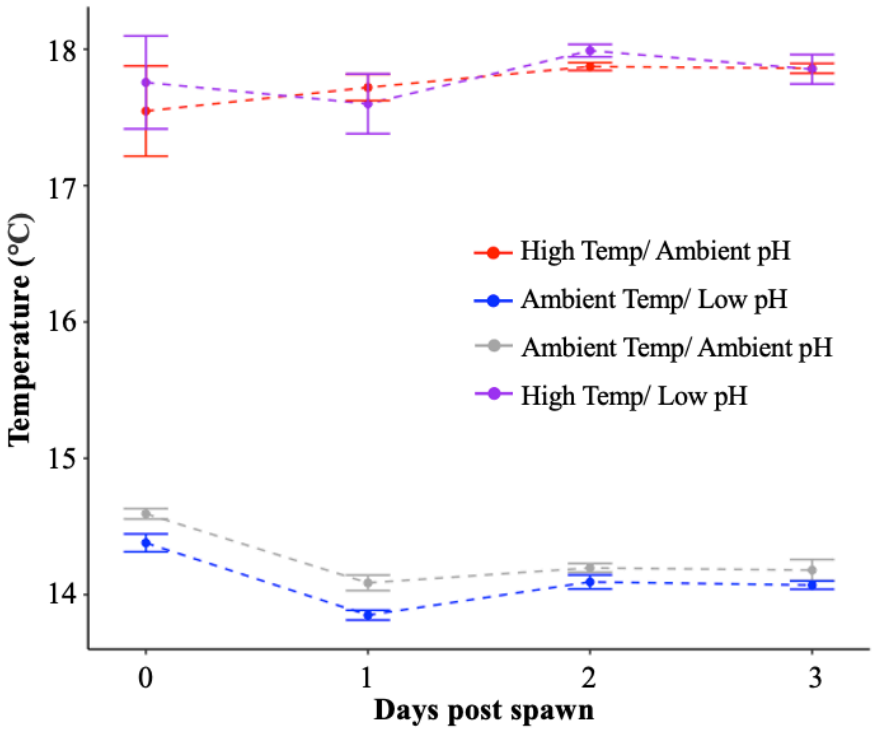

Supplementary Figure 3. Daily temperature reading in each of the embryo tanks grouped by treatment. Grey=ambient, red= high temperature, blue= low pH, purple=high temperature/ low pH. Error bars show standard deviation.

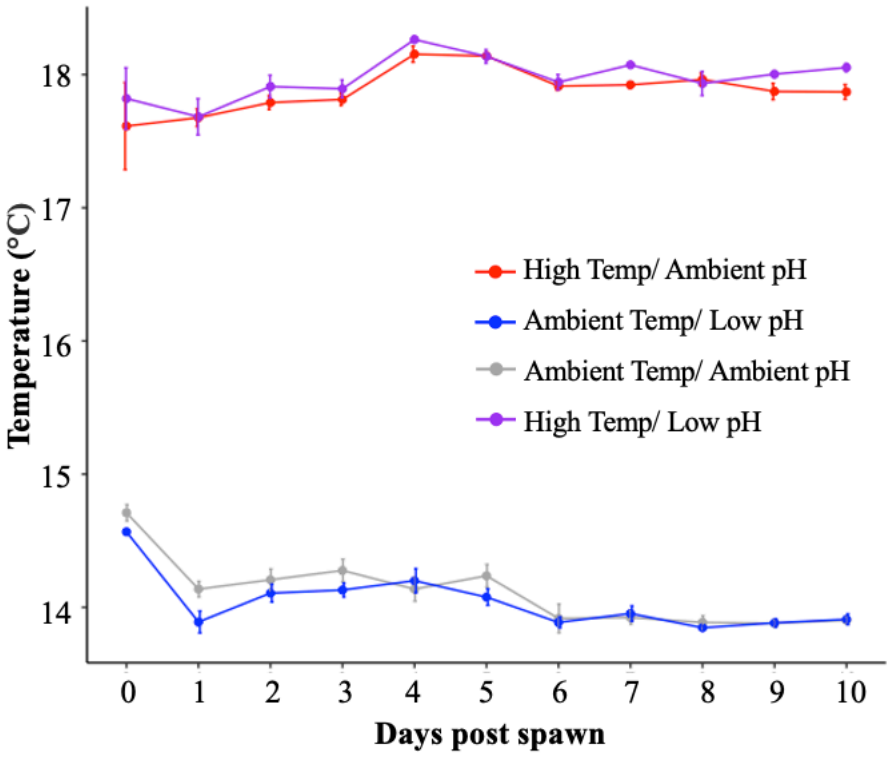

Supplementary Figure 4. Daily temperature reading in each of the larval tanks grouped by treatment. Grey=ambient, red= high temperature, blue= low pH, purple=high temperature/ low pH. Error bars show standard deviation.

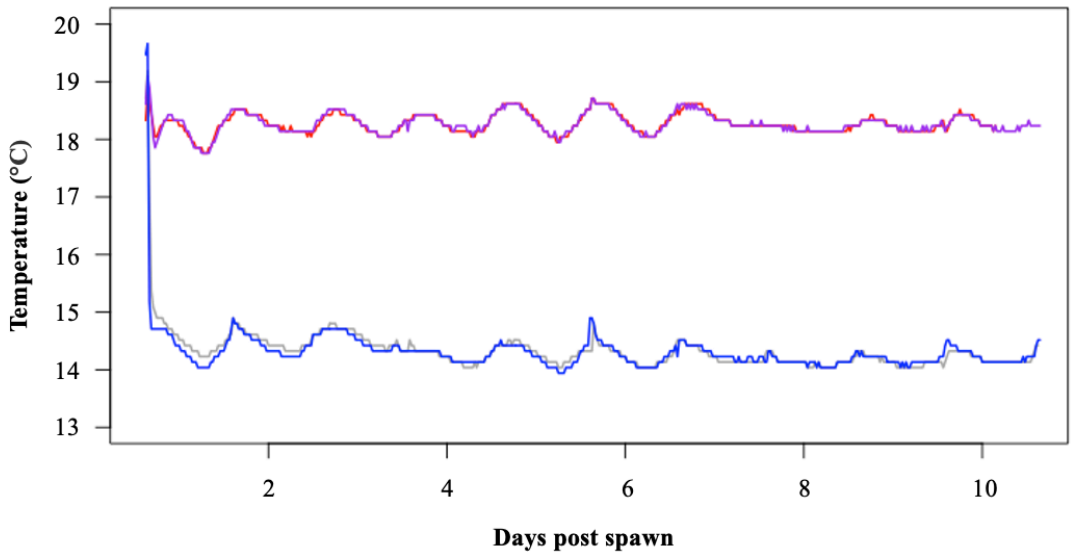

Supplementary Figure 5. Temperature measurements were taken every 30 minutes from one representative larval tank from each treatment (Tanks 1,5,8, and 12) throughout the course of the experiment. The initial high temperatures in the low temperature groups are from just before abalone were added to the system as the temperature dropped to the appropriate level. Grey=ambient, red=high temperature, blue= low pH, purple=high temperature/ low pH.

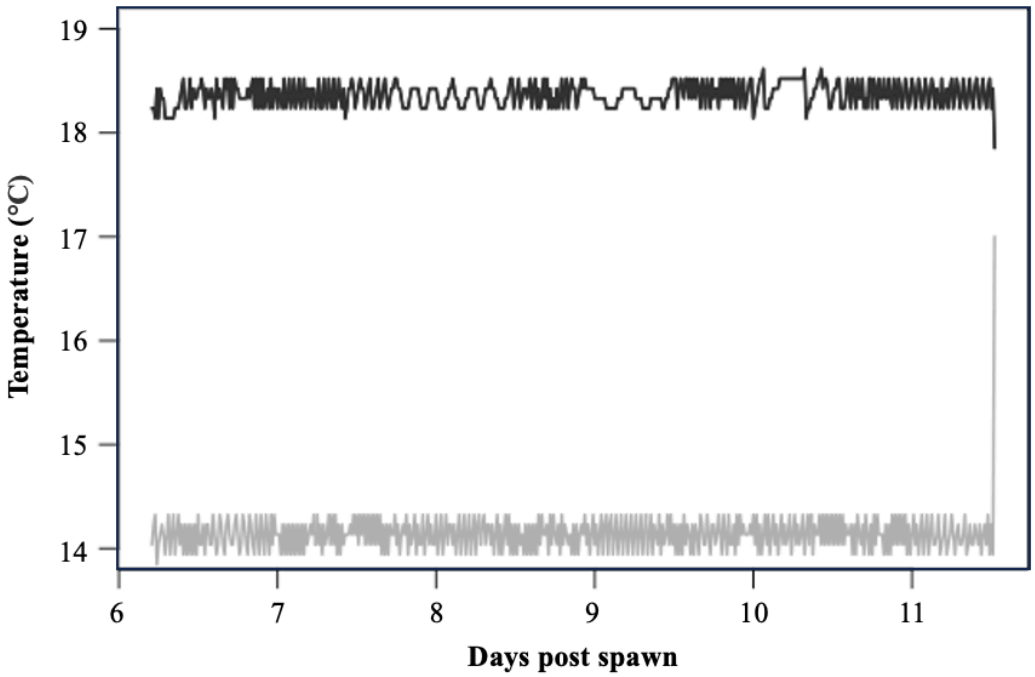

Supplementary Figure 6. Temperature measurements were taken every 15 minutes in the high temperature and low temperature water baths that housed settlement jars during days 6-11 of the experiment.

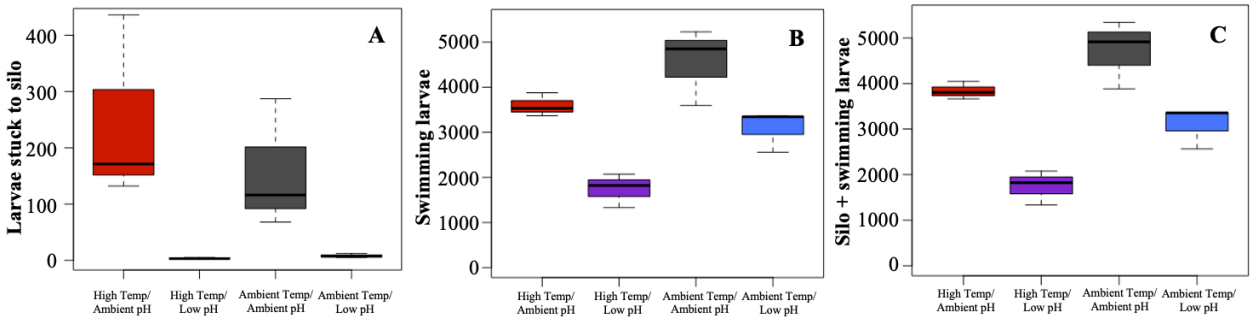

Supplementary Figure 7. (A) Counts of larvae from each replicate tank that were stuck in the silo and removed at the end of the experiment. Larvae that had potentially settled on the sides of the silo vs. larvae that had become stuck in the mesh could not be distinguished, so these larvae were not included in statistical analyses for settlement or survival. (B) Number of larvae approximated in each treatment on day 10. (C) The sum of A and B, or the larvae counted on day 10 plus those stuck in the silo. Minimal difference is observed when those stuck in the silo are added to the counts from day 10.

Chapter 3: Impact of crustose coralline algae, ocean acidification, and ocean warming on larval pinto abalone settlement and juvenile survival

Publication history: This study was co-authored with Ryan Crim, Josh Bouma, Caitlin O'Brien, Jodie Toft, and Jacqueline Padilla-Gamiño. At the time this dissertation was published, this chapter was not published separately.

Abstract

Since 1994, Washington State (USA) has seen a 97% drop in the native pinto abalone (*Haliotis kamtschatkana*) population. Starting in 2007, conservation aquaculture initiatives to restore pinto abalone have been underway to return the wild population to a self-sustaining level. However, the success of depends not only on restoration efforts but also on the capacity of outplanted abalone to survive and reproduce as threats of ocean acidification and warming continue to increase. In a prior study, we found that pH and temperature influence larval survival, but pH has a stronger effect on settlement success. Coralline algae (CA) can play an important role in the success of restoration efforts by serving as a natural settlement inducer and potentially creating a pH refuge for juvenile abalone. In this study, we examined the settlement of pinto abalone under different environmental conditions (7.90 pH/14 °C (ambient), 7.90 pH/18 °C, 7.55 pH/14 °C; and 7.55 pH/18 °C) using two substrates: CA covered fiberglass and clean fiberglass with GABA (a neurotransmitter typically used to induce larval settlement). Larval settlement was negatively impacted by low pH, and though settlement was higher with CA present than in the GABA treatment, this difference was not statistically significant. Juvenile survival was negatively impacted by low pH, but positively impacted by CA presence. Our results show the potential of CA to increase pinto abalone juvenile survival and ameliorate the negative effects of low pH.

Using CA in hatchery culture and selecting sites with CA cover for pinto abalone outplants in the wild may improve the efficiency of restoration efforts in Washington.

Introduction

The mollusc pinto abalone (*Haliotis kamtschatkana*) is the only abalone species native to Washington State and has been listed as a state endangered species since 2019 (Neuman et al., 2019; Sowul et al., 2022). Their densities have been dropping for decades, notably from 0.18 per m^2 in 1992 to 0.04 per m^2 in 2006 (Rothaus et al., 2008), even after the closure of the recreational fishery by the Washington Department of Fish and Wildlife in 1994 (Bouma et al., 2012; Carson et al., 2019; Rothaus et al., 2008). In addition to the decline in abundance, the average size of abalone increased between 1979 and 2017 from 97.6mm to 127.3mm (Rothaus et al., 2008). Further, in surveys from 1992-1996, 16% of abalone were under 90mm, while only 6% were under 90mm in surveys from 2003-2006. These data are an indication that there was no significant recruitment of abalone in that period (Rothaus et al., 2008).

A failure of natural recovery of pinto abalone, likely due to their low density, has led to the use of restoration aquaculture to help regrow the population (Gascoigne & Lipcius, 2004; Rothaus et al., 2008; Sowul et al., 2022). As this restoration takes place, however, climate change increasingly impacts coastal waters of the northeast Pacific, the habitat of pinto abalone (Feely et al., 2004; Ianson et al., 2016; IPCC, 2014; Murray et al., 2015)

Marine calcifiers such as pinto abalone are vulnerable to ocean acidification and warming (Chapter 2; Bouma et al., 2012; Crim et al., 2011; Gazeau et al., 2013; Guo et al., 2022; Kroeker et al., 2013; Parker et al., 2013; Rogers-Bennett et al., 2010). The early life stages of pinto abalone and other molluscs can be particularly vulnerable to these stressors. Thus, it is important to study performance and survival at these stages because they may limit population recovery under climate change conditions (Chapter 2; Byrne, 2011). In the hatchery, larval and early

juvenile phases of pinto abalone also experience high mortality rates, making it crucial to gain a better understanding of these life stages to optimize culture practices.

Abalone have a lecithotrophic larval phase during which they rely on maternally provisioned energy stores (Moran & Manahan, 2003). Larvae settle onto the substrate and metamorphose into their juvenile phase once they are both developmentally competent and after they experience an external cue to initiate settlement (Degnan & Morse, 1995). Settlement from the lecithotrophic larval phase to the benthic phase is a critical step in the life history of abalone species (Figure 1). In hatcheries, gamma-aminobutyric acid (GABA) is typically used as a cue to induce abalone settlement. Flow is stopped, and low concentrations of GABA are added to the water, which causes abalone to drop in the water column. If those abalone are competent to settle, they will settle onto tank surfaces and begin metamorphosis into their juvenile forms (Morse & Morse, 1984; Morse et al., 1979; Searcy-Bernal & Anguiano-Beltrán, 1998).

Increasing temperatures and decreasing pH have both been found to have negative impacts on pinto abalone's early life stages (Chapter 2; Bouma, 2007; Crim et al., 2011). However, previous research on how ocean acidification may impact the settlement specifically of different abalone species has been inconclusive. In pinto abalone, we previously found that low pH levels led to low settlement success when GABA was used as a settlement cue (Chapter 2). Another study on pinto abalone found no impact of pH on metamorphosis after GABA exposure; however, it was noted that abalone appeared able to settle with or without a shell (Crim et al., 2011). Settlement also appeared unimpaired by low pH in European abalone (*Haliotis tuberculata*), but shell formation and shell length were both negatively impacted (Kavousi et al., 2022). In the red abalone (*Haliotis rufescens*), pH had a negative impact on settlement when the exposure was acute (just before settlement) but not chronic (throughout the larval stage).

Understanding the effects of ocean acidification, as well as warming, on pinto abalone settlement is key for restoration efforts for the species because it is currently a bottleneck in the restoration aquaculture process; it is a place where improvements in survival could make a big difference in production of abalone for outplanting.

Coralline algae (CA) is an effective natural settlement inducer for a variety of abalone species (Huggett et al., 2005; A. N. Morse & Morse, 1984; Williams et al., 2008). Both chemical cues from the coralline algae and biological cues from the associated microbiome are thought to play a role in settlement induction (Huggett et al., 2006; Webster et al., 2013). While GABA is present in coralline algae and was initially identified for its role in settlement-induction (D. E. Morse et al., 1979), it is possible that the isolated chemical may not be as effective as coralline algae itself. This is because coralline algae may induce settlement through multiple mechanisms, potentially making it more effective than GABA alone.

Coralline algae may offer additional benefits as a settlement substrate under climate change scenarios beyond its potential role as the natural settlement cue. The photosynthesis of coralline algae can increase the pH in the diffusive boundary layer around the surface of the algae (Cornwall et al., 2013; Houlihan et al., 2020) and provide a refuge for early life stages of marine calcifiers vulnerable to ocean acidification (Cornwall et al., 2013; Houlihan et al., 2020).

The combined effects of pH, temperature, and coralline algae substrate have not previously been studied in pinto abalone. In our study, we examine how different levels of pH and temperature along with the presence of crustose coralline algae (CCA, one form of CA) can impact settlement, juvenile survival, and the number of individuals the hatchery can produce. Our study also provides a hatchery-based assessment of the importance of coralline algae as an abalone habitat under different climate change scenarios.

Methods

Experimental Treatment Summary

Our experiment used two pH levels (7.90 and 7.55), two temperature levels (14°C and 18°C), targeting levels used in Chapter 2, and three substrates/settlement cues (CCA-covered rocks, clean rocks with GABA chemical settlement inducer, and clean rocks with no settlement inducer). Water was filtered through 20um and 5um filters, then circled through a degassing tank and a degassing column where it was heated to ~19°C. From there, water was UV sterilized and flowed to the experimental header tanks. Four 190 L header tanks were used that fed 16 treatment tanks (~18L) for embryos and 16 treatment tanks (~18L) for larvae (Figure 2a). Larvae from the tanks were transferred into 500mL jars to assess settlement and survival 8 days post fertilization (dpf) (Figure 2b). For settlement, one jar from each tank had a clean rock with no settlement cue, one jar had a clean rock with GABA used as a settlement cue, and one jar had a CCA-covered rock (N=48 total). Larval settlement was assessed after the larvae spent one day in jars with the rocks (Figure 2b). For juvenile survival, two jars from each tank had a clean rock with GABA as a settlement cue, and two jars from each tank had a CCA-covered rock (N=58 total, six lost due to breakage or insufficient larvae). Survival in these jars was assessed after three months (Figure 2c).

Spawning of Broodstock

We used embryos from one induced spawning event at the Kenneth K. Chew Center for Shellfish Research and Restoration operated by Puget Sound Restoration Fund at NOAA's Manchester Research Station (Morse et al., 1977). One female and four males, each collected from the San Juan Islands (Washington), produced gametes during this spawn, so the resulting

embryos were from four half-sibling families. Fertilization success was assessed in the hatchery for the four crosses.

Larval Rearing

We used four treatments with two distinct pH and temperature levels during the larval phase of the experiment. For each of these treatments, four replicate tanks were used (Figure 2). After fertilization (0 dpf) embryos were placed on the bottom of the tanks. From there, they would hatch, swim up in the water column, and the flow-through system would push them to a secondary larval tank with a silo (tube with mesh bottoms to allow water flow while preventing larvae from being flushed out of the system) inside. The embryo tanks were removed from the flow-through system 3 dpf. We chose to do this because authors with significant hatchery experience noted from experience that any viable embryos would have hatched by that time and additional decomposition of non-viable embryos could lead to possible bacterial growth in the tanks, which we wanted to avoid (Pers. Comm. Ryan Crim and Joshua Bouma). At this point, the header tanks were altered to flow directly into the larval tanks that contained the larval-rearing silos. Counts were taken by reducing the water volume in each silo to a known level, plunging the water to evenly disperse larvae, and then taking three samples of known volume to count. Counts were taken on 3, 6, and 8 dpf. The outflow on one larval tank from the 7.55 pH/18°C treatment briefly clogged resulting in an overflow, so larval survival was not included for that replicate.

Settlement Trials

At 8 dpf, larvae from each of the 16 larval tanks (four per treatment) were divided among three settlement jars, each with one of the substrate/settlement cue options. Rocks were glued to the bottom of each jar using Gorilla super glue gel and put in flowing seawater to rinse the jars as much as possible before the experiment. Using larval density from counts, we used known volume additions of water to target between 140 and 300 abalone per jar. The number of larvae varied based on the availability of larvae in each tank. Priority was given to ensuring an equal number of larvae in the survival trial jars. For jars with the GABA cue, a 1mmol concentration of the chemical was added to the jar immediately after the larvae were added (Morse et al., 1979; Searcy-Bernal & Anguiano-Beltrán, 1998). For each jar, the water from the corresponding pH and temperature treatment was used to fill the jar, and jars were sealed with plastic lids and placed in water baths to maintain temperature and pH overnight.

This setup resulted in 12 settlement treatments, each with four replicates for a total of 48 jars. These jars were assessed the following day. Non-settled larvae were collected by allowing the jars to overflow onto a screen. These larvae were preserved in alcohol and later counted using a dissecting microscope (Leica M60). Settled larvae were then collected by spraying the jars with freshwater and propanol at high velocities to dislodge adhered abalone onto a separate screen. These abalone were preserved and counted in the same manner as the non-settled (i.e., swimming) larvae.

Survival Trials

At 8 dpf, larvae from the 16 replicate tanks were also transferred into jars to observe juvenile growth and survival over a period of three months. For these, 300 larvae were added to each of four jars per larval tank, two with CCA-covered rock substrate and two with clean rock

substrate and GABA chemical settlement inducer. This resulted in 64 individual jars from eight distinct temperature/pH/substrate treatments. These jars were connected to the flow-through system to maintain each jar at the pH/temperature level that the respective larvae had been raised in. They were housed in four water baths to keep the temperature in the jars consistent even with fluctuating hatchery air temperatures. Diatoms (*Navicula incerta, Amphora salina,* and *Cylindrotheca closterium*) were periodically added to each jar, and the flow stopped for one hour to allow the settlement of these diatoms. This allowed a film to form in each jar to provide food for the juvenile abalone. On day 12 of the experiment, six 48" TrueLumen LED lights were placed over the jars to help maintain the coralline algae substrate. They were kept there for the duration of the experiment and were automatically switched on for eight hours every day. Occasionally, flow to the jars would halt due to clogs in the outflow. However, this was monitored every morning to ensure that flow was not interrupted while the lights were on. Therefore, no significant pH swings should have occurred. Water was pushed backward through the outflow tubes every day with a syringe to clean them out and reduce clogging overnight.

After approximately three months (85 dpf), the deceased and surviving abalone in each jar were assessed using the same methods used to assess settlement rates. Abalone were preserved in alcohol and counted using a dissecting microscope (Leica M60).

After the experiment, an ArcTec Space Spider 3D scanner was used to generate a 3D rendering of each rock from both the settlement and survival experiments in ArcTec Studio. Each rock's surface area was estimated in MeshLab (v2022.02).

Juvenile Size

At the end of the experiment, photographs of juvenile shells on Sedgewick rafters were taken with a camera (Nikon DS-Fi3) under a dissecting scope (Leica M60), and FIJI was used to assess the surface area of each by tracing the edge of each shell. When available, 25 shells from each replicate jar were measured, though lower numbers were used for many replicates due to low survival or shell breakage (Supplementary Table 1). Preservation of shells was unsuccessful for a subset of the jars (N=8), and a subset of jars had no living abalone at the end of the experiment (N=2); therefore, they do not appear in the size analyses.

Carbonate Chemistry

Temperature and pH in each of the four header tanks were measured with Durafet probes (Honeywell). pH was moderated with the automated addition of CO_2 using a solenoid valve system. Temperature was moderated by tank heaters in a degassing tank, then heater/chiller units in each of the four header tanks. During the larval rearing portion of the experiment, temperature, pH, and salinity were assessed in each tank daily using probe measurements (Orion Star A324 pH/ISE Portable Multiparameter meter with Ross Ultra Triode and Orion Star A222 Conductivity Portable Meter) and water samples were taken daily to assess pH via spectrophotometer (Ocean Insight FLAME-S-VIS-NIR). During the juvenile rearing portion of the experiment, salinity, temperature, and spectrometer pH readings were taken approximately twice per week from each header tank and each jar. pH values assessed by spectrophotometer were adjusted for the specific batch of m-cresol purple dye used, salinity, and alkalinity (Dickson et al., 2007).

In addition to point measurements, each header tank had an Apex pH and temperature probe, taking continual measurements. For the larval phase of the experiment, each of the 16 tanks had a temperature logger (Onset HOBO Pendant) collecting data every 15 minutes. Data collection started when the embryos were added to the system and stopped approximately when the larvae were removed for settlement. For the juvenile phase of the experiment, each of the four water baths that contained jars for the juvenile phase of the experiment also contained a temperature logger (Onset HOBO Pendant), collecting data every 15 minutes. Jars from the two cold water treatments were split evenly between the two cold water baths, as was the case for the two warm water treatments.

Alkalinity samples were taken every 1-2 weeks throughout the duration of the experiment. They were taken from header tanks and experimental tanks during the larval rearing phase and taken from header tanks and jars during the juvenile rearing phase. Alkalinity samples (125mL) were poisoned with mercuric chloride on the day of sampling, and a subset were later analyzed in duplicate by titration (Mettler Toledo T5 Excellence Titrator). To temperature correct pH and understand the full carbonate chemistry of each replicate during the experiment, the R package Seacarb was used (Gattuso et al., 2015). Because alkalinity samples were taken less frequently than pH samples, mean treatment alkalinity values from the most recent sampling were used in Seacarb to adjust pH readings on days when we did not take alkalinity samples (Gattuso et al., 2015).

For sampling 10-20 dpf as the sampling schedule was being established, salinity was taken for header tanks only and applied to each jar being fed from that header tank for the purpose of carbonate chemistry calculations. Similarly, the water bath temperature was periodically checked to approximate jar temperature for carbonate chemistry analyses during this

period. On these dates, sampling alternated between even and odd-numbered jars. Starting 21 dpf, temperature and salinity were taken from within every individual jar at the time the spectrometer water samples were taken, and every jar was sampled on the same day twice per week.

Statistical Analysis

To confirm that planned treatments were distinct, analysis of variance was performed for pH, temperature, and salinity values, as well as surface area of settlement rocks. For the rest of statistical analyses, model comparison was used to determine factors that influenced key response variables.

Estimated numbers of surviving larvae 8 days post fertilization were compared using linear fixed effects models. A null model (intercept only), and models with pH, temperature, pH + temperature, and pH + temperature + pH*temperature were compared. For statistical analysis of larval data, one of the replicates from the 7.55 pH/18°C treatment was removed due to a spill of unknown size at the beginning of the experiment; it was decided that larval survival numbers would not be reliable. Enough larvae remained in the spilled replicate tank to use for settlement analyses, but none were used for the 3-month survival experiments.

For settlement, a fraction of successfully settled larvae from each of the 12 treatments (2 pH levels, 2 temperature levels, 3 settlement cues) were compared using mixed-effects linear models. Proportional settlement data (Metric 1 below) was transformed using arcsine transformation so a normal distribution could be used for the models. Larval tank was included as a random effect to account for repeated measures (jars) from the same larval tanks, and possible combinations of temperature, pH, substrate, and interactions of these parameters that

were deemed reasonable were included as fixed effects. When included, temperature and pH were treated as categorical (factor) variables. Residuals were assumed to be normally distributed. We compared settlement success using the following four methods of calculating settlement success to assess the robustness of our settlement metric—models were compared for Metric 1:

$$Metric\ 1.\ Settlement\ success = \frac{counted\ settled\ larvae}{counted\ settled\ larvae + counted\ swimming\ larvae}$$

$$Metric\ 2.\ Settlement\ success = \frac{counted\ settled\ larvae}{theoretical\ larvae\ added\ to\ jar\ (volume\ estimate)}$$

$$Metric\ 3.\ Settlement\ success = \frac{\frac{counted\ settled\ larvae}{counted\ settled\ larvae + counted\ swimming\ larvae}}{surface\ area\ of\ rock}$$

$$Metric\ 4.\ Settlement\ success = \frac{\frac{counted\ settled\ larvae}{theoretical\ larvae\ added\ to\ jar\ (volume\ estimate)}}{surface\ area\ of\ rock}$$

We also compared settlement success (Metric 1) to rock surface area to see if there was a clear positive relationship between the two that could have impacted results.

We used the same set of mixed-effects linear models to assess survival of juveniles to three months. For juvenile size, we used similar models, but jar nested in larval tank was included as a random effect because measurements from multiple shells came from one jar. We compared models with fixed effects of pH, temperature, substrate, along with number of surviving juveniles for the size models.

As with settlement, to ensure robustness of our initial metric of abalone survival, we compared results for four metrics of survival:

$$Metric\ 1.\ Survival = \ Count\ of\ Juvenile\ Abalone$$

$$Metric\ 2.\ Survival = \frac{Count\ of\ juvenile\ abalone}{\%\ settlement * theoretical(by\ vol)\ number\ of\ abalone\ added\ to\ set.jar}$$

$$Metric\ 3.\ Survival = \frac{Count\ of\ juvenile\ abalone}{\%\ settlement * \%\ recovery\ in\ set.jar * theor.(by\ vol)\ number\ of\ abalone\ added\ to\ set.jar}$$

$$Metric\ 4.\ Survival = \frac{Count\ of\ juvenile\ abalone}{SA\ of\ rock\ (cm)}$$

We again visually compared surface area of rocks in the jars and Metric 1 for survival to see if a positive relationship existed that might have impacted results. Two jars in the warmed + low pH treatment broke during the 3-month survival experiment, resulting in N=10 for that treatment and N=16 for the other three treatments.

For all analyses using multi-model inference, we used the lme4 package in R (D. Bates et al., 2015) and used AICc to compare models. We used the gglm (for survival and settlement) and DHARMa (for shell size) packages in R to evaluate standard model diagnostics for well-supported models e.g. dispersion, QQ plot residuals, and homogeneity of variances (Hartig & Hartig, 2022).

Results

Water Chemistry

Our setup maintained four distinct pH x temperature treatments (Supplementary Figure 1). Temperature was distinct (~4°C difference) between the two treatments in the embryo (ANOVA, $F_{1,46}$=2109, p<0.0001) and larval (ANOVA, $F_{1,110}$=4865, p<0.0001) tanks and the juvenile jars (ANOVA, $F_{1,1281}$=28435, p<0.0001).

pH was distinct (~0.38-unit difference) between the two treatment levels in the embryo tanks (ANOVA, $F_{1,46}$=4665, p<0.0001), larval tanks (ANOVA, $F_{1,108}$=4528, p<0.0001), and juvenile jars (ANOVA, $F_{1,1271}$=29,496, p<0.0001) (Supplementary Figure 2).

Salinity was consistent across pH treatments in both the embryo (2-way ANOVA, $F_{1,45}$=0.27, p=0.61) and larval (2-way ANOVA, $F_{1,109}$=0.327, p=0.57) tanks, but differed between temperature treatments in both the embryo tanks (2-way ANOVA, $F_{1,45}$=,10.25 p=0.003) and the larval tanks (2-way ANOVA, $F_{1,109}$=15.891, p<0.001) (Supplementary Figure

3). Salinity was also consistent between pH treatments (3-way ANOVA, $F_{1,1279}$=0.636, p=0.425) and across substrate types (3-way ANOVA, $F_{1,1279}$=0.046, p=0.83) in the juvenile phase of the experiment but did vary between temperature treatments (3-way ANOVA, $F_{1,1279}$=23.816, p<0.001). The difference between the mean salinity values across the two temperature treatments was small and likely not biologically significant: 29.27 PSU and 29.16 PSU in embryo tanks, 29.30 PSU and 29.21 PSU in larval tanks, and 29.87 PSU and 29.74 PSU in juvenile tanks. Salinity increased slowly over the course of the experiment in all tanks due to increasing salinity of inflow water to the hatchery through the summer.

Alkalinity samples were processed from two of the days during the larval phase and six of the days during the juvenile phase (Supplementary Figure 4). Three days of analysis had a subset of samples with inordinately high alkalinity values. These spikes were not consistently seen among the same jars or treatments. We retained these data points because we cannot identify the cause of these values. We recognize they might have been due to some contamination of these samples, as the high values did not appear related to any treatment effect or overall change in the water entering the flowthrough system.

From our spectrometer pH readings, salinity, temperature, and alkalinity readings, the whole carbonate chemistry system of each replicate was analyzed and is summarized in Tables 1 and 2.

Continuous Monitoring of Water Conditions

Continuous monitoring confirmed that abalone were exposed to appropriate temperature treatments throughout the experiment. The peaks in a few 14°C larval tanks likely occurred during larval counts and water changes that day because of the sharp increase for only one data

point (Supplementary Figure 5). For the juvenile phase of the experiment, the logger in one of the two cold water baths failed 22 dpf, but because the two cold water baths received water from the same sources, it can be safely assumed they remained at similar temperatures to each other. Additional tank chillers were added to those baths 27 dpf to reduce temperature variability (Supplementary Figure 6).

Data from Durafet probes that continuously monitored pH and temperature conditions in the header tanks is summarized in Supplementary Figure 7. Spikes in the continuous temperature data collected in the header tanks are explained further in Supplementary Results.

Comparison of rocks in settlement and survival trials

Overall, the rocks in the CCA treatments were significantly larger than the rocks in both the GABA and blank treatments (3-way ANOVA, $F_{2,43}$=6.996, Tukey post-hoc: p=0.002 and p=0.037, respectively) (Supplementary Figure 8). However, when plotted against each other and separated by treatment, there was no clear positive relationship between surface area and settlement success (Supplementary Figure 9). There was no significant difference in rock surface area between the different pH (3-way ANOVA, $F_{1,43}$=0.231, p=0.718) and temperature (3-way ANOVA, $F_{1,43}$=1.112, p= 0.297) treatments. Examples of the 3D scans of rocks are in Supplementary Figure 10.

There was no statistically significant difference in rock surface area between treatments for rocks used in the survival experiment based on settlement substrate (3-way ANOVA, $F_{1,54}$=0.216, p=0.644), temperature (3-way ANOVA, $F_{1,54}$=0.806, p=0.356), or pH (3-way ANOVA, $F_{1,54}$=0.883, p=0.022) (Supplementary Figure 11). There was no clear positive relationship between surface area and settlement success (Supplementary Figure 12).

Larval Survival

The ambient treatment had the highest mean larval survival (4172 larvae), 54%, while the three other treatments had very similar lower levels of survival (warmed = 3523 larvae, 46%, low pH = 3471 larvae, 45%, warmed + low pH = 3490 larvae, 45%) (Figure 3). Model comparison supported the null model over models that included pH, temperature, or an interaction of the two (Table 3).

Larval Settlement

Settlement was impacted most clearly by pH. The proportion of settled larvae was clearly lowest for the no-cue control treatments (Figure 4). As we were more interested in comparison of the GABA and CCA substrates, our models only included data from those two treatments. Our model comparison shows pH as being the only factor the data support as impacting settlement, although the null model still had considerable support (Figure 4, Tables 4-5). Model diagnostics showed a heavy-tailed QQ plot, and slightly larger residuals for smaller fitted values.

Notably, the variance in settlement success was much higher for the low pH treatments (ambient and warmed) than the ambient pH treatments, and while the CCA treatment had higher mean settlement than the GABA treatment for every pH + temperature group pair, the difference in settlement between the CCA and GABA cue treatments was greater in the low pH treatments. Mean settlement was 3.8% higher in the CCA treatment than in the GABA treatment for the control group and 1.1% higher for the high temperature group, whereas mean settlement was 15.4% higher in the CCA treatment than in the GABA treatment for the low pH group and 12.3% higher for the low pH + high temperature group.

To assess the robustness of our settlement metric, we visually compared three other settlement success metrics (see Methods) and found very similar trends in the data (13).

Fertilization

Since fertilization occurred before the exposure to the pH and temperature treatments, it can be assumed that fertilization success was consistent for all embryos used in the experiment. For the four crosses, 87%, 87%, 97%, and 90% of eggs were successfully fertilized, respectively.

Juvenile Survival

pH and substrate both substantially impacted juvenile survival. The treatment with highest mean survival (raw count) was warmed + CCA (97.4±27.7) followed by ambient + CCA (91.6±31.8), then ambient + GABA (49.8±12.7) and warmed + GABA (46.5±24.0). Survival for the low pH + CCA treatment was the best of the low pH treatments (16.5±14.7), followed by the warmed + low pH + CCA (10.2±5.7). The worst two survival treatments were low pH + GABA (3.4±2.6) and warmed + low pH + GABA (6.0±4.6). Survival was 87% higher in ambient pH treatments compared to low pH treatments. On average, survival was 55% higher in CCA treatments than in GABA treatments (Figure 5).

We compared 14 general linear mixed models for survival and found the best-performing model included pH, temperature, substrate, and all three two-way interactions, though as was expected from visual inspection of the data, the effect sizes for pH, substrate, and pH*substrate were much larger than other effect sizes. Model comparison using AIC indicated high support for this mode, but also modest support for two simpler models that excluded either the pH * substrate or temperature * substrate term, while other models had very little support from the

data (Table 6). Term estimates for the best-performing model are summarized in Table 7. Model diagnostics revealed slight heteroskedasticity in residuals vs. fitted values; QQ plot showed approximately normal data.

We compared three other metrics of survival, two of which were corrected for surface area (see Methods). These metrics did not have different trends in results (Supplementary Figure 14).

Juvenile Size

There was substantial variability in juvenile size within and between treatments, though overall, juveniles were larger in the low pH treatments (Figure 6, Supplementary Figure 15). The warmed + low pH treatment had the largest mean shell size of 2.45±1.72mm for the GABA treatment and 2.43±1.59mm for the CCA treatment. The low pH treatment had the next largest mean shell sizes, with 1.13±0.91mm for the GABA treatment and 1.05±0.73mm for the CCA treatment. The next largest shell size was in the warmed + GABA treatment with 0.85±1.0mm, followed by the ambient + CCA treatment with 0.84±0.59mm. The two smallest mean shell sizes were in the warmed + CCA treatment with 0.76±0.60 and the ambient + GABA treatment with 0.51±0.35mm.

Model comparison revealed that the model including temperature and pH had by far the greatest support, with high temperature and low pH positively impacting size (Tables 8-9). QQ plot residuals revealed that there was significant deviation in the KS test, but non-significant deviation in the dispersion and outlier tests. Variances were not the same between prediction categories. We therefore acknowledge that not all assumptions of the model were met given the

complicated nature of this hierarchical data, but given the large difference in AICc, we believe that the model assumption violations did not have undue influence on the inference.

Discussion

This study investigated how ocean warming, acidification, and the presence of coralline algae affect the development and survival of larvae and juveniles of the state-endangered pinto abalone. Our study supports the hypothesis that settlement on coralline algae can bolster pinto abalone survival and growth in the juvenile phase. Exposure to temperature 4°C warmer than normal hatchery conditions did not affect abalone survival, but low pH negatively impacted settlement and survival in the juvenile phase, regardless of settlement substrate.

Larval settlement and survival

Our study confirmed that rearing pinto abalone larvae to competency in low pH conditions negatively affects settlement, consistent with findings from studies on pāua (*Haliotis iris*) and previous work on pinto abalone (Chapter 2; Espinel-Velasco, Lamare, et al., 2021). The 4°C temperature increase did not impact settlement success, which aligns with previous work culturing pinto abalone larvae at 14°C and 18°C (Chapter 2). While temperature has been shown to influence settlement in other studies (Leighton, 1972; Mzozo et al., 2021; O'Connor et al., 2007), it could be that the primary impacts of temperature are related to settlement timing and the development rate rather than affecting overall settlement success. Alternatively, the 4°C increase to 18°C could be a range on thermal performance curve of pinto abalone where settlement success it not impacted—the choice of our temperature treatments could be influencing the apparent sensitivity to pH over temperature.

In contrast to earlier evidence of additive adverse effects of warming and low pH on pinto abalone larval survival (Chapter 2), our study found no significant difference in larval survival between treatments. However, it is worth noting that the ambient treatment had better survival, while all three stressor treatments had a similar lower survival. Genetic differences in the broodstock used for these two experiments could have played a role, and further studies with more genetic diversity would allow us to better understand the familial effects of possible resilience to climate change. Currently, the scarcity of adult pinto abalone in Washington and the difficulty of spawning them in captivity pose challenges to achieving high genetic diversity for experiments.

A study on the more abundant red abalone found negative impacts of ocean acidification on the larval phase in terms of maturation impairment, shell formation, and hatching (Gómez-Reyes et al., 2023). Another study on white abalone (*Haliotis sorenseni*) in California found highest larval survival at 12°C, with decreases at 15°C and 18°C, and complete larval mortality at 21°C (Mccormick et al., 2016). In multiple experiments on white abalone, the temperature at which they can develop fastest also results in low survival (Leighton, 1972; Mccormick et al., 2016). One study found 56% survival from fertilization to settlement stage at 14°C, similar to the survival we saw in our ambient treatment, but where they saw only 2% survival at 18°C, we saw 46% (Mccormick et al., 2016). A broader examination of the impacts of warming and acidification on early life stages of marine invertebrates suggests that embryonic stages are particularly vulnerable to warming. In certain regions, this population bottleneck during larval stages may overshadow the significance of larvae being more vulnerable than other life stages to acidification (Byrne, 2011). However, the absence of negative impacts of temperature and pH on larvae in our experiment is inconsistent with findings from these other studies.

Juvenile survival and size

Impacts of low pH on juvenile abalone survival in previous studies have yielded mixed results. In European abalone and pāua, minimal differences in juvenile survival between ambient and low pH treatments were found (Auzoux-Bordenave et al., 2020; Cunningham et al., 2016). Another study on European abalone found that adult abalone exposed to reduced pH can maintain metabolism by compromising growth and shell integrity (Avignon et al., 2020). In our study we observed a significant impact of low pH on juvenile abalone survival. This could be attributed to the continuous exposure of our juveniles to low pH conditions from the larval phase through the first three months of the juvenile phase. Other studies focus on older juveniles, and exposure to low pH typically begins after the larval phase has concluded (Auzoux-Bordenave et al., 2022; Avignon et al., 2020; Cunningham et al., 2016).

Thermal effects on post-settlement abalone vary significantly between species; one study noted that adult green abalone (*Haliotis fulgens*) are more robust to temperature increase than adult red abalone (Vilchis et al., 2005). Juvenile white abalone had higher survival at 12°C than at 18°C, but the increased mortality at high temperature was attributed to withering syndrome, highlighting the influence of temperature on disease susceptibility (Mccormick et al., 2016). In pinto abalone, trials between 11°C and 21°C found no significant impact of temperature on juvenile survival (Bouma, 2007). Our treatments, falling within this range, corroborate the finding that juvenile survival is not impacted at these temperatures.

While we observed significant treatment effects on abalone size, the results were contrary to expectations based on previous studies (Cunningham et al., 2016). Abalone in the low pH treatments exhibited larger sizes overall. However, these treatments had far fewer abalone surviving until the end of the experiment. This larger size could have been a result of reduced

competition for food or space in the jars, which has been noted in farmed species (Morash & Alter, 2016). Nonetheless, we do not believe either of these factors should have been limiting in our experimental setup. The diatoms used as abalone food could have been influenced by the different pH conditions, although we lack data to clarify the extent of these effects. The larger size observed in the lower pH treatments might be linked to specific traits that enabled these surviving abalone to endure while others in their groups perished—potentially, naturally faster-growing abalone had a greater likelihood of survival. This result is counter to our expectations because less favorable environmental conditions typically lead to more energy allocation for maintaining homeostasis and less energy available for growth (Morash & Alter, 2016). In European abalone, a low pH treatment resulted in slower shell growth and altered shell texture and porosity (Auzoux-Bordenave et al., 2020). A study on pāua in New Zealand noted that slowed growth impacted shell weight in smaller juveniles, while shell weight was better preserved under low pH for larger juveniles (Cunningham et al., 2016). As we only used shell surface area as a metric of size and did not use weight, we may have missed a similar phenomenon in our study if it occurred.

Coralline algae

The presence of coralline algae demonstrated clear benefits for juvenile abalone survival and likely contributed to improved settlement rates. Survival was, on average, 55% higher in the coralline algae treatments compared to those with clean rocks where GABA was used as the cue. Previous research conducted in Washington showed that juvenile pinto abalone preferred habitats with coralline algae-encrusted rocks over those with kelp holdfasts or sea urchins (Rogers-Bennett et al., 2011). Given observed preference by pinto abalone for habitats with

coralline algae and the observed increased survival, there is strong evidence for the importance of integrating coralline algae into abalone restoration efforts.

While not measured quantitatively, we noted a decline in the health of coralline algae during the experiment. As a calcifying alga, coralline algae have been found particularly vulnerable to decreases in pH across various studies conducted in tropical to Arctic regions (Anthony et al., 2008; Asnaghi et al., 2013; Büdenbender et al., 2011; Kuffner et al., 2008; Martin & Gattuso, 2009). Alterations such as dissolution or reduced abundance of coralline algae could diminish the availability of habitat essential for abalone settlement. Changes in marine biofilms due to pH changes have impacted their effectiveness as settlement cues for marine polychaetes (Espinel-Velasco, Tobias-Hünefeldt, et al., 2021). Similarly, shifts in the coralline algae microbiome or biochemistry due to decreased pH have been found to reduce their effectiveness as settlement inducers for two coral species (Webster et al., 2013). A study on abalone, however, found that even though coralline algae growth was reduced under low pH, pre-exposure to low pH did not impact coralline algae's effectiveness as a settlement cue for red abalone (O'Leary et al., 2017). Future studies isolating the impacts of chemical and biological cues on abalone settlement and analyzing how these different cues will be impacted by ocean acidification and warming, could help us better understand how abalone settlement will be impacted in the future.

Ocean warming

Increased temperatures are known to hasten abalone development and increase settlement (Mzozo et al., 2021), but thermal limits vary by species (Bouma, 2007; Morash & Alter, 2016; Rogers-Bennett et al., 2010). The absence of negative impacts from the warmed treatment on

settlement, larval, and juvenile survival shows that the 18°C temperature we chose is likely still within the thermal tolerance window of pinto abalone in Washington. Given that pinto abalone typically inhabit subtidal rather than surface waters, it is unlikely that they frequently encounter temperatures above 18°C in their natural habitats, where temperatures are more commonly between 8°C and 14°C (Chapter 4; Weigel et al., 2023). Best estimates of sea surface temperature increase by 2100 are between 2 and 4.5°C of warming, so it is possible that temperatures above 18°C could be experienced more regularly in the coming century (IPCC, 2007) These results suggest that in Washington specifically, changes in pH are likely to impact abalone well before changes in temperature will. However, evidence from California indicates that alongside warming, additional stressors, such as disease and starvation, can emerge (Rogers-Bennett et al., 2010). Thus, even if pinto abalone early life stages are not directly impacted by ocean warming in the coming decades, warming might lead to other changes in the ecosystem that could act as stressors to abalone.

Transgenerational impacts

Selective breeding of molluscs is increasingly being incorporated into farming practices to enhance growth rates and resilience to changing ocean conditions (Kube et al., 2007; Tan et al., 2020). Evidence of adaptive transgenerational plasticity has been found in Japanese abalone (*Haliotis discus hannai*) and various colored abalone (*Haliotis diversicolor*) (Guo et al., 2022). A study on red abalone found that larvae from parents exposed to lower pH conditions due to upwelling were more resistant to ocean acidification (Swezey et al., 2020). However, another study on red abalone found that early life exposure to ocean acidification did not confer benefits to future generations and had lasting negative impacts on adult growth (Neylan et al., 2023). In

European abalone, no carry-over effects were seen after parental exposure to ocean acidification (Auzoux-Bordenave et al., 2022). Therefore, investigating the effects of parental exposure to ocean acidification and warming could provide valuable insights into how Washington's pinto abalone may respond to climate change. If early life stage exposure confers transgenerational benefits, it could inform restoration strategies for this species.

Conclusions

This study represents the first experiment exposing pinto abalone to low pH and increased temperatures from embryos through the first months of the juvenile phase. As we continue to update best practices for restoring pinto abalone in Washington, oceanographic and habitat factors are critical considerations. This study highlights the potential of coralline algae in hatcheries to enhance abalone production, based on the significant improvement of juvenile survival in treatments with CCA substrate, especially at low pH. In the future, we want to investigate the combined use of GABA and coralline algae to induce settlement. If we can mitigate the high mortality typically observed during the juvenile phase in hatcheries, it could significantly increase the number of abalone available for outplanting by organizations like the Puget Sound Restoration Fund and the Washington Department of Fish and Wildlife.

Our research supports the continued buffering of the pH of hatchery water to levels near 8.0 and the maintenance of water temperature in the hatchery between 14°C and 18°C. Our findings also advocate the use of coralline algae encrusted rocky reefs as habitat for outplanting pinto abalone. However, beyond benthic habitat considerations, we must also consider water conditions. Research on green abalone in Mexico found that juvenile growth and mortality were correlated with site-specific oceanographic variability (Boch et al., 2018). In natural ecosystems,

numerous factors, such as current speed and direction, site rugosity, presence of predators, algal cover, and water chemistry, can influence pinto abalone survival. Our future work aims to incorporate more of these variables and integrate them with our findings on temperature, pH, and coralline algae.

Acknowledgements

The authors thank Malise Yun, Rachel Dalthorp, Sarah Henneford, Mackenzie Weers, Mackenzie Gavery, and Larken Root for their assistance with sample and data collection during the experiment. We thank Sara Ghandour and Ella Persson for their assistance in photographing shells, and Sarah Hendricks for 3D scanning cobbles. Thanks to Paul McElhany, Danielle Perez, Mike Maher, and Larken Root for helping design spec methods and providing dye. We thank Katie Craighill for her graphics contribution. Finally, we thank Kathleen Sowul, Henry Carson, and Will Love for their assistance in planning and executing dives to collect CCA-encrusted cobbles for the experiment.

Figures and Tables

Table 1. Carbonate chemistry data for culture tanks during the larval phase of the experiment as mean and standard deviation. Sample size shown in parenthesis for each metric.

Treatment	pH	Temperature (°C)	Aragonite Saturation	pCO_2 (µatm)	Salinity (PSU)	Alkalinity (µmol/kg)
			Embryo Tanks			
Ambient	7.94±0.02(12)	14.54±0.25(12)	1.86±0.07(12)	589.41±27.71(12)	29.16±0.14(12)	2439.24±67.95(4)
Warmed	7.91±0.02(12)	17.93±0.10(12)	1.96±0.07(12)	628.31±25.72(12)	29.25±0.07(12)	2398.74±50.31(4)
Low pH	7.54±0.02(12)	14.58±0.31(12)	0.82±0.04(12)	1678.07±69.25(12)	29.16±0.16(12)	2552.94±16.30(4)
Warmed +low pH	7.55±0.01(12)	17.76±0.27(12)	0.98±0.03(12)	1637.27±42.58(12)	29.29±0.09(12)	2557.74±95.87(4)
			Larval Tanks			
Ambient	7.96±0.02(27)	14.32±0.33(27)	1.90±0.08(27)	566.17±37.51(27)	29.21±0.16(27)	2472.36±94.65(8)
Warmed	7.93±0.02(28)	17.86±0.17(28)	2.12±0.08(28)	621.00±32.32(28)	29.29±0.07(28)	2505.12±33.22(8)
Low pH	7.53±0.03(28)	14.35±0.32(28)	0.82±0.07(27)	1703.11±137.42(27)	29.21±0.15(27)	2552.40±92.93(8)
Warmed +low pH	7.55±0.04(27)	17.81±0.21(27)	0.97±0.08(28)	1687.91±172.93(28)	29.31±0.09(28)	2580.65±63.28(8)

Table 2. Carbonate chemistry data for culture jars during the juvenile phase of the experiment as mean and standard deviation. Sample size shown in parenthesis for each metric.

Treatment	pH	Temperature (°C)	Aragonite Saturation	pCO_2 (µatm)	Salinity (PSU)	Alkalinity (µmol/kg)
			CCA cue			
Ambient	7.94±0.02(176)	14.34±0.37(176)	1.91±0.13(176)	593.27±43.99(176)	29.74±0.50(176)	2507.62±195.11(48)
Warmed	7.90±0.02(174)	18.00±0.28(174)	2.01±0.12(174)	664.73±45.25(174)	29.88±0.46(174)	2481.94±158.87(48)
Low pH	7.55±0.05(175)	14.36±0.25(175)	0.86±0.12(175)	1640.46±179.88(175)	29.74±0.42(175)	2564.38±88.16(49)
Warmed + low pH	7.57±0.04(114)	18.06±0.39(114)	1.03±0.11(114)	1591.55±138.09(114)	29.86±0.47(114)	2574.48±207.85(32)
			GABA cue			
Ambient	7.94±0.02(173)	14.34±0.33(173)	1.89±0.14(173)	604.41±49.54(173)	29.76±0.43(173)	2524.64±230.79(48)
Warmed	7.89±0.03(175)	17.99±0.28(175)	1.97±0.13(175)	681.68±84.92(175)	29.87±0.48(175)	2450.00±111.44(48)
Low pH	7.52±0.03(175)	14.36±0.37(175)	0.82±0.06(175)	1750.53±125.58(175)	29.74±0.46(175)	2580.75±100.78(49)
Warmed + low pH	7.55±0.04(111)	18.07±0.28(111)	1.02±0.13(111)	1661.91±177.96(111)	29.87±0.42(111)	2615.00±206.22(32)

Table 3. Model comparison for larval survival.

Model Terms	Model Rank	Parameters	ΔAICc
1	1	1	0
pH	2	2	0.185
temp	3	2	0.798
pH + temp	4	3	0.577
pH + temp + pH*temp	5	4	0.946

Table 4. Model comparison for larval settlement.

Model Terms	Model Rank	Parameters	ΔAICc
pH + (1| larval tank)	1	2	0
(1| larval tank)	2	1	0.672
pH + CCA + (1| larval tank)	3	3	4.054
pH + temp + (1| larval tank)	4	3	4.147
pH + temp + pH*temp + (1| larval tank)	5	4	7.627
pH + CCA + pH*CCA + (1| larval tank)	6	4	7.995
pH + CCA + temp + (1| larval tank)	7	4	8.382
pH + CCA + temp + pH*temp + (1| larval tank)	8	5	12.064
pH + CCA + temp + pH*CCA + (1| larval tank)	9	5	12.525
pH + CCA + temp + pH*CCA + pH*temp + (1| larval tank)	10	6	16.432

Table 5. Summary of best performing model for larval settlement

Term	Estimate	Std. Error
Intercept	1.140	0.080
pH (low)	-0.282	0.113

Table 6. Model comparison for juvenile survival.

Model Terms	Model Rank	Parameters	ΔAICc
temp + pH + CCA + pH*CCA + pH*temp + temp*CCA + (1| larval tank)	1	7	0.00
temp + pH + CCA + pH*CCA + pH*temp + (1| larval tank)	2	6	3.88
temp + pH + CCA + pH*CCA + temp*CCA + (1| larval tank)	3	6	4.17
temp + pH + CCA + pH*CCA + (1| larval tank)	4	5	8.15
pH + CCA + pH*CCA + (1| larval tank)	5	4	10.97
temp + pH + CCA + (1| larval tank)	6	4	24.26
pH + CCA + (1| larval tank)	7	3	27.25
temp + pH + (1| larval tank)	8	3	50.51
temp + pH + CCA + temp*CCA + (1| larval tank)	9	5	51.22
pH + (1| larval tank)	10	2	53.99
temp + CCA + (1| larval tank)	11	3	59.03
CCA + (1| larval tank)	12	2	64.45
temp + (1| larval tank)	13	2	83.97
(1| larval tank)	14	1	89.49

Table 7. Summary of best-performing model for juvenile survival

Term	Estimate	Std. Error
(Intercept)	95.44	6.86
Temp (low)	-1.80	9.18
pH (low)	-82.01	10.04
Substrate (GABA)	-47.01	8.45
pH (low)*substrate (GABA)	36.61	10.15
Temp (low)*pH (low)	3.02	11.55
Temp (low)*substrate (GABA)	1.26	10.15

Table 8. Model comparison for juvenile size

Model Terms	Model Rank	Parameters	ΔAICc
(1|larval tank/ jar) + temp + pH	1	3	0.00
(1|larval tank/ jar) + temp + pH + # juveniles	2	4	1.39
(1|larval tank/ jar) + temp + pH + substrate	3	4	1.98
(1|larval tank/ jar) + temp + pH + # juveniles + substrate	4	5	3.30
(1|larval tank/ jar) + pH	5	2	10.84
(1|larval tank/ jar) + pH + # juveniles	6	3	12.09
(1|larval tank/ jar) + temp + # juveniles + substrate	7	4	12.74
(1|larval tank/ jar) + pH + substrate	8	3	12.84
(1|larval tank/ jar)) + temp + # juveniles	9	3	13.16
(1|larval tank/ jar) + pH + substrate + # juveniles	10	4	13.86
(1|larval tank/ jar)	11	1	19.22
(1|larval tank/ jar) + # juveniles	12	2	19.34
(1|larval tank/ jar) + substrate + # juveniles	13	3	20.21

Table 9. Summary of best-performing model for juvenile size

Term	Estimate	Std. Error
(Intercept)	13.447	0.103
pH (low)	0.705	0.137
Temperature (low)	-0.403	0.132

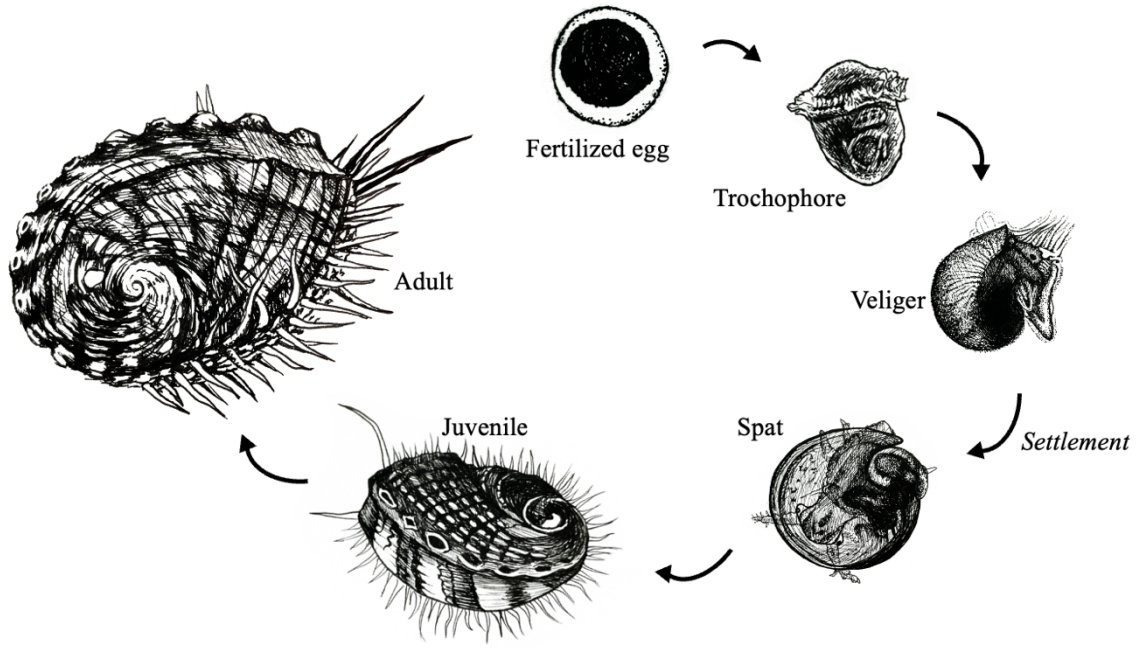

Figure 1. The abalone life cycle begins with fertilized eggs hatching 1-3 days after spawning. This is followed by the larval phase, which includes the trochophore and veliger stages and lasts for 7-10 days. After this, the larvae settle onto the benthos and undergo metamorphosis into spat. The spat then grow into juvenile abalone, eventually reaching adulthood. Illustrations by Katie Craighill

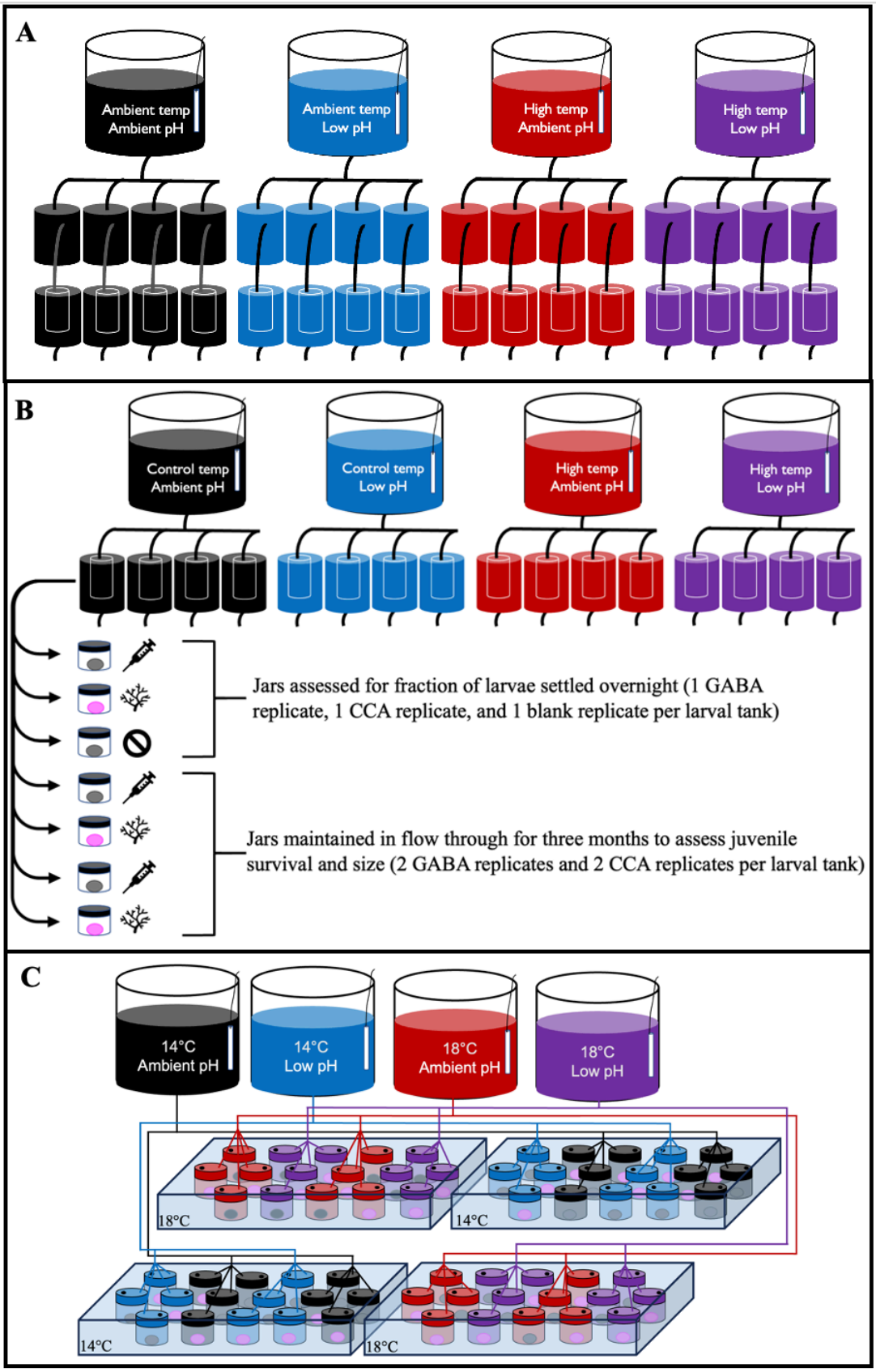
A
Ambient temp
Ambient pH
Ambient temp
Low pH
High temp
Ambient pH
High temp
Low pH
B
Control temp
Ambient pH
Control temp
Low pH
High temp
Ambient pH
High temp
Low pH
Jars assessed for fraction of larvae settled overnight (1 GABA replicate, 1 CCA replicate, and 1 blank replicate per larval tank)
Jars maintained in flow through for three months to assess juvenile survival and size (2 GABA replicates and 2 CCA replicates per larval tank)
C
14°C
Ambient pH
14°C
Low pH
18°C
Ambient pH
18°C
Low pH
18°C
14°C
14°C
18°C

Figure 2. Experimental setup during the larval (A), settlement (B), and juvenile (C) phases of the experiment. (A) Four header tanks fed into tanks with embryos on the bottom. As embryos hatch, larvae would swim up and be pushed into the second tier of tanks where silos kept them in the larval tanks. On day 3 of the experiment, the embryo tanks were removed, and the header tanks fed directly into the larval tanks through day 8. (B) On day eight, larvae from each of the 16 tanks were split into 7 jars from each tank. Three of these jars were used to assess settlement overnight. Four of these jars were put in the juvenile experiment. (C) The four header tanks fed directly into each of the jars for the duration of the larval experiment. This experimental setup kept the jars at the proper pH and temperature. All jars were placed in water baths to ensure temperature did not fluctuate on particularly warm days.

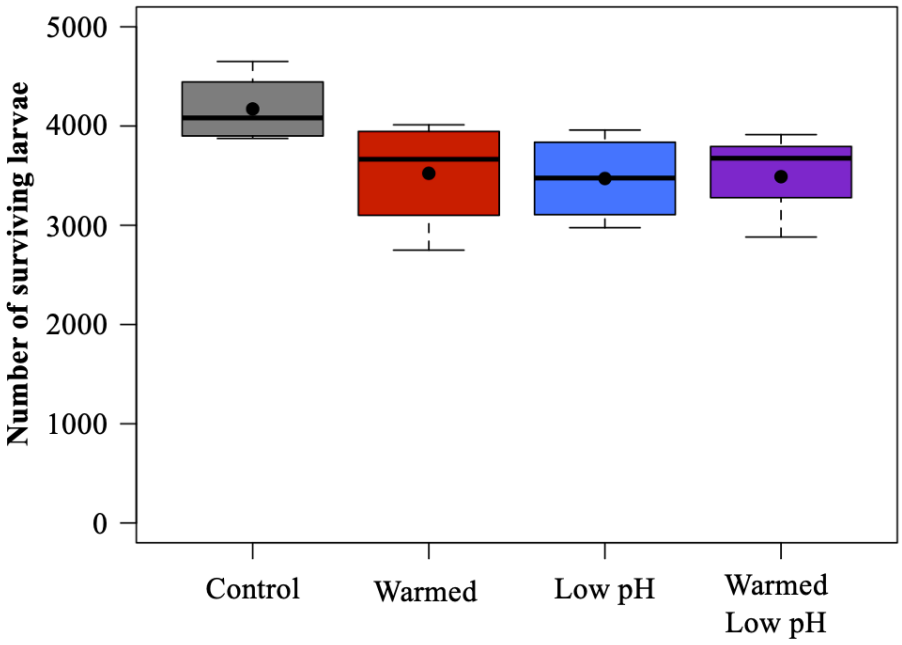

Figure 3. Number of surviving larvae in each treatment on day 8 (immediately pre-settlement).

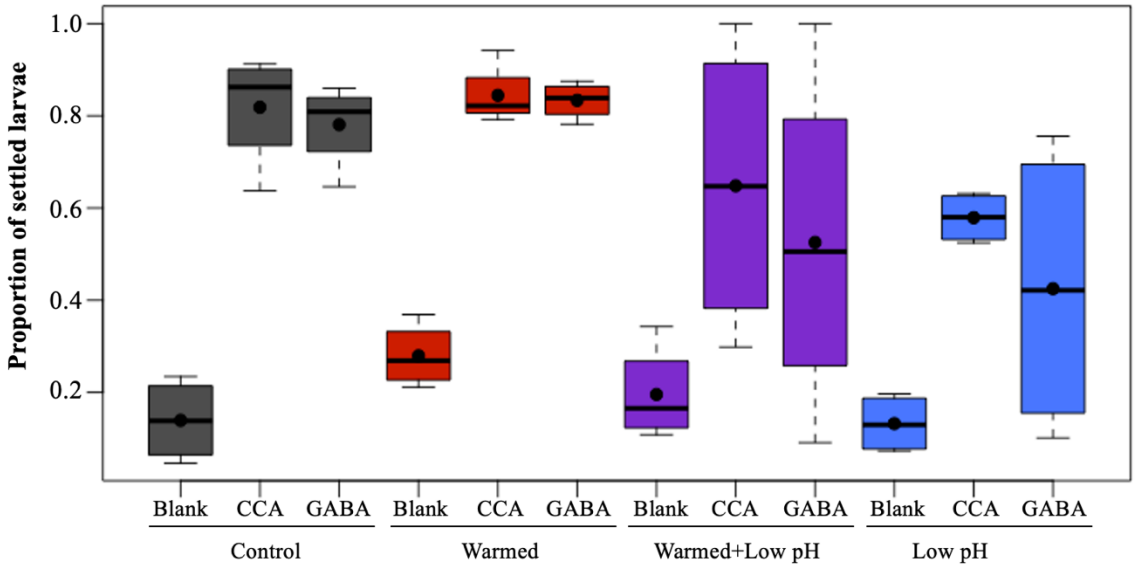

Figure 4. Settlement of larvae, calculated as #setters/(#setters+#swimmers), on day 8 of the experiment.

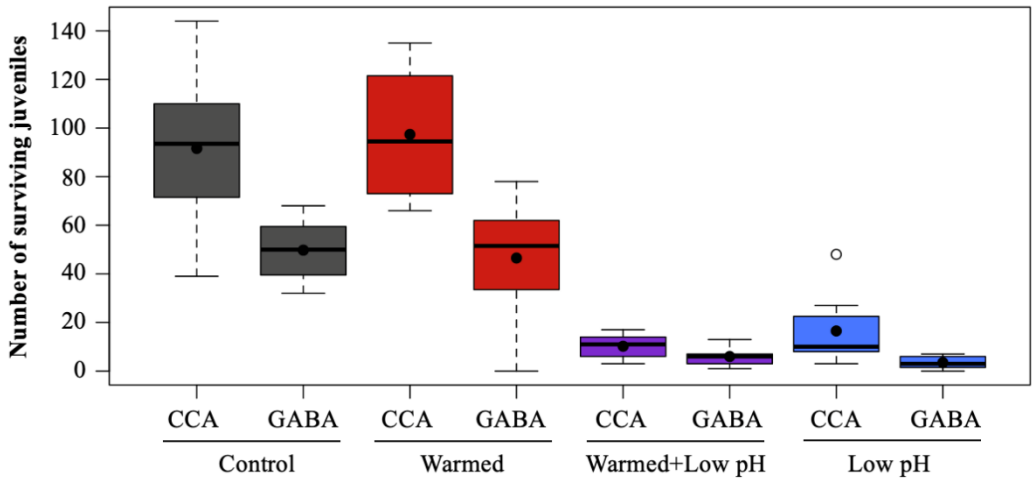

Figure 5. Juvenile survival, calculated as counts of abalone at the end of the experiment.

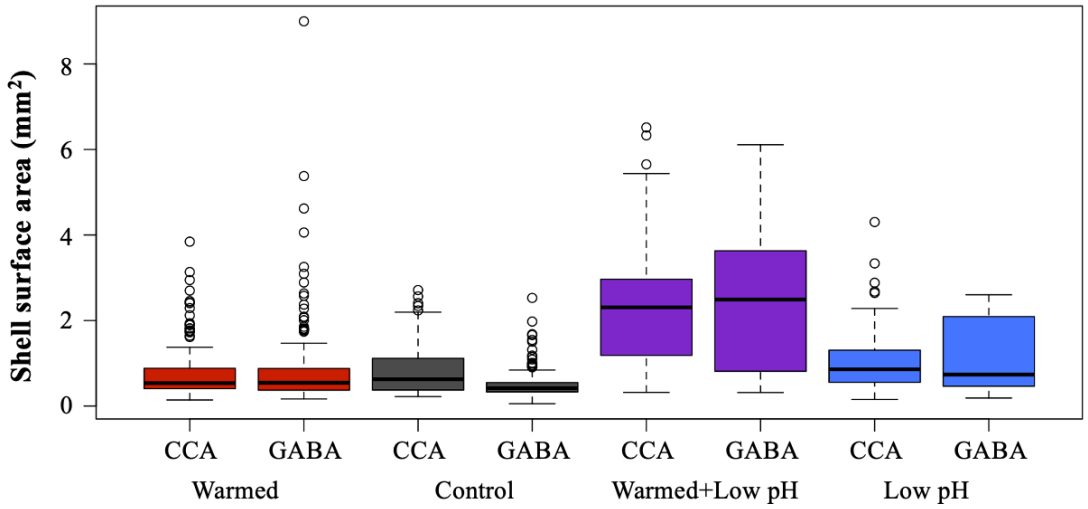

Figure 6. Surface area of juvenile shells at the conclusion of the experiment.

References

Anthony, K. R., Kline, D. I., Diaz-Pulido, G., Dove, S., & Hoegh-Guldberg, O. (2008). Ocean acidification causes bleaching and productivity loss in coral reef builders. *Proceedings of the National Academy of Sciences*, *105*(45), 17442–17446.

Asnaghi, V., Chiantore, M., Mangialajo, L., Gazeau, F., Francour, P., Alliouane, S., & Gattuso, J.-P. (2013). Cascading effects of ocean acidification in a rocky subtidal community. *PloS One*, *8*(4), e61978.

Auzoux-Bordenave, S., Ledoux, A., Martin, S., Di Poi, C., Suquet, M., Badou, A., Gaillard, F., Servili, A., Le Goïc, N., & Huchette, S. (2022). Responses of early life stages of European abalone (*Haliotis tuberculata*) to ocean acidification after parental conditioning: Insights from a transgenerational experiment. *Marine Environmental Research*, *181*, 105753.

Auzoux-Bordenave, S., Wessel, N., Badou, A., Martin, S., M'zoudi, S., Avignon, S., Roussel, S., Huchette, S., & Dubois, P. (2020). Ocean acidification impacts growth and shell mineralization in juvenile abalone (*Haliotis tuberculata*). *Marine Biology*, *167*, 1–14.

Avignon, S., Auzoux-Bordenave, S., Martin, S., Dubois, P., Badou, A., Coheleach, M., Richard, N., Di Giglio, S., Malet, L., & Servili, A. (2020). An integrated investigation of the effects of ocean acidification on adult abalone (*Haliotis tuberculata*). *ICES Journal of Marine Science*, *77*(2), 757–772.

Bates, D., Maechler, M., Bolker, B., Walker, S., Christensen, R. H. B., Singmann, H., Dai, B., Grothendieck, G., Green, P., & Bolker, M. B. (2015). Package 'lme4.' *Convergence*, *12*(1), 2.

Boch, C. A., Micheli, F., AlNajjar, M., Monismith, S. G., Beers, J. M., Bonilla, J. C., Espinoza, A. M., Vazquez-Vera, L., & Woodson, C. B. (2018). Local oceanographic variability influences the performance of juvenile abalone under climate change. *Scientific Reports*, *8*(1), 5501.

Bouma, J. V. (2007). *Early life history dynamics of pinto abalone (Haliotis kamtschatkana) and implications for recovery in the San Juan Archipelago, Washington State*. University of Washington.

Bouma, J. V., Rothaus, D. P., Straus, K. M., Vadopalas, B., & Friedman, C. S. (2012). Low juvenile pinto abalone *Haliotis kamtschatkana kamtschatkana* abundance in the San Juan Archipelago, Washington State. *Transactions of the American Fisheries Society*, *141*(1), 76-83.

Büdenbender, J., Riebesell, U., & Form, A. (2011). Calcification of the Arctic coralline red algae *Lithothamnion glaciale* in response to elevated CO_2. *Marine Ecology Progress Series*, *441*, 79–87.

Byrne, M. (2011). Impact of ocean warming and ocean acidification on marine invertebrate life history stages: Vulnerabilities and potential for persistence in a changing ocean. *Oceanography and Marine Biology Annual Review*, *49*, 1–42.

Carson, H. S., Morin, D. J., Bouma, J. V., Ulrich, M., & Sizemore, R. (2019). The survival of hatchery-origin pinto abalone *Haliotis kamtschatkana* released into Washington waters. *Aquatic Conservation: Marine and Freshwater Ecosystems*, *29*(3), 424–441.

Cornwall, C. E., Hepburn, C. D., Pilditch, C. A., & Hurd, C. L. (2013). Concentration boundary layers around complex assemblages of macroalgae: Implications for the effects of ocean acidification on understory coralline algae. *Limnology and Oceanography*, *58*(1), 121–130.

Crim, R. N., Sunday, J. M., & Harley, C. D. (2011). Elevated seawater CO2 concentrations impair larval development and reduce larval survival in endangered northern abalone (*Haliotis kamtschatkana*). *Journal of Experimental Marine Biology and Ecology*, *400*(1–2), 272–277.

Cunningham, S. C., Smith, A. M., & Lamare, M. D. (2016). The effects of elevated pCO_2 on growth, shell production and metabolism of cultured juvenile abalone, *Haliotis iris. Aquaculture Research*, *47*(8), 2375–2392.

Degnan, B. M., & Morse, D. E. (1995). Developmental and morphogenetic gene regulation in *Haliotis rufescens* larvae at metamorphosis. *American Zoologist*, *35*(4), 391–398.

Dickson, A. G., Sabine, C. L., & Christian, J. R. (2007). *Guide to best practices for ocean CO_2 measurements.* North Pacific Marine Science Organization.

Espinel-Velasco, N., Lamare, M., Kluibenschedl, A., Moss, G., & Cummings, V. (2021). Ocean acidification induces carry-over effects on the larval settlement of the New Zealand abalone, *Haliotis iris*. *ICES Journal of Marine Science*, *78*(1), 340–348.

Espinel-Velasco, N., Tobias-Hünefeldt, S. P., Karelitz, S., Hoffmann, L. J., Morales, S. E., & Lamare, M. D. (2021). Reduced seawater pH alters marine biofilms with impacts for marine polychaete larval settlement. *Marine Environmental Research*, *167*, 105291.

Feely, R. A., Sabine, C. L., Lee, K., Berelson, W., Kleypas, J., Fabry, V. J., & Millero, F. J. (2004). Impact of anthropogenic CO2 on the CaCO3 system in the oceans. *Science*, *305*(5682), 362–366.

Gascoigne, J., & Lipcius, R. N. (2004). Allee effects in marine systems. *Marine Ecology Progress Series*, *269*, 49-59.

Gattuso, J.-P., Epitalon, J.-M., Lavigne, H., Orr, J., Gentili, B., Hagens, M., Hofmann, A., Mueller, J.-D., Proye, A., & Rae, J. (2015). Package 'seacarb.'

Gazeau, F., Parker, L. M., Comeau, S., Gattuso, J.-P., O'Connor, W. A., Martin, S., Pörtner, H.-O., & Ross, P. M. (2013). Impacts of ocean acidification on marine shelled molluscs. *Marine Biology*, *160*, 2207–2245.

Gómez-Reyes, R., Galindo-Sánchez, C. E., Lafarga-De la Cruz, F., Hernández-Ayón, J. M., Valenzuela-Wood, E., & López-Galindo, L. (2023). Individual Pattern Response to CO2-Induced Acidification Stress in *Haliotis rufescens* Suggests Stage-Specific Acclimatization during Its Early Life History. *Sustainability*, *15*(18), 14010.

Guo, X., Huang, M., Luo, X., You, W., & Ke, C. (2022). Effects of one-year exposure to ocean acidification on two species of abalone. *Science of The Total Environment*, *852*, 158144.

Hartig, F., & Hartig, M. F. (2022). Package 'DHARMa.' *R Package.*

Houlihan, E. P., Espinel-Velasco, N., Cornwall, C. E., Pilditch, C. A., & Lamare, M. D. (2020). Diffusive boundary layers and ocean acidification: Implications for sea urchin settlement and growth. *Frontiers in Marine Science*, *7*, 972.

Huggett, M. J., De Nys, R., Williamson, J. E., Heasman, M., & Steinberg, P. D. (2005). Settlement of larval blacklip abalone, *Haliotis rubra*, in response to green and red macroalgae. *Marine Biology*, *147*(5), 1155–1163.

Huggett, M. J., Williamson, J. E., De Nys, R., Kjelleberg, S., & Steinberg, P. D. (2006). Larval settlement of the common Australian sea urchin *Heliocidaris erythrogramma*

in response to bacteria from the surface of coralline algae. *Oecologia*, *149*(4), 604–619.

Ianson, D., Allen, S. E., Moore-Maley, B. L., Johannessen, S. C., & Macdonald, and R. W. (2016). Vulnerability of a semi-enclosed estuarine sea to ocean acidification in contrast with hypoxia. *Geophysical Research Letters*, *43*(11), 5793–5801.

IPCC (2007). *Climate Change 2007: The Fourth Assessment Report of the Intergovernmental Panel on Climate Change (IPCC).* Cambridge University Press.

IPCC (2014). Climate Change 2014: Synthesis Report. Contribution of Working Groups I, II and III to the Fifth Assessment Report of the Intergovernmental Panel on Climate Change [Core Writing Team, R.K. Pachauri and L.A. Meyer (eds.)]. IPCC, Geneva, Switzerland, 151 pp.

Kavousi, J., Roussel, S., Martin, S., Gaillard, F., Badou, A., Di Poi, C., Huchette, S., Dubois, P., & Auzoux-Bordenave, S. (2022). Combined effects of ocean warming and acidification on the larval stages of the European abalone *Haliotis tuberculata*. *Marine Pollution Bulletin*, *175*, 113131.

Kroeker, K. J., Kordas, R. L., Crim, R., Hendriks, I. E., Ramajo, L., Singh, G. S., Duarte, C. M., & Gattuso, J.-P. (2013). Impacts of ocean acidification on marine organisms: Quantifying sensitivities and interaction with warming. *Global Change Biology*, *19*(6), 1884–1896.

Kube, P. D., Appleyard, S. A., & Elliott, N. G. (2007). Selective breeding greenlip abalone (*Haliotis laevigata*): Preliminary results and issues. *Journal of Shellfish Research*, *26*(3), 821–824.

Kuffner, I. B., Andersson, A. J., Jokiel, P. L., Rodgers, K. S., & Mackenzie, F. T. (2008). Decreased abundance of crustose coralline algae due to ocean acidification. *Nature Geoscience*, *1*(2), 114–117.

Leighton, D. L. (1972). Laboratory observations on the early growth of the abalone, *Haliotis sorenseni*, and the effect of temperature on larval development and settling success. *Fishery Bulletin*, *70*(2), 373–381.

Martin, S. & Gattuso, J.-P. (2009). Response of Mediterranean coralline algae to ocean acidification and elevated temperature. *Global Change Biology*, *15*(8), 2089–2100.

Mccormick, T. B., Navas, G., Buckley, L. M., & Biggs, C. (2016). Effect of temperature, diet, light, and cultivation density on growth and survival of larval and juvenile white abalone *Haliotis sorenseni* (Bartsch, 1940). *Journal of Shellfish Research*, *35*(4), 981–992.

Moran, A. L., & Manahan, D. T. (2003). Energy metabolism during larval development of green and white abalone, *Haliotis fulgens* and *H. sorenseni*. *The Biological Bulletin*, *204*(3), 270–277.

Morash, A. J., & Alter, K. (2016). Effects of environmental and farm stress on abalone physiology: perspectives for abalone aquaculture in the face of global climate change. *Reviews in Aquaculture*, *8*(4), 342-368.

Morse, A. N., & Morse, D. E. (1984). Recruitment and metamorphosis of *Haliotis* larvae induced by molecules uniquely available at the surfaces of crustose red algae. *Journal of Experimental Marine Biology and Ecology*, *75*(3), 191–215.

Morse, D. E., Duncan, H., Hooker, N., & Morse, A. (1977). Hydrogen peroxide induces spawning in mollusks, with activation of prostaglandin endoperoxide synthetase. *Science*, *196*(4287), 298-300.

Morse, D. E., Hooker, N., Duncan, H., & Jensen, L. (1979). γ-Aminobutyric acid, a neurotransmitter, induces planktonic abalone larvae to settle and begin metamorphosis. *Science*, *204*(4391), 407–410.

Murray, J. W., Roberts, E., Howard, E., O'Donnell, M., Bantam, C., Carrington, E., Foy, M., Paul, B., & Fay, A. (2015). An inland sea high nitrate-low chlorophyll (HNLC) region with naturally high pCO2. *Limnology and Oceanography*, *60*(3), 957–966.

Mzozo, Z. B., Hugo, S., & Vine, N. G. (2021). Effect of Temperature on the Development and Settlement of the Abalone Larvae *Haliotis midae*: Considerations for Abalone Hatchery Management and Stock Enhancement. *Journal of Shellfish Research*, *40*(1), 119–125.

Neuman, M. J., Wang, S., Busch, S., Friedman, C., Gruenthal, K., Gustafson, R., Kushner, D., Stierhoff, K., Vanblaricom, G. & Wright, S. (2018). A status review of pinto abalone (*Haliotis kamtschatkana*) along the west coast of North America: interpreting trends, addressing uncertainty, and assessing risk for a wide-ranging marine invertebrate. *Journal of Shellfish Research*, *37*(4), 869-910.

Neylan, I. P., Swezey, D. S., Boles, S. E., Gross, J. A., Sih, A., & Stachowicz, J. J. (2023). Within-and transgenerational stress legacy effects of ocean acidification on red abalone (*Haliotis rufescens*) growth and survival. *Global Change Biology*, e17048.

O'Connor, M. I., Bruno, J. F., Gaines, S. D., Halpern, B. S., Lester, S. E., Kinlan, B. P., & Weiss, J. M. (2007). Temperature control of larval dispersal and the implications for marine ecology, evolution, and conservation. *Proceedings of the National Academy of Sciences*, *104*(4), 1266–1271.

O'Leary, J. K., Barry, J. P., Gabrielson, P. W., Rogers-Bennett, L., Potts, D. C., Palumbi, S. R., & Micheli, F. (2017). Calcifying algae maintain settlement cues to larval abalone following algal exposure to extreme ocean acidification. *Scientific reports*, *7*(1), 5774.

Parker, L. M., Ross, P. M., O'Connor, W. A., Pörtner, H. O., Scanes, E., & Wright, J. M. (2013). Predicting the response of molluscs to the impact of ocean acidification. *Biology*, *2*(2), 651–692.

Rogers-Bennett, L., B. L. Allen, and D. P. Rothaus. "Status and habitat associations of the threatened northern abalone: importance of kelp and coralline algae." *Aquatic Conservation: Marine and Freshwater Ecosystems* 21, no. 6 (2011): 573-581.

Rogers-Bennett, L., Dondanville, R. F., Moore, J. D., & Vilchis, L. I. (2010). Response of red abalone reproduction to warm water, starvation, and disease stressors: Implications of ocean warming. *Journal of Shellfish Research*, *29*(3), 599–611.

Rothaus, D. P., Vadopalas, B., & Friedman, C. S. (2008). Precipitous declines in pinto abalone (Haliotis kamtschatkana kamtschatkana) abundance in the San Juan Archipelago, Washington, USA, despite statewide fishery closure. *Canadian Journal of Fisheries and Aquatic Sciences*, *65*(12), 2703-2711.

Searcy-Bernal, R., & Anguiano-Beltrán, C. (1998). Optimizing the concentration of gamma-aminobutyric acid (GABA) for inducing larval metamorphosis in the red abalone *Haliotis rufescens* (Mollusca: Gastropoda). *Journal of the World Aquaculture Society*, *29*(4), 463–470.

Sowul, K., Carson, H., Bouma, J., & Fyfe, D. (2022). *Washington State Recovery Plan for the Pinto Abalone* (p. 65 +iv pp). Washington Department of Fish and Wildlife.

Swezey, D. S., Boles, S. E., Aquilino, K. M., Stott, H. K., Bush, D., Whitehead, A., Rogers-Bennett, L., Hill, T. M., & Sanford, E. (2020). Evolved differences in energy metabolism and growth dictate the impacts of ocean acidification on abalone aquaculture. *Proceedings of the National Academy of Sciences*.

Tan, K., Zhang, H., & Zheng, H. (2020). Selective breeding of edible bivalves and its implication of global climate change. *Reviews in Aquaculture*, *12*(4), 2559–2572.

Vilchis, L. I., Tegner, M. J., Moore, J. D., Friedman, C. S., Riser, K. L., Robbins, T. T., & Dayton, P. K. (2005). Ocean warming effects on growth, reproduction, and survivorship of southern California abalone. *Ecological Applications*, *15*(2), 469–480.

Webster, N. S., Uthicke, S., Botté, E. S., Flores, F., & Negri, A. P. (2013). Ocean acidification reduces induction of coral settlement by crustose coralline algae. *Global Change Biology*, *19*(1), 303–315.

Weigel, B. L., Small, S. L., Berry, H. D., & Dethier, M. N. (2023). Effects of temperature and nutrients on microscopic stages of the bull kelp (*Nereocystis luetkeana*, Phaeophyceae). *Journal of Phycology*, *59*(5), 893–907.

Williams, E. A., Craigie, A., Yeates, A., & Degnan, S. M. (2008). Articulated coralline algae of the genus *Amphiroa* are highly effective natural inducers of settlement in the tropical abalone *Haliotis asinina*. *The Biological Bulletin*, *215*(1), 98–107.

Appendices

Supplementary Results

Continuous temperature measurements through the juvenile phase

Further detail is provided here for Supplementary Figure 5.

The spikes at 0 dpf are from when the tanks were getting to temperature. Abalone were added to the embryo tanks between 1pm and 2:40pm, and flow through was resumed at 3:10pm. All tanks were set to 14°C as abalone were added, and then the two warm water tanks were changed back to 18°C when flow through resumed.

Header tanks were emptied and cleaned 40 dpf, leaving the data loggers out of the water from approximately 10:20 am-12:00 pm and causing the temperature spikes. Individual jars were not influenced by this brief break in flow through.

A power outage at the hatchery facility slightly impacted the tanks 64 dpf. Power was out from approximately 4:30pm to 6:40pm. During this time, the header tanks drained almost fully, and the continuous pH and temperature loggers within them started measuring values in the air. Minimal, if any, air space would have been introduced to the jars during this time, meaning the shift in pH was likely negligible. Temperature loggers in the water baths containing the jars (Supplementary Figure 4) showed that the water baths remained closer to their intended temperatures, with the monitored low-temperature bath only above 15°C for a maximum of 45 minutes and only reaching a peak of 15.36°C. The two warmed temperature baths only reached maximum temperatures of 18.57°C and 18.66°C, respectively. This demonstrates that the peaks

in the header tanks are not representative of the temperature experienced by the abalone during this time. Conditions in the header tanks had returned to set values by approximately 8:00 pm.

From 5:40 am-9:10 am 67 dpf and from 8:20 pm 68 dpf to 9:20 am 69 dpf, clogs in water inflow caused the header tanks to stop refilling, eventually causing the data loggers to not be submerged in water. Both clogs were repaired before grow lights came on for the day, so the brief periods of no flow through would not have occurred when photosynthesis was occurring and likely did not impact jar pH. Data from the water baths shows that jar temperatures were not impacted beyond their usual fluctuations by this brief suspension of flow (Supplementary Figure 4).

Supplementary Tables

Supplementary Table 1. Number of Shells photographed from each replicate.

Ambient		Warmed + Low pH		Low pH		Warmed	
Jar	Shells photographed	Jar	Shells photographed	Jar	Shells photographed	Jar	Shells photographed
1	25	17	0	33	0	49	0
2	25	18	3	34	0	50	25
3*	25	19*	0	35*	25	51*	25
4*	0	20*	6	36*	25	52*	0
5	25	21	0	37	1	53	25
6	25	22	3	38	1	54	25
7*	0	23*	16	39*	3	55*	25
8*	25	24*	0	40*	7	56*	25
9	25	26	10	41	4	57	25
10	25	28*	14	42	5	58	25
11*	25			43*	9	59*	25
12*	25			44*	6	60*	25
13	25			45	2	61	24
14	0			46	2	62	25
15*	25			47*	14	63*	25
16*	25			48*	6	64*	25

*=CCA treatment

Supplementary Figures

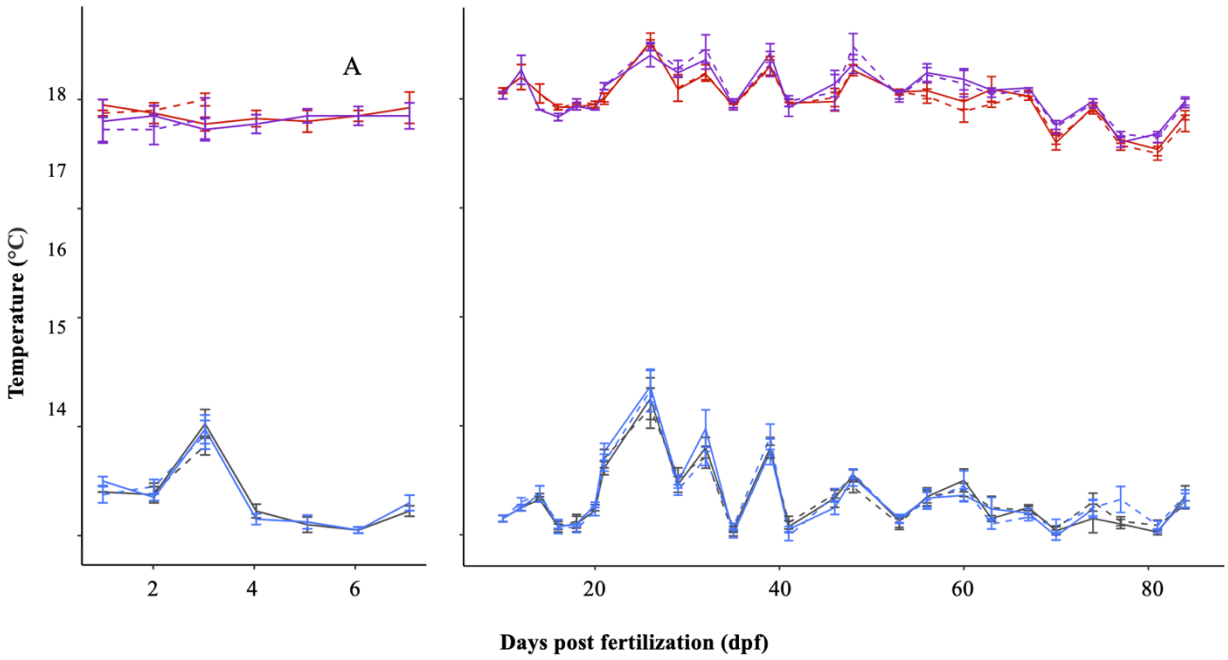

Supplementary Figure 1. Mean temperature in each treatment. (A) Temperature during the larval phase in the larval tanks (solid lines) and embryo tanks (dashed lines). (B) Temperature during the juvenile phase in the CCA treatments (solid lines) and GABA treatments (dashed lines). Black = control, blue = low pH, red = warmed, and purple = warmed + low pH.

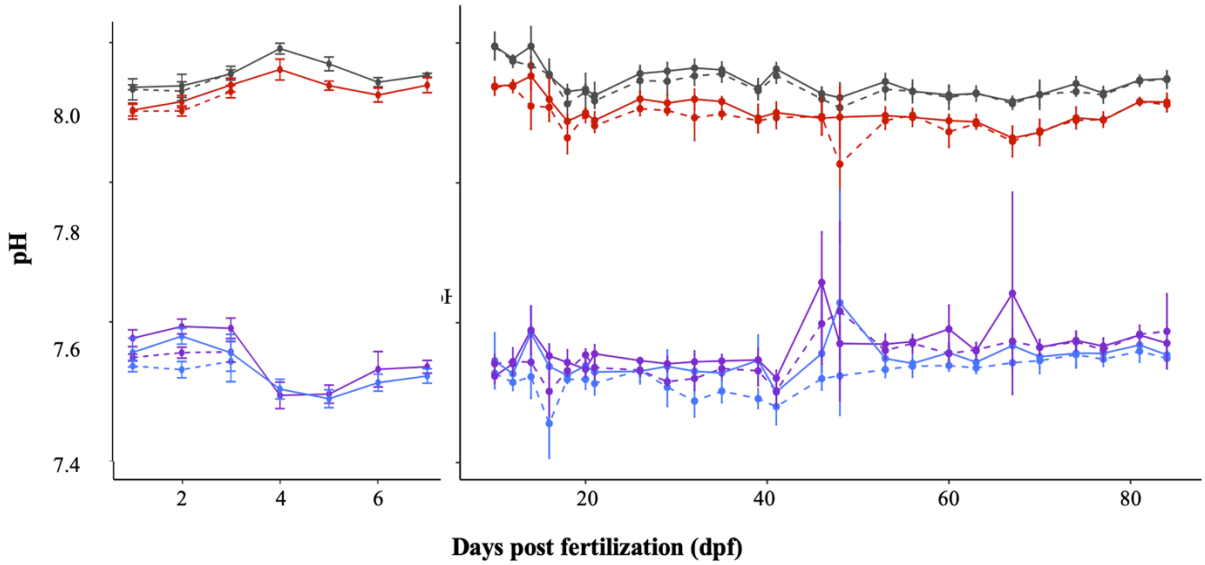

Supplementary Figure 2. Mean pH in each treatment. (A) pH during the larval phase in the larval tanks (solid lines) and embryo tanks (dashed lines). (B) pH during the juvenile phase in the CCA treatments (solid lines) and GABA treatments (dashed lines). Black = control, blue = low pH, red = warmed, and purple = warmed + low pH.

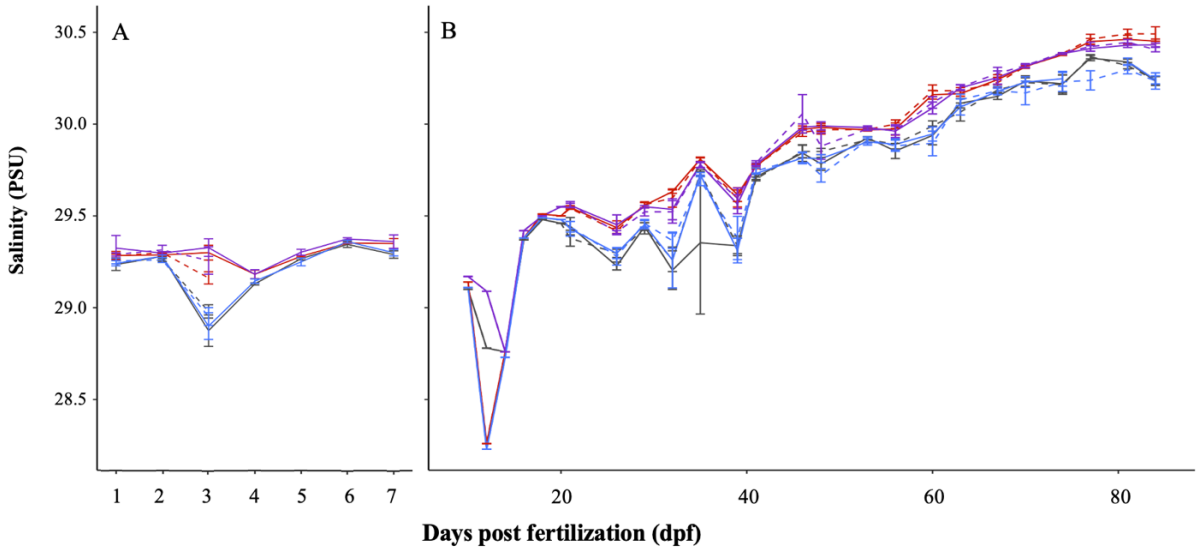

Supplementary Figure 3. Mean salinity in each treatment. (A) Salinity during the larval phase in the larval tanks (solid lines) and embryo tanks (dashed lines). (B) Salinity during the juvenile phase in the CCA treatments (solid lines) and GABA treatments (dashed lines). Black = control, blue = low pH, red = warmed, and purple = warmed + low pH.

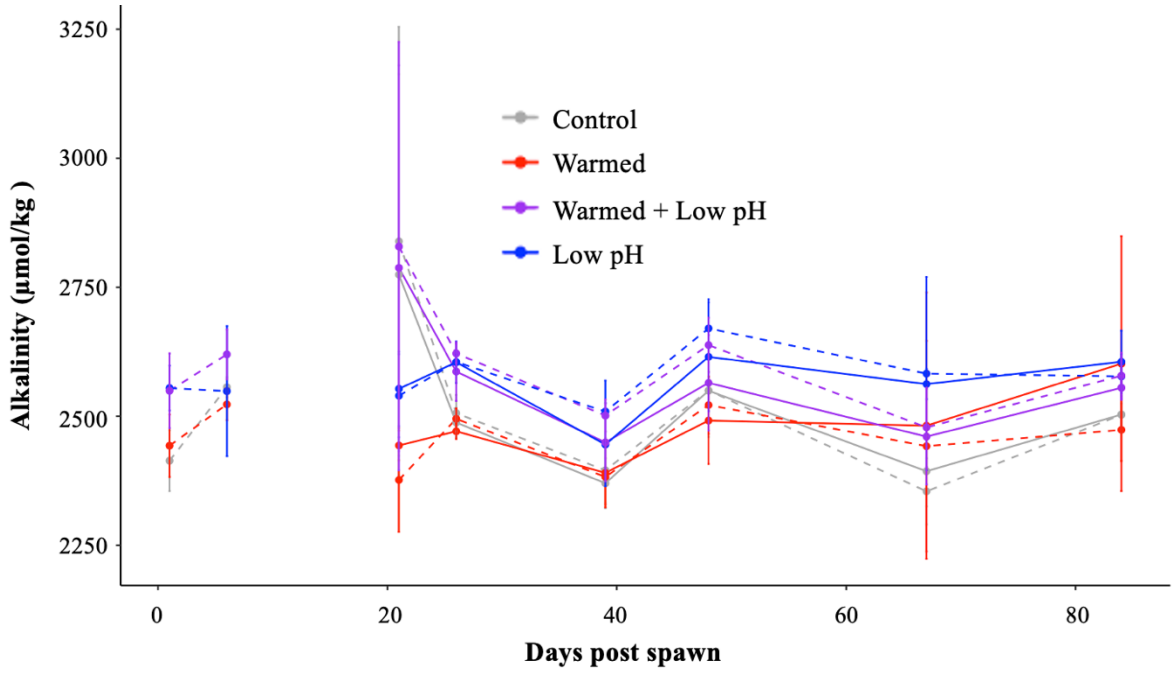

Supplementary Figure 4. Alkalinity samples from each tank for the larval phase (days 0-8), and each jar for the juvenile phase (days 8-85). Grey = control, blue = low pH, red = warmed, and purple = low pH + warmed. For the juvenile phase, solid lines are the CCA treatment and dashed lines are the GABA treatment. Error bars represent standard error.

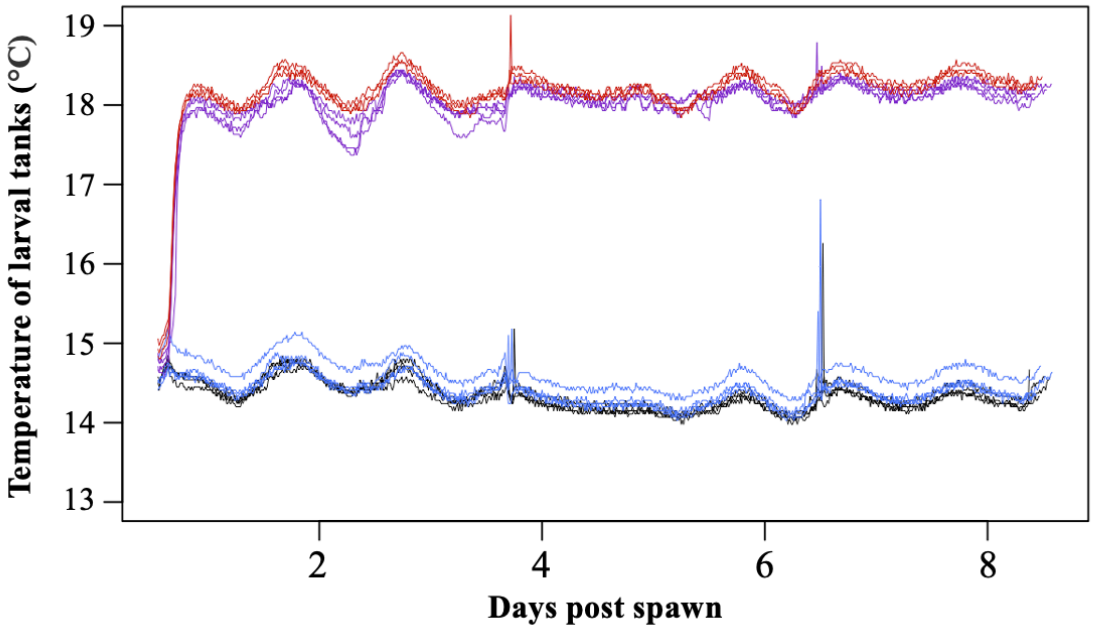

Supplementary Figure 5. The temperature of each larval tank was monitored every 15 minutes for the duration of the larval phase of the experiment.

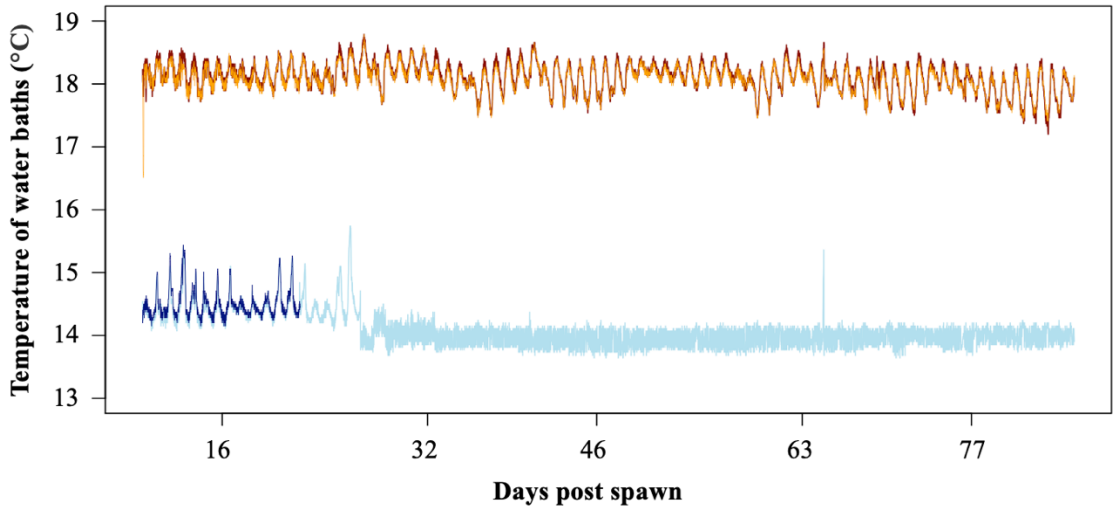

Supplementary Figure 6. Onset HOBO temperature logger data from the two warmed water baths (red and orange) and two low temperature water baths (light blue and dark blue) for the duration of the juvenile phase of the experiment. One of the loggers in a low temperature bath (dark blue) stopped working midway through the experiment.

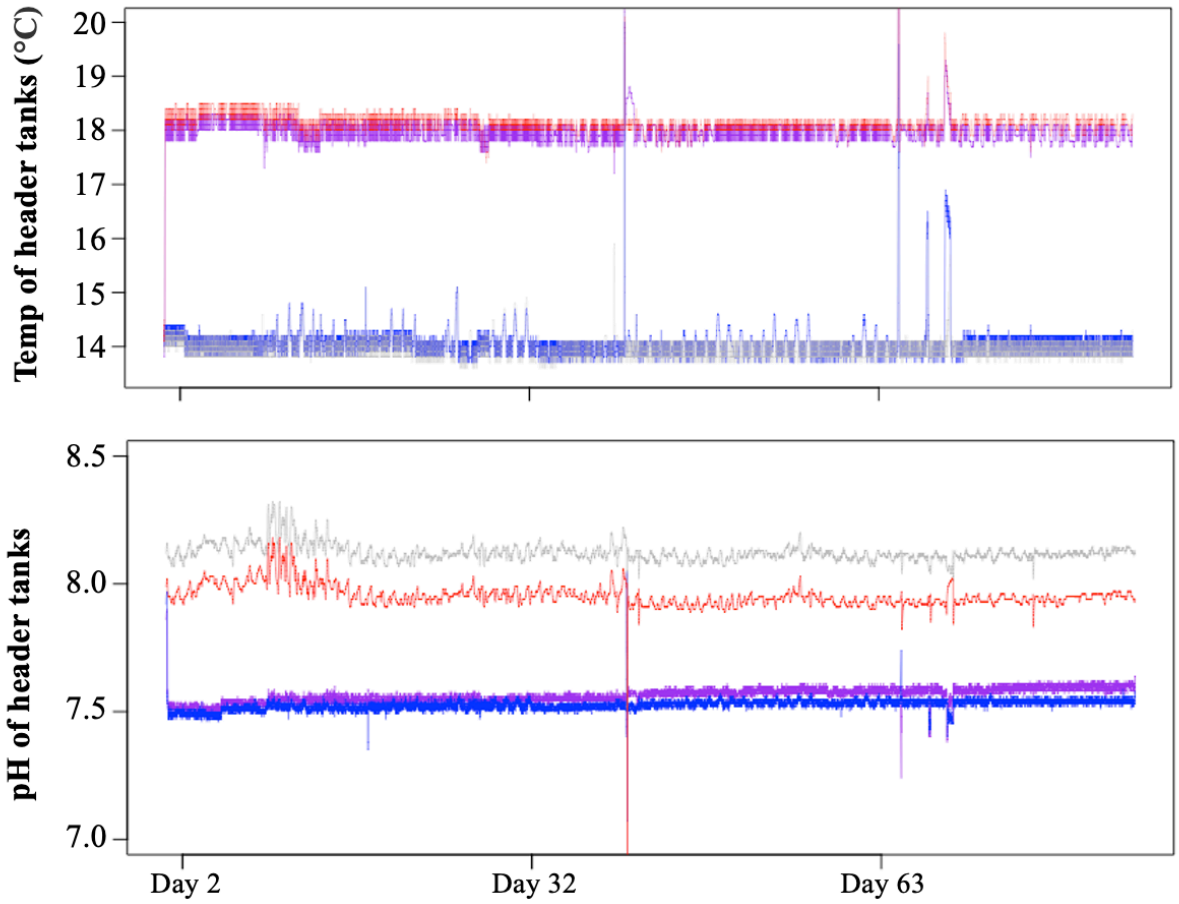

Supplementary Figure 7. Apex temperature (A) and pH (B) data from the four header tanks for the duration of the experiments.

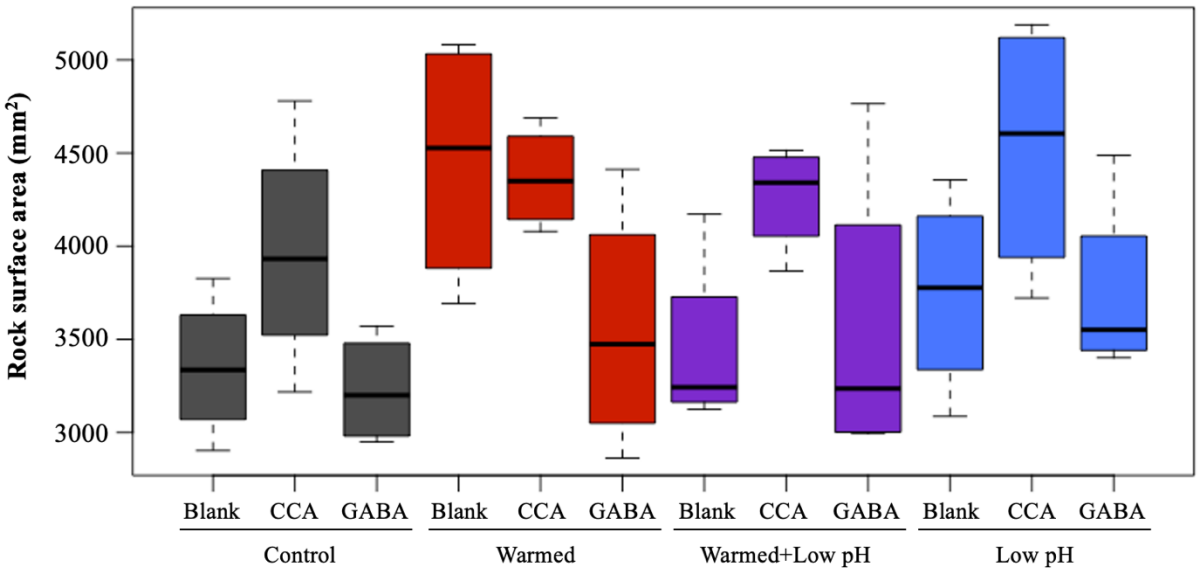

Supplementary Figure 8. Surface area of rocks used in settlement trials grouped by treatment.

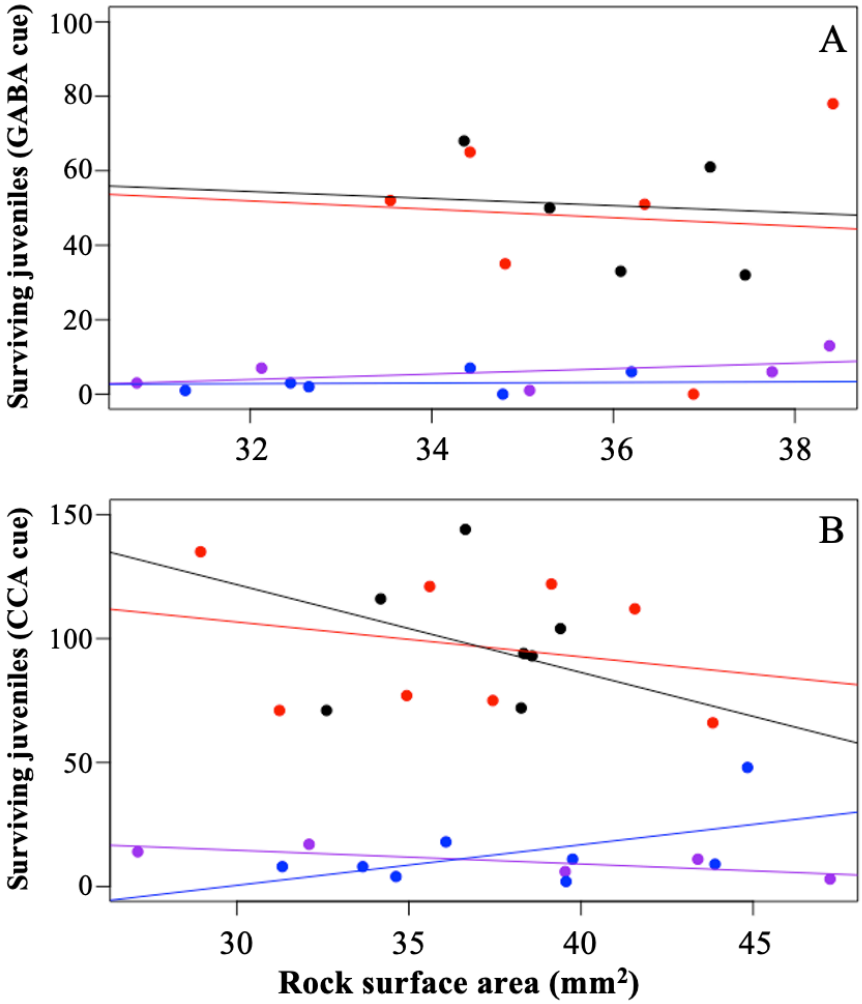

Supplementary Figure 9. Juvenile survival vs. rock surface area in mm^2. (A) shows the relationship for rocks with the GABA cue, (B) shows the relationship for CCA covered rocks.

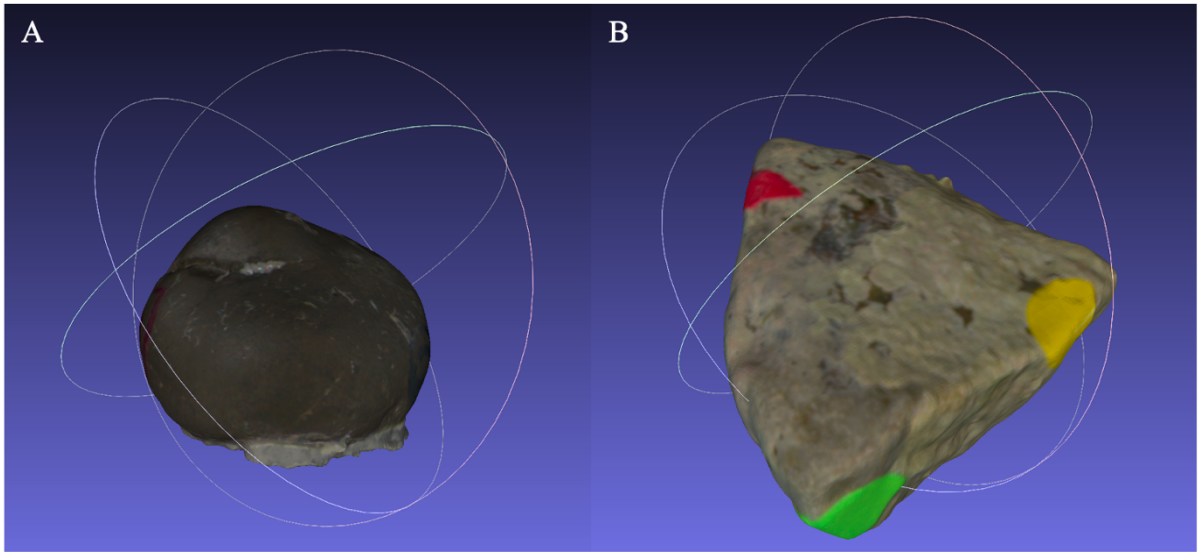

Supplementary Figure 10. Examples of 3D scans of a rock from a GABA treatment (A) and a CCA treatment (B). Colored dots on the rock scans were stickers used to help orient the 3D scanner.

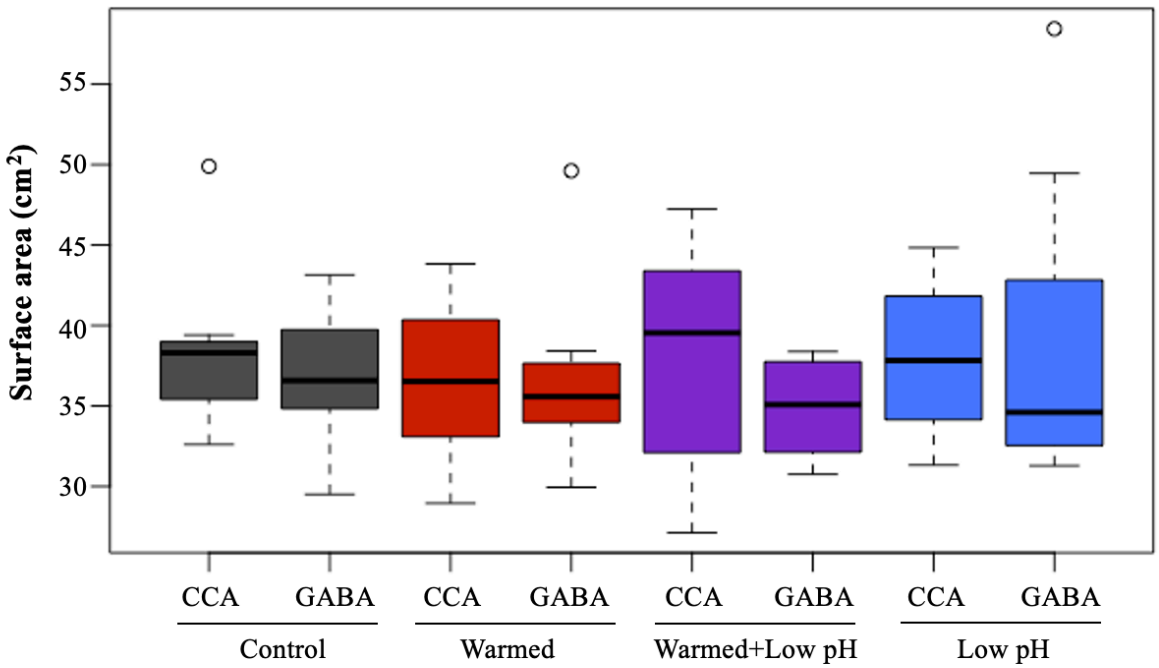

Supplementary Figure 11. Surface area in cm^2 of rocks used for the juvenile survival experiment.

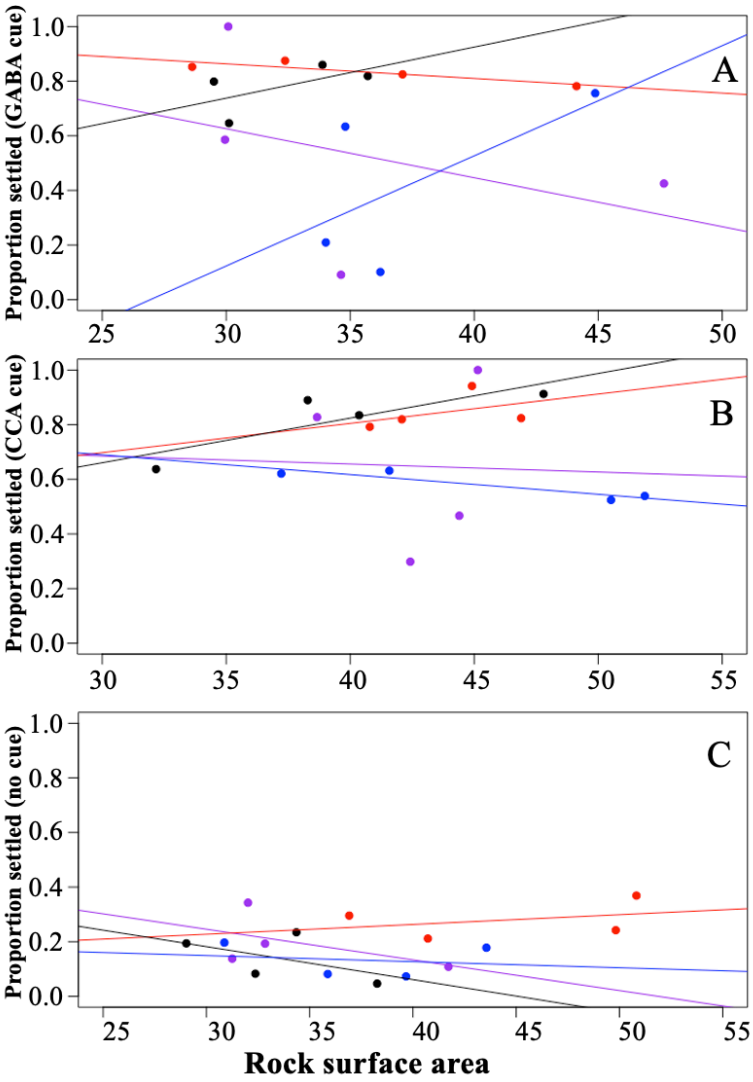

Supplementary Figure 12. Proportion of settled larvae (estimated as count of settled larvae divided by sum of settled and swimming larvae) vs. rock surface area in mm^2. (A) shows the relationship for rocks with the GABA cue, (B) shows the relationship for CCA covered rocks, (C) shows the relationship for rocks with no settlement cue.

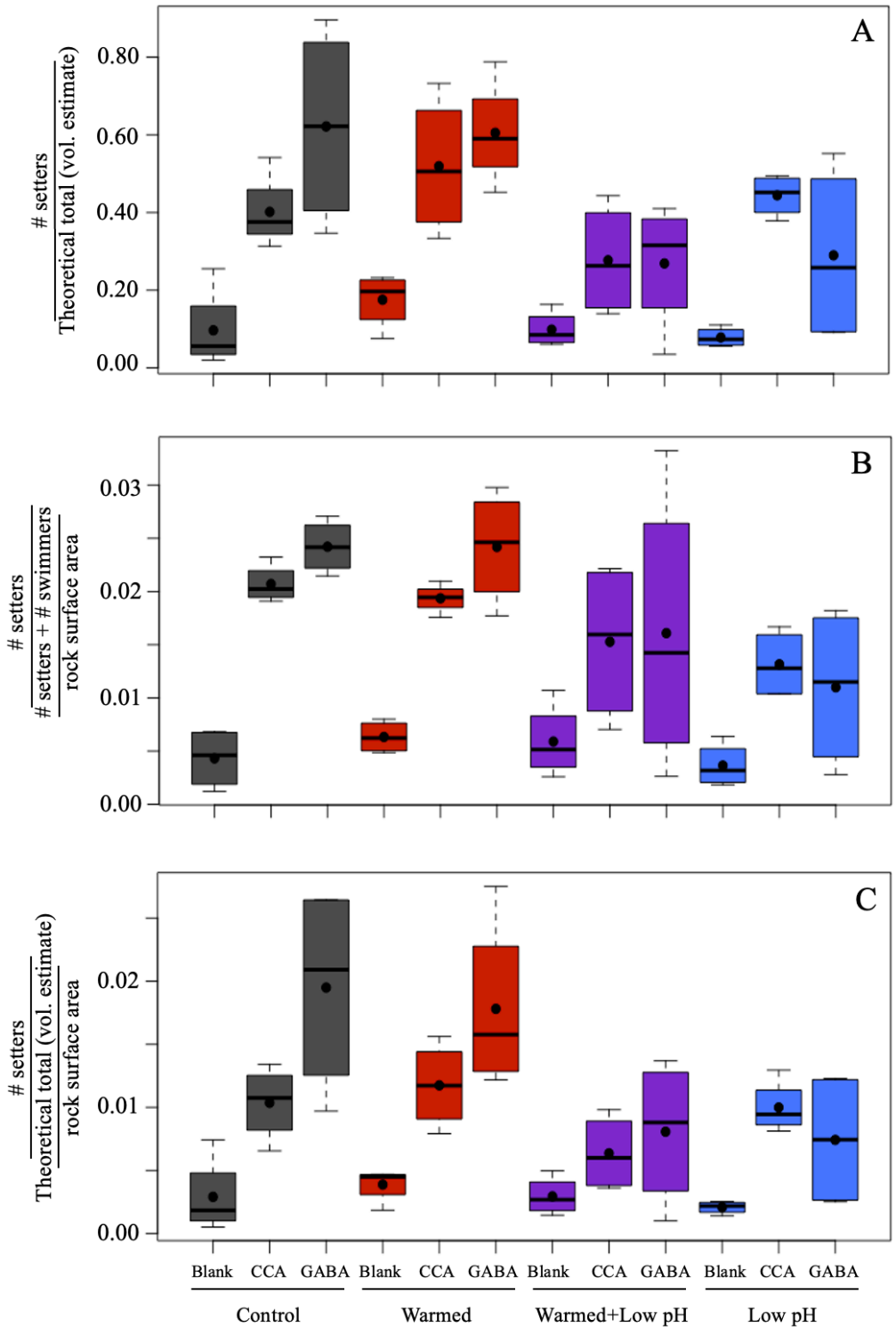

Supplementary Figure 13. Alternative metrics for larval settlement

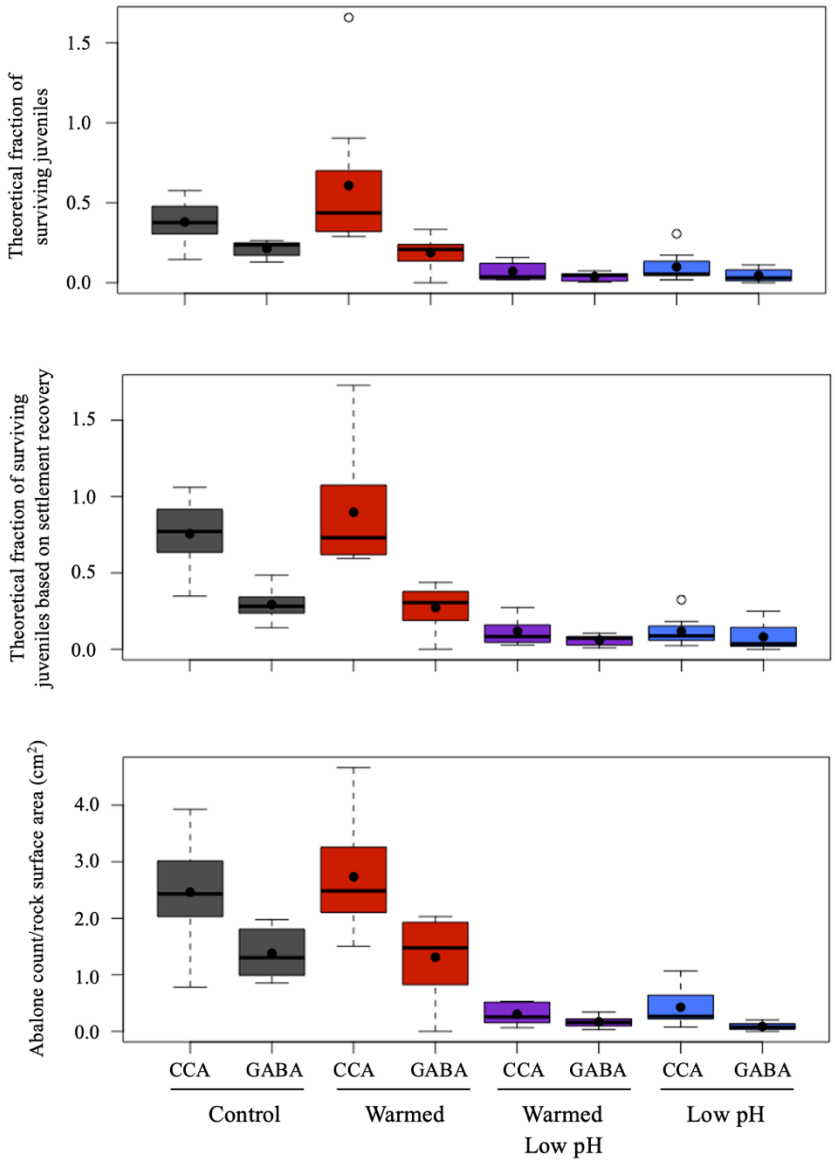

Supplementary Figure 14. Alternative metrics for juvenile survival at the conclusion of the experiment

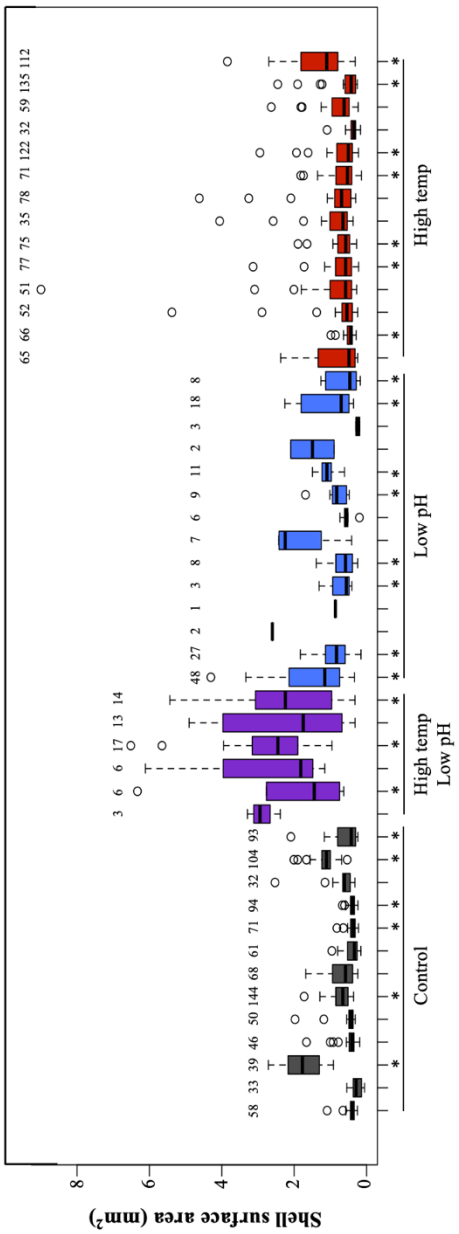

Supplementary Figure 15. Mean juvenile shell surface area (mm^2) at the conclusion of the experiment in each jar used for analysis, grouped by temperature and pH treatment. Number of surviving abalone in each jar is indicated above the box. * indicates CCA treatment jar.

Chapter 4: Juvenile pinto abalone survival and oceanographic dynamics at restoration sites in the San Juan Islands (WA)

Publication history: This study was coauthored by Josh Bouma, Katie Sowul, Henry Carson, Jodie Toft, and Jacqueline Padilla-Gamiño. At the time this dissertation was published, this chapter was not published separately.

Abstract

Pinto abalone (*Haliotis kamtschatkana*), the only native abalone species in Washington, was listed as endangered at the state level in 2019. Efforts to restore pinto abalone to Washington's San Juan Islands have been ongoing since 2009 using conservation aquaculture, but there is considerable variability in abalone survival between the restoration sites where hatchery-reared abalone are outplanted. To see if differences in oceanographic conditions might correlate with these differences in survival, we deployed oceanographic sensor arrays at six abalone restoration sites each year for three years to monitor temperature, salinity, dissolved oxygen, pH, and current speeds. Monitoring spanned the period from when one- to two-year-old abalone were outplanted until sites were surveyed approximately 10 months later to assess abalone survival. Survival at sites ranged from 0.43% - 9.63%. Overall, oceanographic conditions were within known tolerable ranges for pinto abalone. We found clear differences in salinity and temperature variability between sites, especially those sites in the northern islands. Dissolved oxygen and pH both changed seasonally, and variability increased during spring and summer months with algal growth, but clear spatial patterns could not be determined. Current speeds also varied between sites, and currents seemed to be mostly tidally driven as opposed to having seasonal shifts. Despite these measured differences in survival of abalone and in

environmental conditions across sites, the data did not indicate any correlation between oceanographic variables and abalone survival. However, it has provided valuable baseline data on the environmental conditions experienced by abalone in the wild in Washington. This data will facilitate tracking and understanding the evolving environmental conditions over time and their impact on the success of restoration sites.

Introduction

Pinto abalone (*Haliotis kamtschatkana*) range from Southeast Alaska, USA, to Baja California, Mexico, acting as grazers in their subtidal rocky reef habitats. Their population has declined along this entire range, and in Washington State specifically, their numbers declined by 97% at 10 index sites between 1992 and 2017 (WDFW unpublished data, Rothaus et al., 2008). Pinto abalone restoration has been underway in Washington State since 2007. The Washington Department of Fish and Wildlife (WDFW) and Puget Sound Restoration Fund (PSRF), along with other partners, have developed a captive breeding and outplant program to restore pinto abalone above critical densities.

In Washington, wild-collected abalone are spawned, and their offspring are raised at the Kenneth K. Chew Center for Shellfish Research and Restoration (Manchester, WA) for one to two years. Then they are transported to the San Juan Islands (Figure 1), where they are released in dense aggregations. Restoration sites are currently selected during scouting dives, where various factors are qualitatively assessed. Rocky reef sites with high rugosity and high current speed, where minimal sediment accumulation occurs, are preferable, as are sites with abundant coralline algae or bull kelp (Carson et al., 2019). The presence of adult abalone is also used as an indicator of suitable habitat, although the program avoids collecting broodstock and outplanting in the same areas to ensure that broodstock are not hatchery-raised (Carson et al., 2019).

Historically, there has been substantial variability in abalone survival between different outplant sites (Carson et al., 2019). In a study analyzing ten outplant sites from 2011, 2015, and 2016, survival estimates based on SCUBA surveys one year post-outplant showed an average survival at 10.2%, ranging from 0% to 23% among sites (Carson et al., 2019). Each year, distinct genetic families created in the hatchery are split evenly across sites, so this variability cannot be

explained by genetic differences in outplanted juveniles. As the restoration program builds from a pilot to a production phase, optimizing site selection is critical for maximizing abalone survival in the wild. However, there is little understanding of the mechanisms impacting abalone performance at different sites (Carson et al., 2019).

Differences in abalone survival between sites could be due to several factors (Figure 2). Losses could be due to mortality or to outmigration. If mortality, then the bottleneck could include substrate habitat quality, resource availability, water properties, predation, and competition. One potentially crucial aspect that remains unstudied is the variation in seawater characteristics between different sites. Previous laboratory studies have shown that water chemistry impacts growth and survival across different life stages of marine invertebrates, including abalone.

Further, we know that water chemistry is changing globally due to the emission of greenhouse gases and their absorption by oceans, an increase in coastal human populations, and changes in precipitation and other weather patterns (Doney et al., 2009; Fowler & Oregioni, 1976; IPCC, 2023; Wang et al., 2018). As global climate change continues, marine species in coastal areas will face increasing seawater temperatures, continued ocean acidification, and lower dissolved oxygen availability (IPCC, 2014; IPCC, 2023).

Ocean temperature changes are some of the most well-documented impacts of climate change on marine environments, and impacts of temperature have been studied on abalone populations worldwide. A study in Australia assessing size-dependent thermal limits in a hybrid species (*H. rubra* x *H. laevigata*) found evidence that warming may lead to smaller and less fecund abalone, which can impact biomass for farming purposes but can also impact recruitment, which would be more relevant for wild populations (Holland et al., 2024). In pinto abalone, trials

between 11°C and 21°C found no significant impact of temperature on juvenile survival (Bouma, 2007). A study on white abalone (*H. sorenseni*) in California, however, found highest juvenile survival at 12 °C, highest growth at 15 °C, and highest mortality at 18 °C due to withering syndrome (Mccormick et al., 2016). Withering syndrome or other catastrophic abalone diseases have not been identified in Washington State (Sowul et al. 2022) but could pose threats in the future as species ranges shift with climate change. Further, studies have emphasized the significance of considering both mean temperatures and temperature variability to better understand abalone distribution and how it may shift under climate change (Lluch-Cota et al., 2023).

In addition to temperature, pH change is one of the most relevant variables to consider for abalone, especially in coastal waters in the northeast Pacific. Ocean acidification, or a decrease in ocean pH, is caused by the absorption of CO_2 by oceans. Ocean acidification is known to negatively impact many marine invertebrates, particularly calcifying invertebrates (Bates et al., in prep.; Crim et al., 2011; Gazeau et al., 2013; Guo et al., 2022; Kroeker et al., 2013; Parker et al., 2013). Studies on the impacts of ocean acidification on juvenile and adult abalone have shown mixed results. In both European abalone (*H. tuberculata*) and pāua (*H. iris*), juvenile survival was not significantly impacted in low pH treatments (Auzoux-Bordenave et al., 2020; Cunningham et al., 2016). In pinto abalone specifically, we found that survival was negatively impacted after rearing larvae through settlement and into the first months of their juvenile phase in a pH of 7.55 compared to a control of 7.9 (Chapter 3).

Dissolved oxygen, often covarying with pH, is variable in environments like coastal Washington that experience upwelling and will further change as human influences on the climate continue (Feely et al., 2008). Tolerance to low oxygen and hypoxic conditions vary

between abalone species as well and vary with temperature (Shen et al., 2020). In red abalone, prolonged exposure (>24hr bursts as opposed to 3-6hr bursts) led to decreased survival in a laboratory study (Kim et al., 2013). Growth rates of juveniles decreased in this same experiment when exposed to low pH and low dissolved oxygen (DO), as did the variability in growth between individuals, and these changes in growth were less dependent on the duration of exposure (Kim et al., 2013). In a study on South African abalone (*H. midae*), juveniles were found to have significantly less DNA damage than adults after exposure to low DO (~83% saturation) and high DO (~115% saturation) conditions compared to control conditions (~95% saturation) (Vosloo et al., 2013). Juvenile greenlip abalone (*H. laevigata*) exposed to a range of conditions (4.2mg/L-8.9mg/L, or 55-117% saturation) showed declines in growth as oxygen levels decreased across the whole range of experimental treatments (Harris et al., 1999). A study comparing the growth and survival of green abalone on either side of Isla Natividad in Baja California, Mexico, found substantial variability between the two sites, which had distinct temperature and dissolved oxygen regimes (Boch et al., 2018). Dissolved oxygen tolerance of pinto abalone has not been specifically determined. However, it is anticipated that lower oxygen levels could result in sublethal and potentially lethal effects below a certain threshold.

Beyond temperature, pH, and DO, there are other important oceanographic considerations for abalone in Washington. Abalone in Washington's San Juan Archipelago and surrounding areas experience fluctuations in salinity caused by river discharge, primarily from the Fraser River, along with strong tidal currents that influence water mixing (Masson & Cummins, 2004). Historically, lower salinity levels are anticipated during the freshet events from the Fraser River watershed, typically occurring in June due to snowmelt. However, high river discharge regionally can also occur during the winter due to rainfall (Masson & Cummins,

2004). These changes would not be expected to uniformly affect the San Juan Archipelago—distance from river mouths and exposure to tidal currents vary considerably throughout the islands. Pinto abalone are known to be negatively impacted by low salinity—but the extent to which they experience salinities low enough to enter this detrimental range is unknown. Post-larval pinto abalone from Washington exposed to a range of salinities had the highest survival in 26, 29, and 32 PSU treatments, lower survival in 23 PSU treatments, and lowest survival in 14,17, and 20 PSU (Bouma, 2007).

Current speed is also an important oceanographic consideration when analyzing abalone habitat. Abalone anatomy is adapted for living in environments where respiration can be relatively passive, relying on water with high flow to ensure adequate oxygenation (Morash & Alter, 2016). Many studies on flow and abalone occur in captivity (Lin et al., 2024; Wassnig et al., 2010), which makes it challenging to assess how flow rates in tanks compare to tidal currents experienced in their natural environments. A laboratory study on Pacific abalone (*H. discus hannai*) indicated that abalone preferred flow around 5 cm/s and moved and fed less in areas with higher flow (Lin et al., 2024). The correlation between flow and other variables in natural environments—sedimentation rate, oxygenation, or salinity for example—might complicate our understanding of flow effects on wild abalone in Washington State.

Most laboratory studies only focus on one stressor at a time, but there is a growing body of research on the combined impacts of multiple stressors. Similarly, there is growing recognition that exposure to variable conditions has different impacts than to static stressors (Dillon & Woods, 2016). Some laboratory studies have succeeded in exposing abalone and other invertebrates to temporal variability in stressors and have compared acute and chronic exposures

of different durations, but there is still variability and complexity *in situ* that cannot be replicated in a laboratory.

Biological factors can influence water chemistry at local scales (Lowe et al., 2019). Kelp forests in particular can impact pH and dissolved oxygen levels in surrounding water (Murie & Bourdeau, 2020). A study on fjords in the Arctic Ocean found that pH variability was influenced by seasons, horizontal and vertical location in the fjord, and proximity to kelp forests (Krause-Jensen et al., 2015). However, it is important to recognize that the impact of kelp forests on water chemistry is more pronounced within the kelp canopy compared to the benthos, where organisms like abalone live (Murie & Bourdeau, 2020).

Field studies integrating abalone performance with oceanographic conditions are more difficult to conduct and less common than laboratory stressor exposures but are critically important in for crafting robust restoration actions. Assessing survival of abalone in real-world habitat provides unique combinations of oceanographic variables, and unique fluctuations in each of these variables, that we could not successfully mirror in hatchery experiments. In this study, we investigated abalone survival at restoration sites and characterized the variability in water conditions over relatively small spatial scales, focusing on locations relevant to pinto abalone and conservation initiatives. We hypothesized that sites with higher current, higher pH and DO levels, and no extremely high temperature levels or extremely low salinity levels, would likely provide optimal habitat for abalone, and that this would lead to higher survival of outplanted juveniles at sites with these oceanographic conditions. Characterization of the oceanographic conditions at our abalone restoration sites will allow us to see what stressors abalone are experiencing, see the variability in conditions between sites, and could provide us

with data as to what variables are most important to assess when we create new restoration sites in the future.

Methods

Study Sites

Six abalone restoration sites where abalone were to be outplanted were selected for each of three years of oceanographic monitoring. Two sites were selected for monitoring in years two and three because they had received multiple sequential years of outplants. This made for a total of 16 distinct sites that were monitored, 14 of those for one year and two of those for two years of the study.

Sites were located in the San Juan Archipelago and surrounding mainland (Figure 1). Due to concerns over the illegal harvest of pinto abalone, site locations cannot be shown on a map nor fully described. Code names were selected for each site from the names of allied amphibious assaults during World War II and will be used throughout the manuscript. The sites could loosely be grouped into western (Watchtower, Cartwheel, Brushwood), northern (Dracula, Iceberg, and to a lesser extent Landcrab), central (Sword and Agreement), southern (Cherry Blossom and Cottage), and eastern (Husky, Juno, Infatuate, Goodenough, Torch, and Switchback). The sites and corresponding colors used are summarized in Table 1.

The sites were approximately 8 m by 10 m and were demarcated by pitons installed with polylines at all four corners so they could be consistently and repeatedly identified. Sensor arrays (affixed to two half cinderblocks) were placed at a target depth of ~6 m MLLW (mean lower low water) at each site. We attempted to place the blocks on a flat surface, ideally wedged between

rocks or boulders, to reduce the possibility of the sensor flipping in a storm surge (Figure 3). All access to sites was conducted using SCUBA diving.

Oceanographic Sensor Arrays

Oceanographic sensor arrays included pH, temperature, DO, conductivity, and current sensors. Onset temperature (MX2202), dissolved oxygen (U26-001), and conductivity (U24-002-C) sensors were used at each site. For the first year of data collection, Onset HOBO pH loggers (MX2501) were used, and for the second and third years of data collection, Pyroscience AquapHOx-L-pH shallow water pH loggers were used. Sensors logged continuously at 10-minute intervals. Lowell Instruments TCM-1 Tilt Current Meters (no ballast) were used for current speed and direction.

Sensor maintenance and calibration

Sensors were deployed on or around the day of abalone outplants each year, typically in April or May. During deployment dives, readings for dissolved oxygen and salinity were taken with a YSI Professional Series probe for the first two months of the study. Starting in mid-May 2021, a fully submersible YSI Exo Sonde was used to get verification points for sensors instead. Additionally, water samples were taken in triplicate to take verification points for pH. On board the dive boat, these samples were analyzed with a handheld pH probe (Orion Star A324 pH/ISE Portable Multiparameter meter with Ross Ultra Triode). Starting in the second year of the study, these probe calibrations were verified by generating TRIS buffer curves.

Every two to three months, sensor arrays were removed, cleaned, and if necessary, disposable sensor caps replaced and sensors recalibrated (pH and DO sensors). Then, that sensor

array was redeployed at another site at the same time the site's previous sensor array was collected for recalibration. This "leapfrogging" of sensors ensured that any bias between individual instruments would not continually bias results at certain sites. At the same time these sensor swaps occurred, water samples were taken for pH and alkalinity, and YSI readings were taken for salinity and dissolved oxygen.

Data Processing

Salinity: The conductivity assistant tool in HOBOware Pro was used to process salinity data. We used the start and end points from deployment along with corresponding temperature and conductivity measurements from the YSI to correct the raw salinity data. This approach should have effectively corrected for drift during deployment for these samples. For certain files, however, using the start and end corrections created unreasonable peaks in the data, likely due to fouling or sensors flipping over. For these data segments, we used only the starting YSI calibration point and then truncated the data at the time when a sudden incorrect sensor drift appeared to occur.

For the first deployments of the sensors at Landcrab, Switchback, and Infatuate in the first year of the study, we only used the endpoint corrections and the factory settings as the start point corrections. This was due to inaccurate YSI readings for those start measurements, and because the sensors had not been used or fouled yet, we believed the factory settings would be sufficient.

All the salinity loggers experienced fouling during the deployments, which likely caused inaccurate drops in salinity data, as is often seen with long deployments for these sensors. Some of these peaks reached values clearly too low to be realistic salinities for the region, so for the

purposes of graphing, a lower boundary for salinity was set at 25 PSU and minimum and mean salinity values were not calculated for each site.

For analysis, maximum salinity in the summer months (May-September), maximum salinity in the winter months (October-April), and mean salinity based on individual YSI measurements were used. We used YSI points from sensor deployments in April/May, June/July, September/October, November/December, and YSI points from sensor removals in February/March of each year of the study. This totaled to five points for each site in each year. Maximum salinity for Torch in the winter months had to be estimated as a mean of all other maximum winter salinities because the salinity meter at Torch failed for all winter months.

Dissolved Oxygen: The dissolved oxygen assistant tool in HOBOware Pro was used to process dissolved oxygen data. This tool allowed us to adjust dissolved oxygen data for site-specific salinity. Due to the inconsistencies in the salinity loggers, we used the mean of the two salinity measurements taken at the start and end of each deployment with the YSI. We were also able to correct the DO data using the YSI measurements for dissolved oxygen from the start and end of each deployment.

For analysis, we calculated mean, maximum, minimum, and variance of DO values for each site for each year. We also calculated the number of days in total that each site spent at a DO level below 5mg/L. Finally, we calculated the mean daily fluctuation in DO at each site. Although there were gaps in DO data for some sites, these were considered small enough over the course of the year that all available data was used to calculate each metric.

Temperature: Temperature data from the HOBO loggers was left unadjusted. For analysis, we used mean, maximum, minimum, and variance in temperature for each site for each year. When temperature loggers failed, temperature data from DO loggers was used in their

place, and on the rare occasion temperature and DO loggers failed, temperature data from salinity loggers was used. This allowed us to have complete data sets for temperature for each of the three years of the study.

pH: HOBOware Pro was used for the first year of collected data to convert files. The Pyroscience Workbench software was used for the second and third years of data collection, and an automatic drift compensation was applied to address known sensor drift to more basic values.

Fouling, particularly during the first year of data collection, appears to have led to increased variability in pH measurements over time after sensor cleaning. For this reason, we elected to use the two weeks of data after each sensor recalibration as a smaller data set to compare pH between sites.

In addition to our sensor data, we also had point measurements from water samples taken during each sensor deployment, redeployment, and retrieval. We estimated alkalinity values from known salinity values for each time the pH samples were taken using a regression for coastal Washington waters (Fassbender et al., 2017). Using the R package Seacarb, we used our pH values and alkalinity values to calculate temperature-corrected pH values for each deployment time, which we could then compare to sensor measurements.

For analysis, we assessed the minimum, maximum, mean, and variance of pH values for each site from the sensor data. We also calculated a mean based on the discrete water samples taken from sensor deployments in April/May, June/July, September/October, November/December, and YSI points from sensor removals in February/March. This totaled to five points for each site in each year.

Current speed: Current speed data was generated using the Domino software (Lowell Instruments), adjusting for declination, seawater density, and ballast on the sensors.

Unfortunately, battery issues with the current meters caused breaks in data during the first two years of the study. For the third year of the study, enough data was missing that we decided not to include any current data.

Abalone outplant and survival surveys

In April of each year of the study (2021, 2022, 2023), abalone were outplanted to the six sites where sensors would be installed. These abalone were spawned from wild-collected broodstock and reared in the Kenneth K. Chew Center for Shellfish Restoration and Research for 8-20 months. Outplant consisted of loading abalone into 4" or 6" PVC tubes at the hatchery and transporting the abalone in seawater to Anacortes, where they were loaded into a tote on the dive boat. Abalone were then brought to each site, and PVC tubes were placed on the site and wedged into place with rocks. Abalone then crawled out of the PVC tubes over time at each of the sites.

In February of the following year (2022, 2023, 2024), survival surveys of the outplanted abalone were conducted. Divers used the pitons on the plot corners and measuring tape to demarcate the outside border of the site, then laid lead line in 2 m lanes. Lanes were meticulously surveyed, and all abalone were counted and measured in each lane as well as in a 2 m perimeter around the plot. Survival was calculated based on the known number of abalone outplanted at each specific site vs. the number counted the following February.

In Year 3 of the study at Cherry Blossom, Iceberg, and Dracula sites, where abalone had been outplanted the previous year and only two-year-old abalone were tagged, we were unable to directly evaluate the survival of one-year-old abalone. We used data from previous outplant sites that were surveyed two and three years after outplanting to estimate a mortality rate between

year two and year three. This enabled us to estimate the percentage of our abalone counts in 2024 that originated from the 2023 outplants versus counts from earlier previous outplant cohorts.

Comparison of oceanographic data and survival data

To assess the correlation of oceanographic variables, we ran principal component analysis (PCA) on three subsets of the data. First, we did a PCA for years one and two of the study, which included various metrics of salinity (winter maximum, summer maximum, and mean of point measurements), temperature (mean, minimum, and variance), current (variance, mean, and fraction of days where current went above 1 knot), and DO (mean, daily fluctuation, time below 5mg/L, and minimum). Year three was excluded due to a lack of current data. Second, we did a PCA for years two and three of the study that included various metrics for pH (maximum, mean, mean based on point measurements, and variance), temperature, salinity, and DO. Year one was excluded due to pH data from different sensors being incomparable. And finally, we did a PCA for all three years which included just metrics of the DO, temperature, and salinity.

We compared eigenvalues from principal components (PCs) to those expected by chance using a broken-stick model. PCs with eigenvalues higher than the broken stick expectation were extracted for use in linear models, comparing survival data from the corresponding years to those PCs. We used an arcsine transformation on survival data and then used simple linear models to analyze relationships from each PCA analysis. We also added year as a fixed effect in each model. We compared alternate models removing PCs one at a time, in addition to a model with just year, and a null model, for each of the three PCA results.

We compared AICc values for these models to determine if PCs or year improved the model fit compared to a null model. An improvement in the model fit over the null model would suggest a correlation between the oceanographic variables included in that PC and abalone survival.

Results

Abalone survival

For our 18 site surveys, survival ranged from 0.43% to 9.63% when counting one- and two-year-old abalone (estimates used for Cherry Blossom, Dracula, and Iceberg in Year 3 surveys). Overall, survival was low at Agreement (0.47%), Husky (0.83%), Cottage (0.43%), Watchtower (0.79%), Cherry Blossom (1.52%), Sword (1.15%), and Torch (1.20%). Survival was moderate for Infatuate (3.45%), Brushwood (5.39%), Cartwheel (3.67%), and Dracula (Year 2: 3.03%, Year 3: 3.23%). Survival was high for Juno (5.62%), Landcrab (5.85%), Switchback (7.29%), and Iceberg (Year 2: 9.63%, Year 3: 4.34%. For our surveys, the assessment of survivorship is limited to the abalone that are observed on the site and are visible to the divers. Therefore, factors such as outmigration (abalone leaving the survey area) and the cryptic nature of abalone hiding in inaccessible crevices could potentially influence our measurement of survival.

Temperature

Our three years of monitoring provide a description of conditions across various abalone restoration sites across the San Juan Archipelago. The mean temperature across all sites was 10.03°C, and the range in mean values between the 18 sites was only 1.40°C (Figure 5a).

Dracula and Iceberg had the clearest warm peaks in temperature data, followed by Landcrab and Sword. The average minimum temperature across all 18 sites was 7.25°C (Figure 5a).

All sites showed a similar seasonal pattern in temperature change (Figures 5b-d). The warmest period was July-October, with August being the warmest month when looking at all three years together with a mean temperature of 12.02°C. The lowest temperatures for our time series were generally between late December and February, though it should be noted that we collected minimal data in March. The variability in temperature between sites was most pronounced during and was more apparent in years two and three of the study, when sites were more geographically dispersed (Figure 5e).

Salinity

Salinity appeared suitable for abalone at every site we monitored. Average salinity at each site, based on YSI point measurements, ranged between 27.95 PSU (Dracula Year 2) and 30.75 PSU (Cherry Blossom) (Figure 6a). Dracula and Iceberg, the two northernmost sites, had the lowest salinity point values based on our YSI readings (23.88 and 24.95 PSU respectively in June of year 2). All sites other than these two had mean salinity values above 29.5 PSU.

Most sites showed higher salinity values in the summer months, but periodic dips in salinity were also seen throughout the summer at certain sites (Figures 6b-d). Some sites, such as Brushwood and Cottage, showed minimal seasonal changes in salinity, while others, such as Landcrab, had much more defined changes throughout the year. Iceberg (Year 3) and Switchback had the highest maximum salinity values (35.25 PSU and 35.19 PSU respectively) in the summer (May-September), while Infatuate and Watchtower had the highest maximum values (33.13 PSU and 34.36 PSU respectively) in the winter months (October-April). Iceberg (Year 2)

on the other hand had the lowest summer salinity maximum (30.5 PSU) and lowest winter salinity maximum (30.78 PSU).

Dissolved oxygen

Dissolved oxygen levels were relatively consistent between sites (Figure 7a). The mean DO across all sites was 6.95 mg/L, and the range in mean DO levels was 0.82mg/L. Brushwood had the lowest mean DO of all sites at 6.44mg/L, and Dracula (Year 3) had the highest mean DO at 7.26mg/L. The highest DO recorded was 13.73mg/L at Brushwood, and the lowest was 1.3mg/L at Cherry Blossom, although fouling could have impacted the accuracy and precision of measuring these DO extremes. The largest mean daily fluctuation in DO was at Dracula in year 2 at 2.24mg/L, while the smallest was at Agreement with a mean daily fluctuation of 0.72mg/L.

In year 3 of the experiment, Dracula, Iceberg, Torch and Goodenough had DO levels below 5mg/L for less than one cumulative day each. Brushwood spent a total of 32.92 days with DO below 5mg/L, Watchtower spent 21.75 days, and Landcrab and Cartwheel spent 19.76 and 19.45 days with DO under 5mg/L, respectively.

Throughout the study period, all sites exhibited comparable trends of declining dissolved oxygen (DO) levels during the summer months, followed by a gradual increase beginning around October (Figure 7b-d). September had the lowest mean DO level, 5.81mg/L, averaged across all sites and years.

pH

Although pH was higher overall during the first year of the study compared to years two and three, but this difference was likely due to a change in methodology after the initial year.

Specifically, sensors that offered improved correction capabilities due to fouling and drift and were designed for longer deployments were used in subsequent years of the study (Figure 8a). Average pH values calculated from point measurements taken during sensor deployments throughout the year revealed much more similar pH levels across different years and sites (Figure 8a). Based on these point measurements, the range in mean pH between sites was only 0.1 units (Watchtower had the lowest mean pH based on point measurements at 7.79, and Goodenough had the highest at 7.89). Our point measurements indicate that the sensors used in year one overestimated pH, while the sensors used in years two and three tended to underestimate pH.

Because of the risks of drift and fouling, we looked at pH data for only the two weeks following each sensor recalibration (though the full data set is summarized in Figures 8b-d). For these two-week periods across the year, Infatuate had the lowest single pH recorded at 7.6 for the first year of data collection, while Husky had the highest at 8.7. Looking at years two and three together, Cartwheel and Cottage experienced the lowest peaks in pH at 7.41 and 7.46, respectively, while Dracula (Year 2) had the highest pH recorded at 8.31.

Current speed

Current data was collected for the first two years of the study. Our current meters were less precise at higher speeds and cap at 200cm/s (3.89 knots). Even with this potential cap of maximum measured values, there was substantial variability in mean current speeds between sites (Figure 9a). The lowest mean current speed was 4.03cm/s (0.08 knots) at Watchtower, and the highest was 21.62cm/s (0.42 knots) at Husky.

In terms of the duration spent at higher current speeds, Landcrab, Switchback, Iceberg, Juno, Dracula, and Husky experienced currents exceeding 1 knot more than 70% of the time, while the sites Cartwheel, Brushwood, Watchtower, and Cottage had currents exceeding 1 knot for less than 30% of the time (Figure 9b). Only Juno and Dracula spent more than 20% of the time with current speeds over 2 knots (Figure 9c). Brushwood had the slowest maximum current speed recorded at 87.42cm/s, while Dracula, Switchback, and Agreement all showed current speeds over 200cm/s at times. Seasonal variations in current speed were less evident compared to seasonal variation in other oceanographic metrics. Instead, temporal patterns such as tides seemed to have greater influence on variability in current speed.

Assessing the correlation of oceanographic variables and abalone survival

We initially compared data from the first two years of the study, during which we collected current speed data along with temperature, DO, and salinity data to compare to abalone survival across sites. The first three principal components were significant, with 39.4% of variation represented by the first PC, 18.6% of variation represented by the second PC, and 14.3% of variation represented by the third PC (Figure 10). Eigenvectors for mean DO, days where DO was <5mg/L, temperature variance, fraction of days with current >1knot, salinity winter maximum, and mean salinity based on YSI points were all over a magnitude of 0.3. The two largest loadings for PC2 were mean current and variance in current. The two largest loadings for PC3 were low DO and low temperature. Iceberg and Dracula were separated from other sites along both PCs, likely due to high temperature variability, mean temperature and DO, and days with current over 1 knot. Juno and Husky were separated more on PC2, likely due to higher mean and variability of current speed and days with current over 1 knot. Cartwheel, Watchtower,

and Brushwood were on the far side of PC1 from Iceberg and Dracula, likely influenced by slower currents, higher salinity in winter, higher salinity based on YSI point measurements, and from more days with DO below 5mg/L (Table 2).

We then compared data from all three years of the study, this time only with DO, temperature, and salinity variables, as those were the only ones shared by all three years. The first two principal components captured a substantial portion of the variance, with 37.2% of represented by the first PC and 21.8% represented by the second PC (Figure 11). Eigenvectors for PC1 with the highest loadings were those for mean DO, variance in temperature, and mean temperature. Eigenvectors for PC2 with the highest loadings were those for low DO and low temperature. As in the previous PCA, Cartwheel, Brushwood, and Watchtower cluster together on one end of PC1 and correlate with higher salinity and more days with DO below 5mg/L. On the far side of PC1, Dracula and Iceberg (from both Year 2 and Year 3 this time) cluster together, with variation in temperature again a driving force. Cherry Blossom is distinctly separated from other points along PC2, likely because of its slower temperatures, absence of high summer salinity, and fewer instances of low DO values compared to the other sites (Table 3)

Finally, we compared data from years two and three of the study, where we had data for pH in addition to DO, temperature, and salinity. The first two principal components captured a substantial portion of the variance, representing 42.7% and 20.2% respectively (Figure 12). Eigenvectors for PC1 were largest for variance in temperature, mean temperature, and high pH. Eigenvectors for PC2 were largest for low DO, daily fluctuation in DO, and low temperature. As with previous PCAs, Iceberg and Dracula (again, both Year 2 and Year 3) cluster together, with Dracula at a more extreme end of both PC1 and PC2. Cartwheel, Brushwood, Watchtower, and Cottage are clustered closely together on the opposite end of PC1, demonstrating lower pH, less

temperature variability, and lower DO, as well as high winter salinity values. Cherry Blossom was again the most distinct along PC2, followed by Torch and Sword, with lower DO values, lower temperature values, and less variability in temperature, DO, and pH (Table 4).

We used AICc to compare alternate models and found that the null model fit the data better than models with PCs 1, 2, 3, or the Study Year (Tables 5-7). This was the case for models built off data from each of the three PCAs. This is an indication that there is no statistical evidence correlating our oceanographic variables with abalone survival, given the data we have.

Discussion

Abalone survival differed from 1-10% over 10 months between restoration sites in Washington State. Our study aimed to determine if any oceanographic variables were associated with these differences in survival. Most water properties fell well within the ranges known to be suitable for abalone: Low water temperatures, high salinity, strong water flow, and few occasions where DO or pH fell to problematic levels. Although our data do not statistically show a relationship between abalone outplant survival and water properties, there are important trends in each variable that still appear relevant for understanding abalone optimal habitat.

One reason for the lack of association between survivorship and temperature is that seasonal trends at each site were generally between 7°C and 14°C, which falls within the known thermal tolerance of pinto abalone. The mean site temperature (10.03°C) leaves ample room for warming to occur without exceeding the thermotolerance limits of pinto abalone (Chapter 3, Bouma, 2007). Best estimates of sea surface temperature increase by 2100 are between 2 and 4.5°C of warming (IPCC, 2007). Even with these increases, the mean temperature values would remain within a tolerable range for abalone. However, it is difficult to know what dimensions of

temperature will be most relevant to abalone—further study is required to understand on what temporal scales temperature stress can occur and how duration of exposure impacts maximum tolerable temperatures. We did observe sites with significant warm peaks in the summer months. These peaks were most clear at Dracula, Iceberg, Landcrab, and Sword. The first two are the most northern sites that we studied, and Landcrab is southwest of them. These northern sites appear to experience warmer water masses moving through during the summer months for short periods of time. Sword, while technically located in the central San Juan Islands, is relatively close to Landcrab and situated near a channel that connects to the northern sites. The highest temperature peaks were observed during July and August, occurring after the natural spawning season (April-July) for pinto abalone (Neuman et al., 2019). Therefore, vulnerable early life stages such as larvae would likely not encounter temperatures exceeding their thermal tolerance. Our previous research has shown that abalone larvae may be affected by temperatures around 18°C (Chapter 2). However, immediately post-settlement, juvenile abalone should be robust to temperatures that reach 18°C.

While direct impacts of thermal stress do not seem likely to cause mortality in outplanted abalone nor their offspring, other factors can change with increasing temperatures. As temperatures increase, diseases not present at lower temperatures can become threats to abalone populations. Additionally, changes in temperature can affect the prevalence and abundance of other species that abalone rely on for food, as well as species that compete with abalone for resources (Rogers-Bennett et al., 2010). Thus, even if the early stages of pinto abalone are not directly impacted by ocean warming in the coming decades, warming could trigger other changes in the ecosystem that could act as stressors to abalone populations.

The salinity data exhibited a consistent trend where the northern sites differed notably from the other locations. Both Iceberg and Dracula showed dramatically lower salinities than measured elsewhere. Although fouling of our salinity loggers prevents us from building a full picture of the temporal changes and the minimum salinity values experienced at each site, the data indicates that the two northern sites showed lower salinity values. This could be an indication of interannual variability in salinity in the northern end of the San Juan Islands. The Fraser River, the largest output into the Salish Sea, responsible for 50% of river output into the estuary, has flow dominated by snowpack (Broatch & MacCready, 2022; Masson & Cummins, 2004). Given the interannual variability in Fraser River output (Masson & Cummins, 2004), fluctuations in salinities are plausible. However, the precision and accuracy limitations of our salinity loggers may also have contributed to the observed extreme differences between years. Iceberg showed the best survival of any site during the year where it experienced low salinity, and survival at Dracula was reasonably good in both years, irrespective of the change in salinity. This leads us to believe that salinity experienced at these sites is not detrimental, or at least does not cause mortalities. A more detailed and accurate assessment of salinity at these sites would offer a clearer understanding of sustained salinity levels and extremes within which abalone can survive. This enhanced data could provide valuable insights into the habitat preferences and tolerances of abalone in relation to salinity variations.

Coastal salinity patterns are likely to change due to shifts in whether precipitation falls as rain or snow, therefore changes in snowpack, storms, and precipitation could influence freshwater inputs to coastal areas like the Salish Sea (IPCC, 2023). The timing and direction of changes in precipitation could lead to fresher or saltier periods or less variability in salinity. Based on results in other abalone species, it seems that most abalone can tolerate salinity levels

between 25-45 PSU (Morash and Alter, 2016). Therefore, it is unlikely abalone in the San Juan Archipelago would encounter higher salinity levels that can be detrimental to their health. However, we observed a significant decline in the survival of outplanted abalone between the two years at Iceberg. Interestingly, the second year exhibited considerably higher salinity levels in the summer compared to the first year, even though salinity measured the first year we assess conditions at Iceberg was at one point below 25 PSU. Pinto abalone, especially those in Washington, may have tolerance to slightly lower salinity levels than other species, as they have been found tolerant to 23 PSU conditions (Bouma, 2007).

As other studies in the region have found substantial diel variation in pH and DO (Lowe et al., 2019; Murie & Bourdeau, 2020), we expected these might be two of the most dynamic variables at abalone sites. We observed variability on diel scales that was larger in summer and smaller in winter. These seasonal changes were congruent with higher macroalgal biomass in spring and summer, which suggests that photosynthesis was causing DO and pH to increase more during daylight hours. From laboratory studies, we know that both low DO and low pH can negatively impact abalone (Chapter 3, Kim et al., 2013; Morash & Alter, 2016; Shen et al., 2020). After a three-month exposure to low pH, juvenile European abalone showed reductions in shell length, weight, and strength (Auzoux-Bordenave et al., 2020). Juvenile pinto abalone had reduced survival but increased size following a similar exposure (Chapter 3). Most studies examining the effects of low pH and DO on abalone use stable conditions, while our field data makes it very clear that diel variability, especially in the spring and summer, is substantial. Based on our point measurements of pH, abalone may experience conditions at the edge of these stressful levels at certain sites, and it is likely that they experienced lower levels than our point

measurements could capture, based on the pH variability we saw from the sensors we deployed long term.

Given that ocean pH is expected to drop in the coming century, it is likely that abalone will more regularly experience stressful pH conditions (IPCC, 2023). Our YSI point measurements from sensor redeployments indicated minimal variability between sites. This would not support a restoration strategy of intentionally targeting restoration sites that may be pH refugia, but our long-term data show more substantial differences in pH variability between sites. Determining whether the effects of variable pH are positive or negative for pinto abalone would be critical in understanding which of these sites would act as better climate refugia.

Other habitat considerations

Our results highlight the importance of further investigating certain factors that we have not examined in this study. Predation, for example, was not included here, but ongoing research by the Washington Department of Fish and Wildlife using time-lapse cameras aims to answer the question of how much predation may impact abalone immediately after outplant. Similarly, potential competition with other benthic species for space or food may also influence site suitability. Habitat quality and complexity, or the presence of cryptic habitat in the form of crevices or other protected spaces could also influence abalone habitat preferences and could help in predator avoidance at certain sites.

The abundance of abalone food in the form of benthic diatoms or other algae and seaweeds, the quality of that food, and the consistency of that food throughout the year could also contribute to abalone survival. While not quantified in this study, the types and extent of algal cover varied substantially across sites and seasons and should be studied further.

Outmigration is another variable that we cannot directly account for in surveys due to limitations in time and resources to allocate to diving efforts. However, it could lead to a substantial discrepancy between our calculated survival numbers and actual survival from a given outplant. For the purpose of selecting optimal restoration sites, outmigration may just be as relevant as mortality, as it suggests a deficiency in the habitat that prompts abalone to leave. In many cases, outmigration may result in abalone dispersing from aggregations, potentially impacting their ability to successfully reproduce. Therefore, when assessing abalone fitness and the potential for population growth, outmigration may have a similar effect as mortality.

Conclusions

Our study is the first comprehensive assessment of oceanographic conditions at a range of pinto abalone outplant sites in Washington State. Although it seems unlikely that we can solely rely on oceanographic factors to predict the viability of potential outplant sites, characterizing the environmental conditions where outplanted abalone reside in Washington State yields valuable insights. This knowledge enhances our understanding of how abalone tolerances to many variables, often tested only in a laboratory setting, play out in natural and more variable environments. Future tracking of oceanographic and biological variables at these sites will provide valuable information on how outplant sites change over time. This information is crucial for ensuring the resilience and effectiveness of the pinto abalone recovery program in the face of ongoing climate change.

Acknowledgements

The authors thank Emily Loose, Taylor Frierson, Ocean Working, Bethany Stevick, and Caitlin O'Brien for their help with SCUBA surveys and sensor redeployments. We thank UW DSO Will Love for his help with dive planning and training. We thank Derek Smith, Nate Schwarck, and James Dimond for their assistance in captaining dive boats, as well as James Dimond for his help as a diver. Thanks to Alex Lowe for his advice and help in developing data collection methods. We thank Jennifer Ruesink, Tim Essington, and Jesse Zaneveld for their assistance with manuscript revisions and data analysis strategies.

Figures and Tables

Table 1. Abalone sites that were outplanted and monitored for each year of the study.

Year 1 April 2021-February 2022	Year 2 April 2022-February 2023	Year 3 April 2023-February 2024
Agreement (dark green)	Brushwood (brown)	Cherry Blossom (pink)
Husky (red)	Cartwheel (purple)	Goodenough (light green)
Infatuate (dark blue)	Cottage (light brown)	Dracula (dark red)
Juno (black)	Dracula (dark red)	Iceberg (light grey)
Landcrab (orange)	Iceberg (light grey)	Sword (light blue)
Switchback (dark grey)	Watchtower (dark pink)	Torch (yellow)

Table 2. (A) Sample scores for each site on significant PCs (B) Variable loadings on each PC for PCA1, which includes sites from years 1 and 2.

(A)	Sample Scores			(B)	Eigenvectors		
Site (Year)	PC1	PC2	PC3	Variable	PC1	PC2	PC3
Agreement (1)	3.199	0	1.32	DO minimum	0.024	-0.089	-0.514
Husky (1)	-0.805	2.29	-0.692	DO mean	-0.332	-0.17	-0.252
Infatuate (1)	1.976	-0.072	0.546	DO days below 5mg/L	0.328	0.112	0.336
Juno (1)	0.226	-1.406	-1.458	DO daily fluctuation	-0.141	-0.247	0.267
Landcrab (1)	3.71	-1.366	0.001	Temperature variance	-0.352	-0.283	0.085
Switchback (1)	-1.69	2.589	0.403	Temperature mean	-0.401	-0.173	0.147
Brushwood (2)	0.345	1.35	1.383	Temperature low	0.116	-0.207	0.535
Cartwheel (2)	0.216	-0.85	0.412	Current speed mean	-0.206	0.46	0.287
Cottage (2)	-3.141	-0.608	2.22	Current speed variance	-0.198	0.516	0.1
Dracula (2)	-3.784	-2.67	-0.142	Time current >1 knot	-0.34	0.326	0.069
Iceberg (2)	-0.596	0.855	-2.545	Salinity summer high	0.012	0.282	-0.222
Watchtower (2)	0.346	-0.112	-1.447	Salinity winter high	0.343	-0.152	0.105
				Salinity mean (YSI)	0.384	0.224	-0.125

Table 3. (A) Sample scores for each site on significant PCs (B) Variable loadings on each PC for PCA 2, which includes sites from all three years of the study.

(A)	Sample Scores		(B)	Eigenvectors	
Site (Year)	PC1	PC2	Variable	PC1	PC2
Agreement (1)	-3.233	1.167	DO minimum	0.085	0.483
Husky (1)	-0.56	1.796	DO mean	0.408	-0.243
Infatuate (1)	-2.037	0.834	DO days below 5mg/L	-0.393	0.283
Juno (1)	0.299	0.127	DO daily fluctuation	0.245	0.254
Landcrab (1)	-3.435	0.425	Temperature variance	0.426	0.25
Switchback (1)	0.057	0.101	Temperature mean	0.45	-0.226
Brushwood (2)	-1.401	1.104	Temperature low	-0.019	-0.512
Cartwheel (2)	-0.428	-0.768	Salinity summer high	-0.031	0.34
Cottage (2)	2.469	-0.421	Salinity winter high	-0.319	-0.028
Dracula (2)	4.303	2.026	Salinity mean (YSI)	-0.352	-0.266
Iceberg (2)	-0.057	1.626			
Watchtower (2)	-0.537	0.045			
Cherry Blossom (3)	-0.536	-3.475			
Dracula (3)	2.427	0.609			
Goodenough (3)	0.169	-0.916			
Iceberg (3)	1.662	0.082			
Sword (3)	0.157	-2.301			
Torch (3)	0.683	-2.062			

Table 4. (A) Sample scores for each site on significant PCs (B) Variable loadings on each PC for PCA 3, which includes sites years 1 and 2 of the study.

(A)	Sample Scores		(B)	Eigenvectors	
Site (Year)	PC1	PC2	Variable	PC1	PC2
Brushwood (2)	3.123	1.386	DO minimum	-0.094	0.414
Cartwheel (2)	2.081	1.989	DO mean	-0.27	-0.174
Cottage (2)	0.728	1.351	DO days below 5mg/L	0.286	0.276
Dracula (2)	4.24	1.05	DO daily fluctuation	-0.225	0.371
Iceberg (2)	-2.204	-0.403	Temperature variance	-0.337	0.203
Watchtower (2)	-4.48	1.928	Temperature mean	-0.349	-0.235
Cherry Blossom (3)	1.704	-3.326	Temperature low	0.046	-0.488
Dracula (3)	-2.622	1.094	Salinity summer high	-0.059	0.126
Goodenough (3)	-0.162	-1.037	Salinity winter high	0.297	0.117
Iceberg (3)	-1.551	-0.255	Salinity mean (YSI)	0.288	-0.162
Sword (3)	-0.882	-2.114	pH maximum	-0.33	0.243
Torch (3)	0.025	-1.663	pH minimum	-0.092	-0.241
			pH mean	-0.298	0.079
			pH variance	-0.292	-0.223
			pH mean (points)	-0.287	-0.144

Table 5. Model comparison for a model built off PCA1, using data from Study Years 1-2

	Model Component Estimates ± SD				
	PC1	PC2	PC3	Study Year	ΔAICc
Model 1	--	--	--	--	0
Model 2	--	--	--	-0.0125±0.0504	2.86
Model 3	0.0003 ±0.0143	--	--	-0.0119±0.0617	6.53
Model 4	0.0005±0.1525	0.0022±0.0196	--	0.1924±0.1056	11.22
Model 5	0.0003±0.0144	0.0021±0.0186	-0.0283±0.0204	0.0115±0.0642	14.59

Table 6. Model comparison for a model built off PCA2, using data from Study Years 1-3

	Model Component Estimates ± SD			
	PC1	PC2	Study Year	ΔAICc
Model 1	--	--	--	0
Model 2	--	--	-0.0192±0.0210	1.64
Model 3	0.0039±0.0108	--	-0.0236±0.0248	4.40
Model 4	1.539e-05±1.201e-02	1.340e-02±1.701e-02	-5.218e-03±3.42e-02	6.98

Table 7. Model comparison for a model built off PCA1, using data from Study Years 2-3

	Model Component Estimates ± SD			
	PC1	PC2	Study Year	ΔAICc
Model 1	--	--	--	0
Model 2	--	--	-0.0258±0.0401	2.45
Model 3	-0.0015±0.0090	--	-0.0276±0.0434	6.07
Model 4	-0/0021±0.0098	-0.0042±0.0203	-0.0385±0.0697	10.72

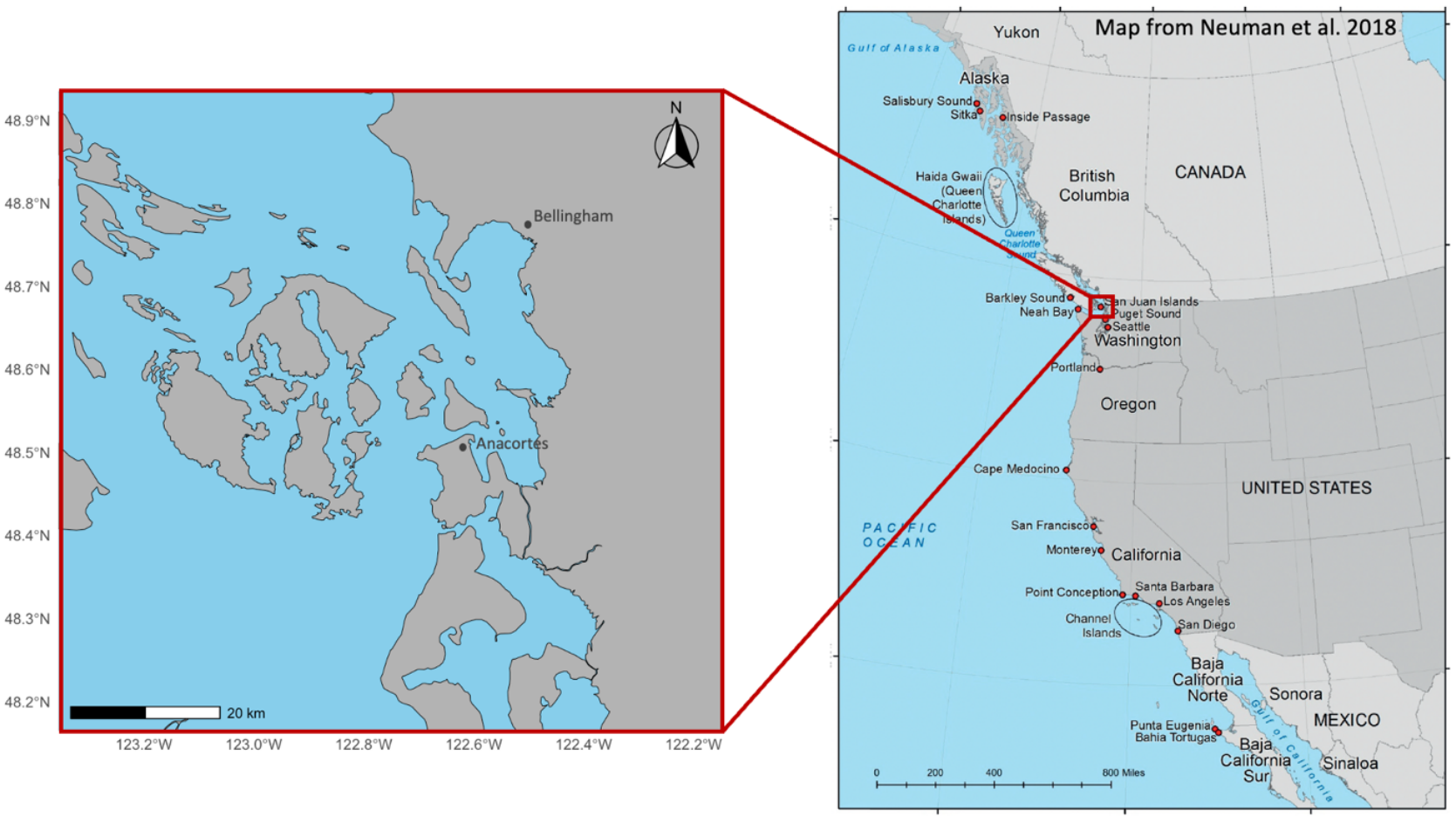

Figure 1. A map of the San Juan Archipelago and surrounding areas where abalone are outplanted in Washington State. Specific outplant sites cannot be included due to risk of illegal harvest. Map of the West coast of North America is from Neuman et al. 2018.

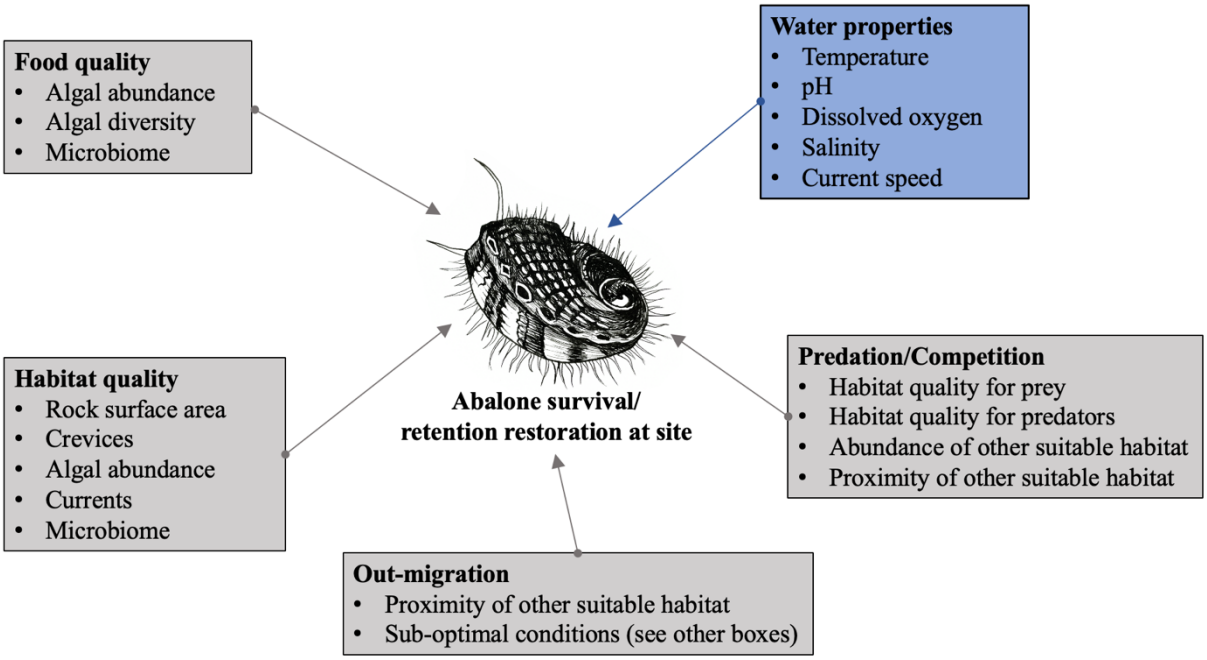

Figure 2. Diagram of factors influencing abalone survival and retention at restoration sites. The blue box shows the variables we focused on in this study.

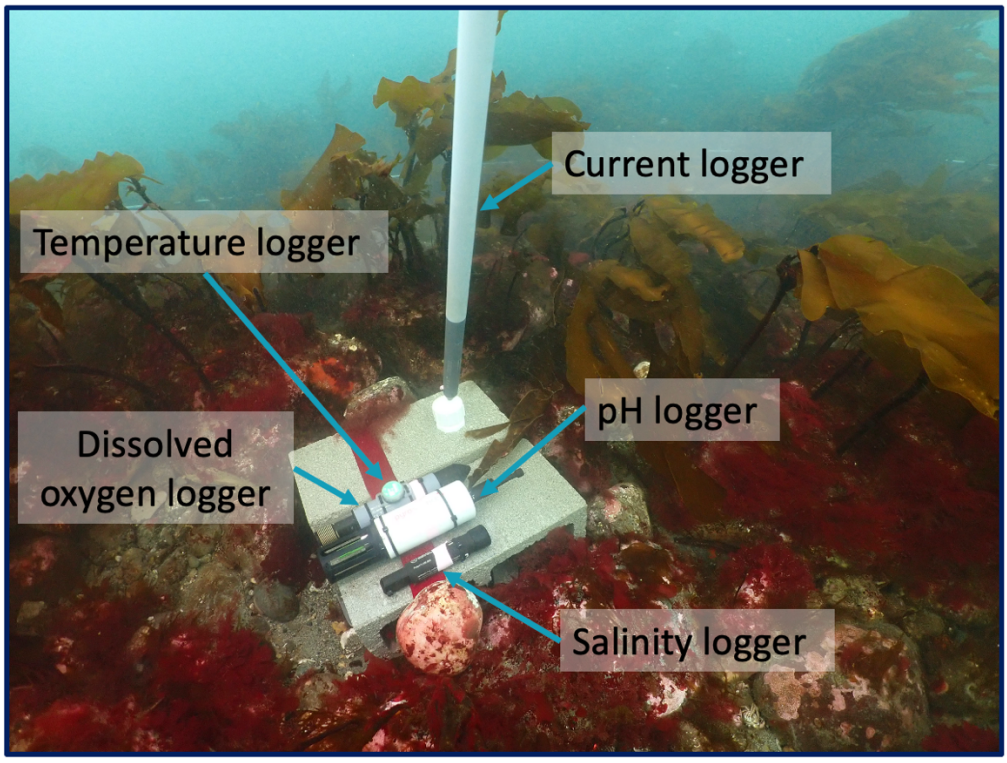

Figure 3. Example of a sensor array deployed at an abalone restoration site. The two half cinder blocks were held together with a nylon strap, and the sensors, on a plastic backing, were strapped to the cinder blocks. The current meter was affixed to the opposite corner of the top surface of the cinderblocks.

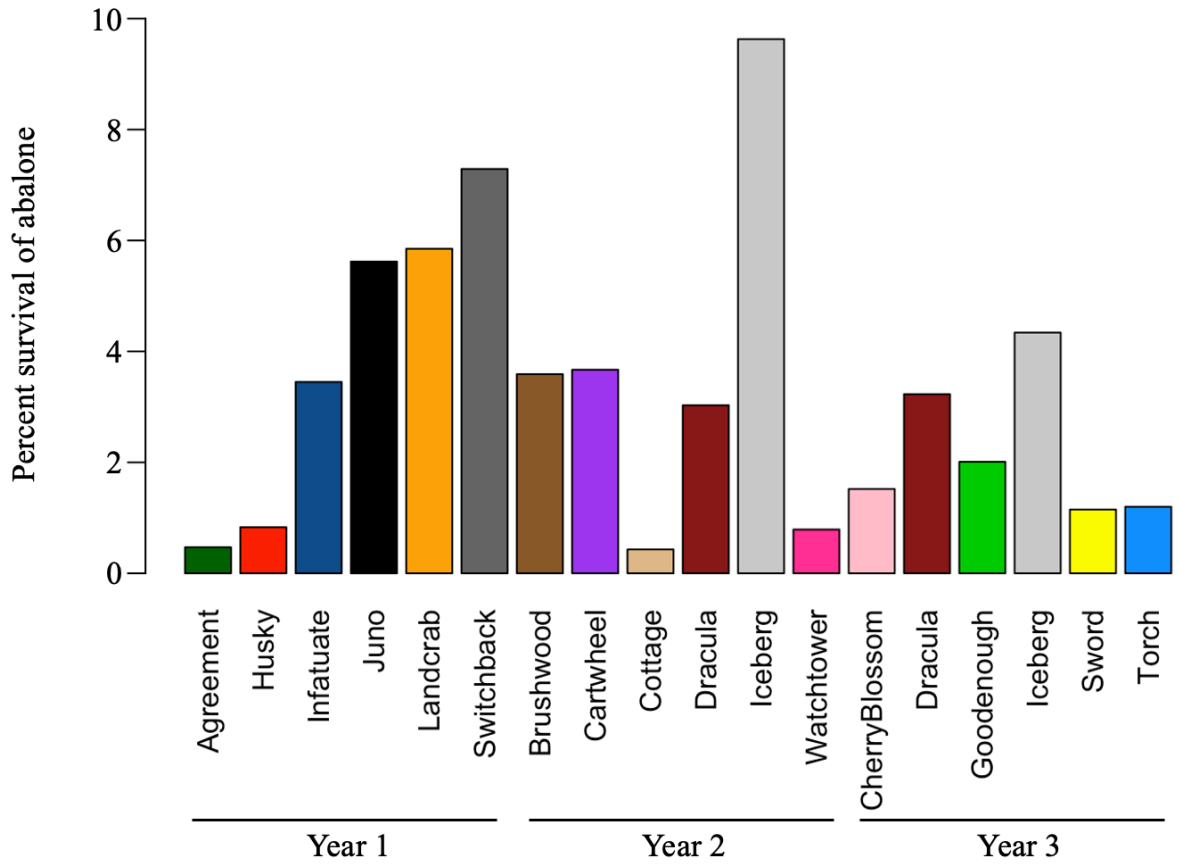

Figure 4. Percent survival of outplanted abalone at each site (1 and 2 years old at time of outplant). Abalone survival was assessed at the end of each outplant year (February or March), approximately 10 months after outplant (April or May). Note that the second time Dracula and Iceberg appear on the graph is the second year in a row that sensors were deployed and abalone outplanted to those sites. For Iceberg, Cherry Blossom, and Dracula in year 3, 1-year-old survival was adjusted based on theoretical survival of abalone from past outplant years because those three sites had received outplants the year before that could not be distinguished from 1-year-olds outplanted in year 3.

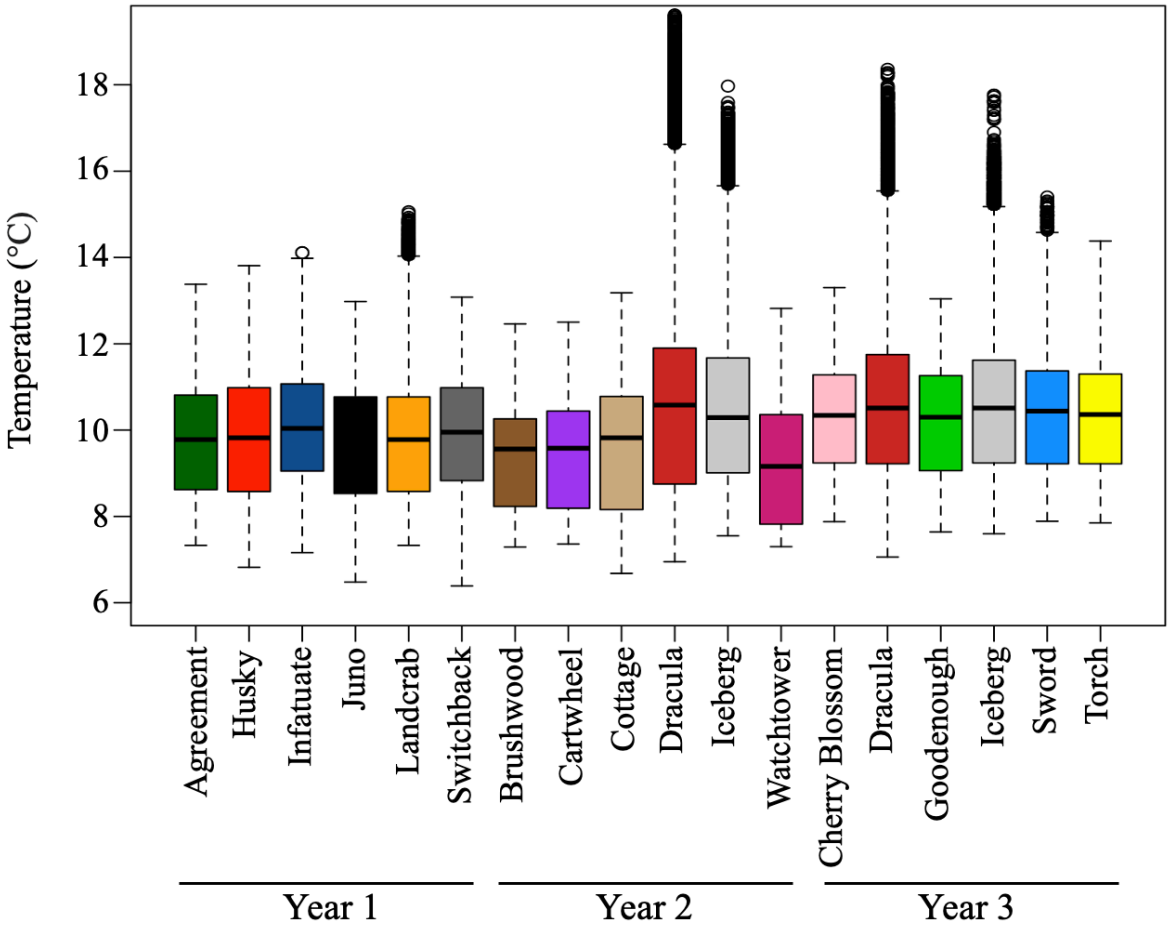

Figure 5a. Temperature (°C) data for each site compiled from the time of outplant to the time of survival surveys the following year. The Number before the site name indicates the year of the study.

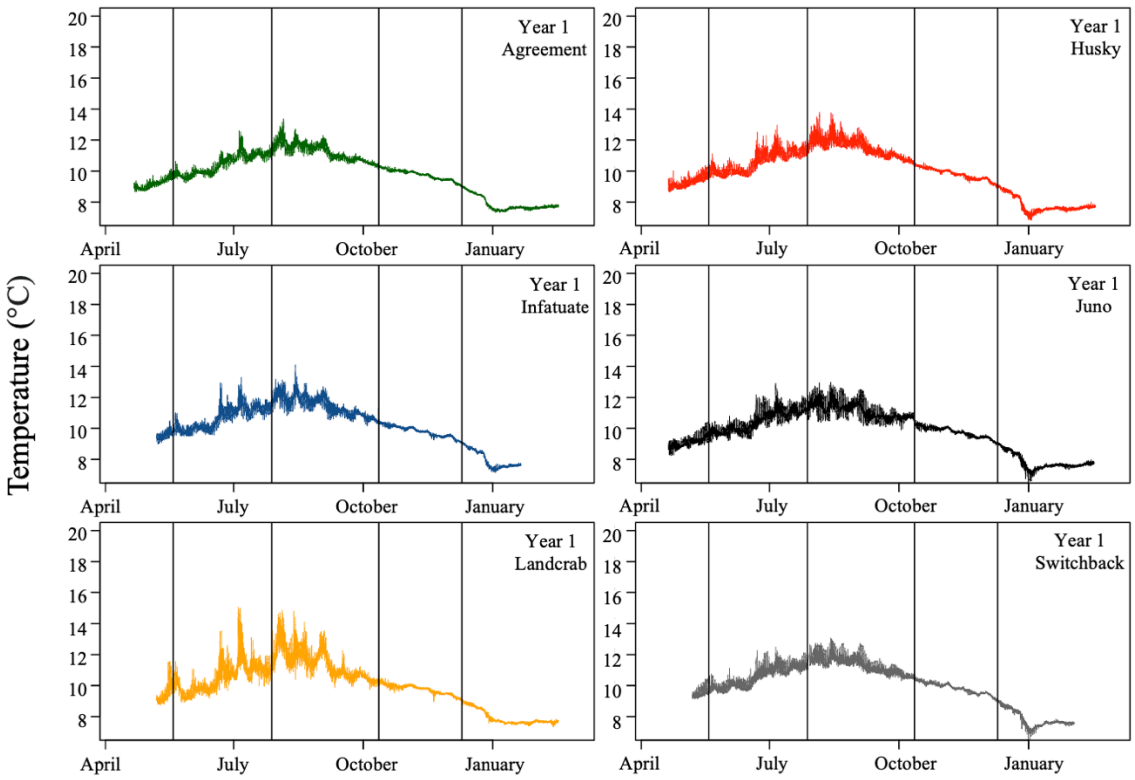

Figure 5b. Temperature profiles (°C) for the six sites used in year one of the study from the day of outplant to the day of survival surveys. Vertical lines indicate when sensors were retrieved and redeployed (moving each specific sensor to a new site each time to avoid possible bias between sensors impacting the data)

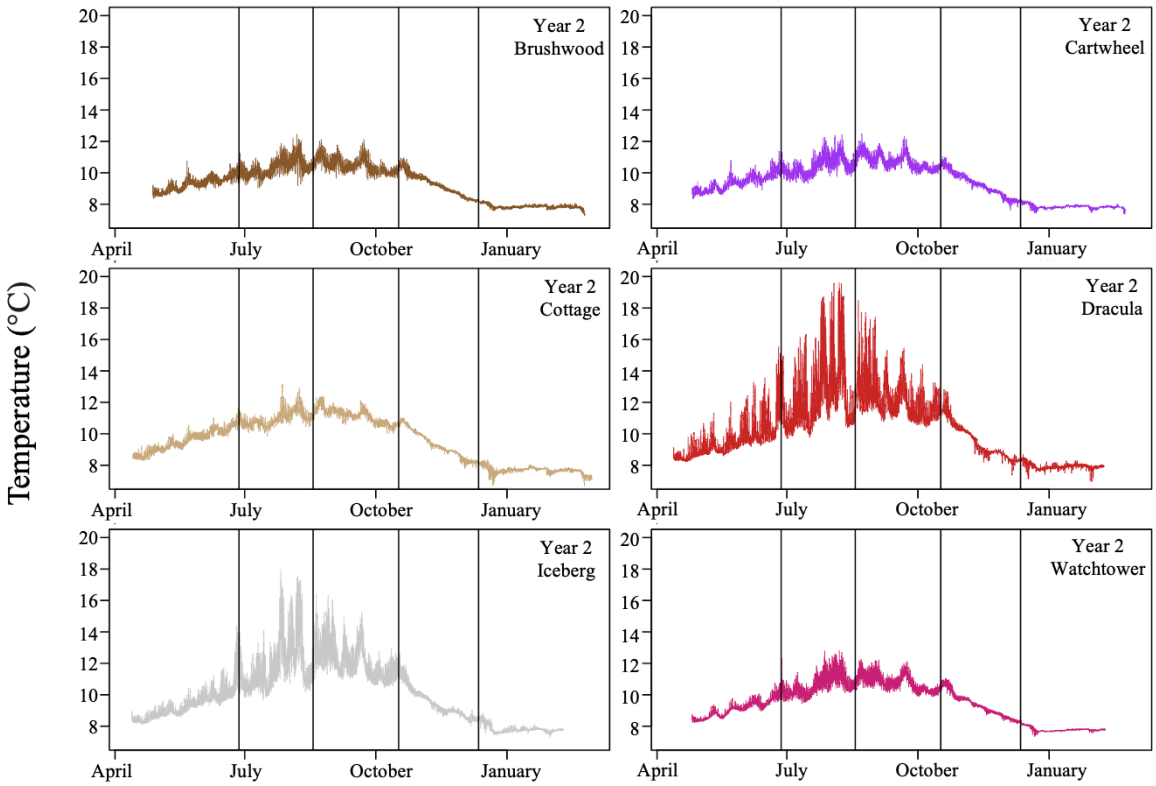

Figure 5c. Temperature profiles (°C) for the six sites used in year two of the study from the day of outplant to the day of survival surveys. Vertical lines indicate when sensors were retrieved and redeployed

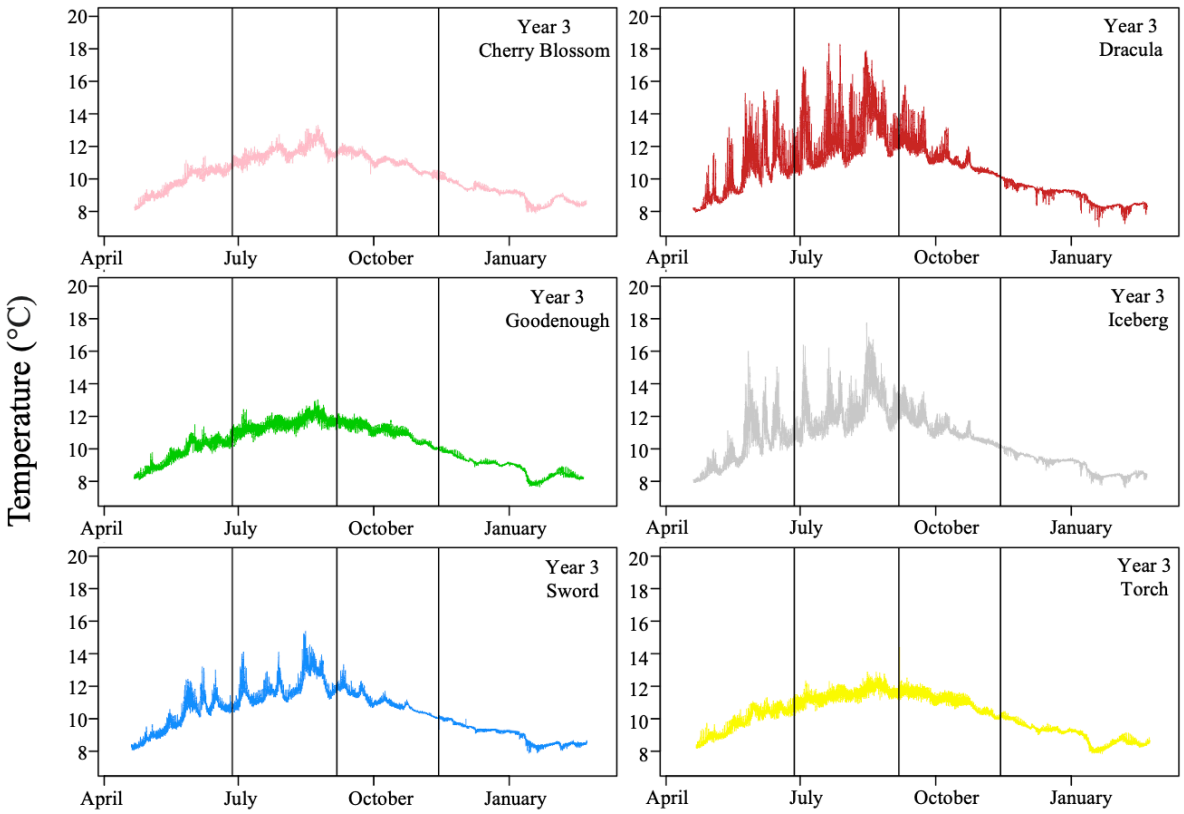

Figure 5d. Temperature profiles (°C) for the six sites used in year three of the study from the day of outplant to the day of survival surveys. Vertical lines indicate when sensors were retrieved and redeployed

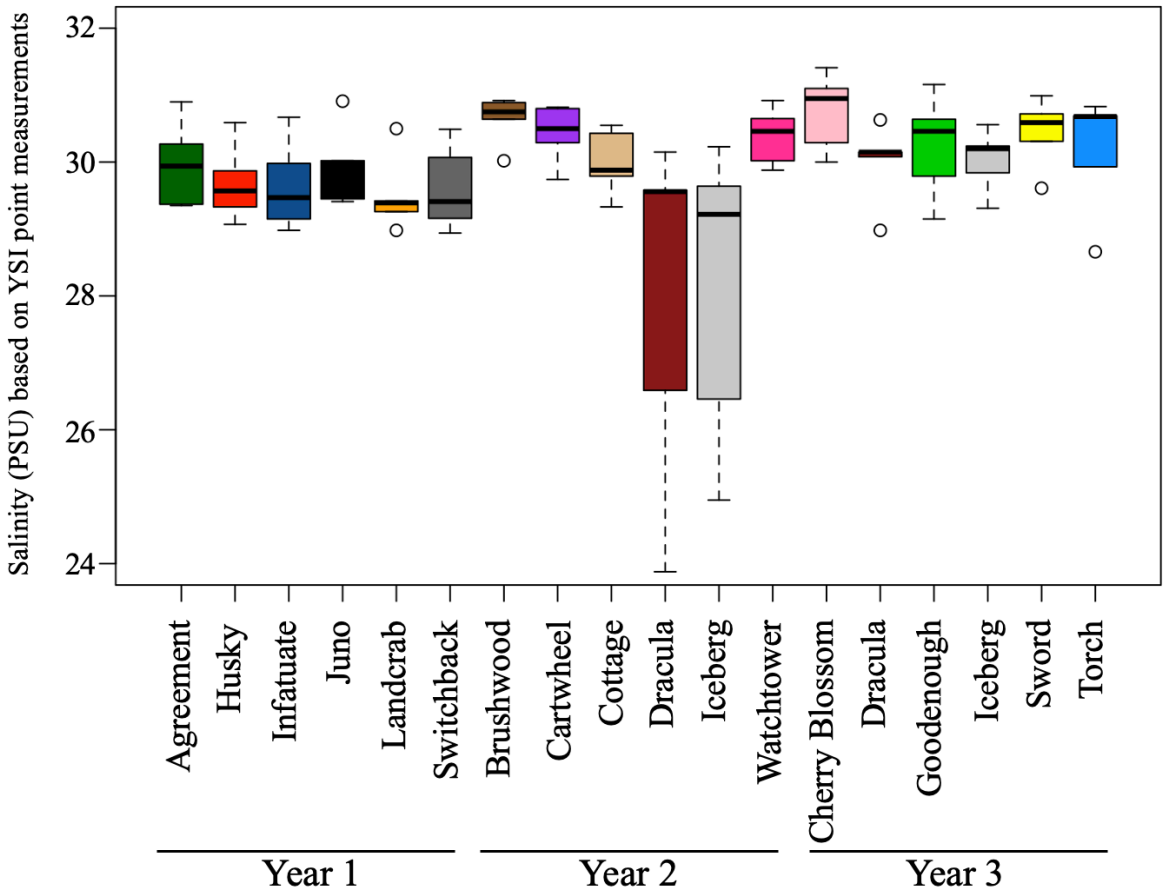

Figure 6a. Salinity (PSU) at each site based on five point-measurements per site taken during sensor deployments/redeployments/retrievals.

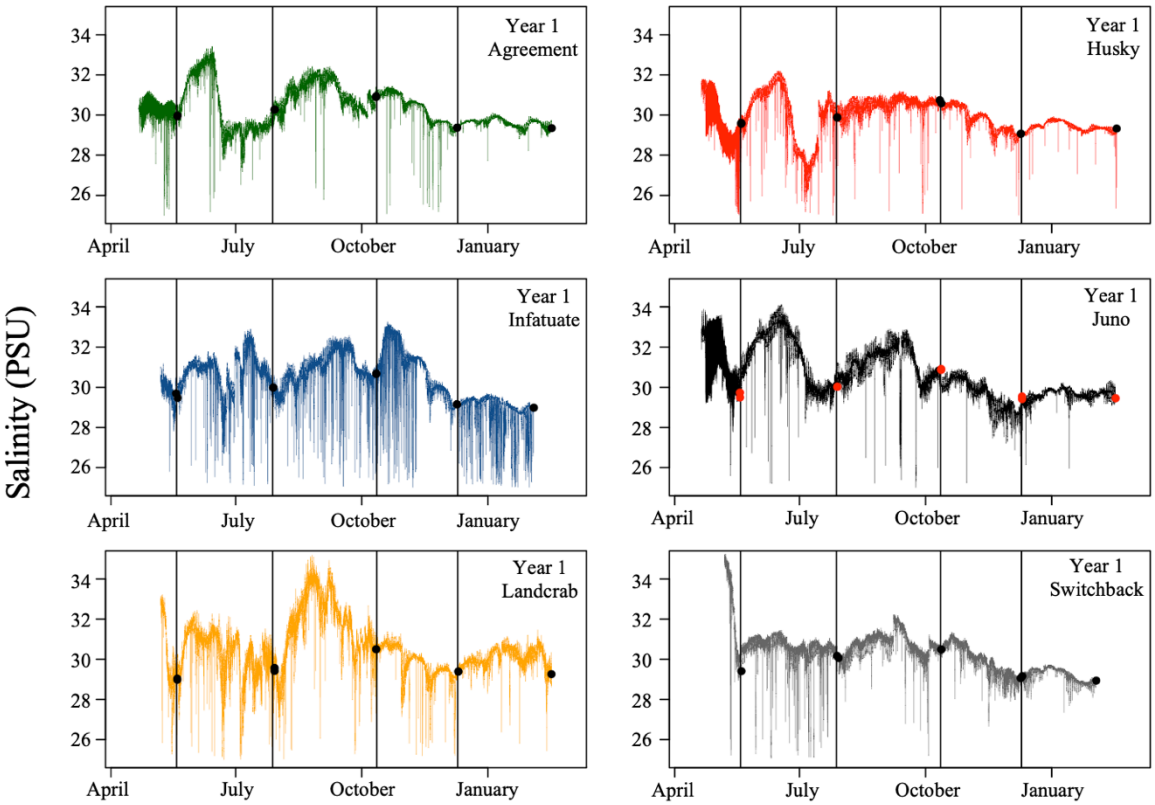

Figure 6b. Salinity profiles (PSU) for the six sites used in year one of the study from the day of outplant to the day of survival surveys. The rapid drops in salinity are likely inaccurate readings due to fouling of sensors during long term deployments. All data was cut off that was below 25PSU, though some drops showed data below 10 PSU. Vertical lines indicate when sensors were retrieved and redeployed (moving the specific sensor to a new site each time to avoid possible bias between sensors impacting the data), which is when YSI measurements were taken to adjust sensor data.

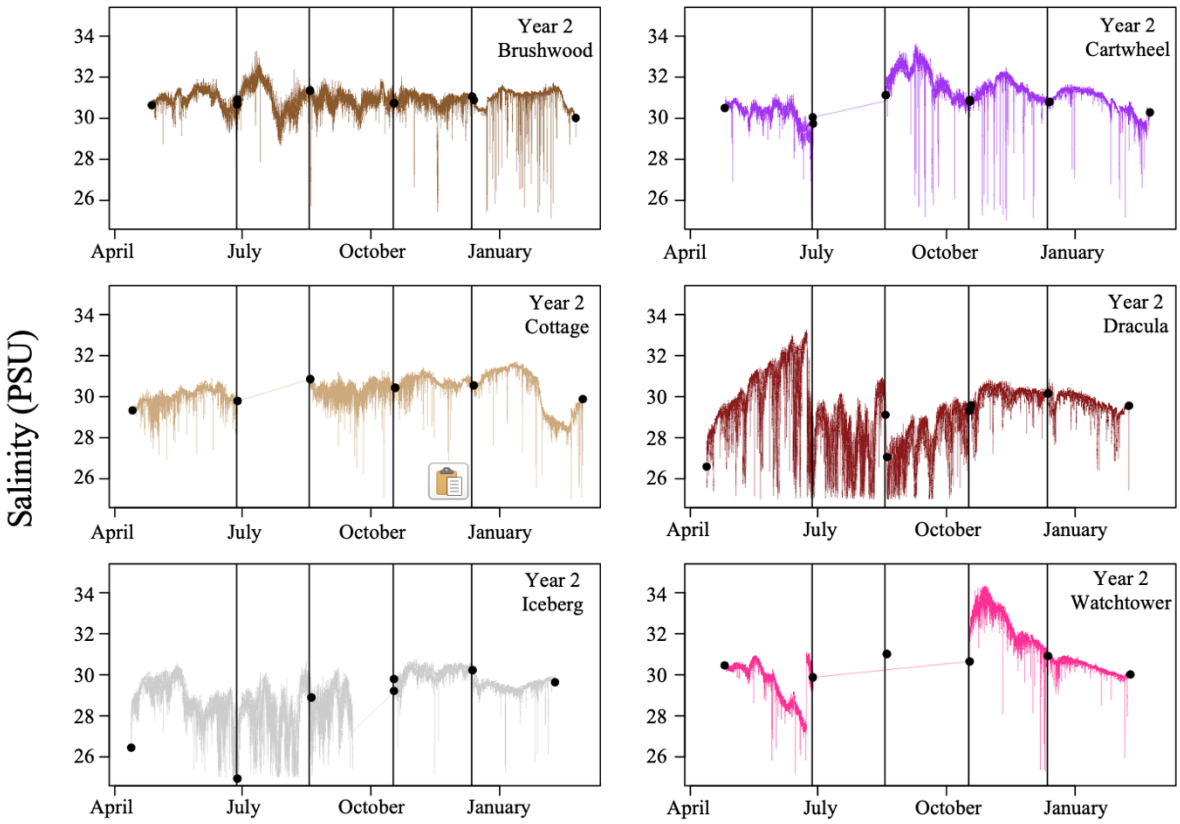

Figure 6c. Salinity profiles (PSU) for the six sites used in year two of the study from the day of outplant to the day of survival surveys. The rapid drops in salinity are likely inaccurate readings due to fouling of sensors during long term deployments. All data was cut off that was below 25PSU. Gaps in the profiles indicate times where sensors failed. Vertical lines indicate when sensors were retrieved and redeployed, which is when YSI measurements were taken to adjust sensor data.

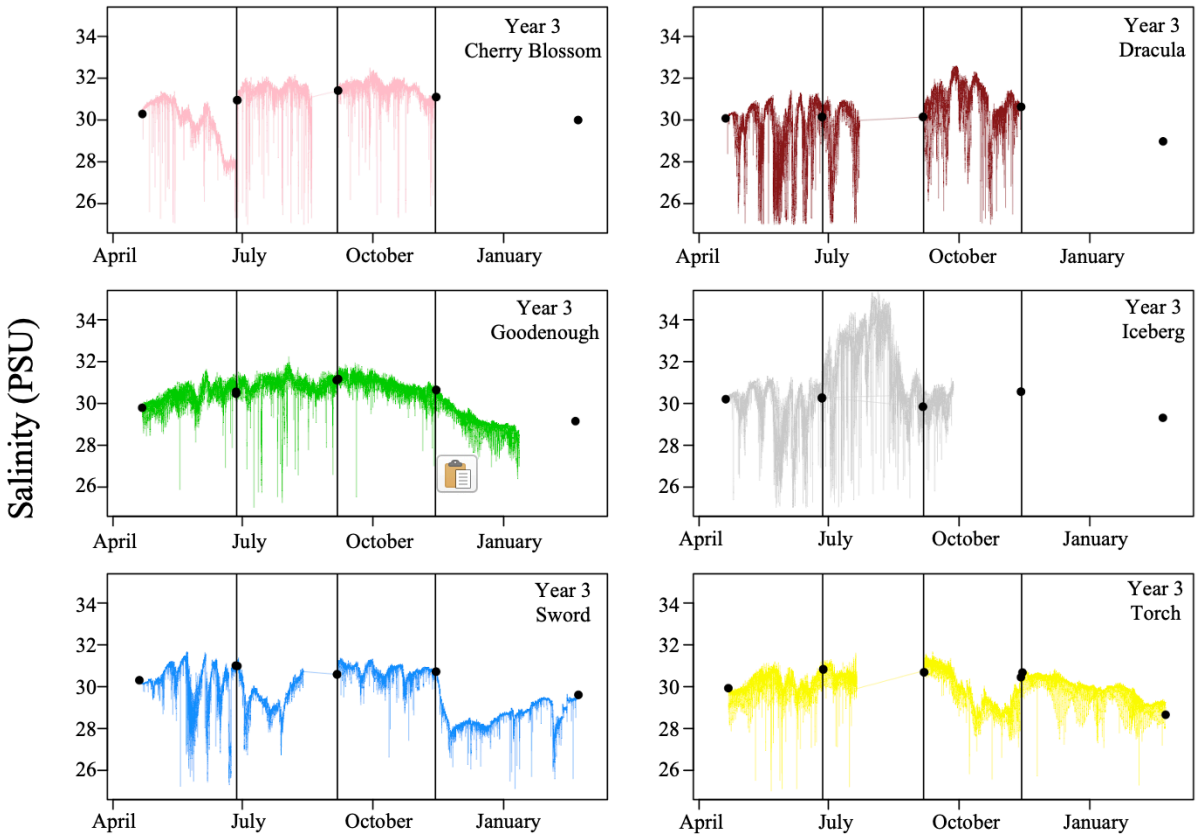

Figure 6d. Salinity profiles (PSU) for the six sites used in year three of the study from the day of outplant to the day of survival surveys. The rapid drops in salinity are likely inaccurate readings due to fouling of sensors during long term deployments. All data was cut off that was below 25PSU. Gaps in the profiles indicate times where sensors failed. Vertical lines indicate when sensors were retrieved and redeployed, which is when YSI measurements were taken to adjust sensor data.

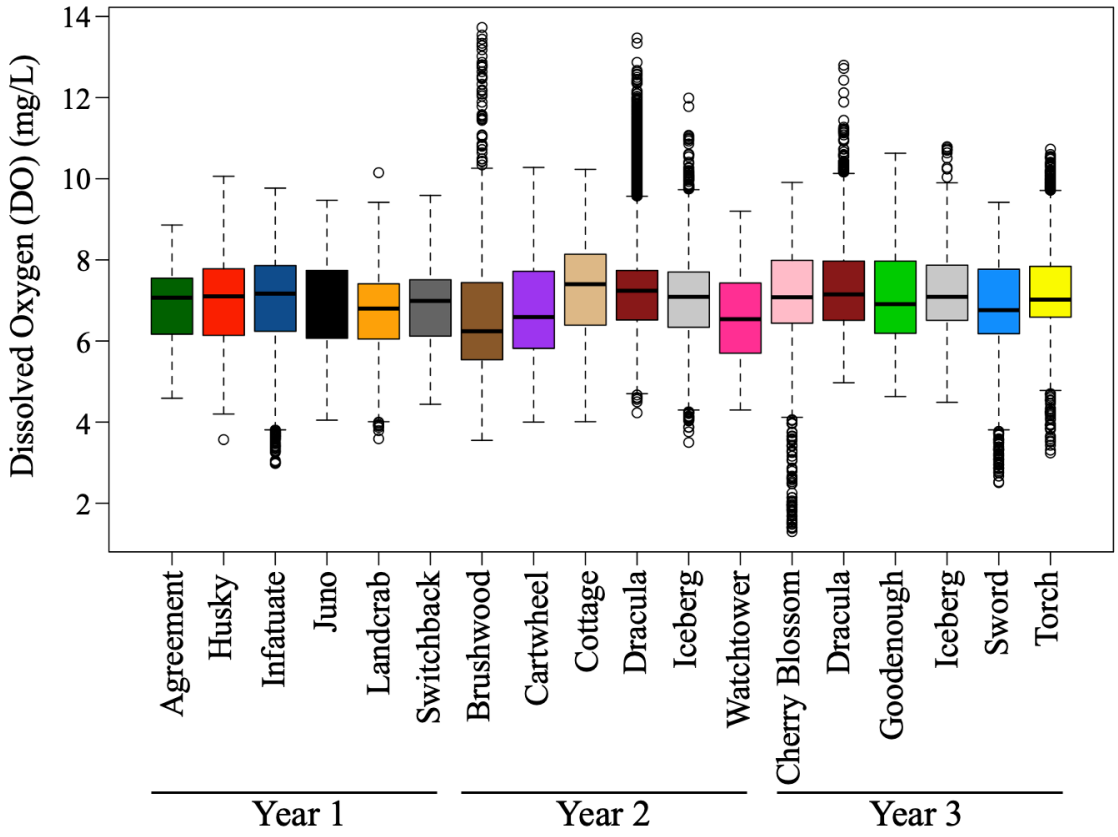

Figure 7a. Dissolved oxygen (mg/L) for each site over the course of sensor deployment. Data gaps (Figures 7b-d) were considered brief enough that the full available data set was used for each site. Number before each site name indicates the year of the study.

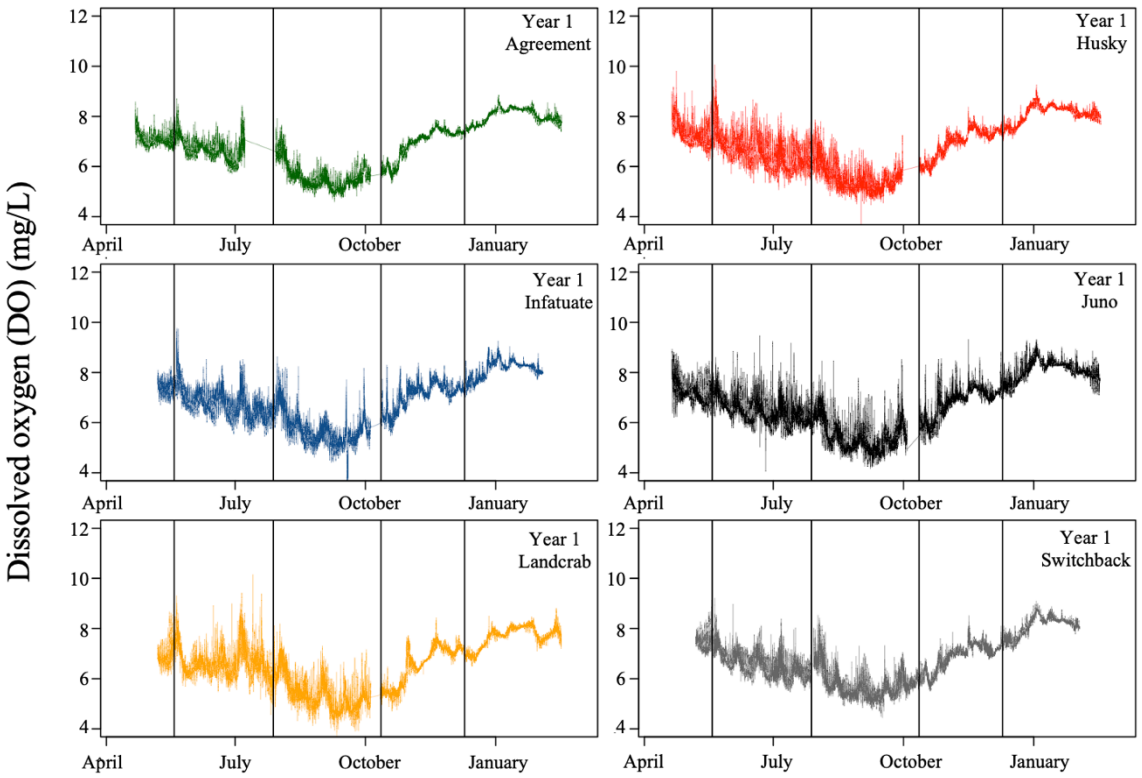

Figure 7b. Dissolved oxygen (mg/L) profiles for the six sites used in year one of the study from the day of outplant to the day of survival surveys. Gaps in the profiles indicate times where sensors failed. Vertical lines indicate when sensors were retrieved and redeployed (moving the specific sensor to a new site each time to avoid possible bias between sensors impacting the data), which is when YSI measurements were taken to adjust sensor data.

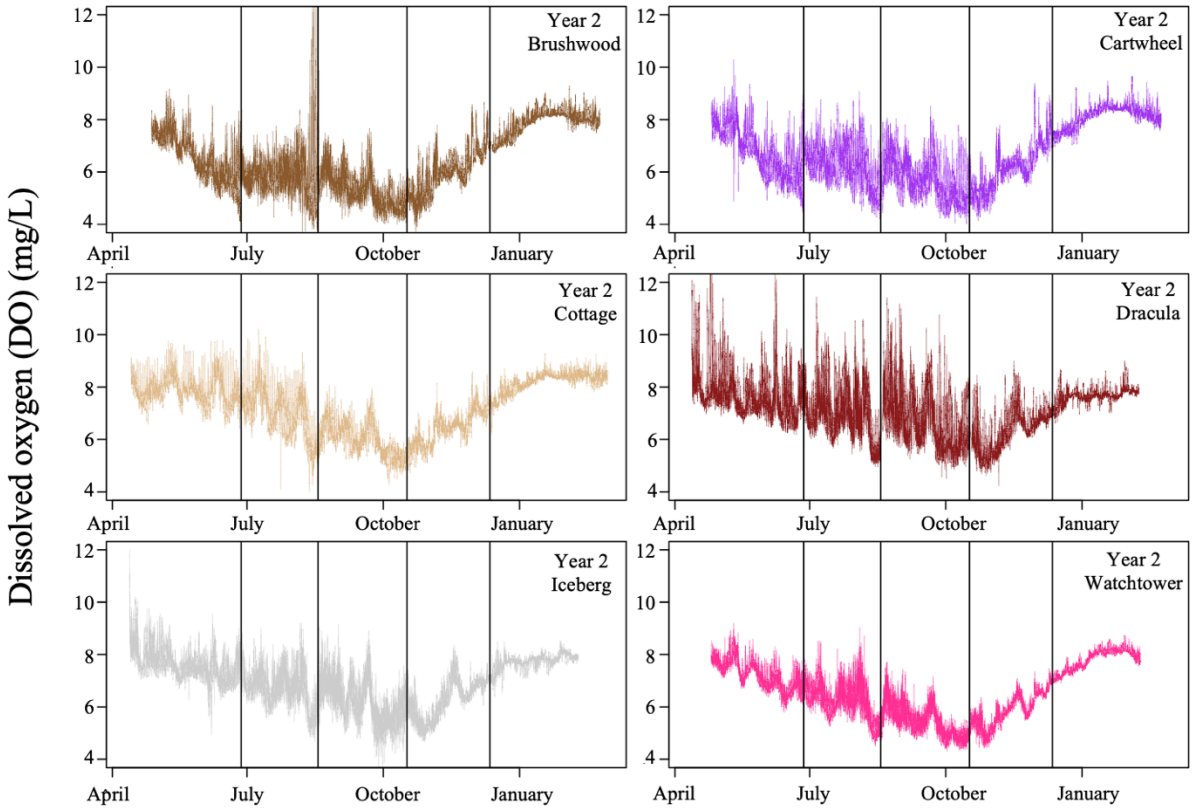

Figure 7c. Dissolved oxygen (mg/L) profiles for the six sites used in year two of the study from the day of outplant to the day of survival surveys. Gaps in the profiles indicate times where sensors failed. Vertical lines indicate when sensors were retrieved and redeployed, which is when YSI measurements were taken to adjust sensor data.

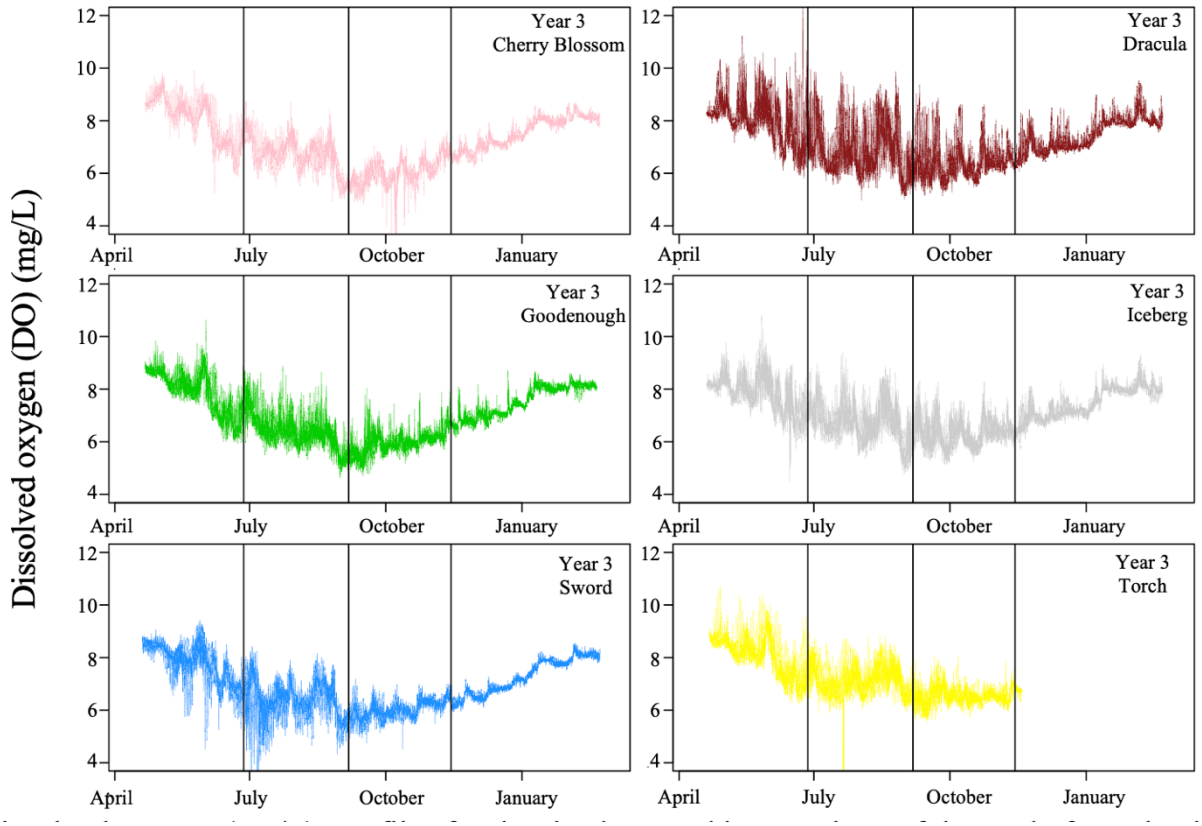

Figure 7d. Dissolved oxygen (mg/L) profiles for the six sites used in year three of the study from the day of outplant to the day of survival surveys. Gaps in the profiles indicate times where sensors failed. Vertical lines indicate when sensors were retrieved and redeployed, which is when YSI measurements were taken to adjust sensor data.

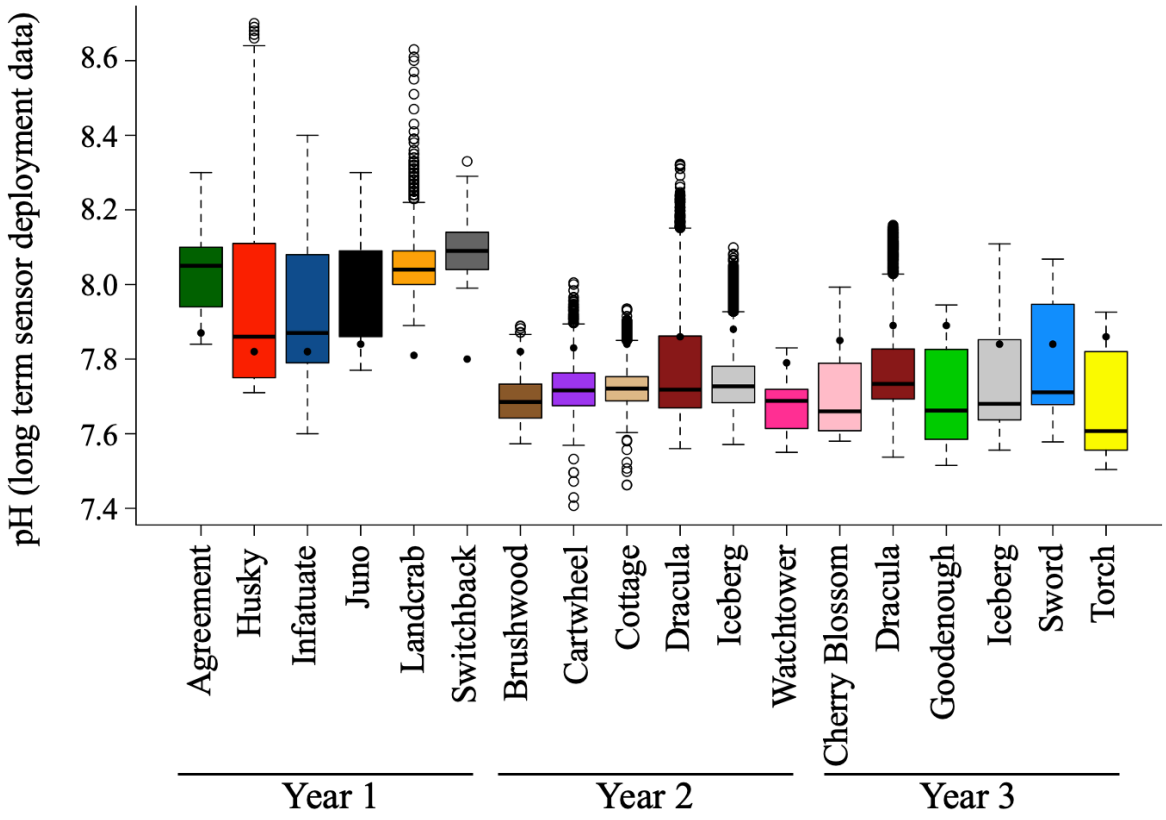

Figure 8a. pH profiles for each site over the course of sensor deployment. This plot shows data from two weeks after each recalibration and deployment, when sensors had less time to drift or become fouled. Data gaps still exist even in this subset of data (Figures 8c–e). Different sensors were used in year one than in years two and three of the study, which may contribute to the higher and more variable pH values in year one. Number before each site name indicates the year of the study. The small black points indicate the mean of the 5 point-pH values calculated from water samples taken each time sensors were deployed and at the end of the experiment. These points allow us to see that the difference in sensors likely cause the discrepancy between year 1 and years 2 and 3.

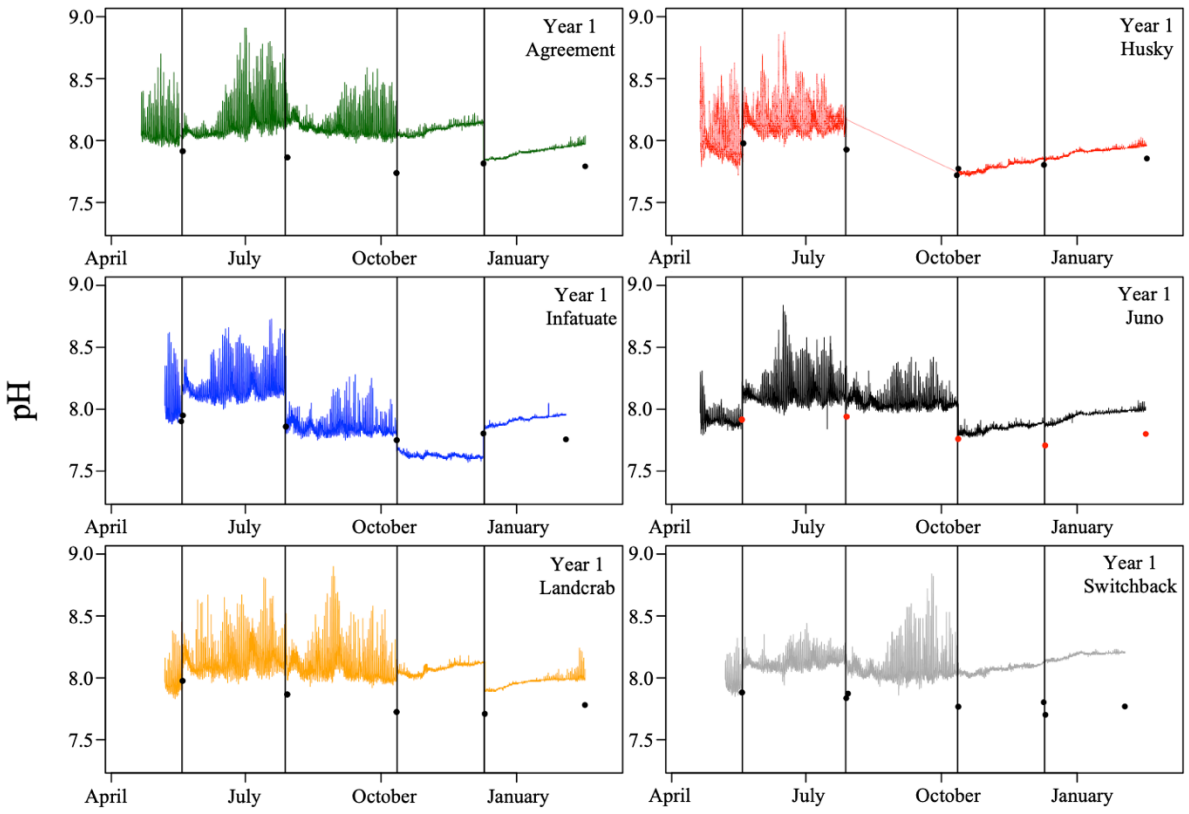

Figure 8b. pH profiles for the six sites used in year one of the study from the day of outplant to the day of survival surveys. Gaps in the profiles indicate times where sensors failed. Vertical lines indicate when sensors were retrieved, recalibrated, and redeployed. Points show the measured pH values based on water samples taken at the time of redeployments.

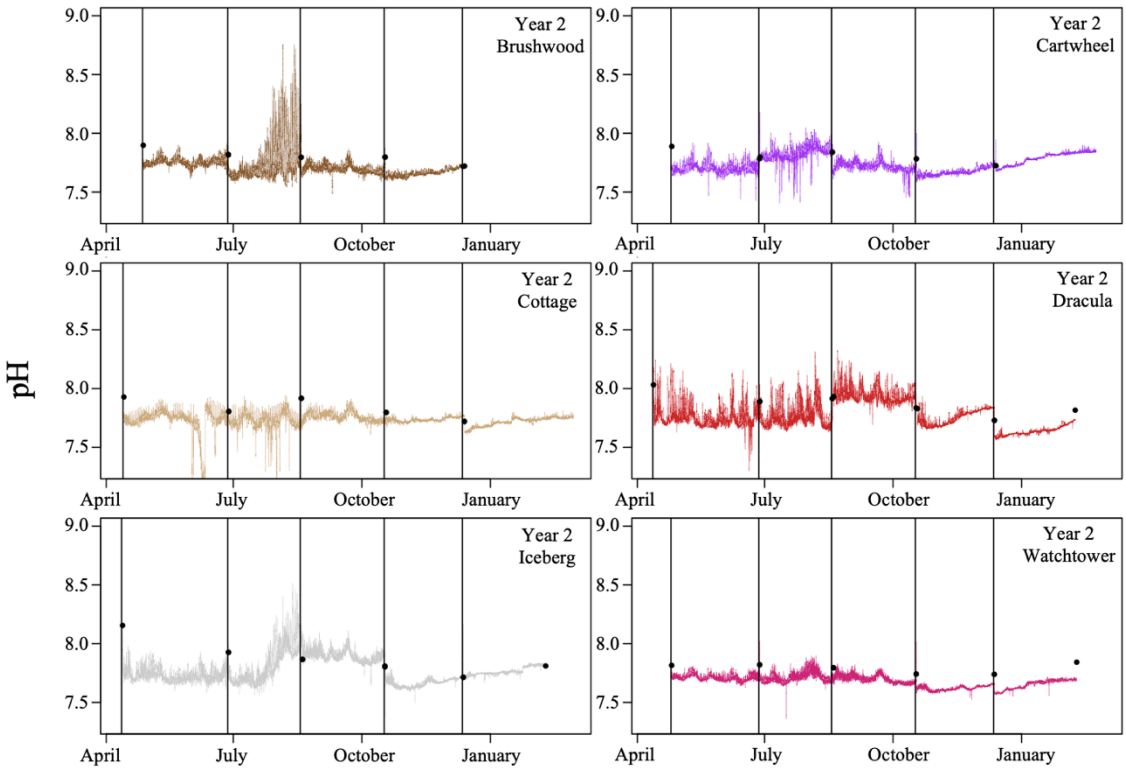

Figure 8c. pH profiles for the six sites used in year two of the study from the day of outplant to the day of survival surveys. Gaps in the profiles indicate times where sensors failed. Vertical lines indicate when sensors were retrieved, recalibrated, and redeployed. Sensor data was corrected based on expected drift over the course of each deployment (PyroScience Workbench software). Points show the measured pH values based on water samples taken at the time of redeployments.

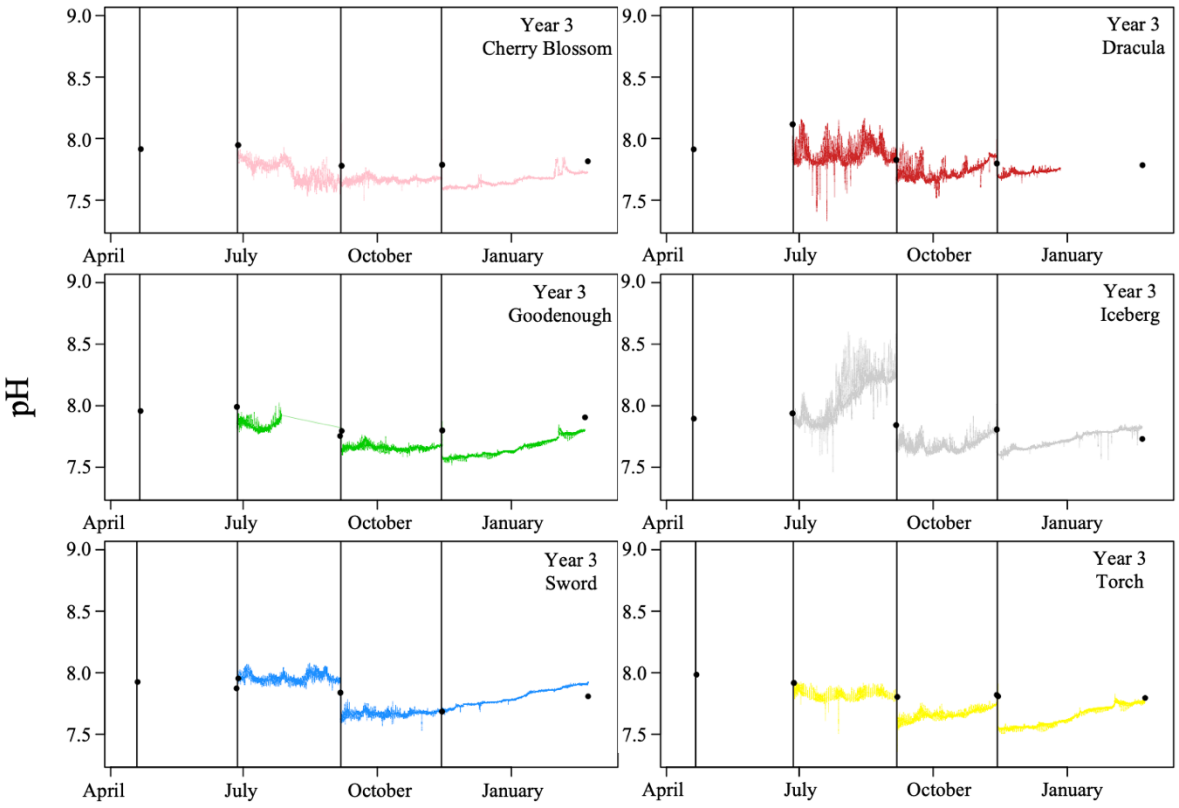

Figure 8d. pH profiles for the six sites used in year three of the study from the day of outplant to the day of survival surveys. Gaps in the profiles indicate times where sensors failed. Vertical lines indicate when sensors were retrieved, recalibrated, and redeployed. Sensor data was corrected based on expected drift over the course of each deployment (PyroScience Workbench software). Points show the measured pH values based on water samples taken at the time of redeployments.

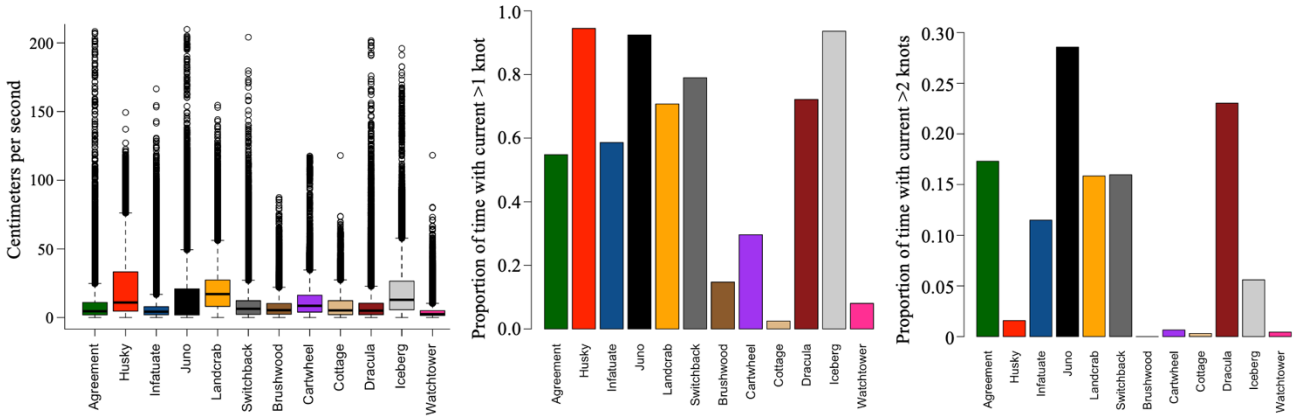

Figure 9a-c. (A) Current speed at each site (cm/s) for years one and two of the study. All available data for each site was used, data gaps can be seen in Figures 9b-c. Sensors took maximum measurements at speed of 120cm/s. Current sensors failed repetitively during year three of the study, so no data from year three is included. (B) Fraction of days where current at each site was above 1 knot (51.44cm/s). (C) Fraction of days where current at each site was above 2 knots (102.89cm/s).

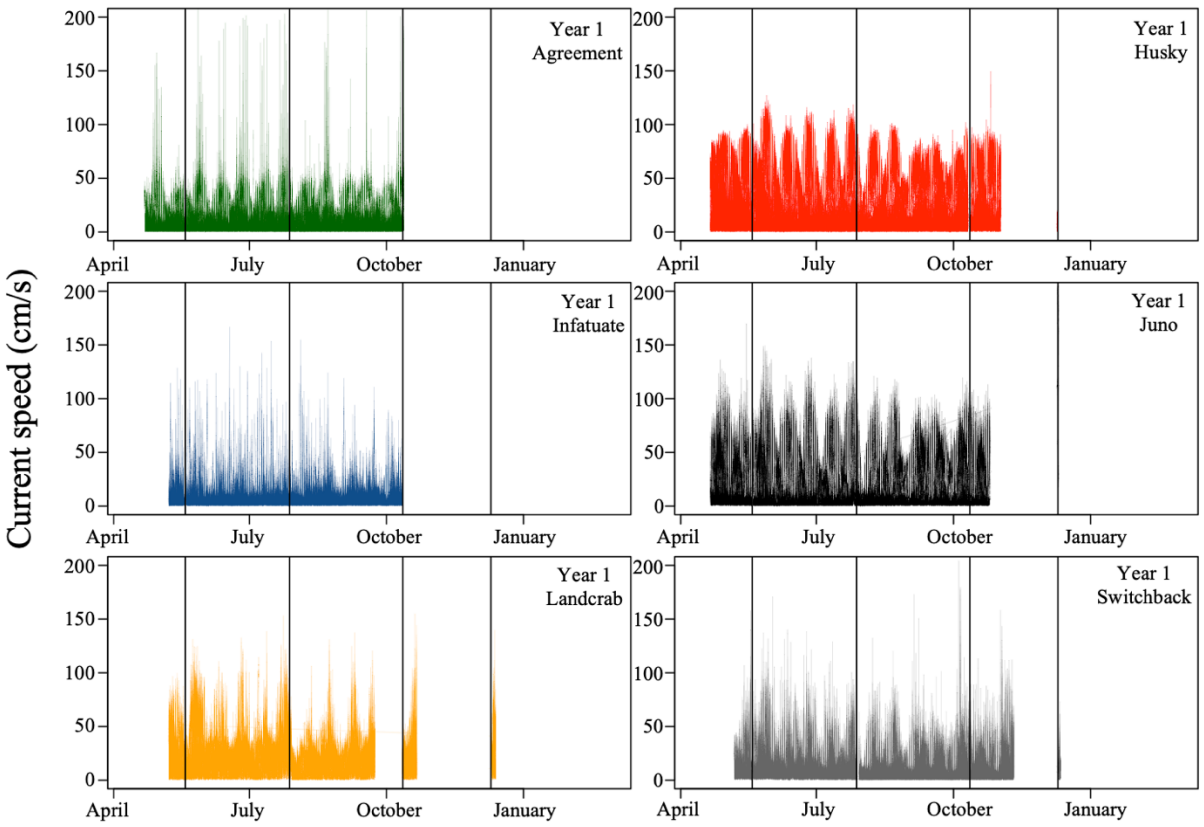

Figure 9b. Current speed (cm/s) profiles for the six sites used in year one of the study from the day of outplant to the day of survival surveys. Gaps in the profiles indicate times where sensors failed. Vertical lines indicate when sensors were retrieved, cleaned, and redeployed.

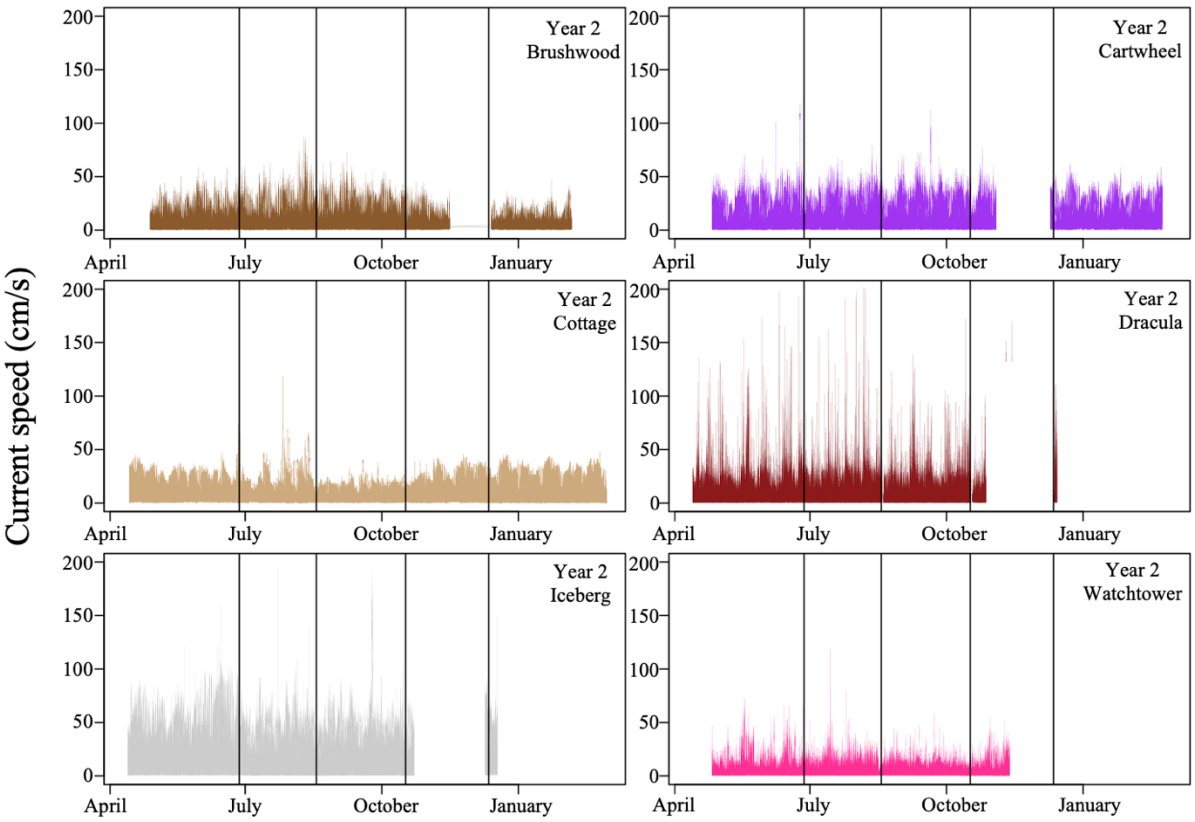

Figure 9c. Current speed (cm/s) profiles for the six sites used in year two of the study from the day of outplant to the day of survival surveys. Gaps in the profiles indicate times where sensors failed. Vertical lines indicate when sensors were retrieved, cleaned, and redeployed.

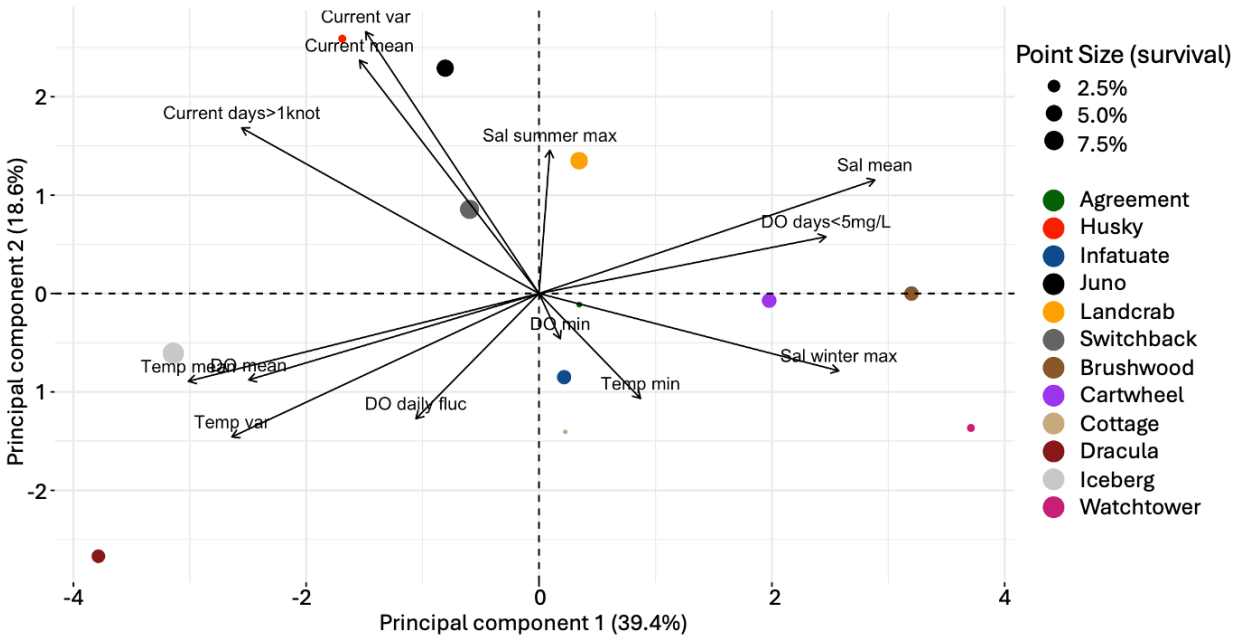

Figure 10. Principal component analysis for oceanographic data from years 1 and 2 of the study. Variables extracted from current, salinity, temperature, and DO data are included.

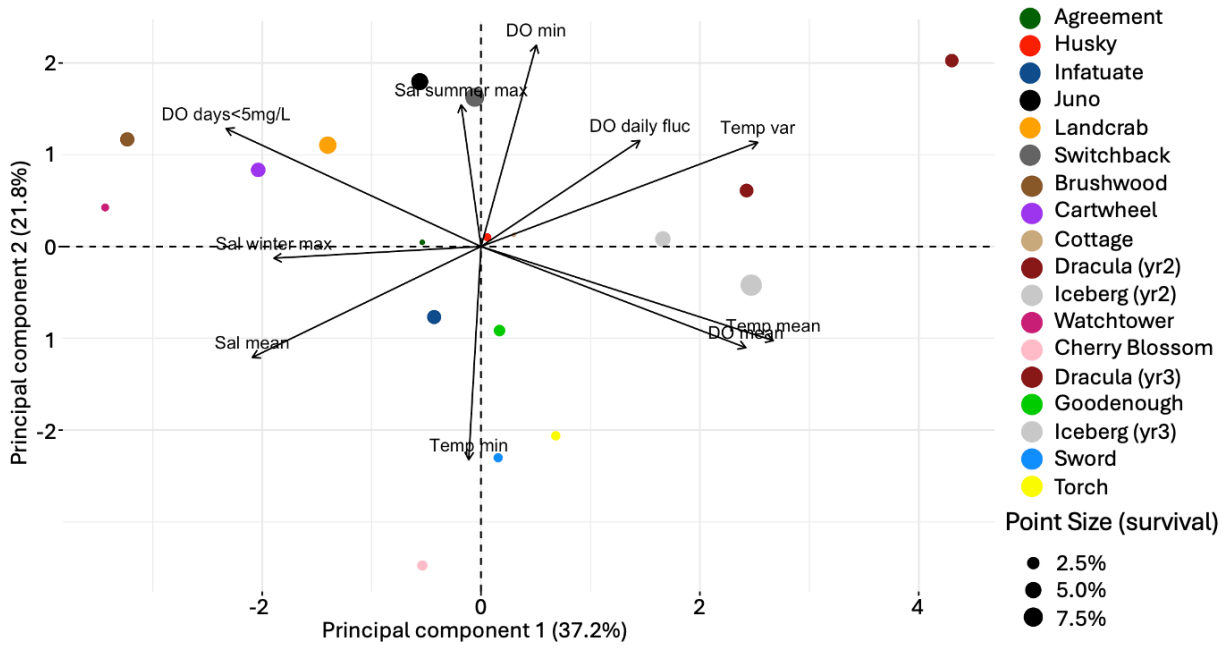

Figure 11. Principal component analysis for oceanographic data from all three years of the study. Variables extracted from salinity, temperature, and DO data are included.

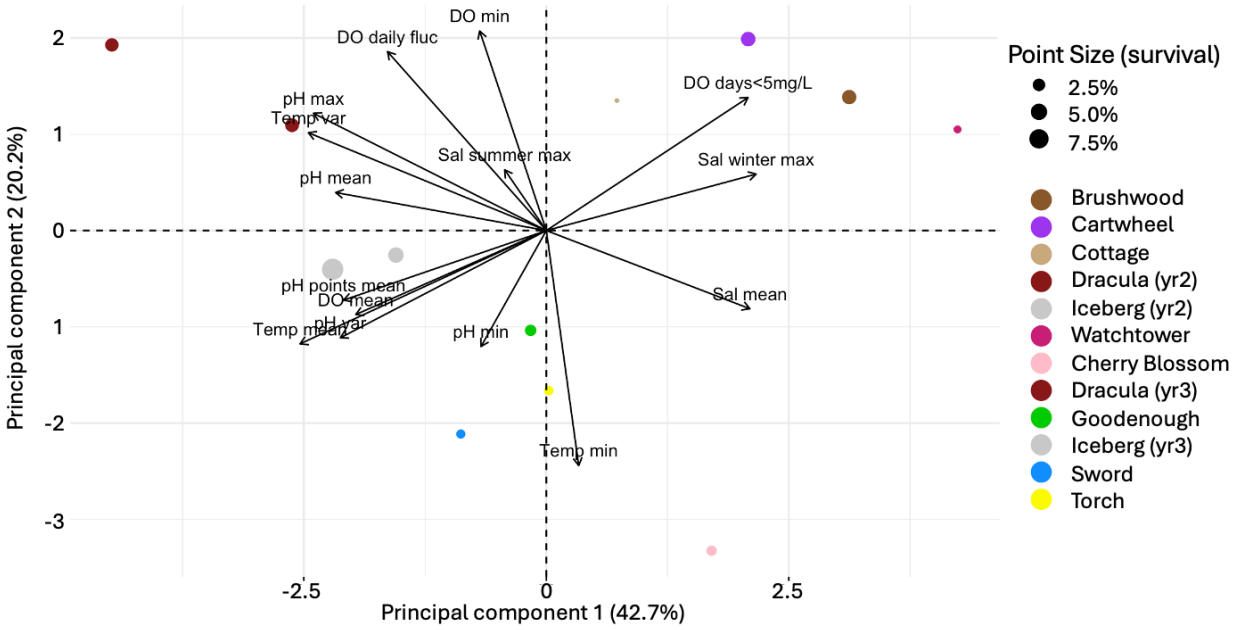

Figure 12. Principal component analysis for oceanographic data from years 2 and 3 of the study.

Variables extracted from pH, salinity, temperature, and DO data are included.

References

Auzoux-Bordenave, S., Wessel, N., Badou, A., Martin, S., M'zoudi, S., Avignon, S., Roussel, S., Huchette, S., & Dubois, P. (2020). Ocean acidification impacts growth and shell mineralization in juvenile abalone (*Haliotis tuberculata*). *Marine Biology*, *167*, 1–14.

Boch, C. A., Micheli, F., AlNajjar, M., Monismith, S. G., Beers, J. M., Bonilla, J. C., Espinoza, A. M., Vazquez-Vera, L., & Woodson, C. B. (2018). Local oceanographic variability influences the performance of juvenile abalone under climate change. *Scientific Reports*, *8*(1), 5501.

Bouma, J. V. (2007). *Early life history dynamics of pinto abalone (Haliotis kamtschatkana) and implications for recovery in the San Juan Archipelago, Washington State*. University of Washington.

Broatch, E. M., & MacCready, P. (2022). Mixing in a salinity variance budget of the Salish Sea is controlled by river flow. *Journal of Physical Oceanography*, *52*(10), 2305–2323.

Carson, H. S., Morin, D. J., Bouma, J. V., Ulrich, M., & Sizemore, R. (2019). The survival of hatchery-origin pinto abalone *Haliotis kamtschatkana* released into Washington waters. *Aquatic Conservation: Marine and Freshwater Ecosystems*, *29*(3), 424–441.

Crim, R. N., Sunday, J. M., & Harley, C. D. (2011). Elevated seawater CO_2 concentrations impair larval development and reduce larval survival in endangered northern abalone (*Haliotis kamtschatkana*). *Journal of Experimental Marine Biology and Ecology*, *400*(1–2), 272–277.

Cunningham, S. C., Smith, A. M., & Lamare, M. D. (2016). The effects of elevated pCO_2 on growth, shell production and metabolism of cultured juvenile abalone, *Haliotis iris*. *Aquaculture Research*, *47*(8), 2375–2392.

Dillon, M. E., & Woods, H. A. (2016). Introduction to the symposium: Beyond the mean: Biological impacts of changing patterns of temperature variation. *Integrative and Comparative Biology*, *56*(1), 11–13.

Doney, S. C., Fabry, V. J., Feely, R. A., & Kleypas, J. A. (2009). Ocean acidification: The other CO_2 problem. *Annual Review of Marine Science*, *1*, 169–192.

Fassbender, A. J., Alin, S. R., Feely, R. A., Sutton, A. J., Newton, J. A., & Byrne, R. H. (2017). Estimating total alkalinity in the Washington State coastal zone: Complexities and surprising utility for ocean acidification research. *Estuaries and Coasts*, *40*(2), 404–418.

Feely, R. A., Sabine, C. L., Hernandez-Ayon, J. M., Ianson, D., & Hales, B. (2008). Evidence for upwelling of corrosive" acidified" water onto the continental shelf. *Science*, *320*(5882), 1490–1492.

Fowler, S. W., & Oregioni, B. (1976). Trace metals in mussels from the NW Mediterranean. *Marine Pollution Bulletin*, *7*(2), 26–29.

Gazeau, F., Parker, L. M., Comeau, S., Gattuso, J.-P., O'Connor, W. A., Martin, S., Pörtner, H.-O., & Ross, P. M. (2013). Impacts of ocean acidification on marine shelled molluscs. *Marine Biology*, *160*, 2207–2245.

Guo, X., Huang, M., Luo, X., You, W., & Ke, C. (2022). Effects of one-year exposure to ocean acidification on two species of abalone. *Science of The Total Environment*, *852*, 158144.

Harris, J. O., Maguire, G. B., Edwards, S. J., & Johns, D. R. (1999). Low dissolved oxygen reduces growth rate and oxygen consumption rate of juvenile greenlip abalone, *Haliotis laevigata* Donovan. *Aquaculture*, *174*(3–4), 265–278.

Holland, O. J., Smythe, C., Clark, T. D., Ragg, N. L., Mondon, J., Corbett, P., & Miller, A. D. (2024). Size-dependent thermal limits in Australian hybrid abalone: Implications for productivity shifts with ocean warming. *Reviews in Fish Biology and Fisheries*, *34*(1), 271–291.

IPCC (2007). *Climate Change 2007: The Fourth Assessment Report of the Intergovernmental Panel on Climate Change (IPCC).* Cambridge University Press.

IPCC (2014). *Climate Change 2014: Synthesis Report. Contribution of Working Groups I, II and III to the Fifth Assessment Report of the Intergovernmental Panel on Climate Change [Core Writing Team* (R. K. Pachauri & L. A. Meyer, Eds.)*]*. IPCC.

IPCC (2023). *Climate Change 2023: Synthesis Report. Contribution of Working Groups I, II and III to the Sixth Assessment Report of the Intergovernmental Panel on Climate Change [Core Writing Team*, H. Lee and J. Romero (eds.*)]. IPCC, Geneva, Switzerland, pp. 35-115.*

Kim, T. W., Barry, J. P., & Micheli, F. (2013). The effects of intermittent exposure to low-pH and low-oxygen conditions on survival and growth of juvenile red abalone. *Biogeosciences*, *10*(11), 7255–7262.

Krause-Jensen, D., Duarte, C. M., Hendriks, I. E., Meire, L., Blicher, M. E., Marbà, N., & Sejr, M. K. (2015). Macroalgae contribute to nested mosaics of pH variability in a subarctic fjord. *Biogeosciences*, *12*(16), 4895–4911.

Kroeker, K. J., Kordas, R. L., Crim, R., Hendriks, I. E., Ramajo, L., Singh, G. S., Duarte, C. M., & Gattuso, J.-P. (2013). Impacts of ocean acidification on marine organisms: Quantifying sensitivities and interaction with warming. *Global Change Biology*, *19*(6), 1884–1896.

Lin, S., Luo, Q., Zhang, M., Lyu, M., Huang, M., Ke, C., & Gao, X. (2024). Selective preferences and behavioral adaptation strategy of Pacific abalone in response to different water flow velocities. *Global Ecology and Conservation*, *50*, e02823.

Lluch-Cota, S. E., Sicard, M. T., Calderón-Liévanos, S., & Velasco-Echavarría, H. (2023). Empirical evidence of temperature variability as a concurrent limiting factor for abalone distribution. *Estuarine, Coastal and Shelf Science*, *282*, 108252.

Lowe, A. T., Bos, J., & Ruesink, J. (2019). Ecosystem metabolism drives pH variability and modulates long-term ocean acidification in the Northeast Pacific coastal ocean. *Scientific Reports*, *9*(1), 1–11.

Masson, D., & Cummins, P. F. (2004). Observations and modeling of seasonal variability in the Straits of Georgia and Juan de Fuca. *Journal of Marine Research*, *62*(4), 491–516.

Mccormick, T. B., Navas, G., Buckley, L. M., & Biggs, C. (2016). Effect of temperature, diet, light, and cultivation density on growth and survival of larval and juvenile white abalone *Haliotis sorenseni* (Bartsch, 1940). *Journal of Shellfish Research*, *35*(4), 981–992.

Morash, A. J., & Alter, K. (2016). Effects of environmental and farm stress on abalone physiology: perspectives for abalone aquaculture in the face of global climate change. *Reviews in Aquaculture*, *8*(4), 342-368.

Murie, K. A., & Bourdeau, P. E. (2020). Fragmented kelp forest canopies retain their ability to alter local seawater chemistry. *Scientific Reports*, *10*(1), 11939.

Neuman, M. J., Wang, S., Busch, S., Friedman, C., Gruenthal, K., Gustafson, R., Kushner, D., Stierhoff, K., Vanblaricom, G. & Wright, S. (2018). A status review of pinto abalone (*Haliotis kamtschatkana*) along the west coast of North America: interpreting trends, addressing uncertainty, and assessing risk for a wide-ranging marine invertebrate. *Journal of Shellfish Research*, *37*(4), 869-910.

Parker, L. M., Ross, P. M., O'Connor, W. A., Pörtner, H. O., Scanes, E., & Wright, J. M. (2013). Predicting the response of molluscs to the impact of ocean acidification. *Biology*, *2*(2), 651–692.

Rogers-Bennett, L., Dondanville, R. F., Moore, J. D., & Vilchis, L. I. (2010). Response of red abalone reproduction to warm water, starvation, and disease stressors: Implications of ocean warming. *Journal of Shellfish Research*, *29*(3), 599–611.

Rothaus, D. P., Vadopalas, B., & Friedman, C. S. (2008). Precipitous declines in pinto abalone (Haliotis kamtschatkana kamtschatkana) abundance in the San Juan Archipelago, Washington, USA, despite statewide fishery closure. *Canadian Journal of Fisheries and Aquatic Sciences*, *65*(12), 2703-2711.

Shen, Y., Huang, M., You, W., Luo, X., & Ke, C. (2020). The survival and respiration response of two abalones under short-term hypoxia challenges. *Aquaculture*, *529*, 735658.

Silbiger, N. J., & Sorte, C. J. (2018). Biophysical feedbacks mediate carbonate chemistry in coastal ecosystems across spatiotemporal gradients. *Scientific Reports*, *8*(1), 1–11.

Sowul, K., H.S. Carson, J.V. Bouma, D. A. Fyfe. 2022. Washington State Recovery Plan for the Pinto Abalone. Washington Department of Fish and Wildlife, Olympia. 65+iv pp.

Vosloo, A., Laas, A., & Vosloo, D. (2013). Differential responses of juvenile and adult South African abalone (*Haliotis midae* Linnaeus) to low and high oxygen levels. *Comparative Biochemistry and Physiology Part A: Molecular & Integrative Physiology*, *164*(1), 192–199.

Wang, W. X., J, M., & Wenig, N. (2018). Trace metals in oysters: Molecular and cellular mechanisms and ecotoxicological impacts. *Environmental Science: Processes & Impacts*, *20*(6), 892–912.

Wassnig, M., Roberts, R. D., Krsinich, A., & Day, R. W. (2010). Effects of water flow rate on growth rate, mortality and biomass return of abalone in slab tanks. *Aquaculture Research*, *41*(6), 839–846.

Conclusion

As humans manage species for commercial use and restoration, the environment changes due to anthropogenic impacts. This creates new challenges in conservation ecology and coastal species management. This dissertation contributes to the ongoing effort to understand and preserve economically and ecologically important species in the face of human-caused stressors.

My findings from chapter one have implications for aquaculture, highlighting depth-related effects on metal accumulation and the importance of continued monitoring of metals in regions with significant shellfish farming. Additionally, my study revealed potential concerns regarding copper and zinc levels exceeding recommended daily intake values. This chapter advances understanding of trace metal bioaccumulation in shellfish, elucidating the complex interplay between environmental factors, species-specific responses, and aquaculture practices. The variability in metal concentrations across different sites and species highlights the need for localized testing to understand better how water properties affect shellfish trace metal accumulation. While metal pollution is a significant threat to shellfish and human health, the inter-site variability observed in this study is particularly noteworthy due to its broader implications. The Salish Sea is a complex environment influenced by various human impacts from increasing population and industry, as well as the area´s intricate bathymetry and complex oceanography. These factors, which might be causing differences in metal concentrations, also affect how climate change impacts are experienced throughout the region.

My final chapter found that oceanographic conditions were quite variable between 16 different abalone restoration sites, all of which were in the San Juan Islands of Washington. Despite this variability, we found that conditions at all sites should be suitable for pinto abalone and that oceanographic conditions did not appear to correlate with differences in abalone

survival between sites. While conditions do not currently seem stressful to pinto abalone or likely to other shellfish and similar species in this region, the results of our study raised a host of related questions.

First, there is a lack of research on how variable conditions, as opposed to constant conditions, impact marine species. Our long-term oceanographic data revealed clear diel, tidal, and seasonal variability. From my hatchery studies (chapters 2 and 3), I found that a constant pH of 7.6 is stressful to juvenile and larval abalone, while a temperature of 18°C is not stressful to juvenile abalone. Based on these data, pH is likely the most problematic variable for abalone in the San Juan Islands, especially as ocean acidification continues. While current mean pH values were not as low as 7.6, all sites experienced pH levels below this threshold at certain times of the day and year. Peak temperatures also varied significantly between sites. More research is needed to determine if variable exposure is more or less stressful than constant exposure to pinto abalone and to identify their tolerance thresholds. Although my second and third chapters provide us with some information on tolerable ranges for pinto abalone in terms of pH and temperature, the variability within and between sites in salinity, current speed, and dissolved oxygen underscored the importance of further study on those variables, including either laboratory studies that use variable exposures or real-world studies that take advantage of natural fluctuation of conditions.

Another question raised by my dissertation work is what factors, aside from oceanography, might be impacting abalone survival at outplant sites. The lack of observed correlation between oceanographic variables and survival suggests that, while oceanography may still play a role, other factors are also likely influencing site suitability. Factors such as site rugosity, food availability, sediment accumulation, or the presence of predators or competitors may play a larger role in determining the success of abalone outplants and restoration efforts.

This does not diminish the importance of our oceanographic data. Our data provide a snapshot of current conditions for future comparisons and represent the first comprehensive long-term quantification of conditions at restoration sites.

One crucial aspect of habitat explored in this dissertation, which could be key to understanding outplant site suitability, is coralline algae. Our hatchery study revealed clear benefits of rearing juvenile abalone on coralline algae substrate—survival was, on average, 55% higher compared to treatments using clean rocks with GABA as a settlement cue. Although cultivating coralline algae is challenging and time-consuming, and complicates the maintenance of hatchery tanks, increasing survival at a hatchery scale could have significant implications for outplant potential.

Outside the hatchery, the role of coralline algae could be more complex. While outplanting to sites with coralline may improve juvenile survival, it is uncertain if future generations would settle in the same locations, as larval abalone might be swept away. Further, the impacts of climate change on coralline algae in Washington have not been clearly studied. As a calcifier, coralline algae will be affected by acidification and warming (Diaz-Pulido et al., 2012; Morse et al. 2006; Ordoñez et al., 2017). It is unknown whether coralline algae have a higher or lower tolerance to these stressors than pinto abalone in Washington. If coralline algae have a lower tolerance, their benefits to abalone in the face of climate change would be minimized. Further study, ideally both in the hatchery and the field, is needed to understand the interactive dynamics between coralline algae and pinto abalone in Washington State.

Looking forward, we have more information than we did previously as we work to restore pinto abalone. This type of in-depth research will be necessary for many species facing stressors linked to climate change, pollution, and other human impacts. Achieving this will

require a combination of laboratory and field-based studies, as well as species-specific research and management strategies, to ensure the sustainability of the Salish Sea's natural resources for generations to come.

References

Diaz-Pulido, G., Anthony, K. R., Kline, D. I., Dove, S., & Hoegh-Guldberg, O. (2012). Interactions between ocean acidification and warming on the mortality and dissolution of coralline algae 1. *Journal of Phycology*, *48*(1), 32-39.

Morse, J. W., Andersson, A. J., & Mackenzie, F. T. (2006). Initial responses of carbonate-rich shelf sediments to rising atmospheric pCO2 and "ocean acidification": Role of high Mg-calcites. *Geochimica et cosmochimica Acta*, *70*(23), 5814-5830.

Ordoñez, A., Kennedy, E. V., & Diaz-Pulido, G. (2017). Reduced spore germination explains sensitivity of reef-building algae to climate change stressors. *PLoS One*, *12*(12), e0189122.